

# Mathematical Modelling of Bacterial Resistance to Anti-microbial Treatment by Bet-hedging Strategy

LAMINU IDRIS

SUPERVISOR:  
Dr ALEX BEST



The  
University  
Of  
Sheffield.

University of Sheffield  
School of Mathematics and Statistics

A thesis submitted in partial fulfilment of the requirements for the degree of  
*Doctor of Philosophy*

November 15, 2022



This thesis has been dedicated to the memory of our parents  
LATE ALHAJI IDRIS KHALIPHA KAURA, and LATE  
MALAMA SA'ADATU MUHAMMAD LADAN for all they  
have done to us until their death, and also to the memory of  
our elder brother LATE SHARHABILU IDRIS KHALIPHA.  
May Aljannar firdaus be their final abode, Amin Ya Allah.





## Acknowledgements

First and foremost I will like to express my gratitude to Almighty Allah for all HE has done to me throughout my life, which are all blessings bestowed upon me by Allah. Almighty Allah I thank you immeasurably.

I also want to express my heartfelt appreciation to my supervisor **Dr. Alex Best**, for his untiring support and guidance throughout my PhD program. I overcame many difficulties, and completed this work successfully because of his scientific, distinctive, and objective criticism; It was a great honor and privilege for me to work under his supervision. I also can't forget the role played by **Prof. Eun – jin Kim** who happened to be my first supervisor before moving to Coventry University. She initiated the process of my admission to the University, suggested the research proposal, and work tirelessly throughout the confirmation review process and beyond. I most say thanks to both of them, and its my pleasure to have both of them as my supervisors.

Notwithstanding, I want to offer my special appreciation to many people for their support and advice, which made the successful completion of this thesis possible.

Special thanks to Nigerian Government, Tertiary Education Trust Fund (Tet-Fund), Federal University Gusau, and also to The University of Sheffield, United Kingdom.



## Declaration of Authorship

I hereby declare that, except where clear reference is made to the work of others, the contents of this dissertation are original and have not, in whole or in part, been submitted to this or any other university for consideration for any other degree or qualification. This dissertation is my own work and contains nothing which is the outcome of work done in collaboration with others, except as specified in the text and Acknowledgements.

Laminu Idris  
November 15, 2022



## Abstract

infectious bacteria can be a major threat to humans, animals, and the environment, especially due to increasing levels of antimicrobial resistance (AMR), where certain bacteria are no longer significantly damaged by the antibiotic drug treatment. One example of AMR is through bacteria with a ‘bet-hedging’ strategy, where bacteria may perform well in one environment by sacrificing fitness in another. In this research, we investigated the dynamics of bacterial populations in a varying environment using mathematical models. One strain of bacteria can ‘switch’ to specialize in each environment, while the other grows at the same rate in both. The death rates of the strain, and the antibiotic drug treatment which is held constant (fixed value) are also included in the model. The aim is to study the dynamical behaviors of these strains and the antibiotic drug administered at both constant and fluctuating rates, to find when each strain may be expected to dominate. We analyze the model using both mathematical analysis and computational simulations. We found a particularly interesting behavior by one strain at early time points when there is a high density of the antibiotic drug concentration. Instead of the strain crashing out early, as would be seen in standard models, an initially high density of the antibiotic drug can allow this strain to stay at the equilibrium state for considerable time. These strain(s) can stay long past the time when the drug density has reduced, before finally being replaced by the ultimately stronger strain(s).



# Contents

---

---

<b>1</b>	<b>Introduction</b>	<b>1</b>
1.1	Background of the Study . . . . .	1
1.2	Statement of the Problem . . . . .	7
1.3	Aims and Objectives of the Study . . . . .	8
1.4	Literature Review . . . . .	9
<b>2</b>	<b>A Model for the Dynamics of the Bet-hedging Bacteria in the Absence of a Constant Strain</b>	<b>23</b>
2.1	Introduction . . . . .	23
2.2	The Model of the Bet-hedging Bacteria . . . . .	25
2.3	Constant Growth Rates ( $\beta_i$ ) Value of the Bacteria . . . . .	26
2.4	Different Growth Rate ( $\beta_i$ ) Values of the Bacteria . . . . .	28
2.5	Fluctuating Resources within the Growth Rates ( $\beta_i$ ) of the Bac- teria . . . . .	34
2.6	Time Courses and Densities of Strains with Varying Values of some Parameters for the Fluctuating Environment . . . . .	36
2.6.1	Time Courses of Strains for Some Varying Values of the Amplitude ( $\delta_i$ ) . . . . .	36
2.6.2	Densities of Strains against the Varying Values of the Amplitude ( $\delta_i$ ) . . . . .	37
2.6.3	Time Courses of Strains for Some Varying Values of the frequency ( $\omega$ ) . . . . .	38
2.6.4	Densities of Strains against the Varying Values of the frequency ( $\omega$ ) . . . . .	40
2.7	Conclusion . . . . .	41
<b>3</b>	<b>Modelling the Bet-hedging of Bacterial Dynamics with the Presence of a Constant Strain</b>	<b>43</b>
3.1	Introduction . . . . .	43
3.2	The Model of the Bet-hedging Bacteria with a Constant Strain .	44

3.3	Constant Growth Rates ( $\beta_i$ ) of the Bacteria . . . . .	45
3.4	Different Growth Rates ( $\beta_i$ ) Values of the Bacteria . . . . .	47
3.5	Fluctuating Resources within the Growth Rates ( $\beta_i$ ) of the Bacteria . . . . .	53
3.6	Time Courses and Densities of Strains for Varying Values of the Parameters in the Fluctuating Environment . . . . .	57
3.6.1	Time Courses and Densities of Strains for Varying Values of the Amplitude ( $\delta_i$ ) . . . . .	57
3.6.1.1	When the Value of $\beta_0$ is Less than the Average Value of $\beta_1$ and $\beta_2$ , [ $\beta_0 < \frac{1}{2}(\beta_1 + \beta_2)$ ] . . . . .	57
3.6.1.2	When the Value of $\beta_0$ is Greater than the Average Value of $\beta_1$ and $\beta_2$ , [ $\beta_0 > \frac{1}{2}(\beta_1 + \beta_2)$ ] . . . . .	60
3.6.1.3	When the Value of $\beta_0$ is Equal to the Average Value of $\beta_1$ and $\beta_2$ , [ $\beta_0 = \frac{1}{2}(\beta_1 + \beta_2)$ ] . . . . .	63
3.6.1.4	When the Values of $\beta_0$ , $\beta_1$ and $\beta_2$ are Equal but not a Constant Value in the Strains Growth Rate, [ $\beta_0 = \beta_1 = \beta_2 \neq 1$ ] . . . . .	66
3.6.2	Time Courses and Densities of Strains for Varying Values of frequency ( $\omega$ ) . . . . .	68
3.6.2.1	When the Value of $\beta_0$ is Less than the Average Value of $\beta_1$ and $\beta_2$ , [ $\beta_0 < \frac{1}{2}(\beta_1 + \beta_2)$ ] . . . . .	68
3.6.2.2	When the Value of $\beta_0$ is Greater than the Average Value of $\beta_1$ and $\beta_2$ , [ $\beta_0 > \frac{1}{2}(\beta_1 + \beta_2)$ ] . . . . .	70
3.6.2.3	When the Value of $\beta_0$ is Equal to the Average Value of $\beta_1$ and $\beta_2$ , [ $\beta_0 = \frac{1}{2}(\beta_1 + \beta_2)$ ] . . . . .	72
3.6.2.4	When the Values of $\beta_0$ , $\beta_1$ and $\beta_2$ are Equal but not a Constant Value, [ $\beta_0 = \beta_1 = \beta_2 \neq 1$ ] . . . . .	75
3.7	Conclusion . . . . .	77
<b>4</b>	<b>Bacterial Dynamics with Antimicrobial Treatment</b>	<b>80</b>
4.1	Introduction . . . . .	80
4.2	The Model of the Bacterial Dynamics with the Antibiotic Drug ( $D$ ) Treatment . . . . .	81
4.3	Constant Growth Rates ( $\beta_i$ ) of the Bacteria . . . . .	82
4.4	Different Growth Rates ( $\beta_i$ ) Values of the Bacteria . . . . .	85
4.4.1	When the Value of $\beta_0$ is Greater than the Average Value of $\beta_1$ and $\beta_2$ , [ $\beta_0 > \frac{1}{2}(\beta_1 + \beta_2)$ ] . . . . .	89



4.4.2	When the Value of $\beta_0$ is Less than the Average Value of $\beta_1$ and $\beta_2$ , $[\beta_0 < \frac{1}{2}(\beta_1 + \beta_2)]$ . . . . .	90
4.4.3	When the Value of $\beta_0$ is Equal to the Average Value of $\beta_1$ and $\beta_2$ , $[\beta_0 = \frac{1}{2}(\beta_1 + \beta_2)]$ . . . . .	92
4.4.4	When the Values of $\beta_0$ , $\beta_1$ , and $\beta_2$ are Equal, $[\beta_0 = \beta_1 = \beta_2 \neq 1]$ . . . . .	94
4.5	Fluctuating Resources within the Bacterial Growth Rates ( $\beta_i$ ) . . . . .	96
4.5.1	When the Value of $\beta_0$ is Greater than the Average Value of $\beta_1$ and $\beta_2$ , $[\beta_0 > \frac{1}{2}(\beta_1 + \beta_2)]$ . . . . .	96
4.5.2	When the Value of $\beta_0$ is Less than the Average Value of $\beta_1$ and $\beta_2$ , $[\beta_0 < \frac{1}{2}(\beta_1 + \beta_2)]$ . . . . .	98
4.5.3	When the Value of $\beta_0$ is Equal to the Average Value of $\beta_1$ and $\beta_2$ , $[\beta_0 = \frac{1}{2}(\beta_1 + \beta_2)]$ . . . . .	100
4.5.4	When the Values of $\beta_0$ , $\beta_1$ , and $\beta_2$ are Equal, $[\beta_0 = \beta_1 = \beta_2 \neq 1]$ . . . . .	102
4.6	Fluctuating Resources within the Antimicrobial Treatment . . . . .	104
4.6.1	When the Value of $\beta_0$ is Greater than the Average Value of $\beta_1$ and $\beta_2$ , $[\beta_0 > \frac{1}{2}(\beta_1 + \beta_2)]$ . . . . .	105
4.6.2	When the Value of $\beta_0$ is Less than the Average Value of $\beta_1$ and $\beta_2$ , $[\beta_0 < \frac{1}{2}(\beta_1 + \beta_2)]$ . . . . .	107
4.6.3	When the Value of $\beta_0$ is Equal to the Average Value of $\beta_1$ and $\beta_2$ , $[\beta_0 = \frac{1}{2}(\beta_1 + \beta_2)]$ . . . . .	109
4.6.4	When the Values of $\beta_0$ , $\beta_1$ , and $\beta_2$ are Equal, $[\beta_0 = \beta_1 = \beta_2 \neq 1]$ . . . . .	111
4.7	Conclusion . . . . .	113
<b>5</b>	<b>Bacterial and the Antimicrobial Treatment Dynamics</b> . . . . .	<b>115</b>
5.1	Introduction . . . . .	115
5.2	The Model of the Bacterial and the Antimicrobial Treatment Dynamics . . . . .	115
5.3	Constant Growth Rate ( $\beta_i$ ) Values of the Bacteria . . . . .	116
5.4	Different Growth Rate ( $\beta_i$ ) Values of the Bacteria . . . . .	120
5.4.1	When the Value of $\beta_0$ is Greater than the Average Value of $\beta_1$ and $\beta_2$ , $[\beta_0 > \frac{1}{2}(\beta_1 + \beta_2)]$ . . . . .	123
5.4.2	When the Value of $\beta_0$ is Less than the Average Value of $\beta_1$ and $\beta_2$ , $[\beta_0 < \frac{1}{2}(\beta_1 + \beta_2)]$ . . . . .	125
5.4.3	When the Value of $\beta_0$ is Equal to the Average Value of $\beta_1$ and $\beta_2$ , $[\beta_0 = \frac{1}{2}(\beta_1 + \beta_2)]$ . . . . .	126

5.5	Fluctuating Resources within the Strains	
	Growth Rates ( $\beta_i$ ) . . . . .	128
5.5.1	When the Value of $\beta_0$ is Greater than the Average value of $\beta_1$ and $\beta_2$ , [ $\beta_0 > \frac{1}{2}(\beta_1 + \beta_2)$ ] . . . . .	128
5.5.2	When the Value of $\beta_0$ is Less than the Average Value of $\beta_1$ and $\beta_2$ , [ $\beta_0 < \frac{1}{2}(\beta_1 + \beta_2)$ ] . . . . .	130
5.5.3	When the Value of $\beta_0$ is Equal to the Average Value of $\beta_1$ and $\beta_2$ , [ $\beta_0 = \frac{1}{2}(\beta_1 + \beta_2)$ ] . . . . .	131
5.6	Fluctuating Resources within the Antimicrobial Treatment Ad- ministration Rate ( $a$ ) . . . . .	132
5.6.1	When the Value of $\beta_0$ is Greater than the Average Value of $\beta_1$ and $\beta_2$ , [ $\beta_0 > \frac{1}{2}(\beta_1 + \beta_2)$ ] . . . . .	132
5.6.2	When the Value of $\beta_0$ is Less than the Average Value of $\beta_1$ and $\beta_2$ , [ $\beta_0 < \frac{1}{2}(\beta_1 + \beta_2)$ ] . . . . .	133
5.6.3	When the Value of $\beta_0$ is Equal to the Average Value of $\beta_1$ and $\beta_2$ , [ $\beta_0 = \frac{1}{2}(\beta_1 + \beta_2)$ ] . . . . .	134
5.7	Conclusion . . . . .	136
<b>6</b>	<b>Conclusions</b>	<b>138</b>
6.1	Overview of Thesis . . . . .	138
6.2	Discussion of Results . . . . .	139
6.2.1	Chapter 2 . . . . .	139
6.2.2	Chapter 3 . . . . .	140
6.2.3	Chapter 4 . . . . .	141
6.2.4	Chapter 5 . . . . .	143
6.3	Future work . . . . .	144
	<b>Bibliography</b>	<b>146</b>

## List of Figures

---

---

- 2.1 The Numerical graphs for the intrinsic dynamics of the 2D bet-hedging model, with a constant growth rates of the bacterial strain:  $\beta_1 = \beta_2 = \beta$ , both strains having the same initial values:  $s_1(0) = s_2(0) = 0.2$ , with different amount of nutrients contents in the environments to be utilized by the bacterial strain:  $\alpha_1 = 5$  and  $\alpha_2 = 1$ , the same range of time for each of the plots  $t = 0 : 0.001 : 200$ , with the transition rates values of:  $\epsilon_1 = 0.01$ ,  $\epsilon_2 = 0.02$ , and the whole plots show the two strains in each case become stable at  $s_1 + s_2 = \beta = 1$ . . . . . 28
- 2.2 The numerical graphs for the eigenvalues of the non-zero equilibrium point for 2D bet-hedging model, with different values of the strains growth rates ( $\beta_1 \neq \beta_2$ ), against some parameters  $\beta_1$ ,  $\beta_2$ ,  $\epsilon_1$ , and  $\epsilon_2$  respectively, which show the two eigenvalues are always negative (*i.e.*  $\lambda_i < 0$ ,  $i = 1, 2$ ). In plot (a),  $\beta_2 = 80$ ,  $\epsilon_1 = 15$ , and  $\epsilon_2 = 50$ . In plot (b) as well,  $\beta_1 = 1$ ,  $\epsilon_1 = 0.01$ , and  $\epsilon_2 = 0.02$ , Also in plot (c),  $\beta_1 = 11$ ,  $\beta_2 = 25$ , and  $\epsilon_2 = 30$ . And lastly in plot (d),  $\beta_1 = 15$ ,  $\beta_2 = 33$ , and  $\epsilon_1 = 0.01$  respectively. The plot obtained in panel (e) is a zoom of the result obtained in the plot of panel (b), which clearly show the result is negative. . . . . 32

- 2.3 The Numerical graphs for the dynamics of the 2D bet-hedging model, with different values of the strains growth rates ( $\beta_1 \neq \beta_2$ ), with both strains having the same initial values ( $s_1(0) = s_2(0) = 0.2$ ), and different amount of nutrient contents in the environments ( $\alpha_1 = 5$  and  $\alpha_2 = 1$ ), with the same range of time for each of the plots  $t = 0 : 0.001 : 200$ , with plots (a), (b) and (c) having different amount or concentration of enzymes  $r_1 = 0.5$ , and  $r_2 = 0.7$ , with plot (a) having  $\epsilon_1 = 0.01$ , and  $\epsilon_2 = 0.02$ , plot (b) having the same transition rate values between the strains  $\epsilon_1 = \epsilon_2 = 0.02$ , and plot (c) having  $\epsilon_1 = 0.02$ , and  $\epsilon_2 = 0.01$ . Also, plots (d), (e) and (f) have the same amount or concentration of enzymes  $r_1 = r_2 = 0.7$ , with plot (d) having  $\epsilon_1 = 0.01$ , and  $\epsilon_2 = 0.02$ , plot (e) having the same transition rate values between the strains  $\epsilon_1 = \epsilon_2 = 0.02$ , and plot (f) having  $\epsilon_1 = 0.02$  and  $\epsilon_2 = 0.01$ , which show all the strains become stable at their respective equilibrium points. 33
- 2.4 The Numerical graphs for the fluctuating dynamics of the bet-hedging model, with all of the plots having the same initial values ( $s_1(0) = s_2(0) = 0.2$ ), with plot (a), (b) and (c) having different values of enzymes ( $r_1 = 0.5$  and  $r_2 = 0.7$ ), with plot (a) having  $\epsilon_1 = 0.01$  and  $\epsilon_2 = 0.02$  plot (b) having the same values of the transition rates  $\epsilon_1 = \epsilon_2 = 0.02$ , and plot (c) having  $\epsilon_1 = 0.02$  and  $\epsilon_2 = 0.01$ . Also, plots (d) to (f) have the same values of enzymes ( $r_1 = r_2 = 0.7$ ), with plot (d) having  $\epsilon_1 = 0.01$  and  $\epsilon_2 = 0.02$ , plot (e) having the same values of the transition rates  $\epsilon_1 = \epsilon_2 = 0.02$ , and plot (f) having  $\epsilon_1 = 0.02$  and  $\epsilon_2 = 0.01$ , with the amplitude value  $\delta = 0.25$ , the frequency of oscillation  $\omega = 1$ , and it is more evident that one strain dominates at some point. . . . . 35
- 2.5 Time courses of strains for the 2D bet-hedging model with the fluctuating environment, and the varying amplitude ( $\delta_i$ ) values of oscillation, with the parameters:  $r_1 = 0.5$  and  $r_2 = 0.7$ , different values of the transition rates  $\epsilon_1 = 0.01$  and  $\epsilon_2 = 0.02$  respectively, with the frequency value of oscillations  $\omega = 1$ , and the initial values of the strains densities ( $s_1(0) = s_2(0) = 0.2$ ). 37

2.6	Maximum and minimum densities of strains for the 2D bet-hedging model, with the fluctuating environment and the same range of the amplitude ( $\delta_i$ ) values, with the parameters: $r_1 = 0.5$ and $r_2 = 0.7$ , plots (a) and (d) having different transition rate values $\epsilon_1 = 0.01$ and $\epsilon_2 = 0.02$ , plots (b) and (e) having the same transition rate values $\epsilon_1 = \epsilon_2 = 0.01$ , also plots (c) and (f) having different transition rate values $\epsilon_1 = 0.02$ and $\epsilon_2 = 0.01$ as well, with the frequency of oscillations $\omega = 1$ , and the initial values of the strain densities ( $s_1(0) = s_2(0) = 0.2$ ).	38
2.7	Time courses of strains for the 2D bet-hedging model with the fluctuating environment, and the varying frequency ( $\omega$ ) values of oscillations, with the parameters: $r_1 = 0.5$ and $r_2 = 0.7$ , different values of the transition rates $\epsilon_1 = 0.01$ and $\epsilon_2 = 0.02$ respectively, with the amplitude value of oscillations $\delta = 0.25$ , and the initial values of the strains densities ( $s_1(0) = s_2(0) = 0.2$ ).	39
2.8	Maximum and minimum densities of strains for the 2D bet-hedging model, with the fluctuating environment ( $\delta * \sin(\omega t) + 1$ ) and the same range of the frequency ( $\omega$ ) values, with the parameters: $r_1 = 0.5$ and $r_2 = 0.7$ , plots (a) and (d) having different transition rate values $\epsilon_1 = 0.01$ and $\epsilon_2 = 0.02$ , plots (b) and (e) having the same transition rate values $\epsilon_1 = \epsilon_2 = 0.01$ , also plots (c) and (f) having different transition rate values $\epsilon_1 = 0.02$ and $\epsilon_2 = 0.01$ as well, with the amplitude value of oscillations $\delta = 0.25$ , and the initial values of the strain densities ( $s_1(0) = s_2(0) = 0.2$ ).	40
2.9	The maximum and minimum densities of strains for the 2D bet-hedging model, with the fluctuating environment ( $\delta * \sin(\omega t) + 1$ ) and the same range of the frequency ( $\omega$ ) values of oscillations, with the parameters: $r_1 = 0.5$ and $r_2 = 0.7$ , different values of the transition rates $\epsilon_1 = 0.01$ , $\epsilon_2 = 0.02$ , and $\epsilon_1 = \epsilon_2 = 0.01$ respectively, with the amplitude value of oscillations $\delta = 0.25$ , and the initial values of the strain densities ( $s_1(0) = s_2(0) = 0.2$ ).	41

- 3.1 The Numerical graphs for the intrinsic dynamics of the 3D bet-hedging model, with a constant growth rates of the bacterial strain ( $\beta_0 = \beta_1 = \beta_2 = \beta = 1$ ), both strains having the same initial values ( $s_0(0) = s_1(0) = s_2(0) = 0.2$ ), with different amount of nutrients to be utilized by the bacterial strain  $\alpha_0 = 3$ ,  $\alpha_1 = 5$  and  $\alpha_2 = 1$ , the same range of time for each of the plots  $t = 0 : 0.001 : 300$ , with (a) having different transition rate values  $\epsilon_1 = 0.01$  and  $\epsilon_2 = 0.02$ , (b) having the same values of the transition rates  $\epsilon_1 = \epsilon_2 = 0.02$ , whereas (c) has different transition rates values as well  $\epsilon_1 = 0.02$  and  $\epsilon_2 = 0.01$ . . . . . 47
- 3.2 The Numerical graphs for the intrinsic dynamics of the 3D bet-hedging model when there is a presence of enzyme(s) to utilize the nutrients available ( $\beta_0 \neq \beta_1 \neq \beta_2$ ), both strains having the same initial values ( $s_0(0) = s_1(0) = s_2(0) = 1$ ), with different values of  $\beta_0$  as; 8, 3 and 6 respectively, where as  $\beta_1 = 5$ , and  $\beta_2 = 7$  all through, with plots (a, d) and (g) having different transition rate values  $\epsilon_1 = 1$  and  $\epsilon_2 = 10$ , plots (b, e) and (h) having the same values of the transition rates  $\epsilon_1 = \epsilon_2 = 1$ , whereas plots (c, f) and (i) has different transition rate values as well  $\epsilon_1 = 10$  and  $\epsilon_2 = 1$ , and both plots show all the strains become stable at some points. . . . . 51
- 3.3 The Numerical graphs for the intrinsic dynamics of the 3D bet-hedging model when there is a presence of enzyme(s) to utilize the nutrients available ( $\beta_0 = \beta_1 = \beta_2 \neq 1$ ), both strains having the same initial values ( $s_0(0) = s_1(0) = s_2(0) = 1$ ), the same growth rate values for the strains  $\beta_0 = \beta_1 = \beta_2 = 5$ , with plot (a) having different transition rates values  $\epsilon_1 = 1$  and  $\epsilon_2 = 10$ , plot (b) having the same values of the transition rates  $\epsilon_1 = \epsilon_2 = 1$ , whereas plot (c) has different transition rates values as well  $\epsilon_1 = 10$  and  $\epsilon_2 = 1$ , and both plots show all the three strains co-exists as a special case. . . . . 53

- 3.4 The Numerical graphs for the intrinsic dynamics of the fluctuating 3D bet-hedging model for  $(\beta_0 \neq \beta_1 \neq \beta_2)$ , with both strains having the same initial values  $(s_0(0) = s_1(0) = s_2(0) = 0.2)$ , with different values of  $r_0$  as; 0.8, 0.3 and 0.6 respectively, where as  $r_1 = 0.5$ , and  $r_2 = 0.7$  all through, with  $(a, d)$  and  $(g)$  having different transition rates values  $\epsilon_1 = 1$  and  $\epsilon_2 = 10$ ,  $(b, e)$  and  $(h)$  having the same values of the transition rates  $\epsilon_1 = \epsilon_2 = 1$ , whereas  $(c, f)$  and  $(i)$  has different transition rates values as well  $\epsilon_1 = 10$  and  $\epsilon_2 = 1$ , with the amplitude value of fluctuation  $\delta = 0.25$ , and the frequency value of oscillation  $\omega = 1$ , and both plots show all the strains become stable at some points. . . . . 55
- 3.5 The Numerical graphs for the intrinsic dynamics of the 3D bet-hedging model for the fluctuating environment, when the growth rate  $(\beta_i)$  of the strains are the same, but not equal to the constant value in their growth rates (*i. e.*  $\beta_0 = \beta_1 = \beta_2 \neq 1$ ), both strains having the same initial values  $[s_0(0) = s_1(0) = s_2(0) = 1]$ , the same growth rate values  $\beta_0 = \beta_1 = \beta_2 = 5$ , with  $(a)$  having different transition rates  $\epsilon_1 = 1$  and  $\epsilon_2 = 10$ ,  $(b)$  having the same values of the transition rates  $\epsilon_1 = \epsilon_2 = 1$ , whereas  $(c)$  has different transition rates as well  $\epsilon_1 = 10$  and  $\epsilon_2 = 1$ , and both plots show the co-existence of all the strains, which is a special case. . . . . 56
- 3.6 Time courses of strains for the 3D bet-hedging model with the fluctuating environment against the varying amplitude  $(\delta_i)$  values with parameters;  $r_0 = 0.3$ ,  $r_1 = 0.5$ ,  $r_2 = 0.7$ , different transition rates values  $\epsilon_1 = 1$  and  $\epsilon_2 = 10$ , frequency value of fluctuation  $\omega = 1$ , and the initial values of the bacterial densities  $s_0(0) = s_1(0) = s_2(0) = 0.2$ , which show the non-switching strain  $(s_0)$  can never invade. . . . . 58

3.7	The maximum and minimum densities of strains for the 3D bet-hedging model with the fluctuating environment, against the varying amplitude ( $\delta_i$ ) values with parameters; $r_0 = 0.3$ , $r_1 = 0.5$ , $r_2 = 0.7$ , plots (a) and (d) having different transition rate values $\epsilon_1 = 1$ , and $\epsilon_2 = 10$ , plots (b) and (e) having the same transition rate values $\epsilon_1 = \epsilon_2 = 1$ , also plots (c) and (f) having different transition rate values as well $\epsilon_1 = 10$ and $\epsilon_2 = 1$ , with the frequencyic value of oscillation $\omega = 1$ , and the initial values of the bacterial densities $s_0(0) = s_1(0) = s_2(0) = 0.2$ , which show in the whole plots the non-switching ( $s_0$ ) strain can never invade. . . . .	59
3.8	Time courses of strains for the 3D bet-hedging model with the fluctuating environment against the varying amplitude ( $\delta_i$ ) values with parameters; $r_0 = 0.8$ , $r_1 = 0.5$ , $r_2 = 0.7$ , different values of the transition rates $\epsilon_i$ , as $i = 1$ and 10 respectively, $\omega = 1$ and the initial values of the bacterial densities $s_0(0) = s_1(0) = s_2(0) = 0.2$ , which show $s_0$ can never be invaded. . . . .	60
3.9	The maximum and minimum densities of strains for the 3D bet-hedging model with the fluctuating environment against the varying amplitude ( $\delta_i$ ) values with parameters; $r_0 = 0.8$ , $r_1 = 0.5$ , $r_2 = 0.7$ , different conditions of transition rates ( $\epsilon_i$ ) as $i = 1$ and 10 respectively, $\omega = 1$ and the initial values of the bacterial densities $s_0(0) = s_1(0) = s_2(0) = 0.2$ , which show $s_0$ can never be invaded. . . . .	62
3.10	Time courses of strains for the 3D bet-hedging model with the fluctuating environment against the varying amplitude ( $\delta_i$ ) values with parameters; $r_0 = 0.6$ , $r_1 = 0.5$ , $r_2 = 0.7$ , different values of the transition rates $\epsilon_i$ , as $i = 1$ and 10 respectively, $\omega = 1$ and the initial values of the bacterial densities $s_0(0) = s_1(0) = s_2(0) = 0.2$ . . . . .	64
3.11	The maximum and minimum densities of strains for the 3D bet-hedging model in the fluctuating environment against the varying amplitude ( $\delta_i$ ) values with parameters; $r_0 = 0.6$ , $r_1 = 0.5$ , $r_2 = 0.7$ , different conditions of transition rates ( $\epsilon_i$ ) as $i = 1$ and 10 respectively, $\omega = 1$ and the initial values of the bacterial densities $s_0(0) = s_1(0) = s_2(0) = 0.2$ . . . . .	65



3.12	Time courses of strains for the 3D bet-hedging model in the fluctuating environment against the varying amplitude ( $\delta_i$ ) values with parameters; $r_0 = r_1 = r_2 = 0.5$ , different values of the transition rates $\epsilon_i$ , as $i = 1$ and $10$ respectively, $\omega = 1$ and the initial values of the bacterial densities $s_0(0) = s_1(0) = s_2(0) = 0.2$ , which show the co-existence of all the strains. . . . .	66
3.13	The maximum and minimum densities of strains for the 3D bet-hedging model in the fluctuating environment against the varying amplitude ( $\delta_i$ ) values with parameters; $r_0 = r_1 = r_2 = 0.5$ , different conditions of the transition rates ( $\epsilon_i$ ), as $i = 1$ and $10$ respectively, $\omega = 1$ and the initial values of the bacterial densities $s_0(0) = s_1(0) = s_2(0) = 0.2$ , which show the co-existence of all the strains. . . . .	67
3.14	Time courses of strains for the 3D bet-hedging model in the fluctuating environment against the varying frequency ( $\omega$ ) values with parameters; $r_0 = 0.3$ , $r_1 = 0.5$ , $r_2 = 0.7$ , different values of the transition rates $\epsilon_i$ , as $i = 1$ and $10$ respectively, $\delta = 0.25$ and the initial values of the bacterial densities $s_0(0) = s_1(0) = s_2(0) = 0.2$ , which show $s_0$ can never invade. . . . .	69
3.15	The maximum and minimum densities of strains for 3D bet-hedging model in the fluctuating environment against the varying frequency ( $\omega$ ) values with parameters; $r_0 = 0.3$ , $r_1 = 0.5$ , $r_2 = 0.7$ , different conditions of the transition rates ( $\epsilon_i$ ), as $i = 1$ and $10$ respectively, $\delta = 0.25$ and the initial values of the bacterial densities $s_0(0) = s_1(0) = s_2(0) = 0.2$ , which show $s_0$ can never invade. . . . .	70
3.16	Time courses of strains for the 3D bet-hedging model in the fluctuating environment against the varying frequency ( $\omega$ ) values with parameters; $r_0 = 0.8$ , $r_1 = 0.5$ , $r_2 = 0.7$ , different values of the transition rates $\epsilon_i$ , as $i = 1$ and $10$ respectively, $\delta = 0.25$ and the initial values of the bacterial densities $s_0(0) = s_1(0) = s_2(0) = 0.2$ , which show $s_0$ can never be invaded. . . . .	71

- 3.17 The maximum and minimum densities of strains for 3D bet-hedging model in the fluctuating environment against the varying frequencyic ( $\omega$ ) values with parameters;  $r_0 = 0.8$ ,  $r_1 = 0.5$ ,  $r_2 = 0.7$ , different conditions of the transition rates ( $\epsilon_i$ ), as  $i = 1$  and 10 respectively,  $\delta = 0.25$  and the initial values of the bacterial densities  $s_0(0) = s_1(0) = s_2(0) = 0.2$ , which show  $s_0$  can never be invaded. . . . . 72
- 3.18 Time courses of strains for the 3D bet-hedging model in the fluctuating environment against the varying frequencyic ( $\omega$ ) values with parameters;  $r_0 = 0.6$ ,  $r_1 = 0.5$ ,  $r_2 = 0.7$ , different values of the transition rates  $\epsilon_i$ , as  $i = 1$  and 10 respectively,  $\delta = 0.25$  and the initial values of the bacterial densities  $s_0(0) = s_1(0) = s_2(0) = 0.2$ . . . . . 73
- 3.19 The maximum and minimum densities of strains for 3D bet-hedging model in the fluctuating environment against the varying frequencyic ( $\omega$ ) values with parameters;  $r_0 = 0.6$ ,  $r_1 = 0.5$ ,  $r_2 = 0.7$ , different conditions of the transition rates ( $\epsilon_i$ ), as  $i = 1$  and 10 respectively,  $\delta = 0.25$  and the initial values of the bacterial densities  $s_0(0) = s_1(0) = s_2(0) = 0.2$ . . . . . 74
- 3.20 The maximum and minimum densities of strains for 3D bet-hedging model in the fluctuating environment against the varying frequencyic ( $\omega$ ) values with parameters;  $r_0 = 0.6$ ,  $r_1 = 0.5$ ,  $r_2 = 0.7$ , different conditions of the transition rates ( $\epsilon_i$ ), as  $i = 1$  and 10 respectively,  $\delta = 0.25$  and the initial values of the bacterial densities  $s_0(0) = s_1(0) = s_2(0) = 0.2$ . . . . . 75
- 3.21 Time courses of strains for 3D bet-hedging model in the fluctuating environment against the varying frequencyic ( $\omega$ ) values with parameters;  $r_0 = r_1 = r_2 = 0.5$ , different values of the transition rates  $\epsilon_i$ , as  $i = 1$  and 10 respectively,  $\delta = 0.25$  and the initial values of the bacterial densities  $s_0(0) = s_1(0) = s_2(0) = 0.2$ , which show the co-existence of all the strains. . . . . 76

3.22	The maximum and minimum densities of strains for 3D bet-hedging model in the fluctuating environment against the varying frequencyic ( $\omega$ ) values with parameters; $r_0 = r_1 = r_2 = 0.5$ , different conditions of transition rates ( $\epsilon_i$ ), as $i = 1$ and $10$ respectively, $\delta = 0.25$ and the initial values of the bacterial densities $s_0(0) = s_1(0) = s_2(0) = 0.2$ , which show the co-existence of all the strains. . . . .	77
4.1	The Numerical graphs for the intrinsic dynamics of the 3D bet-hedging model with the antibiotic drug (D) treatment and the death rates ( $k_i$ ) of the strains, for the constant growth rates of the bacterial strains: $\beta_0 = \beta_1 = \beta_2 = \beta = 1$ , the antibiotic drug treatment $D = 0.5$ , the respective death rates values of the strains: $k_0 = k_1 = k_2 = 0.1$ , with both strains having the same initial values: $s_0(0) = s_1(0) = s_2(0) = 1$ , and different transition rate values: $\epsilon_1 = 1$ , and $\epsilon_2 = 10$ . . . . .	85
4.2	The Numerical graphs for the dynamics of the 3D bet-hedging model, with the strains death rates ( $k_i$ ) and the antibiotic drug ( $D$ ) treatment, for $\beta_0 > \frac{1}{2}(\beta_1 + \beta_2)$ , with both strains having the same initial values ( $s_0(0) = s_1(0) = s_2(0) = 1$ ), different values of the strains growth rates ( $\beta_0 = 8, \beta_1 = 5, \beta_2 = 7$ ), with the antibiotic drug treatment $D = 0.5$ , and different transition rates values $\epsilon_1 = 1$ , and $\epsilon_2 = 10$ . . . . .	89
4.3	The Numerical graphs for the maximum densities of strains for the 3D bet-hedging model with the strains death rates ( $k_i$ ), and the antibiotic drug ( $D$ ) treatment against the different strains death rates ( $k_i$ ) for $\beta_0 > \frac{1}{2}(\beta_1 + \beta_2)$ , with both strains having the same initial values ( $s_0(0) = s_1(0) = s_2(0) = 0.2$ ), different values of the strains growth rates ( $\beta_0 = 8, \beta_1 = 5, \beta_2 = 7$ ), with the antibiotic drug treatment $D = 0.5$ , and different transition rates values $\epsilon_1 = 1$ , and $\epsilon_2 = 10$ . . . . .	90
4.4	The Numerical graphs for the dynamics of the 3D bet-hedging model with the strains death rates ( $k_i$ ), and the antibiotic drug ( $D$ ) treatment for $\beta_0 < \frac{1}{2}(\beta_1 + \beta_2)$ , with both strains having the same initial values ( $s_0(0) = s_1(0) = s_2(0) = 1$ ), different values of the strains growth rates ( $\beta_0 = 3, \beta_1 = 5, \beta_2 = 7$ ), with the antibiotic drug treatment $D = 0.5$ , and the different transition rates values $\epsilon_1 = 1$ , and $\epsilon_2 = 10$ . . . . .	91

- 4.5 The Numerical graphs for the maximum densities of strains for the 3D bet-hedging model with the strains death rates ( $k_i$ ) and the antibiotic drug ( $D$ ) treatment, against the different strains death rates ( $k_i$ ), for  $\beta_0 < \frac{1}{2}(\beta_1 + \beta_2)$ , with both strains having the same initial values ( $s_0(0) = s_1(0) = s_2(0) = 0.2$ ), different range of values for the strains death rates ( $k_i$ ), different values of the strains growth rates ( $\beta_0 = 3, \beta_1 = 5, \beta_2 = 7$ ), with the antibiotic drug treatment  $D = 0.5$ , and the different transition rates values  $\epsilon_1 = 1$ , and  $\epsilon_2 = 10$ . . . . . 92
- 4.6 The Numerical graphs for the dynamics of the 3D bet-hedging model with the strains death rates ( $k_i$ ) and the antibiotic drug ( $D$ ) treatment for  $\beta_0 = \frac{1}{2}(\beta_1 + \beta_2)$ , with both strains having the same initial values ( $s_0(0) = s_1(0) = s_2(0) = 1$ ), same range of time for each of the plots  $t = 0 : 0.001 : 30$ , different values of the strains growth rates ( $\beta_0 = 6, \beta_1 = 5, \beta_2 = 7$ ), with the antibiotic drug treatment  $D = 0.5$ , and different transition rates values  $\epsilon_1 = 1$ , and  $\epsilon_2 = 10$ . . . . . 93
- 4.7 The Numerical graphs for the maximum densities of strains for the 3D bet-hedging model with the strains death rates ( $k_i$ ) and the antibiotic drug ( $D$ ) treatment, against the different strains death rates ( $k_i$ ) for  $\beta_0 = \frac{1}{2}(\beta_1 + \beta_2)$ , with both strains having the same initial values  $s_0(0) = s_1(0) = s_2(0) = 0.2$ , different range of values for the strains death rates, different values of the strains growth rates  $\beta_0 = 6, \beta_1 = 5, \beta_2 = 7$ , with the antibiotic drug treatment  $D = 1$ , and different transition rates values  $\epsilon_1 = 1$ , and  $\epsilon_2 = 10$ . . . . . 94
- 4.8 The Numerical graphs for the maximum densities of strains for the 3D bet-hedging model with the strains death rates ( $k_i$ ) and the antibiotic drug ( $D$ ) treatment, against the different strains death rates ( $k_i$ ) for  $\beta_0 = \beta_1 = \beta_2 \neq 1$ , with both strains having the same initial values ( $s_0(0) = s_1(0) = s_2(0) = 0.2$ ), the same range of values for the strains death rates, the same values of the strains growth rates ( $\beta_0 = \beta_1 = \beta_2 = 5$ ), with the antibiotic drug treatment  $D = 0.5$ , and different transition rates values  $\epsilon_1 = 1$ , and  $\epsilon_2 = 10$ . . . . . 95

- 4.9 The Numerical graphs for the dynamics of the 3D bet-hedging model with the fluctuating growth resources, the strains death rates ( $k_i$ ), and the antibiotic drug ( $D$ ) treatment for  $\beta_0 > \frac{1}{2}(\beta_1 + \beta_2)$ , with both strains having the same initial values ( $s_0(0) = s_1(0) = s_2(0) = 0.2$ ), different ranges of time for the plots, different amount of enzymes in the strains growth rates ( $r_0 = 0.8, r_1 = 0.5, r_2 = 0.7$ ), with the amplitude  $\delta = 0.25$ , and the frequency of fluctuating resources  $\omega = 1$ , the antibiotic drug treatment  $D = 0.5$ , and different transition rates values  $\epsilon_1 = 0.05$ , and  $\epsilon_2 = 0.1$ . . . . . 97
- 4.10 The Numerical graphs for the maximum densities of strains for the 3D bet-hedging model and the fluctuating growth resources, with the strains death rates ( $k_i$ ) and the antibiotic drug ( $D$ ) treatment for  $\beta_0 > \frac{1}{2}(\beta_1 + \beta_2)$ , with both strains having the same initial values ( $s_0(0) = s_1(0) = s_2(0) = 0.2$ ), same range of values for the strains death rates in each plots ( $k_i = 0 : 0.1 : 2$ ), different amount of enzymes in the strains growth rates ( $r_0 = 0.8, r_1 = 0.5, r_2 = 0.7$ ), with the amplitude  $\delta = 0.25$ , and the frequency of fluctuating resources  $\omega = 1$ , the antibiotic drug treatment  $D = 0.5$ , and different transition rates values  $\epsilon_1 = 0.05$ , and  $\epsilon_2 = 0.1$ . . . . . 98
- 4.11 The Numerical graphs for the dynamics of the 3D bet-hedging model and the fluctuating growth resources, with the strains death rates ( $k_i$ ) and the antibiotic drug ( $D$ ) treatment for  $\beta_0 < \frac{1}{2}(\beta_1 + \beta_2)$ , with both strains having the same initial values ( $s_0(0) = s_1(0) = s_2(0) = 0.2$ ), different ranges of time for the plots, different amount of enzymes in the strains growth rates ( $r_0 = 0.3, r_1 = 0.5, r_2 = 0.7$ ), with the amplitude  $\delta = 0.25$ , and the frequency of fluctuating resources  $\omega = 1$ , the antibiotic drug treatment  $D = 0.5$ , and different transition rates values  $\epsilon_1 = 0.05$ , and  $\epsilon_2 = 0.1$ . . . . . 99

- 4.12 The Numerical graphs for the maximum densities of strains for the 3D bet-hedging model and the fluctuating growth resources, with the strains death rates ( $k_i$ ) and the antibiotic drug ( $D$ ) treatment for  $\beta_0 < \frac{1}{2}(\beta_1 + \beta_2)$ , with both strains having the same initial values ( $s_0(0) = s_1(0) = s_2(0) = 0.2$ ), different ranges of the strains death rates in the plots, different amount of enzymes in the strains growth rates ( $r_0 = 0.3, r_1 = 0.5, r_2 = 0.7$ ), with the amplitude  $\delta = 0.25$ , and the frequency of fluctuating resources  $\omega = 1$ , the antibiotic drug treatment  $D = 0.5$ , and different transition rates values  $\epsilon_1 = 0.05$ , and  $\epsilon_2 = 0.1$ . . . . . 100
- 4.13 The Numerical graphs for the dynamics of the 3D bet-hedging model and the fluctuating growth resources, with the strains death rates ( $k_i$ ) and the antibiotic drug ( $D$ ) treatment for  $\beta_0 = \frac{1}{2}(\beta_1 + \beta_2)$ , with both strains having the same initial values ( $s_0(0) = s_1(0) = s_2(0) = 0.2$ ), different ranges of time for the plots, different amount of enzymes in the strains growth rates ( $r_0 = 0.6, r_1 = 0.5, r_2 = 0.7$ ), with the amplitude  $\delta = 0.25$ , and the frequency of fluctuating resources  $\omega = 1$ , the antibiotic drug treatment  $D = 0.5$ , and different transition rates values  $\epsilon_1 = 0.05$ , and  $\epsilon_2 = 0.1$ . . . . . 101
- 4.14 The Numerical graphs for the maximum densities of strains for the 3D bet-hedging model and the fluctuating growth resources, with the strains death rates ( $k_i$ ) and the antibiotic drug ( $D$ ) treatment for  $\beta_0 = \frac{1}{2}(\beta_1 + \beta_2)$ , with both strains having the same initial values ( $s_0(0) = s_1(0) = s_2(0) = 0.2$ ), the same ranges of the strains death rates in each plots, different amount of enzymes in the strains growth rates ( $r_0 = 0.6, r_1 = 0.5, r_2 = 0.7$ ), with the amplitude  $\delta = 0.25$ , and the frequency of the fluctuating resources  $\omega = 1$ , the antibiotic drug treatment  $D = 0.5$ , and different transition rates values  $\epsilon_1 = 0.05$ , and  $\epsilon_2 = 0.1$ . . . . . 102

- 4.15 The Numerical graphs for the dynamics of the 3D bet-hedging model and the fluctuating growth resources, with the strains death rates ( $k_i$ ) and the antibiotic drug ( $D$ ) treatment for  $\beta_0 = \beta_1 = \beta_2 = \beta$ , with both strains having the same initial values ( $s_0(0) = s_1(0) = s_2(0) = 0.2$ ), the same ranges of time for the plots, the same amount of enzymes in the strains growth rates ( $r_0 = r_1 = r_2 = 0.5$ ), with the amplitude  $\delta = 0.25$ , and the frequency of the fluctuating resources  $\omega = 1$ , the antibiotic drug treatment  $D = 0.5$ , and different transition rates values  $\epsilon_1 = 0.05$ , and  $\epsilon_2 = 0.1$ . . . . . 103
- 4.16 The Numerical graphs for the maximum densities of strains for the 3D bet-hedging model and the fluctuating growth resources, with the strains death rates ( $k_i$ ) and the antibiotic drug ( $D$ ) treatment for  $\beta_0 = \beta_1 = \beta_2 = \beta$ , with both strains having the same initial values ( $s_0(0) = s_1(0) = s_2(0) = 0.2$ ), the same ranges of the strains death rates for each plots, the same amount of enzymes in the strains growth rates ( $r_0 = r_1 = r_2 = 0.5$ ), with the amplitude  $\delta = 0.25$ , and the frequency of the fluctuating resources  $\omega = 1$ , the antibiotic drug treatment  $D = 0.5$ , and different transition rate values  $\epsilon_1 = 0.05$ , and  $\epsilon_2 = 0.1$ . . . . . 104
- 4.17 The Numerical graphs for the dynamics of the 3D bet-hedging model with the strains death rates ( $k_i$ ), and the fluctuations within the antibiotic drug ( $D$ ) treatment for  $\beta_0 > \frac{1}{2}(\beta_1 + \beta_2)$ , with both strains having the same initial values ( $s_0(0) = s_1(0) = s_2(0) = 1$ ), with different ranges of time for the plots, different strains growth rates values ( $\beta_0 = 8, \beta_1 = 5, \beta_2 = 7$ ), with the amplitude  $\delta = 0.25$ , and the frequency of the fluctuation resources  $\omega = 1$ , the antibiotic drug treatment  $D = 0.5$ , with all other death rate ( $k_i$ ) values not specified in each plot equal to 1 (*i. e.*  $k_i = 1$ , as  $i = 0, 1, 2$ ), and different transition rates values  $\epsilon_1 = 1$ , and  $\epsilon_2 = 10$ . . . . . 106

- 4.18 The Numerical graphs for the maximum densities of strains for the 3D bet-hedging model, with the strains death rates ( $k_i$ ) and the fluctuations within the antibiotic drug ( $D$ ) treatment for  $\beta_0 > \frac{1}{2}(\beta_1 + \beta_2)$ , with both strains having the same initial values ( $s_0(0) = s_1(0) = s_2(0) = 0.2$ ), different ranges of the strains death rates ( $k_i$ ) for the plots, different values of the strains growth rates ( $\beta_0 = 8, \beta_1 = 5, \beta_2 = 7$ ), with the amplitude  $\delta = 0.25$ , and the frequency of fluctuating resources  $\omega = 1$ , the antibiotic drug treatment  $D = 0.5$ , and different transition rates values  $\epsilon_1 = 1$ , and  $\epsilon_2 = 10$ . . . . . 107
- 4.19 The Numerical graphs for the dynamics of the 3D bet-hedging model with the strains death rates ( $k_i$ ), and the fluctuations within the antibiotic drug ( $D$ ) treatment for  $\beta_0 < \frac{1}{2}(\beta_1 + \beta_2)$ , with both strains having the same initial values ( $s_0(0) = s_1(0) = s_2(0) = 1$ ), with different ranges of time for the plots, different strains growth rates values ( $\beta_0 = 3, \beta_1 = 5, \beta_2 = 7$ ), with the amplitude  $\delta = 0.25$ , and the frequency of fluctuation resources  $\omega = 1$ , the antibiotic drug treatment  $D = 0.5$ , with all other death rate ( $k_i$ ) values not specified in each plot equal to 1 (*i. e.*  $k_i = 1$ , as  $i = 0, 1, 2$ ), and different transition rates values  $\epsilon_1 = 1$ , and  $\epsilon_2 = 10$ . . . . . 108
- 4.20 The Numerical graphs for the maximum densities of strains for the 3D bet-hedging model, with the strains death rates ( $k_i$ ) and the fluctuations within the antibiotic drug ( $D$ ) treatment for  $\beta_0 < \frac{1}{2}(\beta_1 + \beta_2)$ , with both strains having the same initial values ( $s_0(0) = s_1(0) = s_2(0) = 0.2$ ), different ranges of the strains death rates ( $k_i$ ) for the plots, different values of the strains growth rates ( $\beta_0 = 3, \beta_1 = 5, \beta_2 = 7$ ), with the amplitude  $\delta = 0.25$ , and the frequency of fluctuating resources  $\omega = 1$ , the antibiotic drug treatment  $D = 0.5$ , with all other death rate ( $k_i$ ) values not specified in each plot equal to 1 (*i. e.*  $k_i = 1$ , as  $i = 0, 1, 2$ ), and different transition rates values  $\epsilon_1 = 1$ , and  $\epsilon_2 = 10$ . . . . . 109



- 4.21 The Numerical graphs for the dynamics of the 3D bet-hedging model with the strains death rates ( $k_i$ ), and the fluctuations within the antibiotic drug ( $D$ ) treatment for  $\beta_0 = \frac{1}{2}(\beta_1 + \beta_2)$ , with both strains having the same initial values ( $s_0(0) = s_1(0) = s_2(0) = 1$ ), different ranges of time for the plots, different strains growth rates values ( $\beta_0 = 6, \beta_1 = 5, \beta_2 = 7$ ), with the amplitude  $\delta = 0.25$ , and the frequency of fluctuating resources  $\omega = 1$ , the antibiotic drug treatment  $D = 0.5$ , with all other death rate ( $k_i$ ) values not specified in each plot equal to 1 (*i. e.*  $k_i = 1$ , as  $i = 0, 1, 2$ ), and different transition rates values  $\epsilon_1 = 1$ , and  $\epsilon_2 = 10$ . . . . . 110
- 4.22 The Numerical graphs for the maximum densities of strains for the 3D bet-hedging model, with the strains death rates ( $k_i$ ) and the fluctuations within the antibiotic drug ( $D$ ) treatment for  $\beta_0 = \frac{1}{2}(\beta_1 + \beta_2)$ , with both strains having the same initial values ( $s_0(0) = s_1(0) = s_2(0) = 0.2$ ), different range of strains death rates ( $k_i$ ) for the plots, different values of the strains growth rates ( $\beta_0 = 6, \beta_1 = 5, \beta_2 = 7$ ), with the amplitude  $\delta = 0.25$ , and the frequency of fluctuating resources  $\omega = 1$ , the antibiotic drug treatment  $D = 0.5$ , with all other death rate ( $k_i$ ) values not specified in each plot equal to 1 (*i. e.*  $k_i = 1$ , as  $i = 0, 1, 2$ ), and different transition rates values  $\epsilon_1 = 1$ , and  $\epsilon_2 = 10$ . . . . . 111
- 4.23 The Numerical graphs for the dynamics of the 3D bet-hedging model with the strains death rates ( $k_i$ ), and the fluctuations within the antibiotic drug ( $D$ ) treatment for  $\beta_0 = \beta_1 = \beta_2 = \beta$ , with both strains having the same initial values ( $s_0(0) = s_1(0) = s_2(0) = 1$ ), different ranges of time for the plots, the same strains growth rates values ( $\beta_0 = \beta_1 = \beta_2 = 5$ ), with the amplitude  $\delta = 0.25$ , and the frequency of fluctuations  $\omega = 1$ , the antibiotic drug treatment  $D = 0.5$ , with all other death rate ( $k_i$ ) values not specified in each plot equal to 1 (*i. e.*  $k_i = 1$ , as  $i = 0, 1, 2$ ), and different transition rates values  $\epsilon_1 = 0.05$ , and  $\epsilon_2 = 0.1$ . . . . . 112

- 4.24 The Numerical graphs for the maximum densities of strains for the 3D bet-hedging model, with the strains death rates ( $k_i$ ) and the fluctuations within the antibiotic drug ( $D$ ) treatment for  $\beta_0 = \beta_1 = \beta_2 = \beta$ , with both strains having the same initial values ( $s_0(0) = s_1(0) = s_2(0) = 0.2$ ), the same ranges of strains death rates ( $k_i$ ) for the plots, the same values of the strains growth rates ( $\beta_0 = \beta_1 = \beta_2 = 5$ ), with the amplitude  $\delta = 0.25$ , and the frequency of fluctuating resources  $\omega = 1$ , the antibiotic drug treatment  $D = 0.5$ , with all other death rate ( $k_i$ ) values not specified in each plot equal to 1 (*i. e.*  $k_i = 1$ , as  $i = 0, 1, 2$ ), and different transition rates values  $\epsilon_1 = 1$ , and  $\epsilon_2 = 10$ . . . . . 113
- 5.1 The Numerical graphs for the intrinsic dynamics of the 4D bet-hedging model with the dynamics of the antibiotic drug ( $D$ ) treatment, and the respective death rates ( $k_i$ ) of the strains, which has a constant growth rates value for the strain:  $\beta_0 = \beta_1 = \beta_2 = \beta = 1$ , with both the strains and the antibiotic drug ( $D$ ) treatment having the same initial values:  $s_0(0) = s_1(0) = s_2(0) = D(0) = 1$ , the rate of the antibiotic drug administration  $a = 1$ , the rate of the antibiotic drug decay  $c = 2$ , and different transition rate values:  $\epsilon_1 = 1$ , and  $\epsilon_2 = 10$ . . . . . 120
- 5.2 The Numerical graphs for the intrinsic dynamics of the 4D bet-hedging model with the dynamics of the antibiotic drug ( $D$ ) treatment for the non-fluctuating growth rate ( $\beta_i$ ) of the strains, and their respective death rates ( $k_i$ ), for  $\beta_0 > \frac{1}{2}(\beta_1 + \beta_2)$  and  $\epsilon_1 < \epsilon_2$ , with both strains having the same initial values:  $s_0(0) = s_1(0) = s_2(0) = 1$ , different initial values for the antibiotic drug ( $D$ ) treatment, different values for the growth rates of the strains:  $\beta_0 = 8$ ,  $\beta_1 = 5$  and  $\beta_2 = 7$ , different values for the strains death rate ( $k_i$ ), the rate of the antibiotic drug administration  $a = 1$ , and the rate of the antibiotic drug decay  $c = 2$ , with different transition rate values:  $\epsilon_1 = 1$ , and  $\epsilon_2 = 10$ . . . . . 124

- 5.3 The Numerical graphs for the intrinsic dynamics of the 4D bet-hedging model with the dynamics of the antibiotic drug ( $D$ ) treatment for the non-fluctuating growth rate ( $\beta_i$ ) of the strains, and their respective death rates ( $k_i$ ), for  $\beta_0 < \frac{1}{2}(\beta_1 + \beta_2)$  and  $\epsilon_1 < \epsilon_2$ , with both strains having the same initial values:  $s_0(0) = s_1(0) = s_2(0) = 1$ , different initial values for the antibiotic drug ( $D$ ) treatment, different values for the growth rates of the strains:  $\beta_0 = 3$ ,  $\beta_1 = 5$  and  $\beta_2 = 7$ , different values for the strains death rates ( $k_i$ ), the rate of drug administration  $a = 1$ , and the rate of the antibiotic drug decay  $c = 2$ , with different transition rate values:  $\epsilon_1 = 1$ , and  $\epsilon_2 = 10$ . . . 126
- 5.4 The Numerical graphs for the intrinsic dynamics of the 4D bet-hedging model with the dynamics of the antibiotic drug ( $D$ ) treatment for the non-fluctuating growth rate ( $\beta_i$ ) of the strains, and their respective death rates ( $k_i$ ), for  $\beta_0 = \frac{1}{2}(\beta_1 + \beta_2)$  and  $\epsilon_1 < \epsilon_2$ , with both strains having the same initial values:  $s_0(0) = s_1(0) = s_2(0) = 1$ , different initial values for the antibiotic drug ( $D$ ) treatment, different values for the growth rates of the strains:  $\beta_0 = 6$ ,  $\beta_1 = 5$  and  $\beta_2 = 7$ , different values for the strains death rates ( $k_i$ ), the rate of drug administration  $a = 1$ , and the rate of the antibiotic drug decay  $c = 2$ , with different transition rate values:  $\epsilon_1 = 1$ , and  $\epsilon_2 = 10$ . . . 127
- 5.5 The Numerical graphs for the intrinsic dynamics of the 4D bet-hedging model with the dynamics of the antibiotic drug ( $D$ ) treatment for the fluctuating growth rate ( $\beta_i$ ) of the strains and their respective death rates ( $k_i$ ), for  $\beta_0 > \frac{1}{2}(\beta_1 + \beta_2)$  and  $\epsilon_1 < \epsilon_2$ , with both strains having the same initial values:  $s_0(0) = s_1(0) = s_2(0) = 1$ , different initial values for the antibiotic drug ( $D$ ) treatment, different values for the growth rates of the strains:  $\beta_0 = 8$ ,  $\beta_1 = 5$  and  $\beta_2 = 7$ , different values for the strains death rates ( $k_i$ ), the rate of drug administration  $a = 1$ , and the rate of the antibiotic drug decay  $c = 2$ , with different transition rate values:  $\epsilon_1 = 1$ , and  $\epsilon_2 = 10$ . . . . . 129

- 5.6 The Numerical graphs for the intrinsic dynamics of the 4D bet-hedging model with the dynamics of the antibiotic drug ( $D$ ) treatment for the fluctuating growth rate ( $\beta_i$ ) of the strains and their respective death rates ( $k_i$ ), for  $\beta_0 < \frac{1}{2}(\beta_1 + \beta_2)$  and  $\epsilon_1 < \epsilon_2$ , with both strains having the same initial values:  $s_0(0) = s_1(0) = s_2(0) = 1$ , different initial values for the antibiotic drug ( $D$ ) treatment, different values for the growth rates of the strains:  $\beta_0 = 3$ ,  $\beta_1 = 5$  and  $\beta_2 = 7$ , different values for the strains death rates ( $k_i$ ), the rate of drug administration  $a = 1$ , and the rate of the antibiotic drug decay  $c = 2$ , with different transition rate values:  $\epsilon_1 = 1$ , and  $\epsilon_2 = 10$ . . . . . 130
- 5.7 The Numerical graphs for the intrinsic dynamics of the 4D bet-hedging model with the dynamics of the antibiotic drug ( $D$ ) treatment for the fluctuating growth rate ( $\beta_i$ ) of the strains and their respective death rates ( $k_i$ ), for  $\beta_0 = \frac{1}{2}(\beta_1 + \beta_2)$  and  $\epsilon_1 < \epsilon_2$ , with both strains having the same initial values:  $s_0(0) = s_1(0) = s_2(0) = 1$ , different initial values for the antibiotic drug ( $D$ ) treatment, different values for the growth rates of the strains:  $\beta_0 = 6$ ,  $\beta_1 = 5$  and  $\beta_2 = 7$ , different values for the strains death rates ( $k_i$ ), the rate of drug administration  $a = 1$ , and the rate of the antibiotic drug decay  $c = 2$ , with different transition rate values:  $\epsilon_1 = 1$ , and  $\epsilon_2 = 10$ . . . . . 131
- 5.8 The Numerical graphs for the intrinsic dynamics of the 4D bet-hedging model with the dynamics of the antibiotic drug ( $D$ ) treatment for the fluctuating antibiotic drug administration rate ( $a$ ), and the respective death rates ( $k_i$ ) of the strains, for  $\beta_0 > \frac{1}{2}(\beta_1 + \beta_2)$  and  $\epsilon_1 < \epsilon_2$ , with both strains having the same initial values:  $s_0(0) = s_1(0) = s_2(0) = 1$ , different initial values for the antibiotic drug ( $D$ ) treatment, different values for the growth rates of the strains:  $\beta_0 = 8$ ,  $\beta_1 = 5$  and  $\beta_2 = 7$ , different values for the strains death rates ( $k_i$ ), the rate of drug administration  $a = 1$ , and the rate of the antibiotic drug decay  $c = 2$ , with different transition rate values:  $\epsilon_1 = 1$ , and  $\epsilon_2 = 10$ . 133

- 5.9 The Numerical graphs for the intrinsic dynamics of the 4D bet-hedging model with the dynamics of the antibiotic drug ( $D$ ) treatment for the fluctuating antibiotic drug administration rate ( $a$ ), and the respective death rates ( $k_i$ ) of the strains, for  $\beta_0 < \frac{1}{2}(\beta_1 + \beta_2)$  and  $\epsilon_1 < \epsilon_2$ , with both strains having the same initial values:  $s_0(0) = s_1(0) = s_2(0) = 1$ , different initial values for the antibiotic drug ( $D$ ) treatment, different values for the growth rates of the strains:  $\beta_0 = 3$ ,  $\beta_1 = 5$  and  $\beta_2 = 7$ , different values for the strains death rates ( $k_i$ ), the rate of drug administration  $a = 1$ , and the rate of the antibiotic drug decay  $c = 2$ , with different transition rate values:  $\epsilon_1 = 1$ , and  $\epsilon_2 = 10$ .[134](#)
- 5.10 The Numerical graphs for the intrinsic dynamics of the 4D bet-hedging model with the dynamics of the antibiotic drug ( $D$ ) treatment for the fluctuating antibiotic drug administration rate ( $a$ ), and the respective death rates ( $k_i$ ) of the strains, for  $\beta_0 = \frac{1}{2}(\beta_1 + \beta_2)$  and  $\epsilon_1 < \epsilon_2$ , with both strains having the same initial values:  $s_0(0) = s_1(0) = s_2(0) = 1$ , different initial values for the antibiotic drug ( $D$ ) treatment, different values for the growth rates of the strains:  $\beta_0 = 6$ ,  $\beta_1 = 5$  and  $\beta_2 = 7$ , different values for the strains death rates ( $k_i$ ), the rate of drug administration  $a = 1$ , and the rate of the antibiotic drug decay  $c = 2$ , with different transition rate values:  $\epsilon_1 = 1$ , and  $\epsilon_2 = 10$ .[135](#)



# CHAPTER 1

## Introduction

---

### 1.1 Background of the Study

Bacterial resistance to anti-microbial treatment has become a major threat to public health, and is a worldwide problem for many decades in both hospital settings, within-host, and communal environments. With the advent of antibiotic drugs for the treatment of different infections caused by bacteria, scientists/pharmacologists hoped they had overcome this lingering problem, but bacteria started evolving and mutating to acquire resistance to those antibiotic drugs ([Austin et al., 1999](#); [Makrythanasis et al., 2014](#)).

The constant mutating of the bacteria from one form to another does render an efficient/effective antibiotic drug being used at a particular time ineffective, thereby necessitating the introduction of a new antibiotic drug to address the new infection caused by the bacteria, which in turn is time-consuming and costly.

Since the inception of antibiotic drugs for the treatment of infections caused by bacteria, medical personnel recognize the emergence of resistance to those antibiotic drugs by bacteria, with the most frustrating frequency of the resistance strain emerging within the last two (2) decades, causing great concern to public health. Because of this increasing evolution of bacterial resistance frequency to the antibiotic drugs, some have started pointing out the possibilities of having a post-antibiotic period, which may cause a serious death threat

as it was during the pre-antibiotic drug time ([Appelbaum, 2012](#); [Fair Richard and Yitzhak, 2014](#)).

In order to address the problem of this resistance to antibiotic drugs caused by the bacterial infections, several measures were put in place with the most efficient/effective method of keeping the patients in the hospital, to ensure strict compliance to the laid down rules and regulations of administering the antibiotic drugs treatment were adhered to, with the aim of curtailing the problem of antibiotic drugs abuse, which yield a significant result in addressing the antibiotic drugs resistance problem caused by the bacterial infections.

When the bacteria realized a significant measure of addressing the resistance problem is widely accepted, the bacteria was left with no option than to device another method or strategy in ensuring this resistance problem is not overcome, and suddenly it (bacteria) adopted a new strategy called Bet-hedging.

The term "Bet-hedging" is defined as the ability of an organisms or species to sacrifice some part of their physical fitness, with the hope of an increased gain when in a devastating or harmful situation. In other words, it simply means Insurance ([Ripa et al., 2010](#)). In the bet-hedging strategy, some fractional part of the bacteria will not take part in the bacterial reproduction by deactivating their metabolism, which causes them (bacteria) not to divide and can not be killed by the antibiotic drugs. When the antibiotic drug treatment is finished or removed, some resistant bacteria can "wake up" and continue growing to form some nucleus for their reappearances ([Balaban et al., 2004](#); [Müller et al., 2013](#)). For the purpose of explaining the biological context of bet-hedging strategy, we will discuss some experimental results that are relevant to it.

[Bigger et al. \(1944\)](#) explained how certain experiments were conducted and the result best described bet-hedging strategy in related to bacterial



(*Staphylococcal*) resistance to antibiotic treatment. A very important group of bacterial pathogens that require a serious clinical attention are the genus *Staphylococcus* with a serious threat to human life, which acquire (MRSA) Methicillin-resistant *Staphylococcus aureus*, also known as (super-bug). In the paper, the authors mentioned that penicillin was used to cure gonorrhoeal infection completely, but when used for the treatment of *Staphylococcal* infection, it could only cure some part of the bacteria, and no matter the concentration of penicillin used or how long the treatment is extended, it leaves some *cocci* of the bacteria (*Staphylococcus*) untreated. This causes serious arguments among scientists as to either penicillin is Bactericidal or Bacteriostatic antibiotic in the treatment of *Staphylococcal* infection. They (authors) further mentioned that, many scientists argued about the inability of penicillin to treat *Staphylococcal* infection completely, which they believed is caused either due to an insufficient supply of blood to the main focus of infection, or because of tissue barriers. They (authors) confirmed it in their experiment that 1 unit of penicillin per c.cm killed 99.96% of 250,000 *cocci* within 6 weeks, and when in extension up to 3 and 11 days, the remaining 0.04% of the *cocci* could not be eradicated, and they (bacteria) are termed those with the highest natural resistance to penicillin.

Based on the aforementioned resistance of bacteria to the antibiotic treatment by (Bigger et al., 1944), they (authors) believed the bacterial resistance to the antibiotic drugs fall on either of the following theories;

- The bacteria which possess highest natural resistance to the antibiotic drug treatment.
- The bacteria which acquired resistance to the antibiotic drugs when exposed to the treatment.
- The bacteria which have lower level of resistance to the antibiotic drug

treatment, but acquired it (resistance) when exposed to the environment where the antibiotic drug cannot act (Temporary Phase).

Constantly administering high concentration of the antibiotic drugs to the bacteria with no growing time, it make some of the bacteria to become used to those antibiotic drugs, and they (bacteria) acquire resistance to such antibiotic drugs. From the study of the above experiment, the authors described those bacteria who moved to temporary phase to hide, and wait for the antibiotic drugs to finish acting on the available bacteria are acting as bet-hedgers, and once the antibiotic drugs become ineffective, or whenever treatment is removed they (bacteria) start reproducing without any difficulty and later become dangerous to human life (Bigger et al., 1944).

There have been several investigations also in the causes of *Staphylococcus aureus* resistance to antibiotic drugs (Luria and Delbrück, 1943; Demerec, 1945a,b; Meads et al., 1945; North et al., 1945; Oakberg and Luria, 1947; Demerec, 1948; Hiramatsu, 2001; Wu et al., 2003; Gardete et al., 2006; Tuscherr et al., 2016; Kuok et al., 2017; Kebriaei et al., 2020) and others too numerous not mentioned here.

In 1943, (Luria and Delbrück, 1943) pointed out some of the ways in which *Staphylococcus* acquired resistance to streptomycin and penicillin in their experiment. The resistance was inspired through the interactions of the bacteria and the antibiotic drugs. It also arises through mutation of sensitive bacteria, which is contrary to the actions of the antibiotic drugs being a destructive agents to the sensitive bacteria.

The experimental realisation of the genesis/causes of *Staphylococcus aureus* resistance to streptomycin and penicillin by (Demerec, 1945b, 1948) discovered that, the resistance of the bacteria to those antibiotic drugs treatment is not only inspired by the presence of these two compounds, but also through the genetic evolution similar to the natural gene mutations. Before the adminis-

tration of the antibiotic drugs (streptomycin and penicillin) reaches a certain threshold concentration level, some of the bacteria persist with low administration of the antibiotic drugs concentration in both cases. But when the administration of the antibiotic drugs concentration were increased above the threshold level, there was a massive decrease in numbers among the existing bacteria, indicating the presence of both sensitive and resisting bacteria within the entire population of the bacteria.

A very important aspect that was observed during the conduct of the experiment was the individualistic resistance of the bacteria from one antibiotic drug to the other. Those strain with an escalating resistance to streptomycin were sensitive to penicillin and vice versa.

Because of the prevailing nature of resistance, Pharmacologists keeps changing the families of antibiotic drugs from one form to another with the aim of defeating resistance, and bacteria itself kept on metabolising from one form to another, as it is a too way battle, while human are trying to eliminate it (bacteria) by all means, it want to survive like any other living organisms.

The concept of bet-hedging has been discussed extensively in some disciplines apart from the mathematical discipline, which in some paragraphs below I picked some few to mention how the concept is been describe or explained in those disciplines.

Randomly switching of population cells from one phenotype to another can benefit from an environmental changes, but there is a tremendous challenge in identifying the exact link between environmental changes and switching rates. A simple model was developed which study a finite population of phenotype switching evolution caused by stochastic environmental shocks. Different switching rates successes among the competing genotypes were compared and examined in detailed how the most favourable switching rates due to environmental changes largely depend on its frequency ([Fudenberg and Imhof](#),

2012).

In the paper of (Friedman et al., 2014) they realized that multiplicity of phenotypes was typically linked to two different observations of bet-hedging and hysteresis in biological systems. Hysteresis is usually viewed as a system which normally continue to reflect on environmental previous condition, whereas bet-hedging does not necessarily associated it action with any memory, but increases the population growth when there is a phenotype changes due to environmental inputs. A simple model was used in a population growth which consider phenotype switching and lag-phase that occurred after phenotype switching, which show both memory and hysteresis are linked to bet-hedging when the species attempt to make the best use of their population growth rate. They (authors) further show that hysteresis switching strategy does not bestow any additional advantage in the population growth once the environment varies periodically in a deterministic situation which bet-hedging does.

Environmental fluctuation causes a serious problems to bacterial populations. It is evident that individual cells randomly change phenotype in rapidly changing environment for the pathogen population to survive, and bet-hedging generally adapt this random switching strategy. Traditional deterministic models can not describe the random switching of phenotype with relation to bet-hedging. A non-linear stochastic model of multi-stable bacterial system was introduced which clearly provides an insight understanding of multidimensional analysis from an experimental data. They (authors) also provide a quantitative technique of driven data from the multi-stable bacterial system without using any specific mathematical models (Jia et al., 2014).

Takahashi et al. (2015) pointed out the relevance of bet-hedging which was extensively discussed in a cell population heterogeneity of an environment, where zinc was used as a nutrient (medium) of cells growth. A stochastic model simulation was used to hypothesize that, to maintain population heterogeneity

is just like a bet-hedging response which normally allow the population of cells to exist in a varied and fluctuating environment.

Diauxic growth was related to bet-hedging in cells that are grown in a defined medium with two sugars (mainly; glucose and lactose) where there was a lengthy period of arrested growth, which is termed as "lag-phase". Stochastic simulation model was used to predict how the lag-phase will evolve subject to distribution of condition (Chu and Barnes, 2016).

The concept of population heterogeneity become widely present in almost all bio-processes including homogeneous environment, and can be well understood through bet-hedging process, which can be obtained from experimental studies by producing a computer model of dynamics in industrial scale bio-processes. The distinct parts of single cell studies in the processes was summarized (Heins and Weuster-Botz, 2018).

## 1.2 Statement of the Problem

Despite various research works by different authors and the different measures that were put in place by those concerned in order to curtail the increasing frequency of this resistant to antimicrobial treatments, bacterial resistant to antimicrobial treatment is increasingly growing at a very high frequency. Instead of seen the resistant to the antimicrobial treatment by the bacteria decreasing or even been eradicated completely as a results of keeping the patients in the hospitals with the sole aim of ensuring strict compliance in taken up the treatments administered by the doctors, bacteria developed a new strategy of resisting the antimicrobial treatment called bet-hedging. This necessitated a new research work to critically look in to the problems caused by the bacteria as a result of adopting the new strategy (bet-hedging), in order to know the parameters that are sensitive in causing the bacterial resistance to antimi-

crobial treatment, with the hope of coming up with the best feasible way of minimizing or even eradicating the resistance to the antimicrobial treatment by the bacteria.

### 1.3 Aims and Objectives of the Study

The aim of this research is to study the dynamics of the various models in order to observe the behaviors of the different strains, within the non-fluctuating and the fluctuating environments without/with the death rates of the strains, and also together with the antimicrobial treatment which is held at a constant (fixed) value and its dynamics as well, to find out which among the switching ( $s_1, s_2$ ) strain can perform better or worse in any of the environments with different conditions, or if possible which between the non-switching ( $s_0$ ) and the switching ( $s_1, s_2$ ) strains can be eliminated.

The objectives of the study include but not limited to:

- Finding the equilibrium points of the various models for the non-fluctuating environments with different conditions.
- Finding the eigenvalues of each model mentioned above by using the characteristic equation  $\left| J - \lambda I \right| = 0$
- Use the eigenvalues obtained from the characteristic equation above in order to determine the stability state of each model in question.
- Use the fluctuating resources to observe the behaviors of the different strains with different conditions.
- To observe if the presence of a particular strain(s) can cause an elimination of the other strain(s).
- To find out which among the switching ( $s_1, s_2$ ) strain perform better or worse at different environments with different conditions.

- To find out how the non-switching ( $s_0$ ) strain grow at a constant rate in any environment with different conditions.
- To observe the effects of the antimicrobial treatment in the behaviors of the strains administered at a constant (fixed) value, and also at its dynamics.

## 1.4 Literature Review

For over three and a half decades, several mathematical models were designed by different researchers, in order to address the problems caused by bacterial resistance to antimicrobial treatment (AMR) based on population dynamics in different settings, which causes a lot of harm, and even loss of lives to different communities.

Increases in the prevalence of infections due to antibiotic-resistant by the bacteria have often been traced back to the antibiotic use. [Garber \(1987\)](#) developed simple models of resistance development in order to clarify the effects of antibiotic exposure on bacterial antibiotic-resistance. The model assumes logistic growth, equal inhibition by resource limitation effects or crowding and a deterministic behavior. The growth of competing bacterial strains whose antibiotic sensitivities differ were described in the model. The effects of antibiotic exposure on the rate of growth of the isolated bacterial population, its resistance characteristics, the equilibrium population size and characteristics, as well as the approach to equilibrium were all elucidated in the models. The author emphasized that the models extend beyond the growth of bacterial population only. The models can be used to analyze populations of competing species such as insecticide-resistance and insecticide-susceptible agricultural pests, drug-resistant malarial parasites, or cancer cells whose resistance to chemotherapeutic drugs varies. Analysis were carried on multiple strains in

the presence of several antibiotics as well as on changes in the resistance of mixed bacterial populations. The results reveal that;

- Antibiotics decrease the equilibrium population size.
- Resistance to any other antibiotic or even to the same antibiotic might not increase due to application of one antibiotic.

The analysis further reveals that to reduce the population size below the minimum attainable under a single antibiotic combination, two sequences of antibiotic combinations will be optimal.

Castillo-Chavez and Feng (1997) observed that despite tuberculosis' sociological and historical importance, research on the transmission dynamics of the disease using statistical and mathematical models has not received enough attention. The authors developed one-strain and two-strain tuberculosis (TB) models. The one-strain model studied the effects of basic epidemiological factors such as the latent and infectious periods on the dynamics of tuberculosis on a homogeneously mixing population. The two-strain TB model studied the possible mechanisms that may allow for the survival and spread of naturally resistant strains of TB as well as the antibiotic-genetic resistant strains of TB. The basic reproductive numbers for both the one-strain and two-strain models were obtained (computed) and hence, conditions for stability or otherwise of the equilibrium states were proved. The authors determined the role that lack of drug treatment compliance by TB patients plays on the prevalence of antibiotic resistant strains. They first consider a special case of the two-strains model with two competing strains of TB which are the typical strain and a resistant strain that was not as the result of antibiotic resistance. The results show that non-antibiotic co-existence is possible but rare for the naturally resistant strains. They also consider a special case of a typical strain and a resistant strain that was as a result of the antibiotic resistance. In this case



they noticed that co-existence is almost certain.

At the end of the twentieth century, ([Austin and Anderson, 1999](#)) developed a mathematical model, which focuses on the emanation and escalation of bacterial resistance to antimicrobial treatment in communities, within patients, and in hospitals settings. The concepts of pharmacodynamics, and pharmacokinetics were initially combined to develop their model in patients already treated, in a structure that reflects the relationship between the antibiotic drug treatment, the population growth of the bacteria, and immunological responses aimed at the pathogen. The model also determined the area needing exact information, especially within the circumstances surrounding the rates of birth and death of the pathogens, being influenced by the antibiotic drug treatment (pharmacodynamics). They further addressed the issue of multiplied bacterial escalation to antibiotic drug treatment resistance in hospital settings. In order to provide the standard for control and elimination of the multiplied escalation, the model for the pathogens transmission dynamics was used to provide a basis for rating different intervention measures, applied in an intensive care settings for controlling the escalation of vancomycin-resistant enterococci.

[Bhunu \(2011\)](#) observed that despite the development of a number of effective treatments over the past half century, tuberculosis remain one of the most destructive bacterial infections in humans. Though various mathematical models on the spread of TB drug resistance have been considered by [Castillo-Chavez and Feng \(1997\)](#), [Blower and Gerberding \(1998\)](#), [Rodrigues et al. \(2007\)](#), [Gumel and Song \(2008\)](#), and [Zhou et al. \(2008\)](#). However, [Bhunu \(2011\)](#) noted that factors contributing to the emergence of multi-drug resistant TB, its spread and containment are not well defined. Improving on the works of the authors named above, [Bhunu \(2011\)](#) considered a three (3) strain TB model incorporating drug sensitive, multidrug-resistant (MDR-TB), ex-

tensively drug-resistant strains (XDR-TB), as well as the likely benefits of quarantining individuals detected to have extensively drug resistant (XDR-TB). The total human population  $N(t)$  were divided into 9 mutually exclusive compartment of: Susceptible  $S(t)$ ; Latently Infected  $E_i(t)$ ; Infectives  $I_i(t)$ ; the Recovered  $R(t)$  and the Quarantined  $Q(t)$ , for  $i = 1, 2, 3$  denote the drug-sensitive strain, multidrug-resistant strain and extensively drug-resistant strain of Mycobacterium Tuberculosis (Mtb) respectively.

Thus:

$$N(t) = S(t) + E_1(t) + E_2(t) + E_3(t) + I_1(t) + I_2(t) + I_3(t) + R(t) + Q(t)$$

Following [Van den Driessche and Watmough \(2002\)](#), the reproduction numbers  $R_i (i = 1, 2, 3)$  of the model were obtained and used to establish the local asymptotical stability of the disease-free equilibrium of the model. Four (4) different cases of possible scenarios for the model endemic equilibrium were analysed with respect to the reproduction numbers. The following three (3) findings were concluded by the author:

- Treatment of drug sensitive Mycobacterium Tuberculosis (Mtb) strains will help reduce the spread of drug sensitive TB, and if not properly used results in the increase of multi-drug resistant (MDR-TB) cases.
- Treatment of multi-drug-resistant strain (MDR-TB) will help reduce the spread of the MDR-TB, and if not properly used results in an increase of extensively drug-resistant (XDR-TB) strain cases.
- Quarantining of extensively drug-resistant (XDR-TB) strain has a positive impact in the control of the XDR-TB, as it reduces the rate at which individuals having that form of TB interact with other non-infected people in the community.

Presented in the work of ([Cooper and Julius, 2011](#)) is a hybrid system model for the dynamics of the populations of normal and persister bacterial cells in

favorable growth conditions under antibiotic attacks. The model captures a long-term persistent health problem that is common for some infections, such as tuberculosis. The model posed the problem of designing an optimal infection treatment strategy so as to minimize the number of persister cells that go into long-term dormancy. After which, the model characterized the optimal treatment strategy, which turns out to be non-unique and it can be expressed as a feedback law using the information about the population sizes of normal and persister cells. The theoretical lower bound on the number of persister cells that transition into long-term dormancy under the optimal treatment scheduling was then computed.

Due to the increasing bacterial resistance to antibiotics in hospital settings, a new movement to re-examine the need for the development of new antibiotics was carried out by [Joyner et al. \(2012\)](#). The authors discussed four different mathematical models. To begin with they modified ([Chow et al., 2011](#)) model to have the Base and the Isolation models that described the spread of both single and dual resistant in a hospital setting with no drug available to aid in treating patients colonized with dual resistant bacterial strain. In addition, the Random Drug and the Targeted Drug models were also developed to introduce a new drug into hospital settings. The Random Drug model was used to treat all patients with the new drug, while the Targeted Drug model was used to treat those patients with identified dual resistant bacteria. In their model emphasis was given to the introduction of an entirely new antibiotics, and not simply an upgrade of an existing antibiotics within the same class. This was so, as the use of upgrade antibiotics on patients already colonized with bacterial resistant to the older antibiotics could lead to a new high-level resistant strain. The complete equilibrium analyses on the Random Drug model were carried out. At first, they used the next generation approach to establish the local stability of the resistant-free equilibrium for the Random Drug model. In

addition, sensitivity analysis was carried out in order to determine the effects of introducing a new drug in combating resistance within a hospital setting. The researchers find out that introducing a new drug into the hospital resulted in a significant reduction of the average patients carrying dual resistant bacteria, a reduction from approximately 65 – 72% of the hospital down to between 28 – 36% of the hospital. The authors also find out from their sensitivity analysis that introduction of a new antibiotic aids in the fight against the spread of antibiotic resistance in a hospital setting, however decreasing the rate of transmission, the per capita treatment rate of drugs, the overall per capita treatment rate and increasing the turnover rate in the hospital, and the portion of patients identified with dual resistant bacteria and treated will result in the greatest decrease in the overall resistance.

In an attempt to predict the effects of pollution on the persistence of resistant bacteria in a river, (Mostefaoui, 2014) studied the qualitative properties of the model of (Lawrence et al., 2010). The model considered both river and land bacteria, and each is subdivided into resistant and non-resistant, thus we have: River non-resistant bacteria, River resistant bacteria, Land non-resistant bacteria, and Land resistant bacteria. So that at any arbitrary equilibrium we have  $E_* = (R_s, R_I, L_S, L_I)$ . Mostefaoui (2014) established the non-negativity and boundedness of the model solutions, and obtained three equilibria of the model:  $E_0(0, 0, 0, 0)$ ,  $E_1(K, 0, 0, 0)$  and  $E_2(\frac{\beta}{\alpha}, K - \frac{\beta}{\alpha}, 0, 0)$ , where  $K$  is the carrying capacity of the river,  $\alpha$  is the transmission rate of the antibiotic resistance gene, and  $\beta$  is the loss rate of the antibiotic resistance gene. As bacteria are always present, the analysis of  $E_0$  is not of any important. For the extinction of the resistant bacteria in both river and land, using the Jacobian stability technique the author established that  $E_1$  is locally asymptotically stable, if and only if  $\alpha K < \beta$ . Using an appropriate Lyapunov function,  $E_1$  was proven to be globally asymptotically stable, if  $\alpha K + r < \beta$ . Where  $r$  is

the birth-death rate due to  $K$ . Furthermore, the author established that the global stability of  $E_2$  holds if  $\alpha K > \beta + \alpha$ . Thus, if there is a large enough loss rate of gene of resistance between bacteria then there will be a reduction of resistance against antibiotic in the river. And on the other hand, a large enough transmission gene of resistance between bacteria when the river is not diluted will result in persistence of the resistant bacteria in the river. And finally, (Mostefaoui, 2014) find out that the pollutants are not eliminated by the stream of the water if the pollutant enter the river periodically from the shore as the system has at least one positive periodic solution.

Discovery of antibiotics and their widespread introduction did not bring an end to the war against infectious diseases as expected. The overuse of antibiotic drugs has resulted in the prevalence of antibiotic resistant bacteria and thus, an unfolding catastrophe has resulted due to antimicrobial resistance (Godlee, 2013). As the long-term competitive ending between susceptible strains and resistant strains of bacteria within the host under different concentrations of antibiotic remains unknown, (Huang and Fan, 2014) proposed a competitive population dynamical model in order to explore the competitive interactions between the susceptible strain and the resistant strain with antibiotic exposure. The authors focused on the relationship between antibiotics resistance and the concentration of antibiotics. The model has two variables, namely: the number of susceptible and the number of resistant strains at time  $t$ , denoted by  $x(t)$  and  $y(t)$  respectively. Both qualitative and quantitative analysis were carried out, and by following the concept of Dulac criterion (McCluskey and Muldowney, 1998; Osuna and Villaseñor, 2011), the results indicated that the resistant strain will ultimately survive along with the long-term high strength antibiotic treatment and prevention. This agrees with the literature on many recurrent and chronic diseases (Lewis, 2007; LaFleur et al., 2010; Allison et al., 2011). Thus, the authors emphasized on the needs to be more evidence based,

and more efficiently targeted in the prescription of antibiotic drugs so as to impede or slow resistance to antibiotics.

Reported in the work of ([Ibargüen-Mondragón et al., 2014](#)) is a mathematical modeling on bacterial resistance to multiple antibiotics caused by spontaneous mutations. The model described population dynamics of bacteria exposed to multiple antibiotics simultaneously on the assumption that the acquisition of resistance is through mutations due to antibiotics exposure. The results of the model qualitative analysis show the existences of a bacteria free equilibrium state, a resistant bacteria equilibrium state, and an endemic bacteria equilibrium state as well, and in the later there are co-existence of all the bacteria. The results of the model suggest that if bacteria can infect but do not produce sufficient progeny then they can be removed. Also when resistant bacteria persist, the model predicts two possible scenarios: sensitive bacteria are eliminated totally by antibiotics or had acquired resistance, or the bactericidal action is not enough to eliminate them, and therefore both types of bacteria coexist. Furthermore, the results also suggest that it would be more appropriate to use treatments combining bactericidal and bacteriostatic drugs, thus the bactericidal antibiotics would eliminate sensitive bacteria and bacteriostatic antibiotics would control bacterial reproduction. The sensitivity analysis of the model established that bacterial reproduction and antibiotics uptake, are the most significant factors on the population dynamics of bacteria followed by antibiotics treatment action.

The economic and social impacts of Methicillin-resistant *Staphylococcus aureus* (MRSA) can not be over-emphasized. It causes substantial morbidity and mortality globally and it is endemic in hospital and nursing homes ([Agusto et al., 2015](#)). Both health-care associated MRSA (HA-MRSA) and community-associated MRSA (CA-MRSA) models have been studied by many authors in order to quantify the possible effect of the disease burden. [Agusto \(2016\)](#)

improved on the existing mathematical models of CA-MRSA and HA-MRSA in hospital settings by incorporating health-care workers interactions with patients and contamination of the environment, the isolation of infected patients, time dependent optimal control strategies associated with the decolonization of healthcare workers, as well as environmental contamination rates. Thus, he addressed some problems such as: knowing the parameter that has the greatest impact on MRSA transmission in a hospital setting; the optimal control strategy required to reduce disease transmission, as well as the implication of increased control cost combination. The authors model contains 9 mutually exclusive compartments. The qualitative analyses of the model equations were carried out beginning with the positivity and boundedness of the solutions, and then the condition for local stability of the disease-free equilibrium using the next generation approach was established. In order to assess the impacts of uncertainty as well as the sensitivity on the outcomes of the numerical simulation of the model, the author carried out global sensitivity analysis using Latin hypercube sampling (LHS) and partial rank correlation coefficients (PRCCs). The numerical simulations revealed that applying time-dependent controls on the decontamination rate for health-care workers, and on the environment contamination rate reduces MRSA in both patients and health-care workers.

[Daşbaşı and Öztürk \(2016\)](#) formulated a mathematical model of bacterial resistance to immune system response and multiple antibiotics simultaneously. The qualitative analysis found out infection-free equilibrium point, and other equilibrium points where resistant bacteria and immune system cells exist, only resistant bacteria exists, and the point where the sensitive bacteria, resistant bacteria and immune system cells exist. The model also highlights the fact that when an individual's immune system weakens, he/she suffers more from the bacterial infections which are believed to have been confined or terminated. To evaluate the effectiveness of antibiotic treatments with respect

to specific changes in bacterial DNA sequence as the only mechanism of bacterial resistance acquisition, the model suggests that if sensitive bacteria can infect but do not produce sufficient progeny, they can be removed and resistant bacteria continue to survive in balance with the immune cells in the host.

Beams et al. (2016) developed a mathematical model using ordinary differential equations in which hosts can have dual-stain infections with different strains, but cannot be doubly infected by the same strain. They considered hosts mixing homogeneously and transmission occurs freely according to mass action. The total population is divided into uninfected susceptible individuals; infected individuals with antibiotic-vulnerable strain and who are susceptible to infection by the antibiotic resistance type; individuals infected with the antibiotic-resistant strain and who are susceptible to infection by the antibiotic vulnerable type; and the individuals who are infected by both types (dual-strain infections). Using the next-generation matrix approach their analysis reveals how the competition within hosts and the costs of resistance determine whether vulnerable and resistance strains persist, coexist, or drive each other to extinction. They found out that if vulnerable strains competitively suppress resistant strains inside dually infected host, using strong antibiotics could competitively release a resistance strain and allow it to invade and establish itself. Their analysis also reveals that screening patients to determine whether they are dually infected may limit the potential of resistance to spread provided the antibiotic effect is not too powerful, otherwise, treating dual infections or not becomes irrelevant and resistance proliferates.

Zilonora and Bratus (2016) extended on the work of De Leenbeer and Cogan (2009) by formulating a mathematical model for optimal strategies in antibiotic treatment of microbial populations. Two microbial populations of susceptible and persister cells were described in their model. The theory of optimal control of Pontryagin's maximum principle was used to find the best



treatment strategies. Three different methods were used to solve the model numerically, which yielded good allowable controls. They found out that the most effective treatment option is gradually reducing the initial dose of an antibiotic during the treatment process (upon condition that initial dose exceeds a certain value), and the periodic treatment with constant antibiotic does not provide any positive result.

Merden et al. (2017) observed that many of the numerical values of the parameters used in modelling studies, especially for newly emerging diseases are determined from the statistical investigation of the limited number of data available on the event and thus, neglected the uncertainty of the parameters in deterministic models. In order to model the uncertainty in the equation system, they implement random components into the deterministic equation system and analyzes the statistical properties of the results. Their work extends previous works by developing a deterministic model of immune system and bacterial resistance with antibiotic therapy to form random and stochastic models of the event. The random analysis for the dynamics of their model shows that even under small random effects, some of the components produce very unlikely results. Their analysis also revealed that the non-negligible deviation and volatility in the random and stochastic models shows the incapability of the deterministic analysis of bacterial resistance of modelling the real-life randomness of the event.

As a continuation of previous works given in [15-20], Esteva and Ibargüen-Mondragon (2018) introduce the concentrations of bactericidal and bacteriostatic drugs as a dynamical variable. They studied the interaction between Mtb resistant to antibiotics, macrophages and T cells within the granuloma formation, considering bacterial resistance to multiple bactericidal and bacteriostatic antibiotics simultaneously. Both qualitative and quantitative analysis were carried out by the authors. The results of their model reveal that in the

presence of TB, control measures should be focus on the reduction of fitness cost and elimination of resistant bacteria by improving the immune system and with appropriate multi-drugs treatment.

[Ibargüen-Mondragón et al. \(2019\)](#) formulated and analysed a deterministic model for the population dynamics of susceptible and resistant bacteria to antibiotics, they assumed that drug resistance is acquired through mutations and plasmid transmission. The qualitative analysis revealed the following: the existence of a bacteria-free equilibrium, a resistant bacteria equilibrium, a coexistence equilibrium and a limit cycle arising from Hopf bifurcation. The stability of the equilibria were given in terms of the growth rate of bacteria, the acquisition of resistance, as well as the elimination of bacteria due to the immune system and the action of antibiotics. The numerical simulations corroborated their analytical results, which illustrated the temporal dynamics of the susceptible and resistant bacteria.

[Das et al. \(2020\)](#) have developed and analysed a delayed model of hospital acquired infection of multidrug-resistant bacteria *Acinetobacter baumannii* (MRAB) using three separate patient states, two healthcare worker states and environmental bacterial load. The study has enabled the researchers to assess the effect of delay in diagnostic process as well as decontamination process on prevalence of MRAB infection. The bacteria was characterized by longevity in hospital environment, and the effect of delay in decontamination was then investigated in detail. Another delay was considered in diagnostic procedure for treatment of multidrug-resistant bacteria. The researchers observed that, the increment in delay values initiate periodic dynamics of endemic state, which was demonstrated both analytically and numerically. An optimal control technique was used to estimate the effectiveness of various controls in reducing infection, while minimizing the associated cost. The sensitivity analysis carried out indicated that antibiotic stewardship program has stronger impact

on delayed antibiotic-resistant infection dynamics, compared to hand hygiene compliance of healthcare workers.

Presented in the work of (Piommas and Farida, 2021) is a mathematical model that takes into account bacterial conjugation and drug effects, to investigate the presence of sensitive and resistant bacteria in a human host. The researchers considered two types of drugs: antibiotic  $M$  that kills only sensitive bacteria and antibiotic  $N$  that kills both bacteria. Their results highlighted that, larger doses and longer dosing interval of antibiotic  $M$  might result in the higher prevalence of resistant bacteria, while they do the opposite for the antibiotic  $N$ . When delays in administering initial and second doses were incorporated, they found that the delays might lead to the higher prevalence of resistant bacteria when antibiotic  $M$  or  $N$  is administered, with the longer time of bacteria remaining at the lower prevalence of the latter. They also found that, switching antibiotic agents during a treatment course with different bacterial strain characteristics, result in a significant impact on the prevalence of resistant bacteria, and that treatment was more effective for bacteria with the higher probability of losing a plasmid, and the higher conjugation rate. They concluded that their results are in agreement with some preceding studies, that highlighted the importance of interval between treatments to plasmid-borne antibiotic resistance, and that their study would help gain a better understanding into the population dynamics of sensitive and resistant bacteria under a therapeutic treatment, and the effects involving bacterial mechanisms such as drug regimens, drug efficacy, delays in administrations, antibiotic switching, and characteristics of the bacterial strains.

Considering the studies of the aforementioned authors and others too numerous to mention, we developed a mathematical model which investigates the work of (Müller et al., 2013), focusing on the population dynamics of bet-hedging and constant strains under different scenarios using the deterministic

model approach, instead of the adaptive dynamics approach used by the authors. The new model incorporates the death rates of the various strains with the antibiotic drug treatment which is held constant (fixed value), and later includes the dynamics of the antibiotic drug treatment with its administration rate, and the rate at which the antibiotic drug decays (degradation rate). The various death rates of the strains and the antibiotic drug treatment used, are very important elements towards reducing or eradicating the densities of the bacterial strains in all situations.

## CHAPTER 2

# A Model for the Dynamics of the Bet-hedging Bacteria in the Absence of a Constant Strain

---

### 2.1 Introduction

Bacterial pathogens are a major source of human and animal diseases worldwide. A particular challenge is caused by bacterial resistance to anti-microbial treatment. In this context, we will look at some particular forms of bacterial resistance to anti-microbial treatment (AMR) by a bet-hedging strategy.

A bet-hedging strategy is the ability of organisms or species to sacrifice some part of their physical fitness, with the hope of an increased gain when in a devastating or harmful situation. In other words, it simply means Insurance ([Ripa et al., 2010](#)).

One of the particular form of bacterial resistance to anti-microbial treatment, that require a serious clinical attention are the genus *Staphylococcus* with a serious threat to human life, which acquire Methicillin-resistant *staphylococcus aureus* (MRSA), also known as (super-bug). Penicillin was used to cure gonorrhoea completely, but when used for the treatment of *Staphylococcal* infection, it could only eradicate some parts of the bacterial symptoms, and no matter the amount of the penicillin concentration used, or how long the treatment is extended, it leaves some *cocci* of the bacteria untreated [Bigger et al. \(1944\)](#).

*Bacillus Mycobacterium* is another example of bacteria with a strong resistance to anti-microbial treatment, which causes an infectious disease called "Tuberculosis", generally known as TB. Pulmonary TB typically affects the lungs, and sometimes can affect other parts of the body. Rifampicin became the earliest effective drug for the treatment of TB in 1960s, but adversely didn't eradicate it completely, and because of TB resistance to Rifampicin, there was the need for multidrug treatment to the bacteria. Currently, the bacteria are being treated with a combination of a quadruple antibiotic drugs,

for a minimum period of 6-months, and in some cases up to a year and half ( $1\frac{1}{2}$  year), but still only about 85% success of the bacterial infection treatment was recorded (Stewart et al., 2003).

Mathematical modelling has been used by different researchers to investigate the concept of anti-microbial resistant (AMR) treatment. Balaban et al. (2004) developed a mathematical model which focused on the growth rates of the normal and resistant cells and the transition rates between them. The model usually address many problems that discussed bacterial growth and AMR. Ibargüen-Mondragón et al. (2014) also developed a mathematical model that looked at the population dynamics of bacteria which is introduced to simultaneous multiple antibiotics, with the expectations that resistance is acquired through mutations when exposed to antibiotics.

Müller et al. (2013) used an adaptive dynamics model technique, to explore the evolution of bet-hedging within a population that experiences a stochastic changing environment. To learn more about the adaptive dynamics approach refer to (Geritz et al., 1998). The aim of that biological paper, was to deepen the understanding of the outcomes obtained in their research as at then to the present situation, and also to extend the understanding of its scope for the legitimacy of the outcomes obtained. In the outcomes of their research, three different forms of evolutionary stable strategies (ESS's) were found, depending on the frequencyicity at which the environment switches. A monomorphic phenotype familiarized to the instant environment, caused by a gradually switching environment, a bimorphic bet-hedging phenotype, caused by a central point of a dimension, and a monomorphic phenotype which is also familiarized to the average environment. From the findings of their research, the last two outcomes were based on the study of Lyapunov exponents for stochastically changing environment, while the earlier outcome was only attained by means of examining (heuristic) arguments and simulations. The research in that article looked at the evolution aspect of the mathematical model.

In this chapter 2, we will look at the model dynamics of the switching ( $s_1, s_2$ ) strains, from the paper of Müller et al. (2013) mentioned above for the bet-hedging strains in isolation, which will form a basis for the later full models in the next chapter. In their paper, the authors didn't obtain the basic stability analysis of the full model, which we explicitly obtained in this research work.

## 2.2 The Model of the Bet-hedging Bacteria

The model equations for the bet-hedging strain which can ‘switch’ their phenotype to specialize in each environment, by performing better or worse in any environment Müller et al. (2013), based on the bacterial growth rates ( $\beta_i$ ), the amount or concentration of enzymes ( $r_i$ ) for the bacteria, their interactions with the environment ( $\alpha_i$ ), and the transition rates ( $\epsilon_i$ ) between each other is given by;

$$\begin{aligned} s_1' &= s_1 [\beta_1 (r_1, \alpha_1) - \epsilon_1 - S] + \epsilon_2 s_2 \\ s_2' &= s_2 [\beta_2 (r_2, \alpha_2) - \epsilon_2 - S] + \epsilon_1 s_1 \end{aligned} \quad (2.1)$$

where;  $S = s_1 + s_2$

$\beta_1$  and  $\beta_2$  are the growth rates of the bacteria that depends on the respective number or concentration of enzymes concentrations  $r_1$  and  $r_2$  the bacteria needed, to utilize the nutrient contents in the respective environmental states  $\alpha_1$  and  $\alpha_2$ .  $\epsilon_1$  and  $\epsilon_2$  are the transition rates from one type to the opposite one, where as ( $s_1, s_2$ ) are the switching strains which can perform better or worse in any environment.

The bacterial rate of growth ( $\beta_i$ ) is defined as;

$$\beta_i (r_i, \alpha_i) = 1 + r_i e^{\frac{-r_i}{\alpha_i}} \quad (2.2)$$

with all parameters defined as above.

Considering the bacterial rate of growth in the environments, we sometimes considered the number or the amount of enzymes concentration ( $r_i$ ) to be the same values (equal), or different values (not equal) at some conditions, and also that of the environment ( $\alpha_i$ ) to be either the same, or different too. This means, the growth of each population depends on the parameters  $r_i$  and  $\alpha_i$ . We later assumed the environments ( $\alpha_i$ ) to fluctuate as well.

For a given environment ( $\alpha_i$ ), the growth rate ( $\beta_i$ ) will attain a maximum value, when  $r_i = \alpha_i$ . That is;

$$\frac{\partial \beta_i}{\partial r_i} = \left(1 - \frac{r_i}{\alpha_i}\right) e^{\frac{-r_i}{\alpha_i}} = 0 \quad (2.3)$$

Stability analysis were performed on the model equations by considering different conditions, to check the behavior of the strains, by finding the equilibrium points of the system, stability of the model, and the eigenvalues of the system from the characteristic equation below;

$$|J - \lambda I| = 0 \quad (2.4)$$

where;  $J$  is the Jacobian matrix of the system,  $I$  as the identity matrix, and  $\lambda$  are the eigenvalues of the system, which helped to find the state of the equilibrium points of the system as either stable, unstable or a saddle point (Murray, 2002) and references therein.

## 2.3 Constant Growth Rates ( $\beta_i$ ) Value of the Bacteria

The research began by investigating the system of equation (2.1) when  $r_1 = r_2 = 0$ , meaning the growth rates of the bacteria has a constant value (*i. e.*  $\beta_1 = \beta_2 = \beta = 1$ ).

By solving the above equation (2.1) with the stated condition, the system produced two equilibrium points, which are the zero and the non-zero points as:

$$\begin{aligned} (s_1^*, s_2^*) &= (0, 0) \\ (s_1^*, s_2^*) &= \left( \frac{\beta\epsilon_2}{\epsilon_T}, \frac{\beta\epsilon_1}{\epsilon_T} \right) \end{aligned} \quad (2.5)$$

With the stated condition at the beginning of this section 2.3, we obtained the Jacobian matrix of the model from equation (2.1) above as;

$$J = \begin{pmatrix} \beta - \epsilon_1 - 2s_1^* - s_2^* & -s_1^* + \epsilon_2 \\ -s_2^* + \epsilon_1 & \beta - \epsilon_2 - s_1^* - 2s_2^* \end{pmatrix} \quad (2.6)$$

After substituting the zero equilibrium point  $(s_1^*, s_2^*) = (0, 0)$  obtained from equation (2.5) in equation (2.6), the Jacobian matrix now becomes;

$$J = \begin{pmatrix} \beta - \epsilon_1 & \epsilon_2 \\ \epsilon_1 & \beta - \epsilon_2 \end{pmatrix} \quad (2.7)$$

To find the eigenvalues, an identity matrix, together with the Jacobian matrix obtained in equation (2.7) were substituted in the characteristic equation (2.4) above, which resulted to;

$$\begin{vmatrix} \beta - \epsilon_1 - \lambda & \epsilon_2 \\ \epsilon_1 & \beta - \epsilon_2 - \lambda \end{vmatrix} = 0 \quad (2.8)$$



After evaluating the above expression in equation (2.8) by hand, the two eigenvalues were obtained as;

$$\begin{aligned}\lambda_1 &= \beta \\ \lambda_2 &= \beta - \epsilon_T\end{aligned}\tag{2.9}$$

where;  $\epsilon_T = \epsilon_1 + \epsilon_2$

By carefully looking at the above equation (2.9), one of the eigenvalues is positive (*i. e.*  $\lambda_1 > 0$ ), and it implies the point being locally and asymptotically unstable, which means the bacteria will not settle at the (0, 0) equilibrium point.

After the investigation and found the zero equilibrium point to be unstable, we continued the research by substituting the non-zero equilibrium point  $(s_1^*, s_2^*) = \left(\frac{\beta\epsilon_2}{\epsilon_T}, \frac{\beta\epsilon_1}{\epsilon_T}\right)$  from equation (2.5), in the Jacobian matrix obtained in equation (2.6) above, which gives the new Jacobian matrix as;

$$J = \begin{pmatrix} \beta - \epsilon_1 - 2\frac{\beta\epsilon_2}{\epsilon_T} - \frac{\beta\epsilon_1}{\epsilon_T} & -\frac{\beta\epsilon_2}{\epsilon_T} + \epsilon_2 \\ -\frac{\beta\epsilon_1}{\epsilon_T} + \epsilon_1 & \beta - \epsilon_2 - \frac{\beta\epsilon_2}{\epsilon_T} - 2\frac{\beta\epsilon_1}{\epsilon_T} \end{pmatrix}\tag{2.10}$$

The Jacobian matrix in equation (2.10), together with it corresponding identity matrix were again substituted in the characteristic equation (2.4) above, and the result from that expression produced;

$$\begin{vmatrix} \beta - \epsilon_1 - 2\frac{\beta\epsilon_2}{\epsilon_T} - \frac{\beta\epsilon_1}{\epsilon_T} - \lambda & -\frac{\beta\epsilon_2}{\epsilon_T} + \epsilon_2 \\ -\frac{\beta\epsilon_1}{\epsilon_T} + \epsilon_1 & \beta - \epsilon_2 - \frac{\beta\epsilon_2}{\epsilon_T} - 2\frac{\beta\epsilon_1}{\epsilon_T} - \lambda \end{vmatrix} = 0\tag{2.11}$$

After evaluating the above expression obtained in equation (2.11) by hand, the two eigenvalues were found as;

$$\begin{aligned}\lambda_1 &= -\beta \\ \lambda_2 &= -\epsilon_T\end{aligned}\tag{2.12}$$

where;  $\epsilon_T = \epsilon_1 + \epsilon_2$

Based on the results obtained in equation (2.12) above, it confirmed the two eigenvalues to be negative (*i. e.*  $\lambda_i < 0$ ), as ( $i = 1, 2$ ), which means the system is locally and asymptotically stable at the non-zero equilibrium point.

Since the parameter values used are  $r_1 = r_2 = 0$ , it means the equilibrium point  $(s_1^*, s_2^*) = (0, 0)$  is never stable, and the strain (bacteria) will always reach an equilibrium point where  $S^* = s_1^* + s_2^* = \beta = 1$ , as shown in Figure 2.1 below.

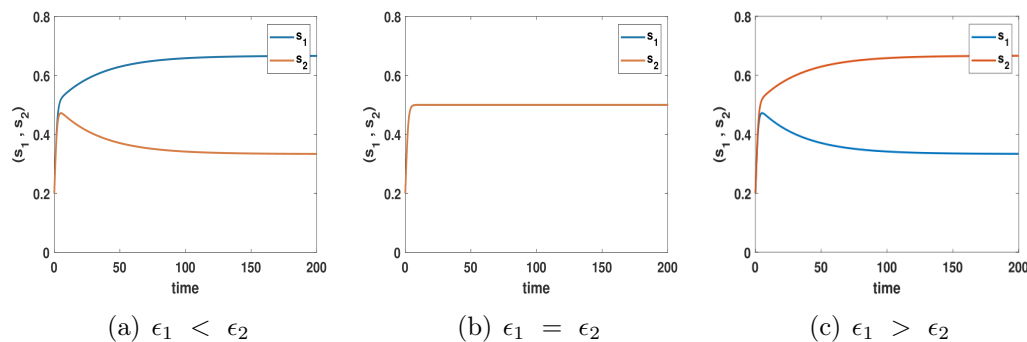


Figure 2.1: The Numerical graphs for the intrinsic dynamics of the 2D bet-hedging model, with a constant growth rates of the bacterial strain:  $\beta_1 = \beta_2 = \beta$ , both strains having the same initial values:  $s_1(0) = s_2(0) = 0.2$ , with different amount of nutrients contents in the environments to be utilized by the bacterial strain:  $\alpha_1 = 5$  and  $\alpha_2 = 1$ , the same range of time for each of the plots  $t = 0 : 0.001 : 200$ , with the transition rates values of:  $\epsilon_1 = 0.01$ ,  $\epsilon_2 = 0.02$ , and the whole plots show the two strains in each case become stable at  $s_1 + s_2 = \beta = 1$ .

## 2.4 Different Growth Rate ( $\beta_i$ ) Values of the Bacteria

Having considered the situation when the strains have a constant growth rate value ( $\beta_1 = \beta_2 = \beta = 1$ ), it is important to look at what happen when the strains have different growth rate values ( $\beta_1 \neq \beta_2$ ).

In this situation we are to consider two cases, either the strains has the same/equal ( $r_1 = r_2 \neq 0$ ), or different/unequal ( $r_1 \neq r_2$ ) number/amount of enzymes, and in either case, the growth rates of the bacteria are different to each other (*i. e.*  $\beta_1 \neq \beta_2$ ), because of the differences in the environmental nutrient contents ( $\alpha_1 \neq \alpha_2$ ).

The model equation based on the above mentioned condition is now defined as;

$$\begin{aligned} s_1' &= s_1 [\beta_1 (r_1, \alpha_1) - \epsilon_1 - S] + \epsilon_2 s_2 \\ s_2' &= s_2 [\beta_2 (r_2, \alpha_2) - \epsilon_2 - S] + \epsilon_1 s_1 \end{aligned} \quad (2.13)$$

where;  $S = s_1 + s_2$ , with all other parameters, and the bacterial growth rate defined as in equations (2.1), and (2.2) respectively.

Solving the above equation (2.13), the system produced two equilibrium points, a zero and non-zero points as;

$$\begin{aligned}
(s_1^*, s_2^*) &= (0, 0) \\
(s_1^*, s_2^*) &= (S - \beta_2)(\beta_1 - \epsilon_1 - \epsilon_2 - S) + (\beta_1 - \beta_2)\epsilon_2
\end{aligned} \tag{2.14}$$

The Jacobian matrix of the system from equation (2.13) above was found as;

$$J = \begin{pmatrix} \beta_1 - \epsilon_1 - 2s_1^* - s_2^* & -s_1^* + \epsilon_2 \\ -s_2^* + \epsilon_1 & \beta_2 - \epsilon_2 - s_1^* - 2s_2^* \end{pmatrix} \tag{2.15}$$

When the zero equilibrium point  $(s_1^*, s_2^*) = (0, 0)$  from equation (2.14) was substituted in equation (2.15) above, the Jacobian matrix became;

$$J = \begin{pmatrix} \beta_1 - \epsilon_1 & \epsilon_2 \\ \epsilon_1 & \beta_2 - \epsilon_2 \end{pmatrix} \tag{2.16}$$

The Jacobian matrix obtained in equation (2.16), together with its corresponding identity matrix were then substituted in the characteristic equation (2.4) above, and the characteristic equation became;

$$\begin{vmatrix} \beta_1 - \epsilon_1 - \lambda & \epsilon_2 \\ \epsilon_1 & \beta_2 - \epsilon_2 - \lambda \end{vmatrix} = 0 \tag{2.17}$$

Having followed the same procedure as before, for solving the above expression in equation (2.17) by hand, the zero equilibrium point for  $\beta_1 \neq \beta_2$  produced the two eigenvalues as;

$$\begin{aligned}
\lambda_1 &= \frac{1}{2} \left[ (\beta_T - \epsilon_T) - \sqrt{(\Delta\beta)^2 - 2\Delta\beta\Delta\epsilon + (\epsilon_T)^2} \right] \\
\lambda_2 &= \frac{1}{2} \left[ (\beta_T - \epsilon_T) + \sqrt{(\Delta\beta)^2 - 2\Delta\beta\Delta\epsilon + (\epsilon_T)^2} \right]
\end{aligned} \tag{2.18}$$

where;  $\beta_T = \beta_1 + \beta_2$ ,  $\epsilon_T = \epsilon_1 + \epsilon_2$ ,  $\Delta\beta = \beta_1 - \beta_2$  and  $\Delta\epsilon = \epsilon_1 - \epsilon_2$

From the eigenvalues obtained in equation (2.18) we can confirm whenever  $\beta_T > \epsilon_T$ , one of the eigenvalues is positive ( $\lambda_i > 0$ ,  $i = 2$ ), which means the point is locally and asymptotically unstable, and the system will not settle to the equilibrium point of  $(0, 0)$ . But when  $\epsilon_T > \beta_T$ , we can't find an analytic proof that is obeyed, but numerical simulation found no examples of  $(0, 0)$  equilibrium point being stable.

After the analysis and found the zero equilibrium point to be unstable, we continued by considering and re-arranging the non-zero equilibrium point  $(S - \beta_2)(\beta_1 - \epsilon_1 - \epsilon_2 - S) + (\beta_1 - \beta_2)\epsilon_2$  obtained from equation (2.14) above, which gives;

$$S^2 - (\beta_T - \epsilon_T)S + (\beta_1\beta_2 - \beta_1\epsilon_2 - \beta_2\epsilon_1) \tag{2.19}$$

Solving the above quadratic equation obtained in equation (2.19) for the values of  $S$ , we obtained;

$$\begin{aligned} S &= \frac{1}{2} \left[ (\beta_T - \epsilon_T) - \sqrt{(\Delta\beta)^2 - 2\Delta\beta\Delta\epsilon + (\epsilon_T)^2} \right] \\ S &= \frac{1}{2} \left[ (\beta_T - \epsilon_T) + \sqrt{(\Delta\beta)^2 - 2\Delta\beta\Delta\epsilon + (\epsilon_T)^2} \right] \end{aligned} \quad (2.20)$$

To identify the real solution of equation (2.19), we substituted the expression  $\beta_1 = \beta_2 = \beta$  in the two values obtained in equation (2.20) above, which gives;

$$\begin{aligned} S &= \beta - \epsilon_T \\ S &= \beta \end{aligned} \quad (2.21)$$

and the second value obtained in equation (2.21) is the same with the value obtained for the non-zero equilibrium point for constant growth rate in equation (2.5) above.

Since the second value of  $S$  obtained in equation (2.21) is the same with the value of the non-zero equilibrium point obtained in equation (2.5) above when  $\beta_1 = \beta_2 = \beta$ , we then used it to obtain the non-zero equilibrium point in this case as well.

To obtain the non-zero equilibrium points ( $s_1^*$ ,  $s_2^*$ ) we refer back to equation (2.13), where we eliminate  $s_2$  in the first equation by using ( $s_2 = S - s_1$ ), and later eliminate  $s_1$  in the second equation by using ( $s_1 = S - s_2$ ), and we respectively obtained;  $s_1^* = \frac{\epsilon_2 S}{S + \epsilon_T - \beta_1}$  and  $s_2^* = \frac{\epsilon_1 S}{S + \epsilon_T - \beta_2}$  where:  $S = \frac{1}{2} \left[ (\beta_T - \epsilon_T) + \sqrt{(\Delta\beta)^2 - 2\Delta\beta\Delta\epsilon + (\epsilon_T)^2} \right]$  from equation (2.20) above.

Therefore, the non-zero equilibrium points for different growth rate values ( $\beta_1 \neq \beta_2$ ) were obtained as;

$$(s_1^*, s_2^*) = \left( \frac{\frac{\epsilon_2}{2} A}{\frac{1}{2} A + \epsilon_T - \beta_1}, \frac{\frac{\epsilon_1}{2} A}{\frac{1}{2} A + \epsilon_T - \beta_2} \right) \quad (2.22)$$

where;  $A = (\beta_T - \epsilon_T) + \sqrt{(\Delta\beta)^2 - 2\Delta\beta\Delta\epsilon + (\epsilon_T)^2}$

Substituting the equilibrium points from equation (2.22) in the Jacobian matrix obtained in equation (2.15) above, the Jacobian matrix is then transformed to;

$$J = \begin{pmatrix} \beta_1 - \epsilon_1 - \frac{2\epsilon_2 A}{A+2\epsilon_T-2\beta_1} - \frac{\epsilon_1 A}{A+2\epsilon_T-2\beta_2} & -\frac{\epsilon_2 A}{A+2\epsilon_T-2\beta_1} + \epsilon_2 \\ -\frac{\epsilon_1 A}{A+2\epsilon_T-2\beta_2} + \epsilon_1 & \beta_2 - \epsilon_2 - \frac{\epsilon_2 A}{A+2\epsilon_T-2\beta_1} - \frac{2\epsilon_1 A}{A+2\epsilon_T-2\beta_2} \end{pmatrix} \quad (2.23)$$

To find the eigenvalues, the Jacobian matrix obtained in equation (2.23), and its corresponding identity matrix were substituted in the characteristic equation (2.4) above, which yielded;

$$\begin{vmatrix} \beta_1 - \epsilon_1 - \frac{2\epsilon_2 A}{A+2\epsilon_T-2\beta_1} - \frac{\epsilon_1 A}{A+2\epsilon_T-2\beta_2} - \lambda & -\frac{\epsilon_2 A}{A+2\epsilon_T-2\beta_1} + \epsilon_2 \\ -\frac{\epsilon_1 A}{A+2\epsilon_T-2\beta_2} + \epsilon_1 & \beta_2 - \epsilon_2 - \frac{\epsilon_2 A}{A+2\epsilon_T-2\beta_1} - \frac{2\epsilon_1 A}{A+2\epsilon_T-2\beta_2} - \lambda \end{vmatrix} = 0 \quad (2.24)$$

After undergoing a series of computations by hand, and making some representations as well, the eigenvalues for the non-zero equilibrium point when  $\beta_1 \neq \beta_2$  were obtained as;

$$\begin{aligned} \lambda_1 &= \frac{1}{2} \left[ (\beta_T - \epsilon_T - 3m) - \sqrt{(\Delta\beta)^2 - 2\Delta\beta(\Delta\epsilon + n) + (\epsilon_T - m)^2} \right] \\ \lambda_2 &= \frac{1}{2} \left[ (\beta_T - \epsilon_T - 3m) + \sqrt{(\Delta\beta)^2 - 2\Delta\beta(\Delta\epsilon + n) + (\epsilon_T - m)^2} \right] \end{aligned} \quad (2.25)$$

where;

$$\begin{aligned} \beta_T &= \beta_1 + \beta_2, & \Delta\beta &= \beta_1 - \beta_2, \\ \epsilon_T &= \epsilon_1 + \epsilon_2, & \Delta\epsilon &= \epsilon_1 - \epsilon_2, \\ m &= p + q, & n &= p - q, \\ p &= \frac{\epsilon_2 A}{F}, & q &= \frac{\epsilon_1 A}{G}, \\ F &= A + 2\epsilon_T - 2\beta_1, & G &= A + 2\epsilon_T - 2\beta_2, \\ A &= (\beta_T - \epsilon_T) + \sqrt{(\Delta\beta)^2 - 2\Delta\beta\Delta\epsilon + (\epsilon_T)^2} \end{aligned}$$

The eigenvalues obtained in equation (2.25) above are too complex to be analysed algebraically. Instead, their behaviours were investigated numerically by plotting them against different parameter values. As the eigenvalues were plotted against these parameters, their results show they were always negatives (*i. e.*  $\lambda_i < 0$ ,  $i = 1, 2$ ) as shown in Figure 2.2 below.

In Figure 2.2, plots (a) to (e) show the two eigenvalues are always negative for any parameter values used. Plot (b) shows an odd behaviour near  $\beta_2 = 1$ , and it was investigated further in plot (e) which clarifies it to be negative as well, and by that we found the non-zero equilibrium point for  $\beta_1 \neq \beta_2$  to be a stable one.

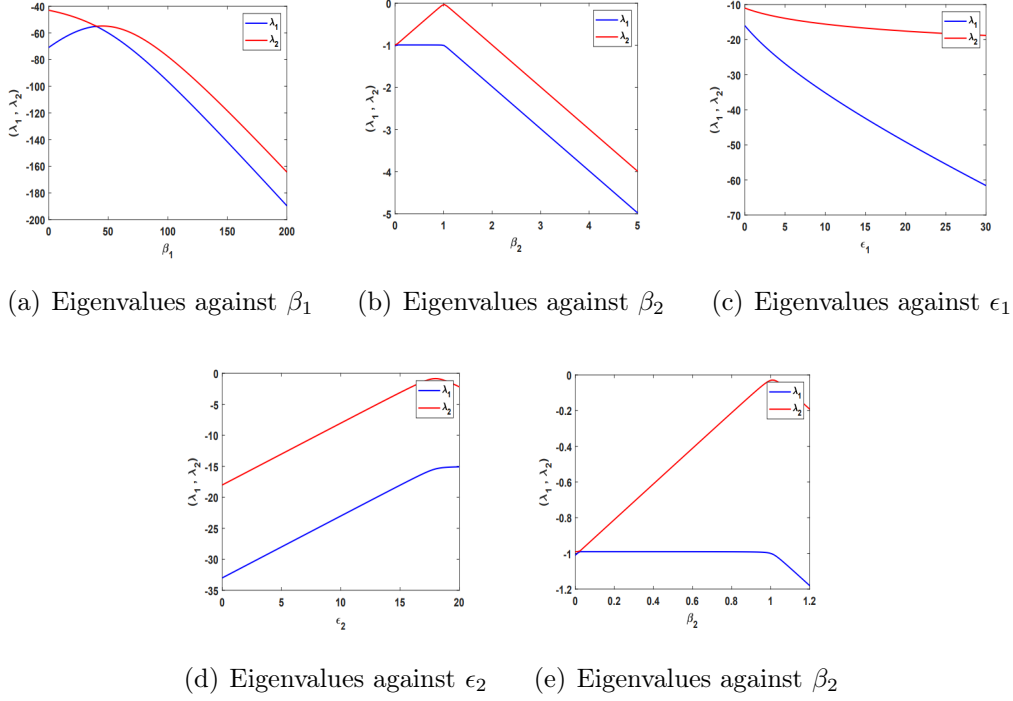


Figure 2.2: The numerical graphs for the eigenvalues of the non-zero equilibrium point for 2D bet-hedging model, with different values of the strains growth rates ( $\beta_1 \neq \beta_2$ ), against some parameters  $\beta_1$ ,  $\beta_2$ ,  $\epsilon_1$ , and  $\epsilon_2$  respectively, which show the two eigenvalues are always negative (*i.e.*  $\lambda_i < 0$ ,  $i = 1, 2$ ). In plot (a),  $\beta_2 = 80$ ,  $\epsilon_1 = 15$ , and  $\epsilon_2 = 50$ . In plot (b) as well,  $\beta_1 = 1$ ,  $\epsilon_1 = 0.01$ , and  $\epsilon_2 = 0.02$ . Also in plot (c),  $\beta_1 = 11$ ,  $\beta_2 = 25$ , and  $\epsilon_2 = 30$ . And lastly in plot (d),  $\beta_1 = 15$ ,  $\beta_2 = 33$ , and  $\epsilon_1 = 0.01$  respectively. The plot obtained in panel (e) is a zoom of the result obtained in the plot of panel (b), which clearly show the result is negative.

In Figure 2.3, plots (a) to (c) show the dynamics of the bet-hedging model when the strains amount or concentration of enzymes for their growth rates are different (*i.e.*  $r_1 \neq r_2$ ), while plots (d) to (f) show the dynamics when the strains amount or concentration of enzymes for their growth rates are equal but not zero (*i.e.*  $r_1 = r_2 \neq 0$ ). In either case, the growth rates of the bacteria are different (*i.e.*  $\beta_1 \neq \beta_2$ ), which show both strains will not settle at  $(0, 0)$  equilibrium point, and will always become stable at the non-zero equilibrium point.

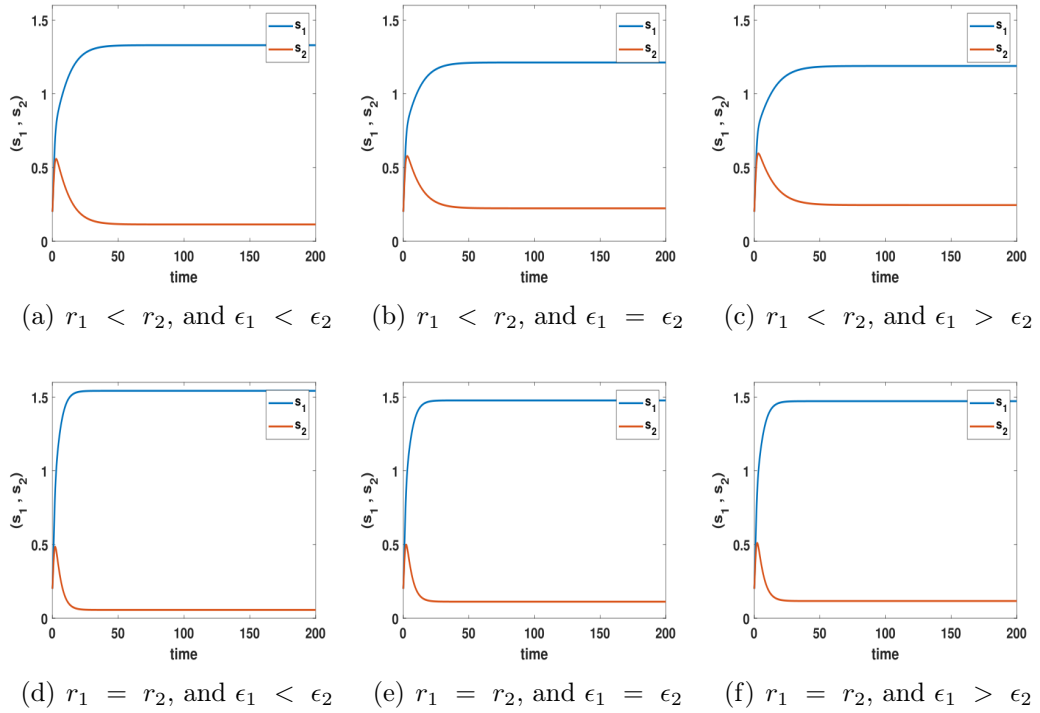


Figure 2.3: The Numerical graphs for the dynamics of the 2D bet-hedging model, with different values of the strains growth rates ( $\beta_1 \neq \beta_2$ ), with both strains having the same initial values ( $s_1(0) = s_2(0) = 0.2$ ), and different amount of nutrient contents in the environments ( $\alpha_1 = 5$  and  $\alpha_2 = 1$ ), with the same range of time for each of the plots  $t = 0 : 0.001 : 200$ , with plots (a), (b) and (c) having different amount or concentration of enzymes  $r_1 = 0.5$ , and  $r_2 = 0.7$ , with plot (a) having  $\epsilon_1 = 0.01$ , and  $\epsilon_2 = 0.02$ , plot (b) having the same transition rate values between the strains  $\epsilon_1 = \epsilon_2 = 0.02$ , and plot (c) having  $\epsilon_1 = 0.02$ , and  $\epsilon_2 = 0.01$ . Also, plots (d), (e) and (f) have the same amount or concentration of enzymes  $r_1 = r_2 = 0.7$ , with plot (d) having  $\epsilon_1 = 0.01$ , and  $\epsilon_2 = 0.02$ , plot (e) having the same transition rate values between the strains  $\epsilon_1 = \epsilon_2 = 0.02$ , and plot (f) having  $\epsilon_1 = 0.02$  and  $\epsilon_2 = 0.01$ , which show all the strains become stable at their respective equilibrium points.

Comparing the plots for the intrinsic dynamics of the bet-hedging model, when the strains have constant growth rates values ( $\beta_1 = \beta_2 = \beta = 1$ ) obtained in Figure 2.1, and those obtained in Figure 2.3 with different values of the strains growth rates ( $\beta_1 \neq \beta_2$ ), we noticed the densities of the strains at the steady state are a bit higher in Figure 2.3, which means there are respective increase in the densities of the strains in all the plots, which are usually determined by the growth rates ( $\beta_i$ ) values together with the transition rates ( $\epsilon_i$ ) of the strains from one type to the other.

## 2.5 Fluctuating Resources within the Growth Rates ( $\beta_i$ ) of the Bacteria

Having considered the two situations in sections 2.3 and 2.4 above, when the strains respectively have equal and constant growth rate values ( $\beta_1 = \beta_2 = \beta = 1$ ), and when they (strains) have different growth rate values ( $\beta_1 \neq \beta_2$ ), we now want to consider a situation when the nature of the environment fluctuates. We know there are lot of factors which could cause the environmental fluctuation, and as a result of those factors the environment fluctuates, which also causes a fluctuation in the strains growth rates.

Based on the aforementioned, the environmental state ( $\alpha_i$ ) in the intrinsic growth rate of the model will be replace by fluctuating resources, which is defined as:  $\alpha_i = \delta_i \sin(\omega t) + 1$ .

where;  $\delta_i$  is the amplitude, and  $\omega$  is the frequency of the fluctuating resources.

In this scenario, the rate of the bacterial growth ( $\beta_i$ ) with respect to time ( $t$ ) becomes;

$$\beta_i (r_i, \alpha_i) = 1 + r_i e^{\frac{-r_i}{\delta_i \sin(\omega t) + 1}} \quad (2.26)$$

meaning that, the growth rates of the bacteria will have a sinusoidal behavior, determined by the amplitude ( $\delta_i$ ), or frequency ( $\omega$ ) of the fluctuations with respect to time ( $t$ ).

Plots (a) to (f) in Figure 2.4 below show the dynamics of the bacterial density, with the sinusoidal function when ( $r_1 \neq r_2$ ), and also when ( $r_1 = r_2 \neq 0$ ), with all of these two conditions confirming that ( $\beta_1 \neq \beta_2$ ) respectively.

Plots (a) to (c) described a situation, when the strains have different/unequal amount of enzymes ( $r_1 \neq r_2$ ) with different transition rate ( $\epsilon_i$ ) values. Whereas, plots (d) to (f) described the strains with the same/equal amount of enzymes ( $r_1 = r_2 \neq 0$ ), and different transition rate ( $\epsilon_i$ ) values as well. And by looking at the whole plots in Figure 2.4 below, one can notice both strains show the same behavior in their fluctuations, and the same densities for the amplitude of their oscillations in plot (e), because in that plot (e) both strains have the same concentration or amount of enzymes ( $r_i$ ), and the same transition rates ( $\epsilon_i$ ) values as well.



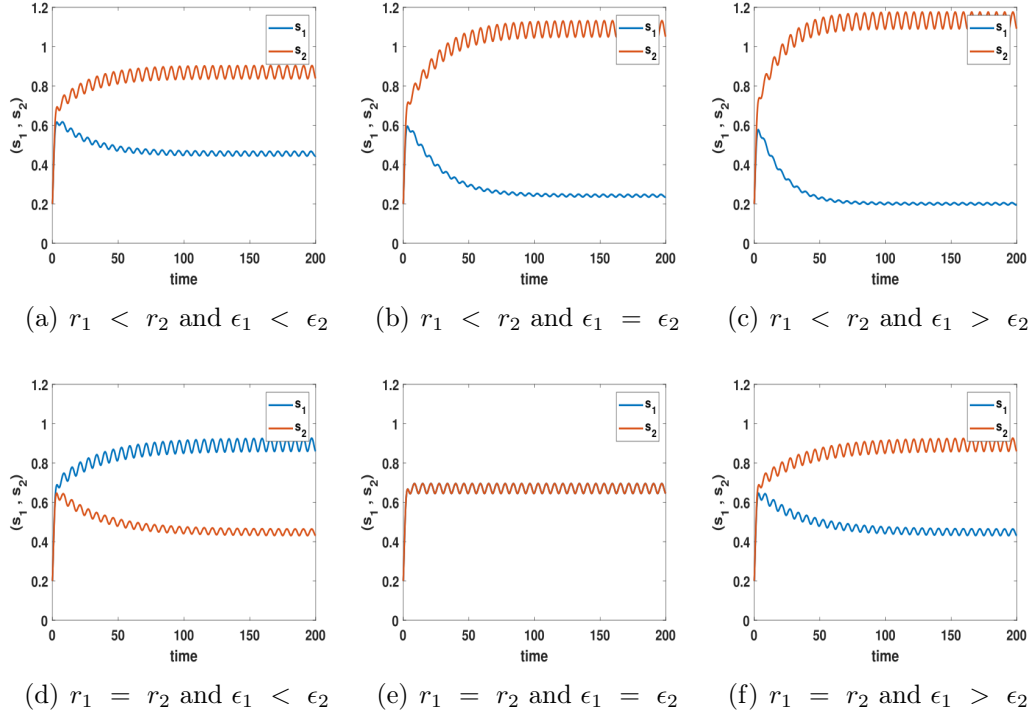


Figure 2.4: The Numerical graphs for the fluctuating dynamics of the bet-hedging model, with all of the plots having the same initial values ( $s_1(0) = s_2(0) = 0.2$ ), with plot (a), (b) and (c) having different values of enzymes ( $r_1 = 0.5$  and  $r_2 = 0.7$ ), with plot (a) having  $\epsilon_1 = 0.01$  and  $\epsilon_2 = 0.02$  plot (b) having the same values of the transition rates  $\epsilon_1 = \epsilon_2 = 0.02$ , and plot (c) having  $\epsilon_1 = 0.02$  and  $\epsilon_2 = 0.01$ . Also, plots (d) to (f) have the same values of enzymes ( $r_1 = r_2 = 0.7$ ), with plot (d) having  $\epsilon_1 = 0.01$  and  $\epsilon_2 = 0.02$ , plot (e) having the same values of the transition rates  $\epsilon_1 = \epsilon_2 = 0.02$ , and plot (f) having  $\epsilon_1 = 0.02$  and  $\epsilon_2 = 0.01$ , with the amplitude value  $\delta = 0.25$ , the frequency of oscillation  $\omega = 1$ , and it is more evident that one strain dominates at some point.

Also, the density of each strain in the fluctuating environment depends on their growth rates ( $\beta_i$ ), and their transition rates ( $\epsilon_i$ ) values as we observed in the non-fluctuating environment. If the two strains have the same or equal amounts of enzymes ( $r_1 = r_2 \neq 0$ ), with one of the strain having a lower transition rate ( $\epsilon_i$ ) value, the density of that particular strain will be higher than its counterpart strain, as shown in plots (d) and (f) respectively.

These defined the environmental state ( $\alpha_i$ ) as a non-autonomous function, and their stability can not easily be found directly. Instead, the functions have to be studied numerically at various points of fluctuations.

## 2.6 Time Courses and Densities of Strains with Varying Values of some Parameters for the Fluctuating Environment

In this section 2.6, we focused on how these parameters amplitude ( $\delta_i$ ), and the frequency ( $\omega$ ) parameters for the fluctuating resources can affect the behavior of each strain. Time courses for the strains with varied values of the parameters (amplitude and frequency) were carefully studied, and in the end their maximum and minimum densities of strains were generated, against the varied values of each parameter in question, with different values of the transition rates ( $\epsilon_i$ ) in order to observe their behaviors.

### 2.6.1 Time Courses of Strains for Some Varying Values of the Amplitude ( $\delta_i$ )

A few out of the many plots for the time courses, with different values of the amplitude ( $\delta_i$ ) were shown here, which gives an insight of how the behavior of those strains looked like, and can be compared with the results obtained in the intrinsic model for the fluctuating resources (with equal/constant or different values of the strains growth rates) in section 2.5 above, to observe if their behaviors are the same, or if there is any differences in their behaviors.

The plots in Figure 2.5 below show, there is always an increase in the densities of strains for the amplitude of oscillations, once the value of the amplitude ( $\delta_i$ ) is increased. But the behavior of the plots (fluctuations within the strains densities) in Figure 2.5 are the same with what were observed with the intrinsic model for the fluctuating environment in Figure 2.4 above.

This means that both the two strains can 'switch' to specialize in any environment as mentioned earlier, but the strain with low transition rate ( $\epsilon_i$ ), and a high value of the amplitude ( $\delta_i$ ), always has a higher density of oscillations at the steady state than the other.

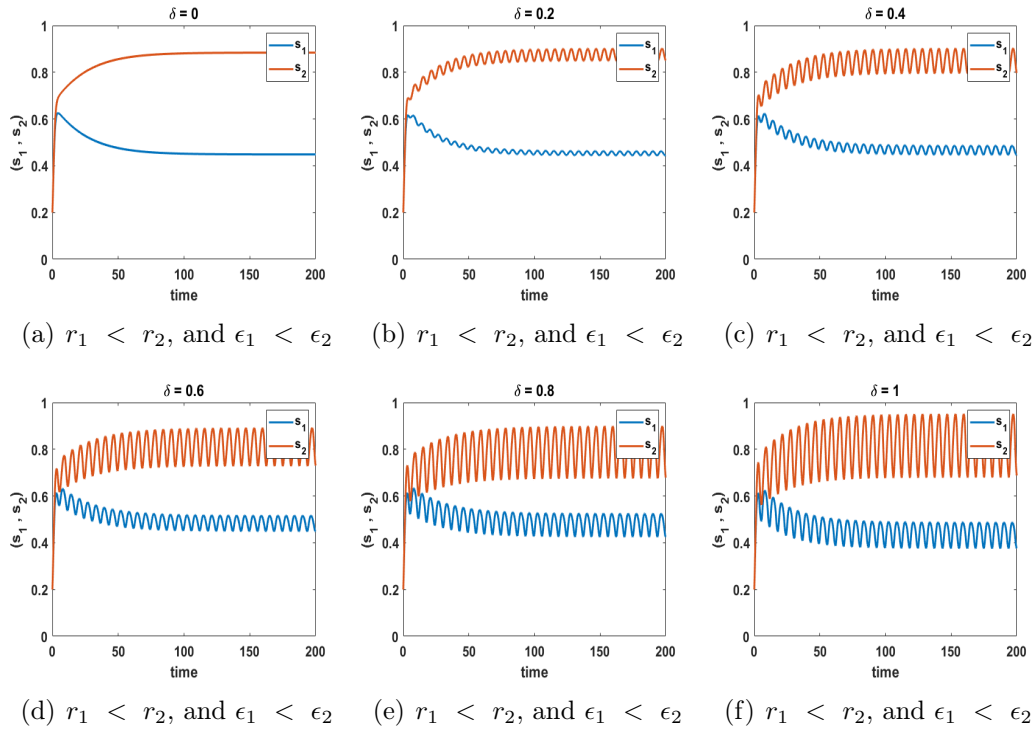


Figure 2.5: Time courses of strains for the 2D bet-hedging model with the fluctuating environment, and the varying amplitude ( $\delta_i$ ) values of oscillation, with the parameters:  $r_1 = 0.5$  and  $r_2 = 0.7$ , different values of the transition rates  $\epsilon_1 = 0.01$  and  $\epsilon_2 = 0.02$  respectively, with the frequency value of oscillations  $\omega = 1$ , and the initial values of the strains densities ( $s_1(0) = s_2(0) = 0.2$ ).

## 2.6.2 Densities of Strains against the Varying Values of the Amplitude ( $\delta_i$ )

The maximum and minimum densities of the strains, against the varying values of the amplitude ( $\delta_i$ ) of oscillations, with different values of the transition rates ( $\epsilon_i$ ), were taken in to consideration in this section 2.6.2, to see exactly the behavior of all the strains, with different values of the amplitude ( $\delta_i$ ) in a single plot.

An interesting pattern observed in it is, the minimum densities are showing the bigger changes than the maximum densities, and generally a reasonable amount of the amplitude ( $\delta_i$ ) value is needed before changes occur.

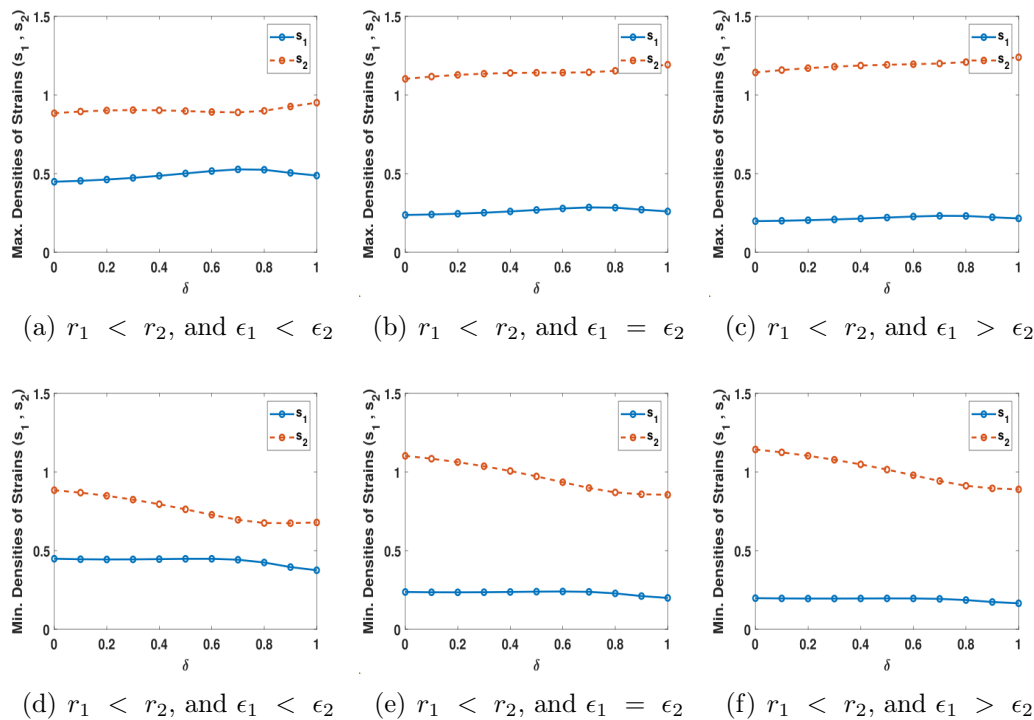


Figure 2.6: Maximum and minimum densities of strains for the 2D bet-hedging model, with the fluctuating environment and the same range of the amplitude ( $\delta_i$ ) values, with the parameters:  $r_1 = 0.5$  and  $r_2 = 0.7$ , plots (a) and (d) having different transition rate values  $\epsilon_1 = 0.01$  and  $\epsilon_2 = 0.02$ , plots (b) and (e) having the same transition rate values  $\epsilon_1 = \epsilon_2 = 0.01$ , also plots (c) and (f) having different transition rate values  $\epsilon_1 = 0.02$  and  $\epsilon_2 = 0.01$  as well, with the frequency of oscillations  $\omega = 1$ , and the initial values of the strain densities ( $s_1(0) = s_2(0) = 0.2$ ).

### 2.6.3 Time Courses of Strains for Some Varying Values of the frequency ( $\omega$ )

Like what was done in section 2.6.1 above, some plots for the time courses of strains with different values of the frequency ( $\omega$ ) of oscillations were shown here too, which give an awareness/insight for the behavior of those strains, and can be compared with the results obtained in Figures 2.4 and 2.5 above, for the intrinsic model of the fluctuating resources, and the time courses for the varied amplitude ( $\delta_i$ ) values respectively, with different values of the strains enzymes ( $r_1 \neq r_2$ ), to distinguish if there exist any differences in the behavior of the strains in those cases, or if their behaviors are the same.

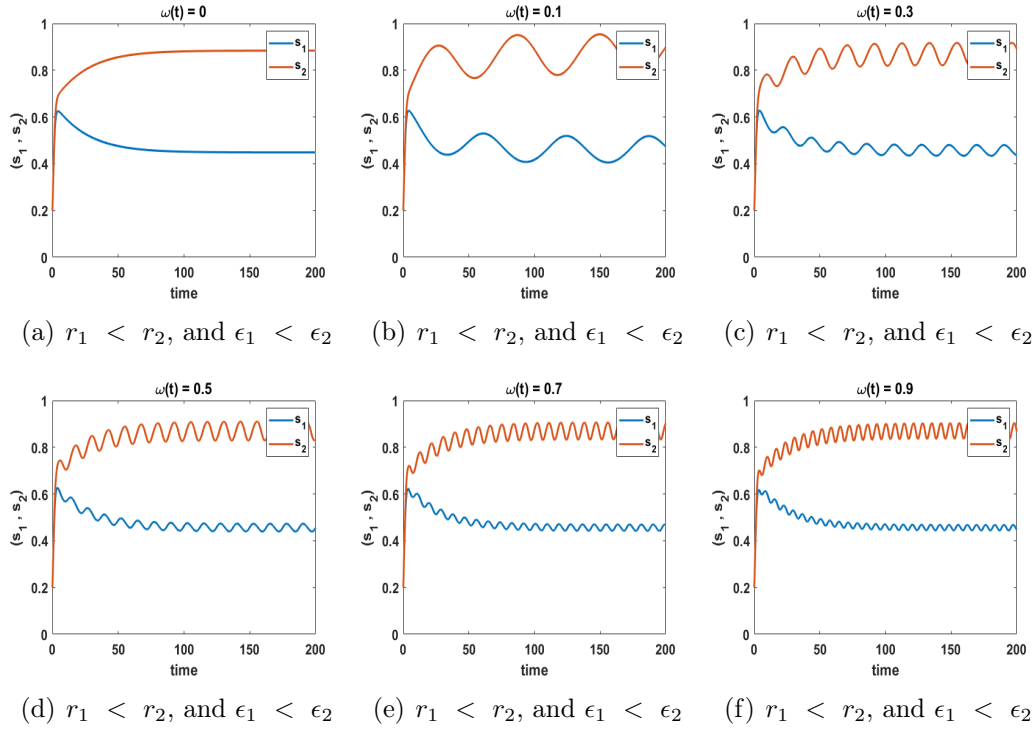


Figure 2.7: Time courses of strains for the 2D bet-hedging model with the fluctuating environment, and the varying frequency ( $\omega$ ) values of oscillations, with the parameters:  $r_1 = 0.5$  and  $r_2 = 0.7$ , different values of the transition rates  $\epsilon_1 = 0.01$  and  $\epsilon_2 = 0.02$  respectively, with the amplitude value of oscillations  $\delta = 0.25$ , and the initial values of the strains densities ( $s_1(0) = s_2(0) = 0.2$ ).

In Figure 2.7 above, we could notice a rapid increase in the strains densities, at the initial values for the frequency ( $\omega$ ) of oscillations, between  $\omega = 0$  to  $\omega = 0.1$  in plots (a) and (b), and a rapid decrease in the strains densities as well in plot (b) and (c), but the latter (rapid decrease) wasn't as much rapid as the former (rapid increase), and also not much difference could be spotted in the pattern of the strains densities in plots (d) to (f), but we could spot an increases in the number of oscillations completed per unit-time interval, when a frequency ( $\omega$ ) value is increased.

This means, the effect of the frequency ( $\omega$ ) in the fluctuating environment is much higher at the beginning than in the long run. Also, the strains ( $s_1, s_2$ ) experienced a rapid increase in their densities at the initial values for the frequency ( $\omega$ ) of oscillations, then a sudden decreased in it as well, before a gradual densities of the strains is maintained later.

## 2.6.4 Densities of Strains against the Varying Values of the frequency ( $\omega$ )

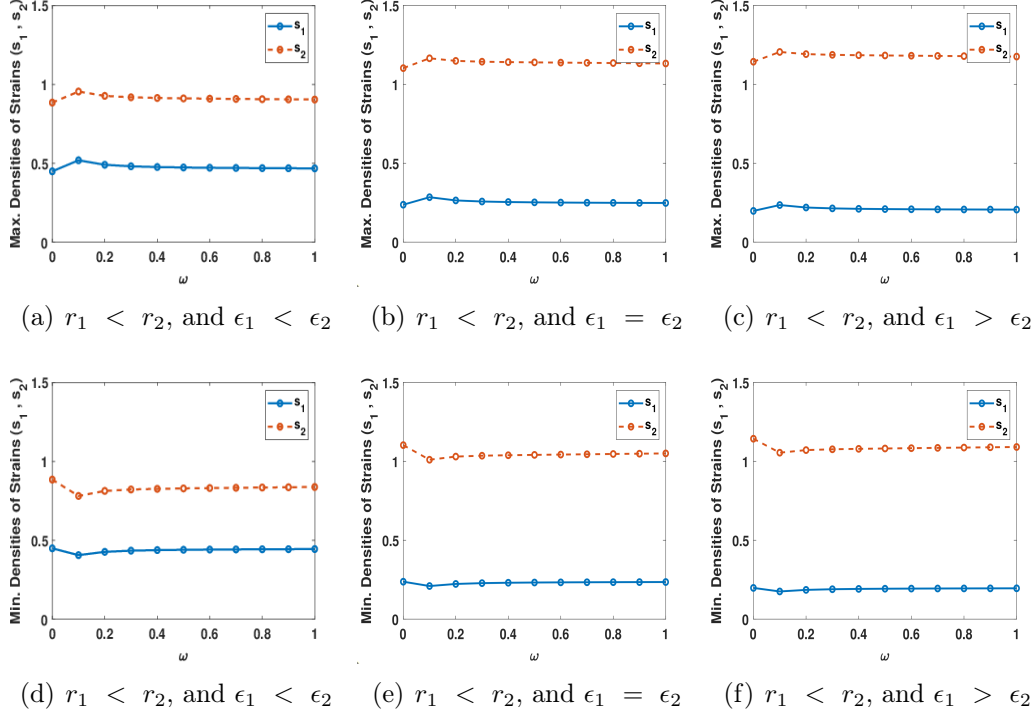


Figure 2.8: Maximum and minimum densities of strains for the 2D bet-hedging model, with the fluctuating environment ( $\delta * \sin(\omega t) + 1$ ) and the same range of the frequency ( $\omega$ ) values, with the parameters:  $r_1 = 0.5$  and  $r_2 = 0.7$ , plots (a) and (d) having different transition rate values  $\epsilon_1 = 0.01$  and  $\epsilon_2 = 0.02$ , plots (b) and (e) having the same transition rate values  $\epsilon_1 = \epsilon_2 = 0.01$ , also plots (c) and (f) having different transition rate values  $\epsilon_1 = 0.02$  and  $\epsilon_2 = 0.01$  as well, with the amplitude value of oscillations  $\delta = 0.25$ , and the initial values of the strain densities ( $s_1(0) = s_2(0) = 0.2$ ).

Plots (a) to (f) in Figure 2.8 above show the maximum and minimum densities of strains, against the varying frequency ( $\omega$ ) values, with some interesting results showing some jumps (up and down) in both the maximums and minimums, at the initial values of the frequency ( $\omega$ ) between  $\omega = 0$  and  $\omega = 0.1$ , with the maximums showing greater changes in the  $s_1$  strain, and the minimums showing greater changes in the  $s_2$  strain, which are quite different from the results obtained in Figure 2.6 above for the densities of the strains against the varied amplitude ( $\delta_i$ ) values.

To further clarify what the jumps (up and down) in the above Figure 2.8 means, we looked at the behaviors of the strains densities, with a short varying values of the frequency ( $\omega$ ) of oscillations, usually around  $\omega = 0$  to  $\omega = 0.1$ .

The results obtained in Figure 2.9 below show a rapid increases and decreases within the strains densities at the initial values for the frequency ( $\omega$ ) of oscillations.

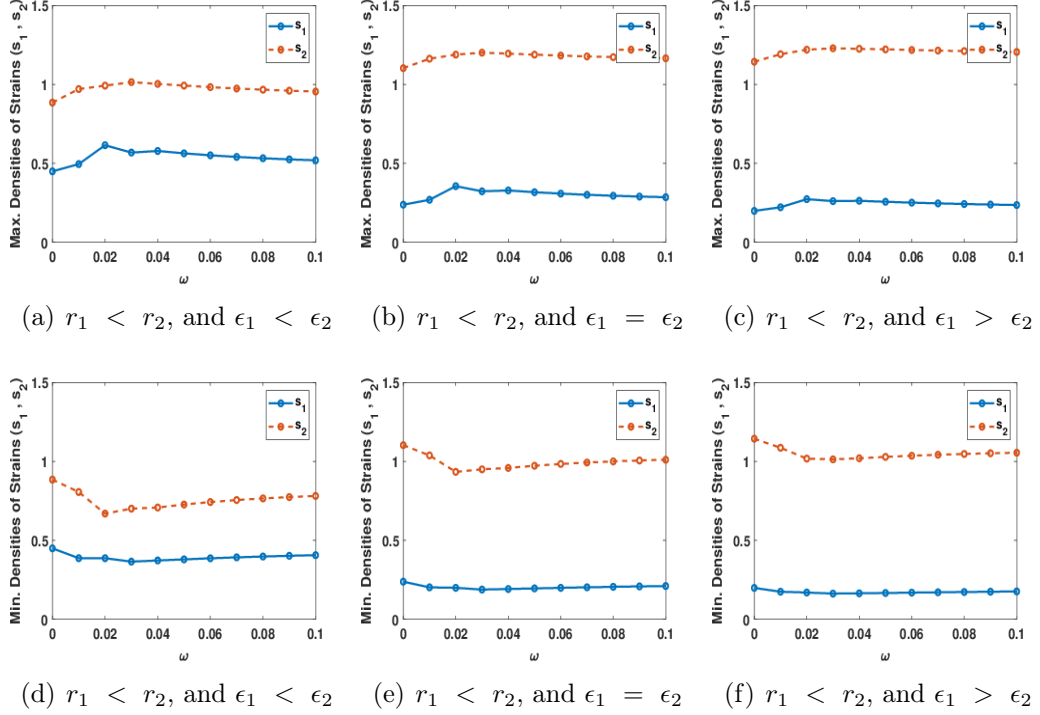


Figure 2.9: The maximum and minimum densities of strains for the 2D bet-hedging model, with the fluctuating environment ( $\delta * \sin(\omega t) + 1$ ) and the same range of the frequency ( $\omega$ ) values of oscillations, with the parameters:  $r_1 = 0.5$  and  $r_2 = 0.7$ , different values of the transition rates  $\epsilon_1 = 0.01$ ,  $\epsilon_2 = 0.02$ , and  $\epsilon_1 = \epsilon_2 = 0.01$  respectively, with the amplitude value of oscillations  $\delta = 0.25$ , and the initial values of the strain densities ( $s_1(0) = s_2(0) = 0.2$ ).

This show the strains respond more quickly to the effect of the frequency ( $\omega$ ) in the fluctuating environment at the early time, than they responds to the amplitude ( $\delta_i$ ) in their densities. It also means the frequency ( $\omega$ ) in the fluctuating resources affects the densities of each strain almost in the same way with a very minor difference, unlike the amplitude ( $\delta_i$ ) of the fluctuating environment which affect their densities, based on the respective amplitude ( $\delta_i$ ) values.

## 2.7 Conclusion

In this chapter 2, we studied the behavior of the two switching ( $s_1, s_2$ ) strains, which can ‘switch’ their phenotype to specialize in each environment, by per-

forming better or worse in any environments (Müller et al., 2013). The results produced two equilibrium points, a zero  $(s_1^*, s_2^*) = (0, 0)$ , and non-zero  $(s_1^*, s_2^*) = \left(\frac{\beta\epsilon_2}{\epsilon_T}, \frac{\beta\epsilon_1}{\epsilon_T}\right)$  equilibrium points in the non-fluctuating environment, which indicates the strains can not settle at the zero equilibrium point, meaning the bacteria always persist at this point, but they (strains) become stable at the non-zero equilibrium point. In the fluctuating environment, we noticed the behavior for the densities of the strains are the same with what were obtained in the non-fluctuating situation, but the only differences is the oscillations in the strains densities for the fluctuating environment, which isn't there in the non-fluctuating situation.

The results in this chapter 2 show, the transition rates ( $\epsilon_i$ ) appear to have a bigger effect, or a greater impact on the strains densities, than the growth rates ( $\beta_i$ ) of the strains in both the non-fluctuating and the fluctuating situations, as seen in the whole plots of Figures 2.1, 2.3, and 2.4 respectively. We also noticed in Figures 2.5 and 2.6 respectively that, once the values of the amplitude ( $\delta_i$ ) are increased in the time courses, the densities of oscillations in the strains are increased too, with the minimum showing a greater changes than the maximum. Meaning, the amplitude ( $\delta_i$ ) makes surprisingly little difference to the maximum/minimum densities, suggesting some strong intrinsic regulation.

Also in Figures 2.7, 2.8 and 2.9, a rapid increase in the strains densities at the early time between  $\omega = 0$  and  $\omega = 0.1$  at the steady state were observed, and a rapid decrease in their densities as well between  $\omega = 0.1$  and  $\omega = 0.2$  at the steady state, but the rapid decrease is not as high as the rapid increase, when the frequency ( $\omega$ ) value of the fluctuating resources is increased. Meaning that, the frequency ( $\omega$ ) makes a bigger differences at the early time, with the amplitudes ( $\delta_i$ ) peaking at very low frequencies.

In the next chapter we will introduce a non-switching ( $s_0$ ) strain, which does not 'switch' its phenotype and can grow at a constant rate in any environment, which is quite different with the phenotype of the switching ( $s_1, s_2$ ) strains discussed in this chapter. The aim is to study the dynamics of the non-switching ( $s_0$ ) and the switching ( $s_1, s_2$ ) strains in the same environmental states, and under the same conditions as we did in this chapter, to observe if there is any changes in their behaviors, or if the behaviors of the strains will be the same. Müller et al. (2013) used stochastic switching in their work, and my work happened to be the first that used deterministic fluctuations toward extending their work.



## CHAPTER 3

# Modelling the Bet-hedging of Bacterial Dynamics with the Presence of a Constant Strain

---

### 3.1 Introduction

After studying and analyzing the results obtained from the dynamics of the two bet-hedging ( $s_1, s_2$ ) strains, that can ‘switch’ their phenotype to specialize and perform better or worse in any environments, with different conditions in the previous chapter (Müller et al., 2013), we found the solutions of the model equations to have two equilibrium points in both situations. The equilibrium points consist of the zero’s and non-zero’s points in the non-fluctuating environment for both the constant and different growth rate ( $\beta_i$ ) values of the strains, which show in all the two cases the strains can’t settle at the zero equilibrium point, but they become stable at the non-zero equilibrium point. In the fluctuating environment, we noticed the strains are more sensitive to the frequency ( $\omega$ ) at relatively lower values than the amplitude ( $\delta_i$ ), and the strains are also more sensitive to the amplitude ( $\delta_i$ ) at relatively intermediate values than the frequency ( $\omega$ ). In this chapter a new strain ( $s_0$ ) which does not ‘switch’ its phenotype like the other strains, and can grow at a constant rate in any environment is introduced in the model equations (Müller et al., 2013).

This is the model structure we were interested in studying, to understand the benefits of bet-hedging between the strains. Müller et al. (2013) used an adaptive dynamics model technique to explore the evolution of bet-hedging within a population that experiences a stochastic changing environment. In the outcomes of their research, three different forms of evolutionary stable strategies (ESS’s) were found, depending on the frequencyicity at which the environment switches. A monomorphic phenotype familiarized to the instant environment caused by a gradually switching environment, a bimorphic bet-hedging phenotype caused by a central point of a dimension, and a monomor-

phic phenotype which is also familiarized to the average environment. In this chapter we will explore, study and analyze the underlying population dynamics model using a deterministic model approach in detail, which is quite different from the method used by the authors to study and analyze the behavior of the model, which is the first research that used the deterministic approach to analyze this particular model.

The aim is to investigate the dynamics of the three strains, the non-switching ( $s_0$ ) and the switching ( $s_1, s_2$ ) strains surviving together in the same environmental states with the same conditions, as we did in chapter 2 with the 'switching' ( $s_1, s_2$ ) strains alone, to ascertain if the behavior of the strains will be the same with what were obtained in chapter 2, or if there is any differences in their behavior. Also to check if any among the strains, the non-switching ( $s_0$ ) and the switching ( $s_1, s_2$ ) can be eliminated by the others, or if there will be competition for survival between them.

## 3.2 The Model of the Bet-hedging Bacteria with a Constant Strain

After investigating and analysing the results for the bet-hedging ( $s_1, s_2$ ) strains, that can switch and perform better or worse in any environment in chapter 2, a non-switching ( $s_0$ ) strain is introduced which grows at a constant rate in any environment (Müller et al., 2013). In this chapter we studied the survival of the non-switching ( $s_0$ ) strain between the switching ( $s_1, s_2$ ) ones in the non-fluctuating environment, and also when the environment fluctuates.

Based on the model equations in chapter 2 and what is introduced in this chapter 3, the new model equations were defined as;

$$\begin{aligned} s'_0 &= s_0 [\beta_0 (r_0, \alpha_0) - S] \\ s'_1 &= s_1 [\beta_1 (r_1, \alpha_1) - \epsilon_1 - S] + \epsilon_2 s_2 \\ s'_2 &= s_2 [\beta_2 (r_2, \alpha_2) - \epsilon_2 - S] + \epsilon_1 s_1 \end{aligned} \quad (3.1)$$

where;  $S = s_0 + s_1 + s_2$

$\beta_0, \beta_1,$  and  $\beta_2$  are the growth rates of the bacteria, which depends on the respective amount or concentration of enzymes  $r_0, r_1,$  and  $r_2$  to utilize the nutrient content in the environmental states  $\alpha_0, \alpha_1,$  and  $\alpha_2$  respectively.  $\epsilon_1,$  and  $\epsilon_2$  are the transition rates from one type to the opposite one,  $s_0$  is the non-switching strain which grow at a constant rate in any environments, where as ( $s_1, s_2$ ) are the switching strains that can perform better or worse in any of the environmental states.

The bacterial rate of growth ( $\beta_i$ ) for the strain(s) in this chapter is defined, as it was defined in equation (2.2) in the previous chapter.

In this research, we wanted to find out how the non-switching ( $s_0$ ) strain will be growing at a constant rate in any of the environmental states, which among the switching ( $s_1, s_2$ ) strains will perform better or worse in those environmental states, and also the level of competition among these strains.

As we did in chapter 2, stability analysis was performed on the model by considering different conditions, in order to check the behavior of the strains through finding the equilibrium points of the system, stability of the model, and the eigenvalues of the system from the characteristic equation (2.4), in which the same procedures were followed in this chapter 3 as well.

### 3.3 Constant Growth Rates ( $\beta_i$ ) of the Bacteria

As we did in chapter 2, we began the research by considering the system of equation (3.1) above with the assumption that ( $r_0 = r_1 = r_2 = 0$ ), which implies the growth rates of the bacteria are equal to one another (*i.e.*  $\beta_0 = \beta_1 = \beta_2 = \beta$ ).

Solving the above equation (3.1), the system produced two equilibrium points, a zero and non-zero points as;

$$\begin{aligned} (s_0^*, s_1^*, s_2^*) &= (0, 0, 0) \\ (s_0^*, s_1^*, s_2^*) &= \left( s_0, \frac{(\beta - s_0)\epsilon_2}{\epsilon_T}, \frac{(\beta - s_0)\epsilon_1}{\epsilon_T} \right) \end{aligned} \quad (3.2)$$

where;  $s_0$  in the second equilibrium in equation (3.2) is a continuum of equilibria, and it is not specified because it can take any value.

The Jacobian matrix of equation (3.1) was obtained as;

$$J = \begin{pmatrix} \beta - 2s_0^* - s_1^* - s_2^* & -s_0^* & -s_0^* \\ -s_1^* & \beta - \epsilon_1 - s_0^* - 2s_1^* - s_2^* & -s_1^* + \epsilon_2 \\ -s_2^* & -s_2^* + \epsilon_1 & \beta - \epsilon_2 - s_0^* - s_1^* - 2s_2^* \end{pmatrix} \quad (3.3)$$

The zero equilibrium point ( $s_0^*, s_1^*, s_2^*) = (0, 0, 0)$  obtained from equation (3.2) was first substituted in equation (3.3), and the Jacobian matrix becomes;

$$J = \begin{pmatrix} \beta & 0 & 0 \\ 0 & \beta - \epsilon_1 & \epsilon_2 \\ 0 & \epsilon_1 & \beta - \epsilon_2 \end{pmatrix} \quad (3.4)$$

The corresponding identity matrix together with the Jacobian matrix obtained in equation (3.4), were substituted in the characteristic equation (2.4), and the below expression was obtained as;

$$\begin{vmatrix} \beta - \lambda & 0 & 0 \\ 0 & \beta - \epsilon_1 - \lambda & \epsilon_2 \\ 0 & \epsilon_1 & \beta - \epsilon_2 - \lambda \end{vmatrix} = 0 \quad (3.5)$$

Evaluating the above expression in equation (3.5) by hand, the three eigenvalues were obtained as;

$$\begin{aligned} \lambda_{1, 2} &= \beta \\ \lambda_3 &= \beta - \epsilon_T \end{aligned} \quad (3.6)$$

where;  $\epsilon_T = \epsilon_1 + \epsilon_2$

Since two of the eigenvalues obtained in equation (3.6) above are greater than zero (*i. e.*  $\lambda_i > 0$ ,  $i = 1$  and  $2$ ), it indicates the zero equilibrium point to be locally, and asymptotically unstable, and the bacteria will not settle at the  $(0, 0, 0)$  equilibrium point.

We then move ahead to consider the non-zero equilibrium point  $(s_0^*, s_1^*, s_2^*) = (s_0, \frac{(\beta-s_0)\epsilon_2}{\epsilon_T}, \frac{(\beta-s_0)\epsilon_1}{\epsilon_T})$  obtained in equation (3.2), and after substituting it in the Jacobian matrix obtained in equation (3.3), we were left with;

$$J = \begin{pmatrix} -s_0 & -s_0 & -s_0 \\ \frac{(s_0 - \beta)\epsilon_2}{\epsilon_T} & \frac{(s_0 - \beta)\epsilon_2 - \epsilon_1\epsilon_T}{\epsilon_T} & \frac{(s_0 - \beta)\epsilon_2 + \epsilon_2\epsilon_T}{\epsilon_T} \\ \frac{(s_0 - \beta)\epsilon_1}{\epsilon_T} & \frac{(s_0 - \beta)\epsilon_1 + \epsilon_1\epsilon_T}{\epsilon_T} & \frac{(s_0 - \beta)\epsilon_1 - \epsilon_2\epsilon_T}{\epsilon_T} \end{pmatrix} \quad (3.7)$$

Substituting the above Jacobian matrix from equation (3.7), together with its corresponding identity matrix in the characteristic equation (2.4), we obtained the below expression as;

$$\begin{vmatrix} -s_0 - \lambda & -s_0 & -s_0 \\ \frac{(s_0 - \beta)\epsilon_2}{\epsilon_T} & \frac{(s_0 - \beta)\epsilon_2 - \epsilon_1\epsilon_T}{\epsilon_T} - \lambda & \frac{(s_0 - \beta)\epsilon_2 + \epsilon_2\epsilon_T}{\epsilon_T} \\ \frac{(s_0 - \beta)\epsilon_1}{\epsilon_T} & \frac{(s_0 - \beta)\epsilon_1 + \epsilon_1\epsilon_T}{\epsilon_T} & \frac{(s_0 - \beta)\epsilon_1 - \epsilon_2\epsilon_T}{\epsilon_T} - \lambda \end{vmatrix} = 0 \quad (3.8)$$

After the rigorous evaluation of the above expression in equation (3.8) by hand, it produces the three eigenvalues as;

$$\begin{aligned} \lambda_1 &= 0 \\ \lambda_2 &= -\beta \\ \lambda_3 &= -\epsilon_T \end{aligned} \quad (3.9)$$

where;  $\epsilon_T = \epsilon_1 + \epsilon_2$

Since one of the eigenvalues obtained here is zero (0), it does not imply stability. It is also evident that a zero (0) eigenvalue is expected, since there is a line of steady states. In the simulation of this kind, the final steady state will definitely depend on the initial conditions of the strains.

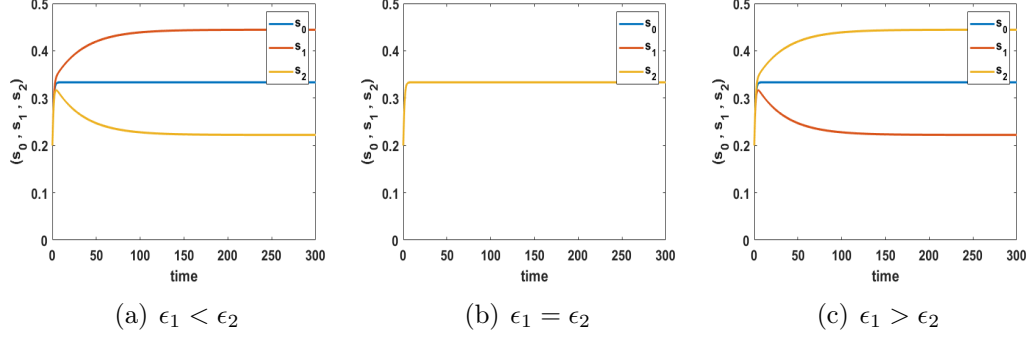


Figure 3.1: The Numerical graphs for the intrinsic dynamics of the 3D bet-hedging model, with a constant growth rates of the bacterial strain ( $\beta_0 = \beta_1 = \beta_2 = \beta = 1$ ), both strains having the same initial values ( $s_0(0) = s_1(0) = s_2(0) = 0.2$ ), with different amount of nutrients to be utilized by the bacterial strain  $\alpha_0 = 3$ ,  $\alpha_1 = 5$  and  $\alpha_2 = 1$ , the same range of time for each of the plots  $t = 0 : 0.001 : 300$ , with (a) having different transition rate values  $\epsilon_1 = 0.01$  and  $\epsilon_2 = 0.02$ , (b) having the same values of the transition rates  $\epsilon_1 = \epsilon_2 = 0.02$ , whereas (c) has different transition rates values as well  $\epsilon_1 = 0.02$  and  $\epsilon_2 = 0.01$ .

The results obtained in figure 3.1 show the same behavior with what were obtained in figure 2.1 in the previous chapter, where the transition rate ( $\epsilon_i$ ) values determines which among the bet-hedging ( $s_1, s_2$ ) strain perform better or worse in any situation. The results also show how the non-switching ( $s_0$ ) strain grow at a constant rate in any situation too.

### 3.4 Different Growth Rates ( $\beta_i$ ) Values of the Bacteria

After carefully studying the situation when ( $r_0 = r_1 = r_2 = 0$ ), meaning the three strains collectively has a constant growth rates value (*i. e.*  $\beta_0 = \beta_1 = \beta_2 = \beta = 1$ ), the research continued by considering what happened when ( $r_0 = r_1 = r_2 \neq 0$ ), or when ( $r_0 \neq r_1 \neq r_2$ ). In either of these mentioned cases, the growth rates of the strains are not the same (*i. e.*  $\beta_0 \neq \beta_1 \neq \beta_2$ ). The growth rates of the bacterial strain for these conditions are not the same,

because the nutrient contents of the environments under study were not the same as well (*i. e.*  $\alpha_0 \neq \alpha_1 \neq \alpha_2$ ).

The model equations for the non-switching ( $s_0$ ) strain, and the switching ( $s_1, s_2$ ) strains based on the aforementioned conditions are governed by;

$$\begin{aligned} s'_0 &= s_0 [\beta_0 (r_0, \alpha_0) - S] \\ s'_1 &= s_1 [\beta_1 (r_1, \alpha_1) - \epsilon_1 - S] + \epsilon_2 s_2 \\ s'_2 &= s_2 [\beta_2 (r_2, \alpha_2) - \epsilon_2 - S] + \epsilon_1 s_1 \end{aligned} \quad (3.10)$$

where;  $S = s_0 + s_1 + s_2$ , with all other parameters as defined in equation (3.1), and the bacterial growth rate ( $\beta_i$ ) of the strains as defined in equation (2.2).

Solving the above equation (3.10), the system produced four equilibrium points, a zero and three non-zero points as;

$$\begin{aligned} (s_0^*, s_1^*, s_2^*) &= (0, 0, 0), \\ (s_0^*, s_1^*, s_2^*) &= (\beta_0, 0, 0), \\ (s_0^*, s_1^*, s_2^*) &= (0, AA, BB), \\ (s_0^*, s_1^*, s_2^*) &= (0, CC, DD) \end{aligned} \quad (3.11)$$

where;

$$\begin{aligned} AA &= \frac{(\beta_2 - 2\beta_1 + 2\epsilon_2)\epsilon_1 - (\beta_1 + \epsilon_2)\beta_2 + (\beta_1^2 + \epsilon_1^2 + \epsilon_2^2)}{2(\beta_1 - \beta_2)} \\ &\quad - \frac{(\beta_1 - \epsilon_1 - \epsilon_2)\sqrt{(\beta_1 - \beta_2)^2 - 2(\beta_1 - \beta_2)\Delta\epsilon + \epsilon_T^2}}{2(\beta_1 - \beta_2)} \\ BB &= \frac{(\beta_2 + \epsilon_1)\beta_1 - (\beta_1 - 2\beta_2 + 2\epsilon_1)\epsilon_2 - (\beta_2^2 + \epsilon_1^2 + \epsilon_2^2)}{2(\beta_1 - \beta_2)} \\ &\quad + \frac{(\beta_2 - \epsilon_1 - \epsilon_2)\sqrt{(\beta_1 - \beta_2)^2 - 2(\beta_1 - \beta_2)\Delta\epsilon + \epsilon_T^2}}{2(\beta_1 - \beta_2)} \\ CC &= \frac{(\beta_2 - 2\beta_1 + 2\epsilon_2)\epsilon_1 - (\beta_1 + \epsilon_2)\beta_2 + (\beta_1^2 + \epsilon_1^2 + \epsilon_2^2)}{2(\beta_1 - \beta_2)} \\ &\quad + \frac{(\beta_1 - \epsilon_1 - \epsilon_2)\sqrt{(\beta_1 - \beta_2)^2 - 2(\beta_1 - \beta_2)\Delta\epsilon + \epsilon_T^2}}{2(\beta_1 - \beta_2)} \\ DD &= \frac{(\beta_2 + \epsilon_1)\beta_1 - (\beta_1 - 2\beta_2 + 2\epsilon_1)\epsilon_2 - (\beta_2^2 + \epsilon_1^2 + \epsilon_2^2)}{2(\beta_1 - \beta_2)} \\ &\quad - \frac{(\beta_2 - \epsilon_1 - \epsilon_2)\sqrt{(\beta_1 - \beta_2)^2 - 2(\beta_1 - \beta_2)\Delta\epsilon + \epsilon_T^2}}{2(\beta_1 - \beta_2)} \end{aligned}$$

$$\epsilon_T = \epsilon_1 + \epsilon_2, \quad \text{and} \quad \Delta\epsilon = \epsilon_1 - \epsilon_2$$

From the equilibrium points obtained above, it show there is no co-existence of the equilibrium states. Meaning that each strain is characterized by its equilibrium point.

The Jacobian matrix of equation (3.10) was obtained as;

$$J = \begin{pmatrix} \beta_0 - 2s_0^* - s_1^* - s_2^* & -s_0^* & -s_0^* \\ -s_1^* & \beta_1 - \epsilon_1 - s_0^* - 2s_1^* - s_2^* & -s_1^* + \epsilon_2 \\ -s_2^* & -s_2^* + \epsilon_1 & \beta_2 - \epsilon_2 - s_0^* - s_1^* - 2s_2^* \end{pmatrix} \quad (3.12)$$

Starting with the zero equilibrium point  $(s_0^*, s_1^*, s_2^*) = (0, 0, 0)$  from equation (3.11), and after it was substituted in equation (3.12), the Jacobian matrix becomes;

$$J = \begin{pmatrix} \beta_0 & 0 & 0 \\ 0 & \beta_1 - \epsilon_1 & \epsilon_2 \\ 0 & \epsilon_1 & \beta_2 - \epsilon_2 \end{pmatrix} \quad (3.13)$$

After substituting the Jacobian matrix obtained in equation (3.13), together with it corresponding identity matrix in the characteristic equation (2.4), we obtained;

$$\begin{vmatrix} \beta_0 - \lambda & 0 & 0 \\ 0 & \beta_1 - \epsilon_1 - \lambda & \epsilon_2 \\ 0 & \epsilon_1 & \beta_2 - \epsilon_2 - \lambda \end{vmatrix} = 0 \quad (3.14)$$

Evaluating the above expression obtained in equation (3.14) by hand, and after some calculations, the three eigenvalues were obtained as;

$$\begin{aligned} \lambda_1 &= \beta_0 \\ \lambda_2 &= \frac{1}{2} \left[ \{(\beta_1 + \beta_2) - \epsilon_T\} + \sqrt{(\beta_1 - \beta_2)^2 - 2(\beta_1 - \beta_2)\Delta\epsilon + \epsilon_T^2} \right] \\ \lambda_3 &= \frac{1}{2} \left[ \{(\beta_1 + \beta_2) - \epsilon_T\} - \sqrt{(\beta_1 - \beta_2)^2 - 2(\beta_1 - \beta_2)\Delta\epsilon + \epsilon_T^2} \right] \end{aligned} \quad (3.15)$$

Since one of the eigenvalues obtained in equation (3.15) above is positive (*i. e.*  $\lambda_i > 0$  as  $i = 1$ ), it confirmed the point to be locally, and asymptotically unstable. And it means the strain (bacteria) will not settle at the zero  $(0, 0, 0)$  equilibrium point.

After finishing with the zero equilibrium point and found it to be unstable, we then considered the first non-zero equilibrium point  $(s_0^*, s_1^*, s_2^*) = (\beta_0, 0, 0)$  obtained in equation (3.11) and substitute the values in the Jacobian matrix obtained in equation (3.12), and the result obtained is;

$$J = \begin{pmatrix} -\beta_0 & -\beta_0 & -\beta_0 \\ 0 & \beta_1 - \beta_0 - \epsilon_1 & \epsilon_2 \\ 0 & \epsilon_1 & \beta_2 - \beta_0 - \epsilon_2 \end{pmatrix} \quad (3.16)$$

The Jacobian matrix obtained in equation (3.16), together with its corresponding identity matrix were both substituted in the characteristic equation (2.4), and we obtained;

$$\begin{vmatrix} -\beta_0 - \lambda & -\beta_0 & -\beta_0 \\ 0 & \beta_1 - \beta_0 - \epsilon_1 - \lambda & \epsilon_2 \\ 0 & \epsilon_1 & \beta_2 - \beta_0 - \epsilon_2 - \lambda \end{vmatrix} = 0 \quad (3.17)$$

The above expression obtained in equation (3.17) was evaluated by hand, and after a series of rigorous computations, it produced the three eigenvalues as;

$$\begin{aligned} \lambda_1 &= -\beta_0 \\ \lambda_2 &= \frac{1}{2} \left[ \{\beta_1 + \beta_2 - 2\beta_0 - \epsilon_T\} - \sqrt{(\beta_1 - \beta_2)^2 - 2(\beta_1 - \beta_2)\Delta\epsilon + \epsilon_T^2} \right] \\ \lambda_3 &= \frac{1}{2} \left[ \{\beta_1 + \beta_2 - 2\beta_0 - \epsilon_T\} + \sqrt{(\beta_1 - \beta_2)^2 - 2(\beta_1 - \beta_2)\Delta\epsilon + \epsilon_T^2} \right] \end{aligned} \quad (3.18)$$

Analysis of equation (3.18) above show, whenever the value of  $\beta_0$  is greater than the average value of  $\beta_1$  and  $\beta_2$  [*i. e.*  $\beta_0 > \frac{\beta_1 + \beta_2}{2}$ ], and the value obtained from the square root is very small (less than the obtained value of  $\beta_0$ ), the strain (bacteria) will become stable at the first non-zero equilibrium point obtained in equation (3.11) which is  $\beta_0$ . Else, if the average value of  $\beta_1$  and  $\beta_2$  is greater than the value of  $\beta_0$  [*i. e.*  $\frac{\beta_1 + \beta_2}{2} > \beta_0$ ], and the value obtained from the square root is very small (less than the obtained average value of  $\beta_1$  and  $\beta_2$ ), the bacteria will become stable at one of the remaining non-zero equilibrium point (the last one) obtained in equation (3.11) above, in which the analytical investigations of their steady states were algebraically unfeasible. In Figure 3.2 we can noticed the effects of the transition rates ( $\epsilon_i$ ) values on the existing strain(s) in plots (d) to (i), which does not show on the existing strain(s) in plots (a) to (c).

Plots (a) to (c) in Figure 3.2 when the value of  $\beta_0$  is greater than the average value of  $\beta_1$  and  $\beta_2$  show no matter the values of the transition rates ( $\epsilon_i$ ) in those plots, it will not affect the equilibrium density of the existing non-switching ( $s_0$ ) strain. This was mentioned earlier that  $s_0$  strain grow at a constant rate in any environment, and that can easily be understood in the model equation, since there is not any transition rate ( $\epsilon_i$ ) associated to it in the equation, but the differences in the transition rates ( $\epsilon_i$ ) values affects the densities of the existing switching ( $s_1, s_2$ ) strains at the steady state which are seen in plots (d) to (i), and also on the extincting strains on plots (a) to (c) respectively.



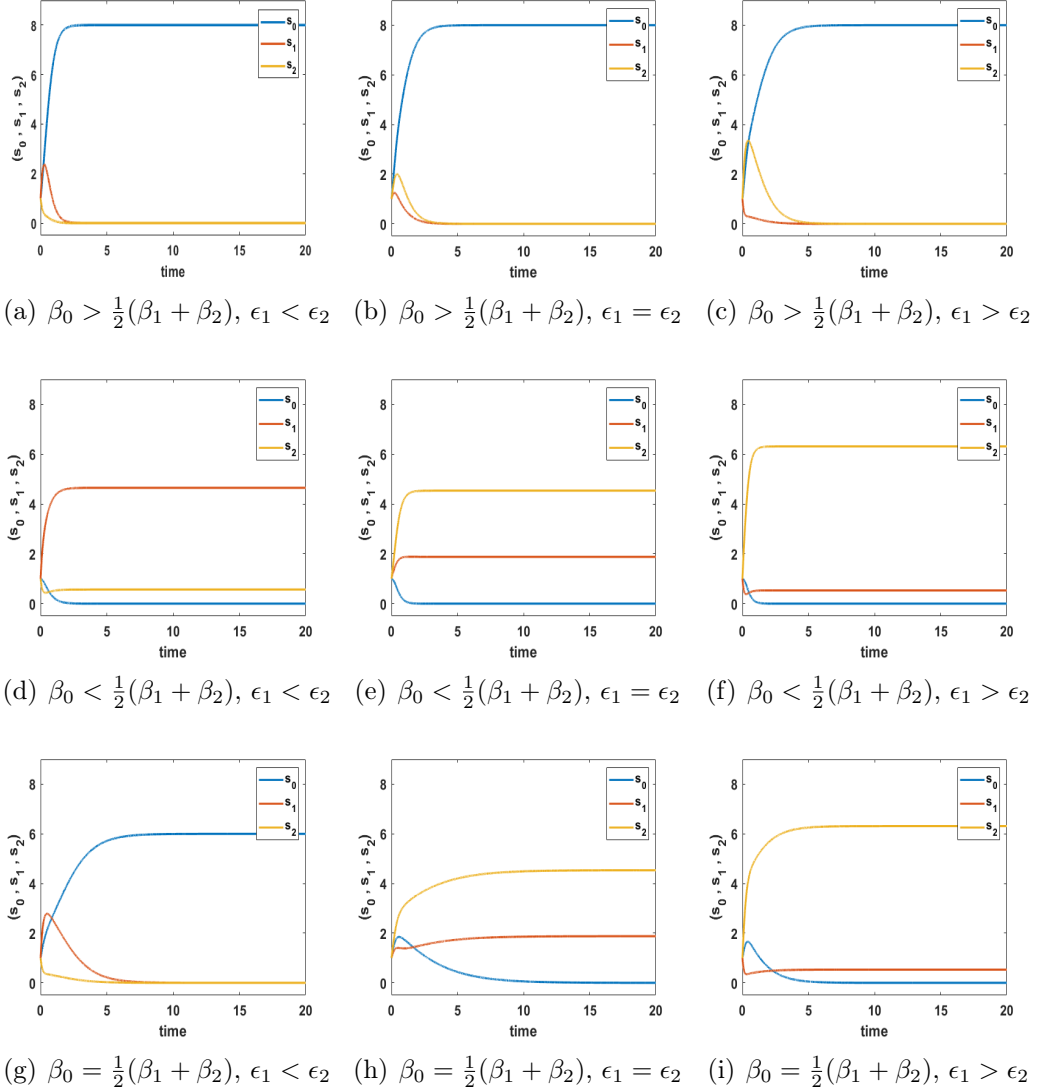


Figure 3.2: The Numerical graphs for the intrinsic dynamics of the 3D bet-hedging model when there is a presence of enzyme(s) to utilize the nutrients available ( $\beta_0 \neq \beta_1 \neq \beta_2$ ), both strains having the same initial values ( $s_0(0) = s_1(0) = s_2(0) = 1$ ), with different values of  $\beta_0$  as; 8, 3 and 6 respectively, where as  $\beta_1 = 5$ , and  $\beta_2 = 7$  all through, with plots (a, d) and (g) having different transition rate values  $\epsilon_1 = 1$  and  $\epsilon_2 = 10$ , plots (b, e) and (h) having the same values of the transition rates  $\epsilon_1 = \epsilon_2 = 1$ , whereas plots (c, f) and (i) has different transition rate values as well  $\epsilon_1 = 10$  and  $\epsilon_2 = 1$ , and both plots show all the strains become stable at some points.

Also in plots (d) to (f) when the value of  $\beta_0$  is less than the average value of  $\beta_1$  and  $\beta_2$ , we could noticed the effects of the transition rates ( $\epsilon_i$ ) values within the existing switching ( $s_1, s_2$ ) strains. It is clear that the values of the transition rates ( $\epsilon_i$ ) does affect the strains densities in those plots at the

steady state. In plot (d), despite the  $s_1$  strain respectively possesses lower values for both its growth rate ( $\beta_1$ ) and the transition rate ( $\epsilon_1$ ) than the  $s_2$  strain, at the steady state the  $s_1$  strain maintains a high density than the  $s_2$  strain, which was due to its lower transition rate ( $\epsilon_i$ ) value. But in plots (e) and (f), when the transition rate ( $\epsilon_1$ ) values of the  $s_1$  strain are respectively equal (the same), and greater than the  $s_2$  strain transition rate ( $\epsilon_2$ ) values, the  $s_2$  strain respectively maintains high densities at the steady state in those plots than the  $s_1$  strain.

There are some interesting results in Figure 3.2 that were spotted in plots (g) to (i), when the value of  $\beta_0$  is equal to the average value of  $\beta_1$  and  $\beta_2$ . In plot (g), despite the value of  $\beta_0$  is not greater than the average value of  $\beta_1$  and  $\beta_2$ , the non-switching ( $s_0$ ) strain wins the competition, because it has a high growth rate ( $\beta_0$ ) value that can compete and win the competition. But in plots (h) and (i), the switching ( $s_1, s_2$ ) strains win the competition, with the  $s_2$  strain having a high density because of its growth rate ( $\beta_2$ ) and transition rate ( $\epsilon_2$ ) values.

Overall the results obtained in Figure 3.2 above show, despite following the concept of  $\beta_0$  value being respectively greater than, or less than, or even equal to the average value of  $\beta_1$  and  $\beta_2$ , the transition rates ( $\epsilon_i$ ) values play a vital role in determining which among the strains (switching and non-switching) wins the competition in some circumstances. This means if a part of a strain moves from one type to the other, definitely the density of that strain will be affected negatively at the steady state, and also it will have a positive effect on the density of the strain it moved to at the steady state as well.

We further investigated what happened under this condition, when the growth rates ( $\beta_i$ ) values of the different strains are equal but not zero (*i.e.*  $\beta_0 = \beta_1 = \beta_2 \neq 1$ ). In this scenario, the three strains both the non-switching ( $s_0$ ), and the switching ( $s_1, s_2$ ) strains co-exist as a special case, which is the stability swapping point between  $(s_0^*, 0, 0)$  and  $(0, s_1^*, s_2^*)$  equilibrium points. At this point stability is lost, which produced a non-isolated fixed point as shown in the Figure 3.3 below.

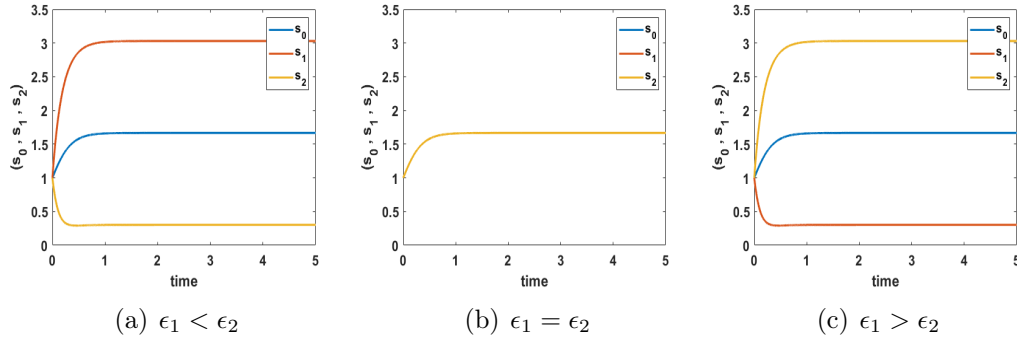


Figure 3.3: The Numerical graphs for the intrinsic dynamics of the 3D bet-hedging model when there is a presence of enzyme(s) to utilize the nutrients available ( $\beta_0 = \beta_1 = \beta_2 \neq 1$ ), both strains having the same initial values ( $s_0(0) = s_1(0) = s_2(0) = 1$ ), the same growth rate values for the strains  $\beta_0 = \beta_1 = \beta_2 = 5$ , with plot (a) having different transition rates values  $\epsilon_1 = 1$  and  $\epsilon_2 = 10$ , plot (b) having the same values of the transition rates  $\epsilon_1 = \epsilon_2 = 1$ , whereas plot (c) has different transition rates values as well  $\epsilon_1 = 10$  and  $\epsilon_2 = 1$ , and both plots show all the three strains co-exists as a special case.

Plots (a) to (c) obtained in Figure 3.3 above show a special cases for the co-existence of the three strains despite using different values of the transition rates ( $\epsilon_i$ ), which show a complete lost of stability when changing an equilibrium state between  $(s_0^*, 0, 0)$  and  $(0, s_1^*, s_2^*)$  in any situation. In the same figure one can notice the strain with the lowest value of the transition rate ( $\epsilon_i$ ) has a high density at the steady state, and the one with the high value of the transition rate ( $\epsilon_i$ ) has a lower density at the steady state as well, as seen in plots (a) and (c) respectively. The switching ( $s_1, s_2$ ) strains co-exists at the steady state with the non-switching ( $s_0$ ) strain, when the switching ( $s_1, s_2$ ) strains have the same transition rates ( $\epsilon_i$ ) values, as seen in plot (b). These definitely show how importance are the transition rates ( $\epsilon_i$ ) values in determining which among the switching ( $s_1, s_2$ ) strain(s) perform better or worse in those situations.

### 3.5 Fluctuating Resources within the Growth Rates ( $\beta_i$ ) of the Bacteria

Since we are done with our investigations in the situations mentioned above, when the strains have constant growth rates values ( $\beta_0 = \beta_1 = \beta_2 = \beta$ ), different growth rates values of the strains ( $\beta_0 \neq \beta_1 \neq \beta_2$ ), and the same (equal) growth rate values ( $\beta_0 = \beta_1 = \beta_2 \neq 1$ ) as well, we now want to

consider an environmental state ( $\alpha_i$ ) with a fluctuating resources, which also caused the growth of the strains to fluctuate as well.

The rate of the bacterial growth ( $\beta_i$ ) in this situation, based on the intrinsic model equations with respect to time ( $t$ ) is defined as in equation (2.26).

In this situation, we will analyze the behavior of the plots, by considering either their amplitude ( $\delta_i$ ), or frequency ( $\omega$ ) of oscillations, for the existing strain(s) with respect to the time ( $t$ ), since the existing strain(s) at the steady state have a sinusoidal behavior.

The whole plots obtained in Figure 3.4 show the same pattern of behavior, with the results obtained in Figure 3.2 for the non-fluctuating resources, except for plot ( $h$ ). The plots displays the same behavior with the result obtained, when the value of  $\beta_0$  is greater than the average value of  $\beta_1$  and  $\beta_2$  [ $\beta_0 > \frac{1}{2}(\beta_1 + \beta_2)$ ], the non-switching ( $s_0$ ) strain exists (wins), and the switching ( $s_1, s_2$ ) strains are extinct. It also show the same pattern, when the reverse is the case [*i. e.*  $\beta_0 < \frac{1}{2}(\beta_1 + \beta_2)$ ], the switching ( $s_1, s_2$ ) strains co-exists (wins), and the non-switching ( $s_0$ ) strain is extinct.

Plot ( $h$ ) in the fluctuating resources below confirms a switch of strain(s) at the steady state, when its result is compared with the results obtained in the non-fluctuating situation in Figure 3.2, where we realized the existence of the non-switching ( $s_0$ ) strain at the steady state, instead of the switching ( $s_1, s_2$ ) strains that were obtained in the non-fluctuating situation, when the value of  $\beta_0$  is equal the average value of  $\beta_1$  and  $\beta_2$  [*i. e.*  $\beta_0 = \frac{1}{2}(\beta_1 + \beta_2)$ ], with the same transition rate values ( $\epsilon_1 = \epsilon_2$ ). This show the environmental fluctuation on the growth rate ( $\beta_i$ ) value on its own might cause the switch of the existing strain(s).

From the results obtained in both the non-fluctuating and the fluctuating environments, they showed the effect of the transition rates ( $\epsilon_i$ ) values in each case. These show the strains densities at the steady state usually depends on both the strain growth rate ( $\beta_i$ ), and its transition rate ( $\epsilon_i$ ) values.

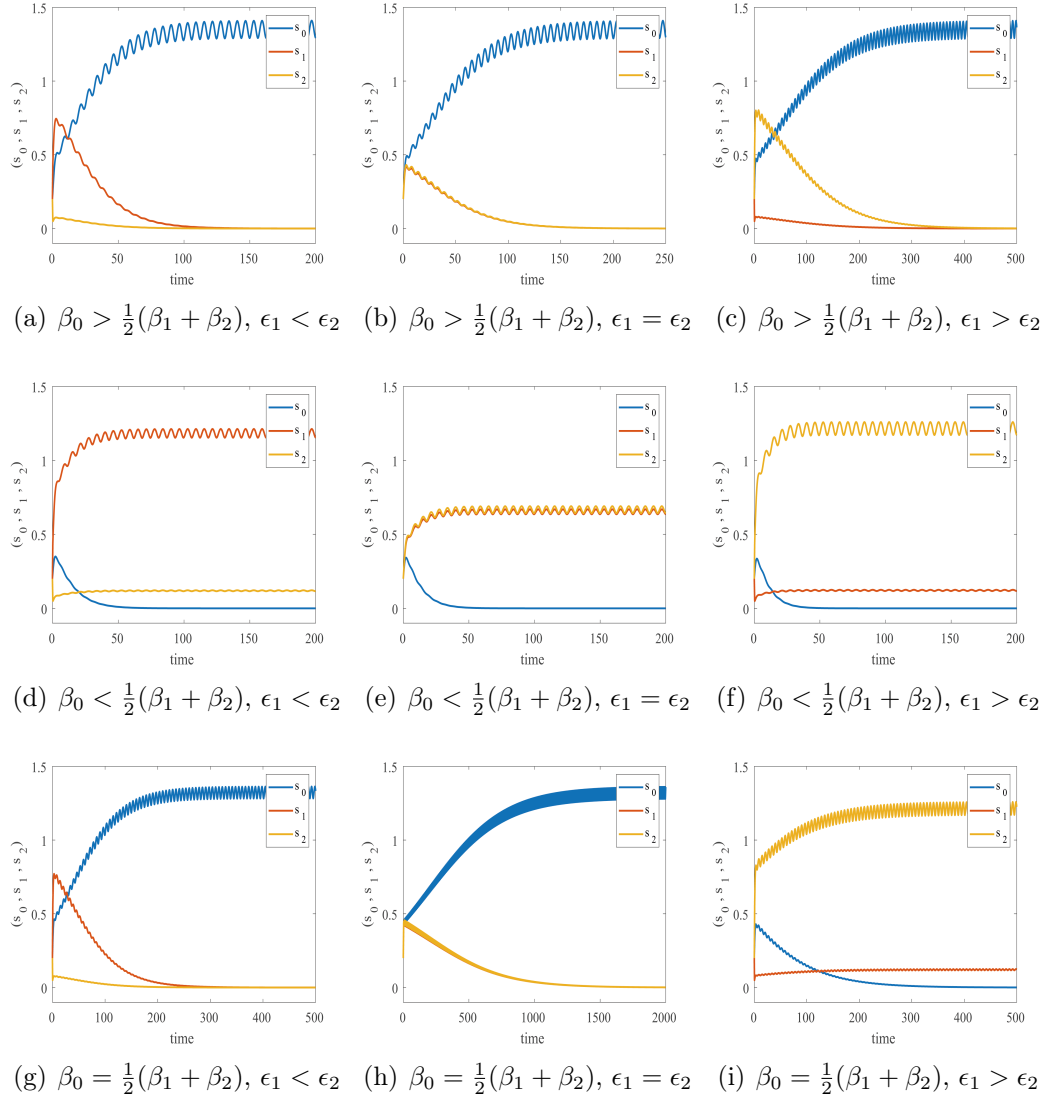


Figure 3.4: The Numerical graphs for the intrinsic dynamics of the fluctuating 3D bet-hedging model for  $(\beta_0 \neq \beta_1 \neq \beta_2)$ , with both strains having the same initial values  $(s_0(0) = s_1(0) = s_2(0) = 0.2)$ , with different values of  $r_0$  as; 0.8, 0.3 and 0.6 respectively, where as  $r_1 = 0.5$ , and  $r_2 = 0.7$  all through, with (a, d) and (g) having different transition rates values  $\epsilon_1 = 1$  and  $\epsilon_2 = 10$ , (b, e) and (h) having the same values of the transition rates  $\epsilon_1 = \epsilon_2 = 1$ , whereas (c, f) and (i) has different transition rates values as well  $\epsilon_1 = 10$  and  $\epsilon_2 = 1$ , with the amplitude value of fluctuation  $\delta = 0.25$ , and the frequency value of oscillation  $\omega = 1$ , and both plots show all the strains become stable at some points.

One important thing we observed in Figures 3.2 and 3.3, is the time ( $t$ ) at which the strains reached a steady state in both the non-fluctuating and the fluctuating environments. In the non-fluctuating environment, we noticed the strain reached the steady state in a shorter time ( $t$ ), unlike in the fluctu-

ating resources where it takes longer time ( $t$ ) to reach the steady state. This means, the fluctuating environment might slow down the eventual steady state behavior.

After all that has been investigated in this section (fluctuating environment), we also looked at what happened when both the non-switching ( $s_0$ ), and the switching ( $s_1, s_2$ ) strains have the same growth rates ( $\beta_i$ ) values, but not equal to the constant value in the strains growth rate (*i. e.*  $\beta_0 = \beta_1 = \beta_2 \neq 1$ ), with different values of the transition rates ( $\epsilon_i$ ) as well, and in the results we found the co-existence of all the three strains in each situation, which are exactly what were obtained in the non-fluctuating situation. As we mentioned in the non-fluctuating situation, we noticed that stability is lost at that point, and it is also a stability swapping point between the equilibrium points  $(s_0^*, 0, 0)$  and  $(0, s_1^*, s_2^*)$ , as shown in Figure 3.5.

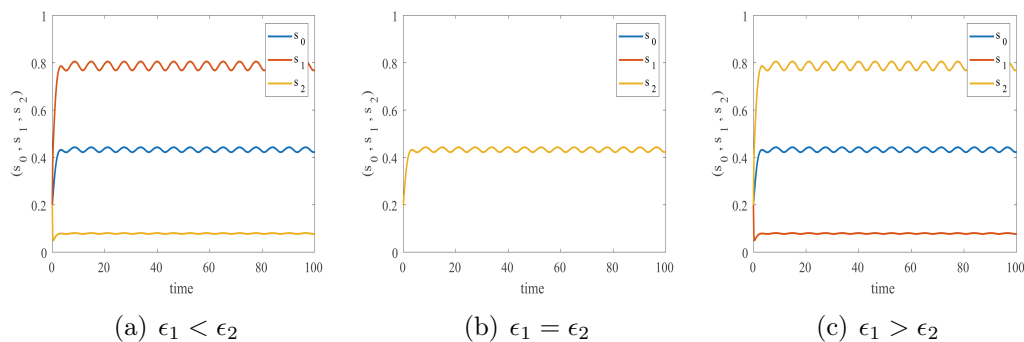


Figure 3.5: The Numerical graphs for the intrinsic dynamics of the 3D bet-hedging model for the fluctuating environment, when the growth rate ( $\beta_i$ ) of the strains are the same, but not equal to the constant value in their growth rates (*i. e.*  $\beta_0 = \beta_1 = \beta_2 \neq 1$ ), both strains having the same initial values [ $s_0(0) = s_1(0) = s_2(0) = 1$ ], the same growth rate values  $\beta_0 = \beta_1 = \beta_2 = 5$ , with (a) having different transition rates  $\epsilon_1 = 1$  and  $\epsilon_2 = 10$ , (b) having the same values of the transition rates  $\epsilon_1 = \epsilon_2 = 1$ , whereas (c) has different transition rates as well  $\epsilon_1 = 10$  and  $\epsilon_2 = 1$ , and both plots show the co-existence of all the strains, which is a special case.

This show even when the resources of the environment fluctuate, there is a loss of stability between the non-switching ( $s_0$ ) strain, and the switching ( $s_1, s_2$ ) strains. From the plots in Figure 3.5, we observed the stability is lost at that point, and the strain with the lower value of transition rate ( $\epsilon_i$ ) among the switching ( $s_1, s_2$ ) strains, has a high density at the steady state than the other, with both having the same (equal) growth rates ( $\beta_i$ ) values, which also strengthen the effect of the transition rate ( $\epsilon_i$ ) in the model.

## 3.6 Time Courses and Densities of Strains for Varying Values of the Parameters in the Fluctuating Environment

As we investigated in chapter 2, how the amplitude ( $\delta_i$ ) and the frequency ( $\omega$ ) parameters affects the behaviors of the switching ( $s_1, s_2$ ) strains in the fluctuating environment, we want to look at how they can affect them as well in this chapter 3, when the non-switching ( $s_0$ ) strain is introduced.

The same techniques (looking at the time courses of the strains against the varying values of the parameters) were applied here as well, to investigate the maximum and minimum densities of the strains, in order to identify if there is any change with the results obtained in chapter 2, before the non-switching ( $s_0$ ) strain is introduced, or if the results obtained are the same.

### 3.6.1 Time Courses and Densities of Strains for Varying Values of the Amplitude ( $\delta_i$ )

Not every plots of the time courses, for varying values of the amplitude ( $\delta_i$ ) in this section were displayed here, but some plots were displayed in order to show an insight of how the densities of either the maximum, or the minimum of the strains behaved.

#### 3.6.1.1 When the Value of $\beta_0$ is Less than the Average Value of $\beta_1$ and $\beta_2$ , [ $\beta_0 < \frac{1}{2}(\beta_1 + \beta_2)$ ]

In this section 3.6.1.1, we looked at some plots of the time courses for the densities of strains, which investigates the behavior of the strains against some varied values of the amplitude ( $\delta_i$ ), when the growth rate ( $\beta_i$ ) value of the non-switching ( $s_0$ ) strain is less than the average value of the switching ( $s_1, s_2$ ) strains as analyzed in equation (3.18).

The aim is to find out if the behavior of the strains will be like that of the non-fluctuating and the fluctuating situations as obtained in their intrinsic models in Figures 3.2 and 3.4 respectively, or if anything different exist.

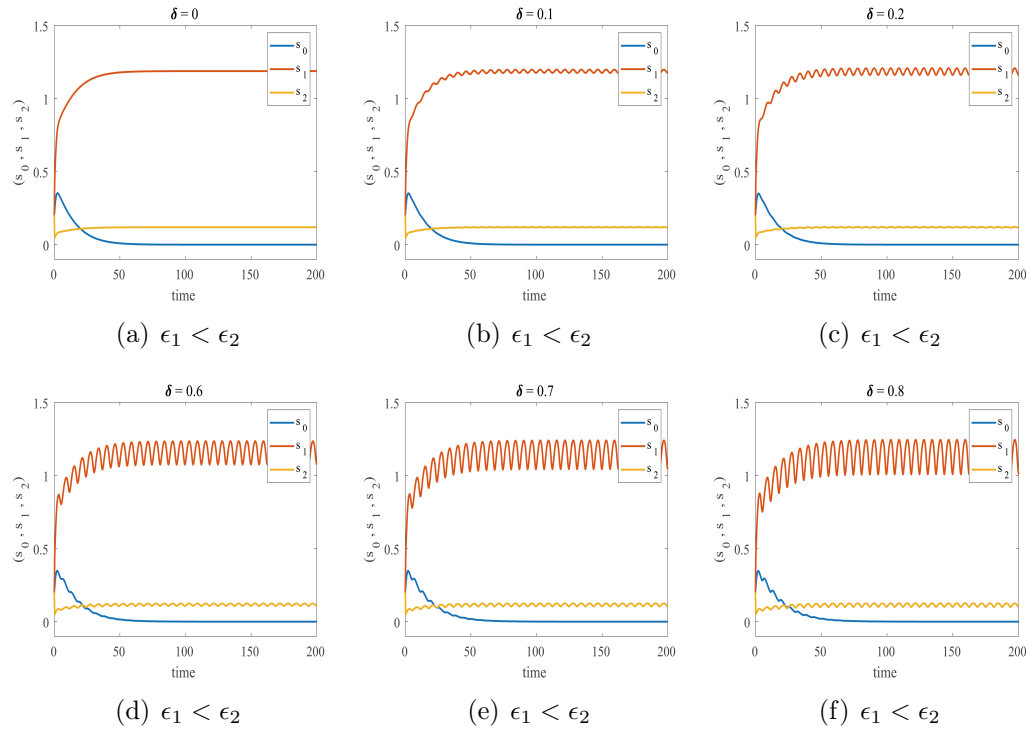


Figure 3.6: Time courses of strains for the 3D bet-hedging model with the fluctuating environment against the varying amplitude ( $\delta_i$ ) values with parameters;  $r_0 = 0.3$ ,  $r_1 = 0.5$ ,  $r_2 = 0.7$ , different transition rates values  $\epsilon_1 = 1$  and  $\epsilon_2 = 10$ , frequency value of fluctuation  $\omega = 1$ , and the initial values of the bacterial densities  $s_0(0) = s_1(0) = s_2(0) = 0.2$ , which show the non-switching strain ( $s_0$ ) can never invade.

Figure 3.6 show some plots for the time courses of strains, with some varying values of the amplitude ( $\delta_i$ ). Plots (a) to (f) in Figure 3.6 show exactly the same behavior with those obtained in the intrinsic models for the non-fluctuating and the fluctuating situations as well. The plots also showed the non-switching ( $s_0$ ) strain can never invade in this section no matter its initial value, but one of the switching ( $s_1$ ,  $s_2$ ) strains will have a high density at the steady state than the other, depending on their growth rate ( $\beta_i$ ) and the transition rate ( $\epsilon_i$ ) values as stated in the analysis of equation (3.18).

One interesting thing we noticed in the whole plots in Figure 3.6 is the ability of the existing strains to gain an increase in their densities once the value of the amplitude ( $\delta_i$ ) for the model under investigation is changed. But the growth is showing the bigger changes towards the minimum value of the density than its maximum value, which indicates the maximum density as being a threshold point that can't be exceeded by the growth of the existing strains.



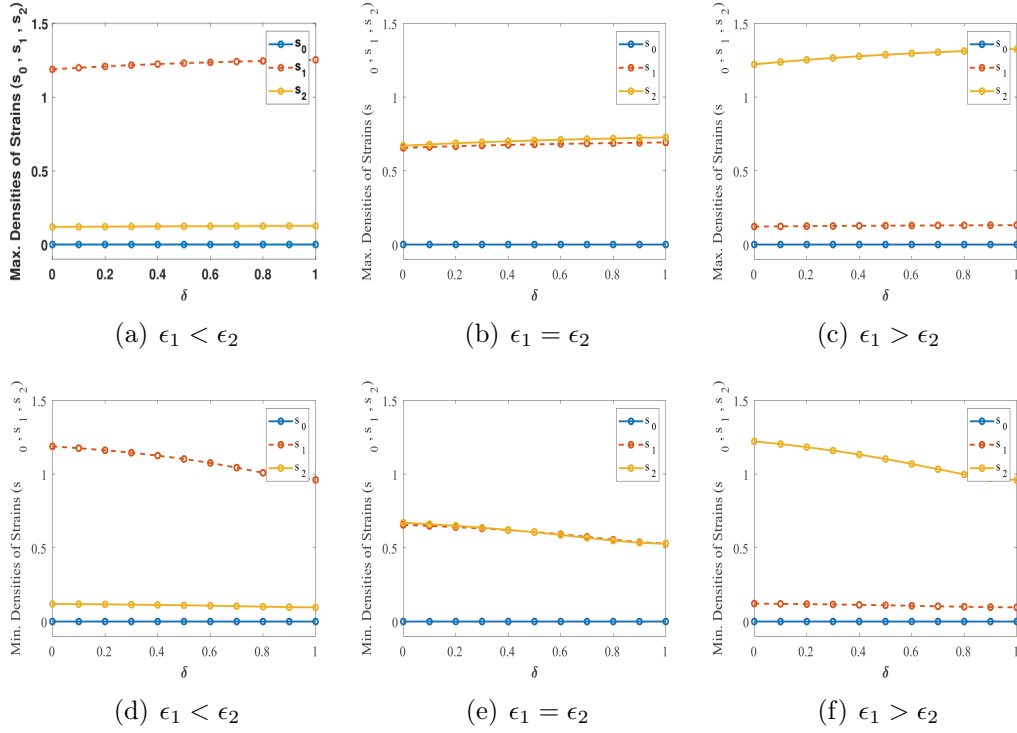


Figure 3.7: The maximum and minimum densities of strains for the 3D bet-hedging model with the fluctuating environment, against the varying amplitude ( $\delta_i$ ) values with parameters;  $r_0 = 0.3$ ,  $r_1 = 0.5$ ,  $r_2 = 0.7$ , plots (a) and (d) having different transition rate values  $\epsilon_1 = 1$ , and  $\epsilon_2 = 10$ , plots (b) and (e) having the same transition rate values  $\epsilon_1 = \epsilon_2 = 1$ , also plots (c) and (f) having different transition rate values as well  $\epsilon_1 = 10$  and  $\epsilon_2 = 1$ , with the frequency value of oscillation  $\omega = 1$ , and the initial values of the bacterial densities  $s_0(0) = s_1(0) = s_2(0) = 0.2$ , which show in the whole plots the non-switching ( $s_0$ ) strain can never invade.

The behaviors of the whole plots in Figure 3.6, which indicates the densities of the existing strains showing bigger changes towards the minimum than its maximum values were summarized in figure (7), where the densities (maximum and minimum) of the strains, with different values of the transition rates ( $\epsilon_i$ ) were plotted against the varied values of the amplitude ( $\delta_i$ ), to clearly figure out what was explained earlier in Figure 3.6.

In Figure 3.7, plots (a) to (f) show both the maximum and minimum densities of strains for the fluctuating model with varying values of the amplitude ( $\delta_i$ ), and with three different conditions of the transition rate ( $\epsilon_i$ ) values as well. Plots (a) and (d) show the maximum and minimum densities of the strains when  $\epsilon_1 < \epsilon_2$ , plots (b) and (e) also when  $\epsilon_1 = \epsilon_2$ , and finally plots (c) and (f) when  $\epsilon_1 > \epsilon_2$ .

The results of the whole plots obtained in Figure 3.7 show the minimums

were showing bigger changes than the maximum, and generally only a reasonable amount of amplitude ( $\delta_i$ ) is needed before changes occur. This means by changing the value of the amplitude ( $\delta_i$ ), the bacteria could keep growth from dropping off, but were unable to really boost it past a threshold, which also means the competition between the strains could probably prevent growth from getting too high.

### 3.6.1.2 When the Value of $\beta_0$ is Greater than the Average Value of $\beta_1$ and $\beta_2$ , [ $\beta_0 > \frac{1}{2}(\beta_1 + \beta_2)$ ]

In the above section 3.6.1.1, we looked at some plots of the time courses, with some varying values of the amplitude ( $\delta_i$ ) based on some conditions extracted from equation (3.18), which are the eigenvalues obtained from the non-zero equilibrium points ( $s_0^*$ , 0, 0) and (0,  $s_1^*$ ,  $s_2^*$ ). In this section 3.6.1.2, we did exactly like what was done in section 3.6.1.1, but with the reverse or opposite condition of the equation (3.18) that was investigated in section 3.6.1.1.

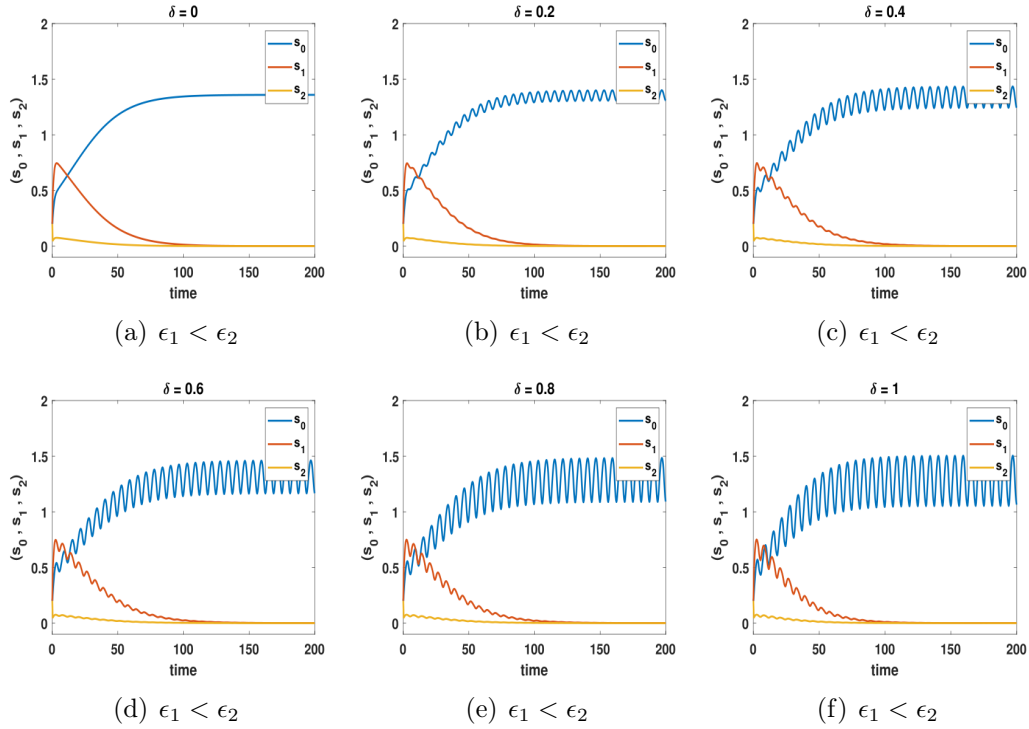


Figure 3.8: Time courses of strains for the 3D bet-hedging model with the fluctuating environment against the varying amplitude ( $\delta_i$ ) values with parameters;  $r_0 = 0.8$ ,  $r_1 = 0.5$ ,  $r_2 = 0.7$ , different values of the transition rates  $\epsilon_i$ , as  $i = 1$  and 10 respectively,  $\omega = 1$  and the initial values of the bacterial densities  $s_0(0) = s_1(0) = s_2(0) = 0.2$ , which show  $s_0$  can never be invaded.

In Figure 3.8 which is shown above, the whole plots produced the same results as those obtained with the intrinsic models, for both the non-fluctuating and the fluctuating situations. In the whole results we realized the non-switching ( $s_0$ ) strain can never be invaded no matter its initial value, or the values of the transition rates ( $\epsilon_i$ ) for the switching ( $s_1, s_2$ ) strains, which simply means the cycling does not change the behavior of the strains under this condition too.

As we noticed in section 3.6.1.1, there is always an increase in the density for the existing strains at the steady state if the value of the amplitude ( $\delta_i$ ) is changed. Likewise in this section 3.6.1.2, the increase is showing a bigger change in the minimum too as in section 3.6.1.1, even though the increase of the maximum density under this condition is slightly different than it appeared to be in section 3.6.1.1, (when the value  $\beta_0$  is less than the average value of  $\beta_1$  and  $\beta_2$ ).

Plots (a) to (f) in Figure 3.9 which are the plots for the densities of strains, against the varying values of the amplitude ( $\delta_i$ ), show the same pattern of behavior with the plots obtained in Figure 3.7, with the same values of the transition rates ( $\epsilon_1 < \epsilon_2$ ,  $\epsilon_1 = \epsilon_2$  and  $\epsilon_1 > \epsilon_2$ ). This is because in the intrinsic model equations, the  $s_0$  strain does not have any transition rate ( $\epsilon_i$ ) value associated to it, which makes the  $s_0$  strain to be the non-switching bacteria, and it indicates the bacteria could show a bigger change in its maximum density since the competition is within the non-switching ( $s_0$ ) strain itself, as we discovered in its time courses plots in Figure 3.8.

We can also conclude by saying, the whole plots obtained in Figure 3.9 were showing the minimum densities are having bigger changes than the maximum densities, and only a reasonable amount of the amplitude ( $\delta_i$ ) were needed before changes could occur as noticed in section 3.6.1.1, and also the cycling does not change the behavior of the strain in this condition too.

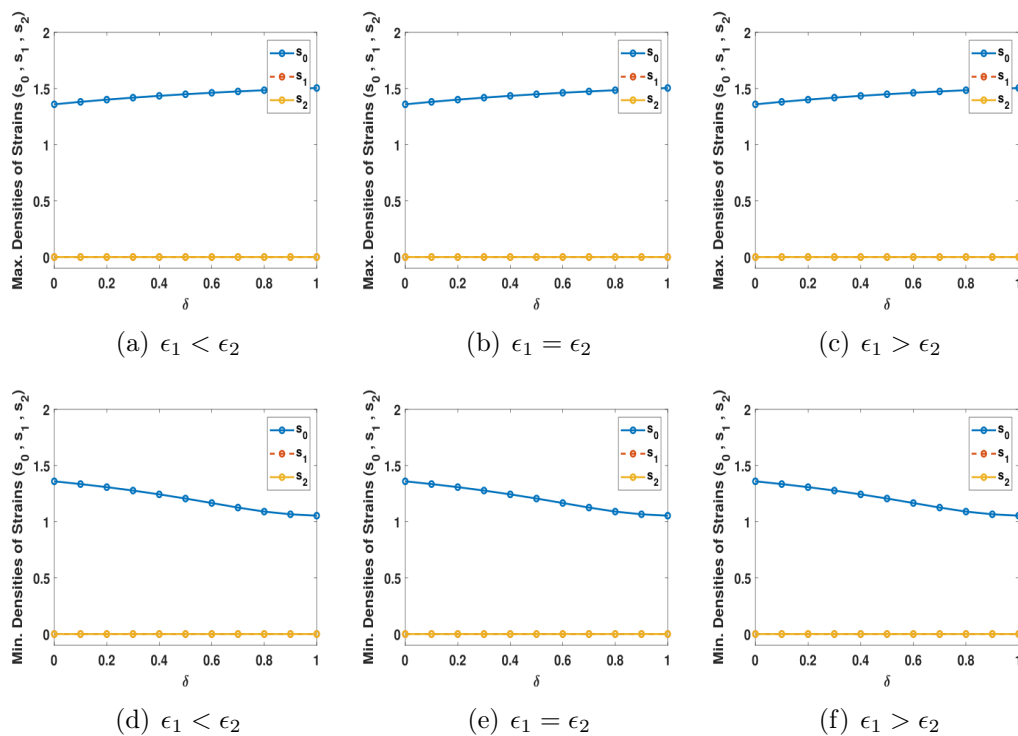


Figure 3.9: The maximum and minimum densities of strains for the 3D bet-hedging model with the fluctuating environment against the varying amplitude ( $\delta_i$ ) values with parameters;  $r_0 = 0.8$ ,  $r_1 = 0.5$ ,  $r_2 = 0.7$ , different conditions of transition rates ( $\epsilon_i$ ) as  $i = 1$  and  $10$  respectively,  $\omega = 1$  and the initial values of the bacterial densities  $s_0(0) = s_1(0) = s_2(0) = 0.2$ , which show  $s_0$  can never be invaded.

As mentioned earlier in this section, the maximums are showing bigger changes than it show in section 3.6.1.1, and this happened because the competition is only between the non-switching ( $s_0$ ) strain, and not with the switching ( $s_1, s_2$ ) strains, which makes the competition less intense than when the other strain were involved. This also means the bacteria could as well keep growth of the strains from dropping off, and were able to also really boost it much better than it does in section 3.6.1.1, but unfortunately couldn't boost it to a much more reasonable growth, which simply indicates the presence of competition within the non-switching strain alone has helped the  $s_0$  strain in improving its growth above what was noticed in section 3.6.1.1 but with not much difference.

The results obtained in this section 3.6.1.2 showed the effect of the transition rate ( $\epsilon_i$ ) value in the growth density for the existing strain is insignificant compared to their respective growth ( $\beta_i$ ) rate values. We also noticed the maximum and the minimum densities in Figure 3.9, with different values of the transition rate ( $\epsilon_i$ ) produced the same results, unlike what we obtained in

section 3.6.1.1. This also happened because the presence of the competition is between the existing strain, and not with the other strains.

### 3.6.1.3 When the Value of $\beta_0$ is Equal to the Average Value of $\beta_1$ and $\beta_2$ , [ $\beta_0 = \frac{1}{2}(\beta_1 + \beta_2)$ ]

Since we investigated what happened in sections 3.6.1.1 and 3.6.1.2 with different conditions, when [ $\beta_0 < \frac{1}{2}(\beta_1 + \beta_2)$ ] and when [ $\beta_0 > \frac{1}{2}(\beta_1 + \beta_2)$ ] respectively, and found out the results obtained were almost the same with those obtained in the non-fluctuating and the fluctuating situations, we then looked at what happened when [ $\beta_0 = \frac{1}{2}(\beta_1 + \beta_2)$ ], to find out if the results also match those obtained in the non-fluctuating and the fluctuating situations, or if at all there are some interesting results different from the ones obtained in the previous sections.

The same pattern/technique that were used previously in the investigations, by looking at the time courses of the said condition with some varying values of the amplitude ( $\delta_i$ ) first, and later on we summarized them with the idea of plotting the densities of their strains against the varying values of the amplitude ( $\delta_i$ ), to observe if there exists any differences with the results obtained or if there are not any differences were adhered to.

Based on what we observed in Figure 3.10, there is actually no any differences in the behavior of the existing strains with those obtained in Figure 3.8, because what we plotted in figure 3.10 only looked at one condition of the transition rates ( $\epsilon_1 < \epsilon_2$ ), but the results obtained in Figure 3.11 show the plots of the whole three conditions for the transition rates ( $\epsilon_i$ ) explicitly.

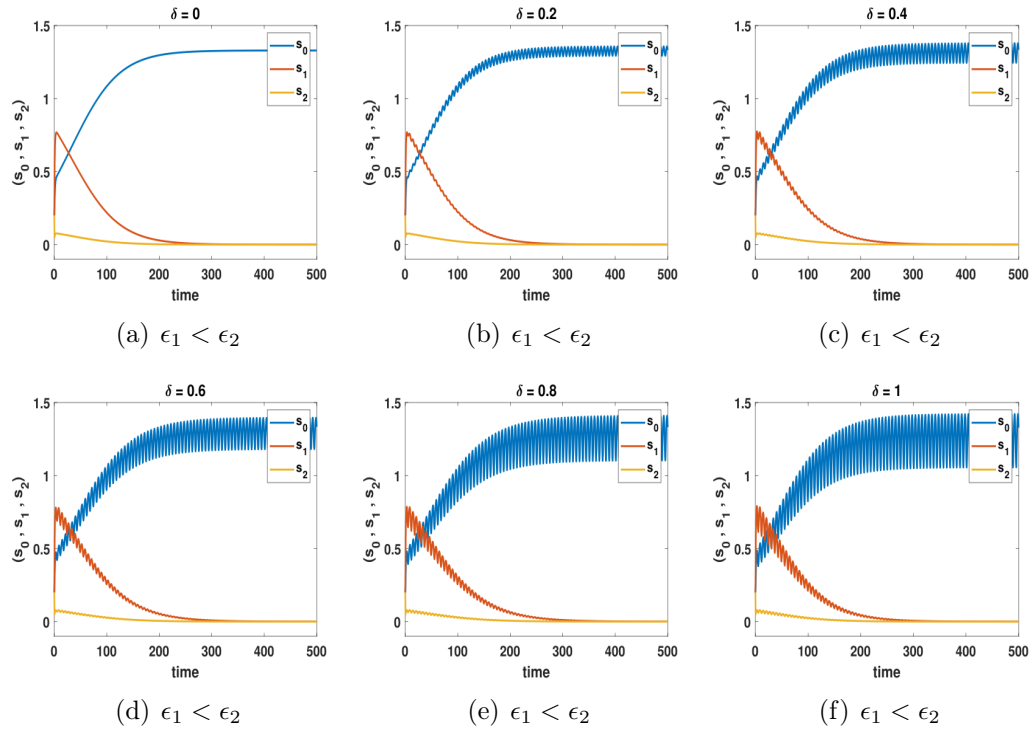


Figure 3.10: Time courses of strains for the 3D bet-hedging model with the fluctuating environment against the varying amplitude ( $\delta_i$ ) values with parameters;  $r_0 = 0.6$ ,  $r_1 = 0.5$ ,  $r_2 = 0.7$ , different values of the transition rates  $\epsilon_i$ , as  $i = 1$  and  $10$  respectively,  $\omega = 1$  and the initial values of the bacterial densities  $s_0(0) = s_1(0) = s_2(0) = 0.2$ .

Plots (g), (h) and (i) obtained in Figure 3.2 in this chapter 3, which are the plots for the non-fluctuating situation, that interprets equation (3.18) with the same condition in this section 3.6.1.3 show the non-switching ( $s_0$ ) strain only exists when  $\epsilon_1 < \epsilon_2$ , whereas in the same plots obtained in Figure 3.4, which are the plots for the fluctuating resources with the same condition again in this section show, the non-switching ( $s_0$ ) strain also exists when  $\epsilon_1 < \epsilon_2$ , and when  $\epsilon_1 = \epsilon_2$ . Likewise in this situation with the same conditions, the non-switching ( $s_0$ ) strain only exists when the transition rates are the same with those used in the fluctuating environment in Figure 3.4, that is when  $\epsilon_1 < \epsilon_2$  and  $\epsilon_1 = \epsilon_2$ , whereas the switching ( $s_1, s_2$ ) strains only exists when  $\epsilon_1 > \epsilon_2$ , which can be seen in Figure 3.11 below.

The interesting results we obtained in Figure 3.11 were on plots (b) and (e), where both the maximum and the minimum densities were showing decreases in the densities of their strains, which is completely different from what we usually obtained, though the minimum were showing the bigger changes than the maximum, which is the tradition we normally obtained in the previous

results.

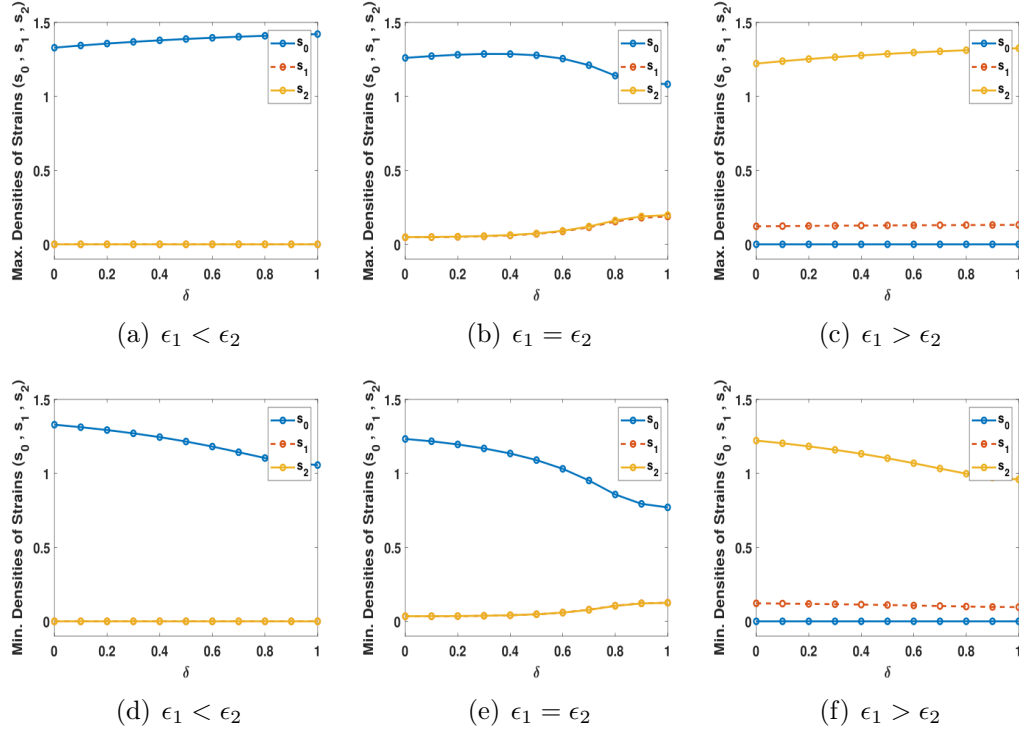


Figure 3.11: The maximum and minimum densities of strains for the 3D bet-hedging model in the fluctuating environment against the varying amplitude ( $\delta_i$ ) values with parameters;  $r_0 = 0.6$ ,  $r_1 = 0.5$ ,  $r_2 = 0.7$ , different conditions of transition rates ( $\epsilon_i$ ) as  $i = 1$  and  $10$  respectively,  $\omega = 1$  and the initial values of the bacterial densities  $s_0(0) = s_1(0) = s_2(0) = 0.2$ .

This simply means the cycling only changed the behavior of the strains in the fluctuating environment for  $\epsilon_1 = \epsilon_2$ , but it doesn't change it for the other conditions of the transition rates ( $\epsilon_i$ ) values. It also showed the bacteria only kept the growth of the strains from dropping off for the mentioned conditions of the transition rate ( $\epsilon_i$ ) values. But for the other two different conditions of the transition rate ( $\epsilon_i$ ) values, it boosted densities up insignificantly, and only needs a relatively high degree of fluctuation to change the behavior of the result substantially.

### 3.6.1.4 When the Values of $\beta_0$ , $\beta_1$ and $\beta_2$ are Equal but not a Constant Value in the Strains Growth Rate, [ $\beta_0 = \beta_1 = \beta_2 \neq 1$ ]

Recall that in sections 3.6.1.1, 3.6.1.2, and 3.6.1.3 above, we investigated the behaviors of the strains against the varying values of amplitude ( $\delta_i$ ) parameter, when the value of  $\beta_0$  is respectively greater than, less than, and even equal to the average values of  $\beta_1$  and  $\beta_2$ . In this section 3.6.1.4, we want to investigate the behaviors of the strains when they all have the same (equal) values, but not equal to the constant value in the strains growth rates ( $\beta_0 = \beta_1 = \beta_2 \neq 1$ ).

In both the non-fluctuating and the fluctuating situations, we spotted the existences of all the three strains ( $s_0$ ,  $s_1$ ,  $s_2$ ) at the steady state, which show at this point there is a lost of stability, and it is a stability swapping point between the non-zero equilibrium points ( $s_0^*$ , 0, 0) and (0,  $s_1^*$ ,  $s_2^*$ ), as they appeared in the plots of Figure 3.3 and 3.5 respectively.

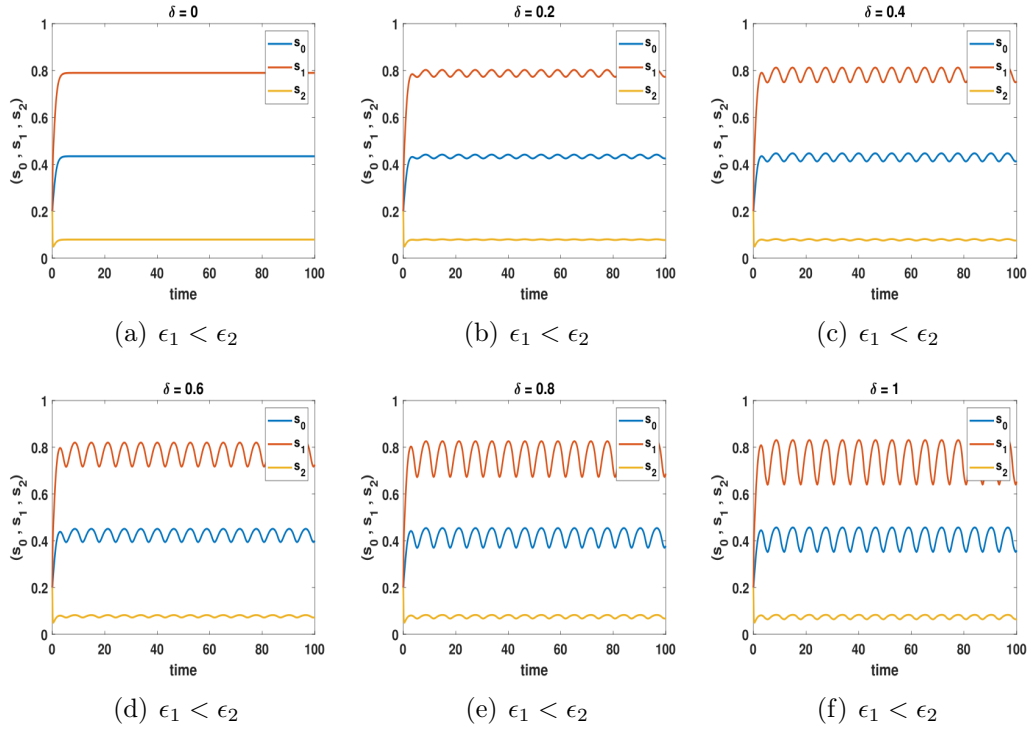


Figure 3.12: Time courses of strains for the 3D bet-hedging model in the fluctuating environment against the varying amplitude ( $\delta_i$ ) values with parameters;  $r_0 = r_1 = r_2 = 0.5$ , different values of the transition rates  $\epsilon_i$ , as  $i = 1$  and 10 respectively,  $\omega = 1$  and the initial values of the bacterial densities  $s_0(0) = s_1(0) = s_2(0) = 0.2$ , which show the co-existence of all the strains.

The plots in Figure 3.12 show nothing is different with the results obtained in the previous sections with the same situations. The only differences noticed



between the plots obtained in Figures 3.3 and 3.5, and the results obtained in Figure 3.12, are the same differences that were seen in the previous conditions for varying values of the amplitude ( $\delta_i$ ), where the densities of the existing strains were subject to the different values of the amplitude ( $\delta_i$ ).

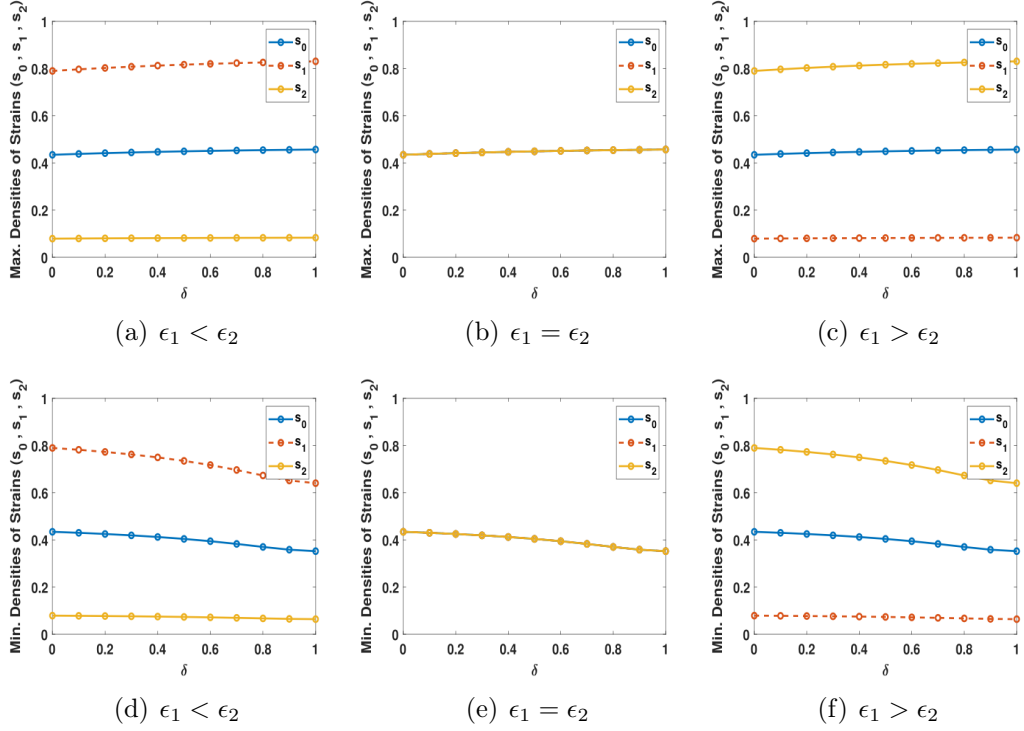


Figure 3.13: The maximum and minimum densities of strains for the 3D bet-hedging model in the fluctuating environment against the varying amplitude ( $\delta_i$ ) values with parameters;  $r_0 = r_1 = r_2 = 0.5$ , different conditions of the transition rates ( $\epsilon_i$ ), as  $i = 1$  and  $10$  respectively,  $\omega = 1$  and the initial values of the bacterial densities  $s_0(0) = s_1(0) = s_2(0) = 0.2$ , which show the co-existence of all the strains.

The plots in Figure 3.13 show the maximum and the minimum densities of strains, when their values of growth rates ( $\beta_i$ ) are equal, and the results obtained show nothing much different compared to what were obtained in the previous sections. If we observe the behavior of the plots, we could notice the bacteria could only keep the growth densities of the strains from dropping off, and were unable to boost it up significantly above a certain threshold, as were seen in the previous plots. This means the cycling does not change the behavior of the strains in this situation, as it happened in the previous situation.

### 3.6.2 Time Courses and Densities of Strains for Varying Values of frequency ( $\omega$ )

Having extensively investigated the behaviors of the strains densities with varying amplitude ( $\delta_i$ ) values, we then looked at the behaviors of the strains densities with varying frequency ( $\omega$ ) values as well, to clarify which among the two parameters can bring any changes in the behaviors of the existing strains at the steady state, when compared with the results obtained from the non-fluctuating and the fluctuating resources.

The same procedures which were used in determining the time courses, and the densities of the strains in section 3.6.1, were also adopted and used in this section 3.6.2.

#### 3.6.2.1 When the Value of $\beta_0$ is Less than the Average Value of $\beta_1$ and $\beta_2$ , [ $\beta_0 < \frac{1}{2}(\beta_1 + \beta_2)$ ]

As mentioned earlier in the section 3.6.1.1, we don't want to present the whole plots for the time courses of the strains for ambiguity, but rather choose to select few of them and present them for clarity, which were later summarized when plotting the densities of the strains against the varying values of the respective parameter in concern.

In Figure 3.14, some plots of the time courses with different values of the frequency ( $\omega$ ) were presented, and the whole plots were showing the non-switching ( $s_0$ ) strain can never invade in this circumstance, which were the same pattern of results obtained for both the non-fluctuating and the fluctuating resources, and also for the densities of the strains with varying amplitude ( $\delta_i$ ) values.

We also noticed the plots show no differences in the amplitudes ( $\delta_i$ ) of the existing strains at the steady state, when the frequency ( $\omega$ ) values were changed, but the number of oscillations in any given time frame were doubled. This means, when the value of the frequency ( $\omega$ ) is increased, the number of oscillations within a particular given time frame were increased too, unlike when the value of the amplitude ( $\delta_i$ ) is increased in section 3.6.1, where the densities of the existing strains also increases, but the number of oscillations remain the same as well.

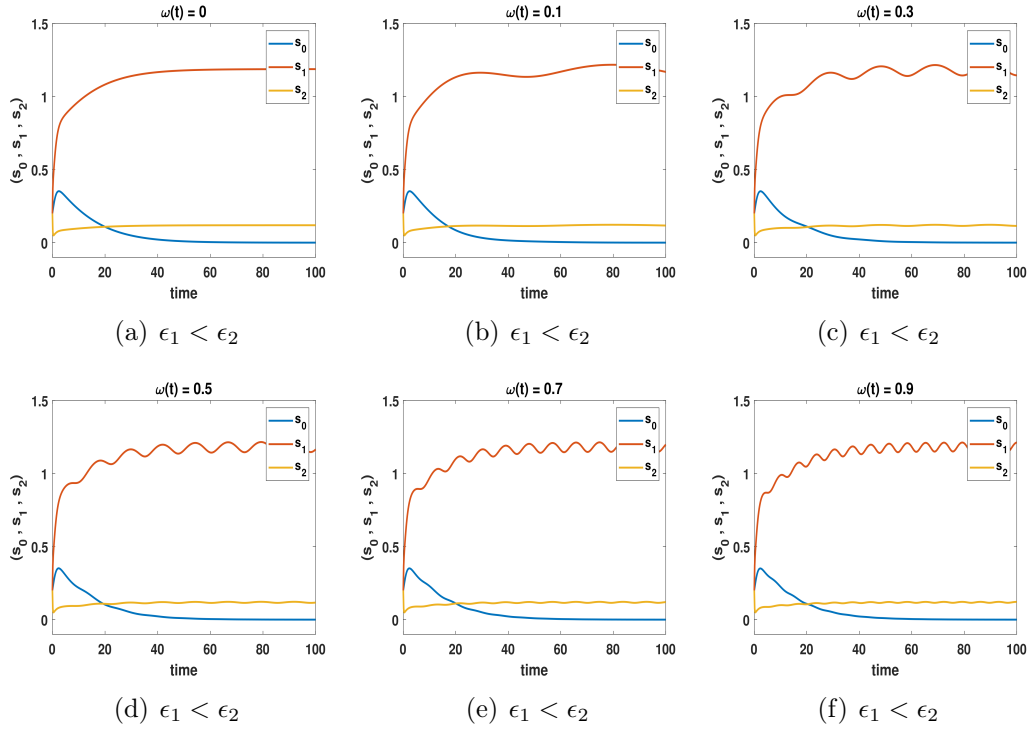


Figure 3.14: Time courses of strains for the 3D bet-hedging model in the fluctuating environment against the varying frequency ( $\omega$ ) values with parameters;  $r_0 = 0.3$ ,  $r_1 = 0.5$ ,  $r_2 = 0.7$ , different values of the transition rates  $\epsilon_i$ , as  $i = 1$  and  $10$  respectively,  $\delta = 0.25$  and the initial values of the bacterial densities  $s_0(0) = s_1(0) = s_2(0) = 0.2$ , which show  $s_0$  can never invade.

The plots obtained in Figure 3.14, and those not presented in the figure were all summarized in Figure 3.15, which plotted the maximum and the minimum densities of the strains against the varying frequency ( $\omega$ ) value, and the results obtained show different patterns with the results obtained in the previous sections in this chapter. The main difference noticed is a slight peak at the lowest values of the frequency ( $\omega$ ) which is exactly the same result obtained in chapter 2 for varying values of the frequency ( $\omega$ ), which seems there is a little interaction between the forcing and the dynamics, which is interesting in itself. This tell us the frequency ( $\omega$ ) makes more difference when  $r_0$  is relatively low.

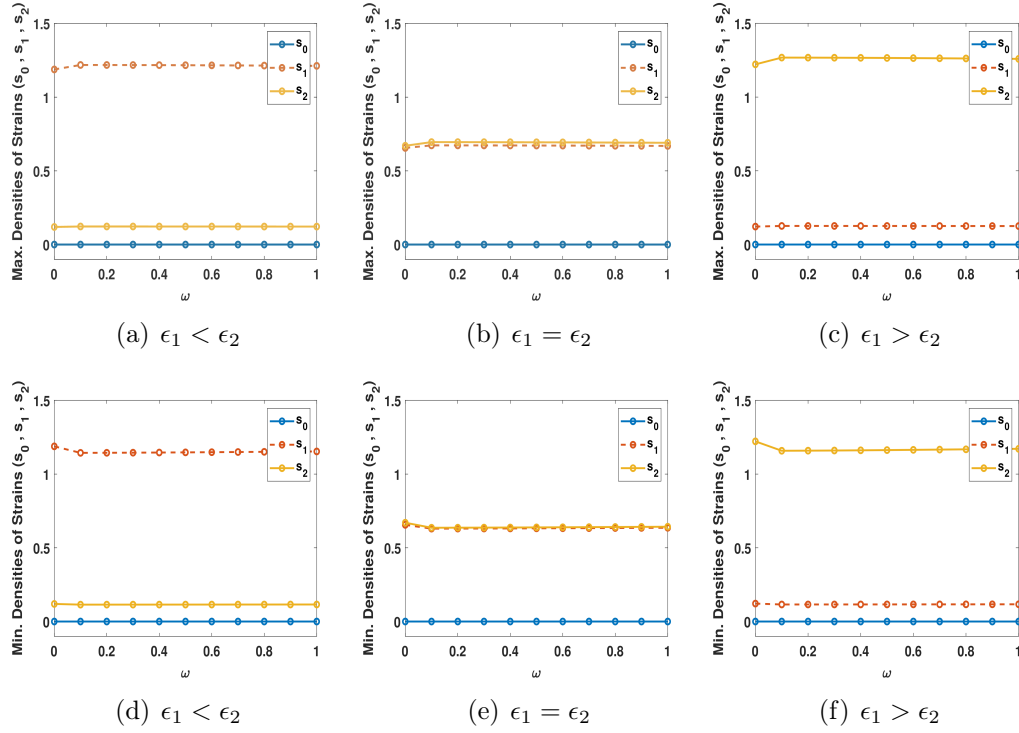


Figure 3.15: The maximum and minimum densities of strains for 3D bet-hedging model in the fluctuating environment against the varying frequency ( $\omega$ ) values with parameters;  $r_0 = 0.3$ ,  $r_1 = 0.5$ ,  $r_2 = 0.7$ , different conditions of the transition rates ( $\epsilon_i$ ), as  $i = 1$  and  $10$  respectively,  $\delta = 0.25$  and the initial values of the bacterial densities  $s_0(0) = s_1(0) = s_2(0) = 0.2$ , which show  $s_0$  can never invade.

### 3.6.2.2 When the Value of $\beta_0$ is Greater than the Average Value of $\beta_1$ and $\beta_2$ , [ $\beta_0 > \frac{1}{2}(\beta_1 + \beta_2)$ ]

In this section 3.6.2.2, we looked at the reverse condition for the strains growth densities with the varying values of the frequency ( $\omega$ ) just discussed in section 3.6.2.1 above, and the results obtained in Figure 3.16 were the same with the results obtained in Figure 3.8, which show the non-switching ( $s_0$ ) strain can never be invaded in this circumstance, and the results obtained are the same with what were obtained in the non-fluctuating and the fluctuating resources in Figure 3.2 and 3.4 respectively.

We also noticed the same pattern of results were obtained in Figure 3.14 and 3.16, which show once a frequency ( $\omega$ ) value is increased, the number of oscillations at the steady state for the existing strain at a particular time also increases, but the amplitude ( $\delta_i$ ) of oscillations at the steady state for the existing strain does not change at all.

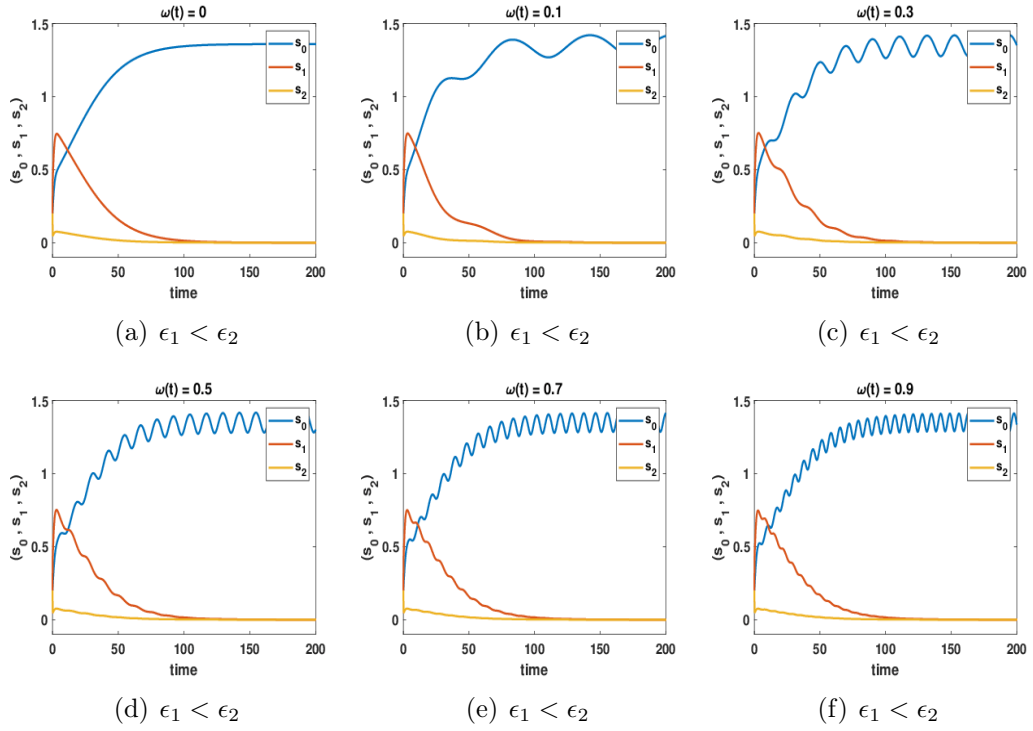


Figure 3.16: Time courses of strains for the 3D bet-hedging model in the fluctuating environment against the varying frequency ( $\omega$ ) values with parameters;  $r_0 = 0.8$ ,  $r_1 = 0.5$ ,  $r_2 = 0.7$ , different values of the transition rates  $\epsilon_i$ , as  $i = 1$  and  $10$  respectively,  $\delta = 0.25$  and the initial values of the bacterial densities  $s_0(0) = s_1(0) = s_2(0) = 0.2$ , which show  $s_0$  can never be invaded.

The whole plots in Figures 3.9 and 3.17 show the same pattern of results as well, meaning the differences in the transition rate ( $\epsilon_i$ ) values does not change the behavior of the existing strain at the steady state, since the existing strain on this condition does not switch (change) at all. This simply means, by increasing the values of the frequency ( $\omega$ ), the bacteria only boosts its growth at the early time (relatively lowest value), but subsequently maintains its growth density uniformly.

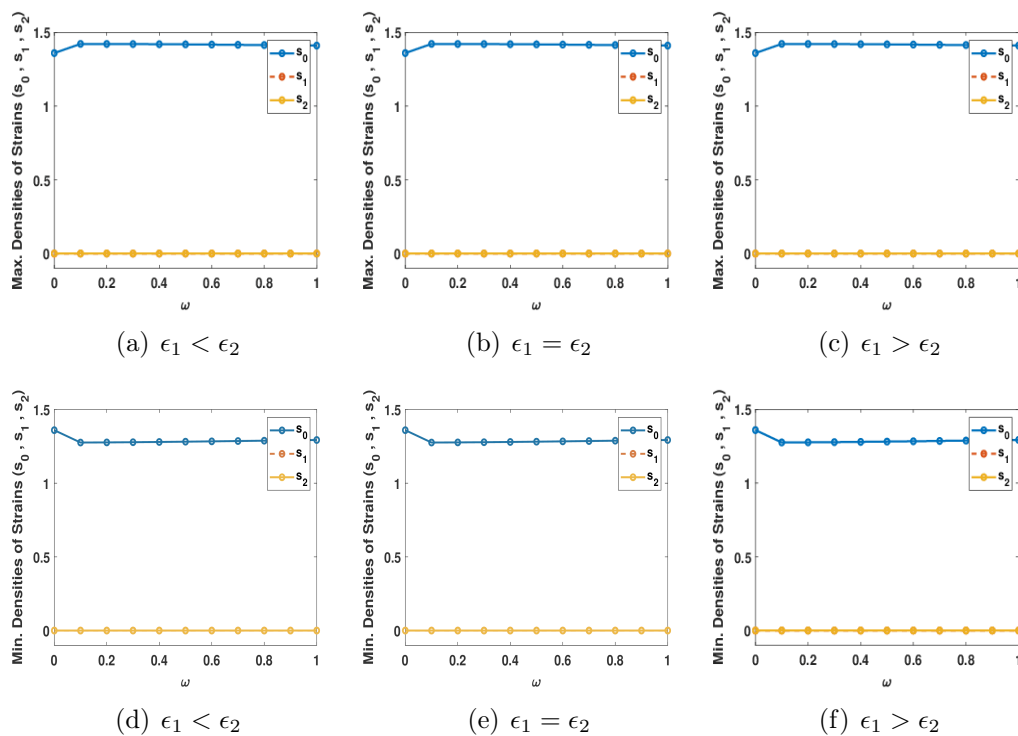


Figure 3.17: The maximum and minimum densities of strains for 3D bet-hedging model in the fluctuating environment against the varying frequency ( $\omega$ ) values with parameters;  $r_0 = 0.8$ ,  $r_1 = 0.5$ ,  $r_2 = 0.7$ , different conditions of the transition rates ( $\epsilon_i$ ), as  $i = 1$  and  $10$  respectively,  $\delta = 0.25$  and the initial values of the bacterial densities  $s_0(0) = s_1(0) = s_2(0) = 0.2$ , which show  $s_0$  can never be invaded.

### 3.6.2.3 When the Value of $\beta_0$ is Equal to the Average Value of $\beta_1$ and $\beta_2$ , [ $\beta_0 = \frac{1}{2}(\beta_1 + \beta_2)$ ]

In this section 3.6.2.3, we considered the growth rate of the non-switching ( $s_0$ ) strain to be equal to the average value of the switching ( $s_1, s_2$ ) strains. Thus, giving us an opportunity to observe the behavior of the existing strains at the steady state, whether they followed the same pattern of behavior, like what were observed in the previous sections, or something different can be obtained.

By carefully observing the whole plots in Figure 3.18, the same pattern of results were obtained with those obtained in Figure 3.16, and this happened because the plots have the same transition rate ( $\epsilon_i$ ) values, with slight differences in the existing strains densities at the steady state, which is caused by the differences in the non-switching ( $s_0$ ) strain growth rate values in the two cases. The densities for the existing strains were uniformly maintained at the steady state, except at the early time (relatively lower values) where there is a rapid growth to the peak, which is exactly the same pattern of growth

obtained in Figure 3.16, with some differences in the results when the values of the transition rates ( $\epsilon_i$ ) differ with those used in this section.

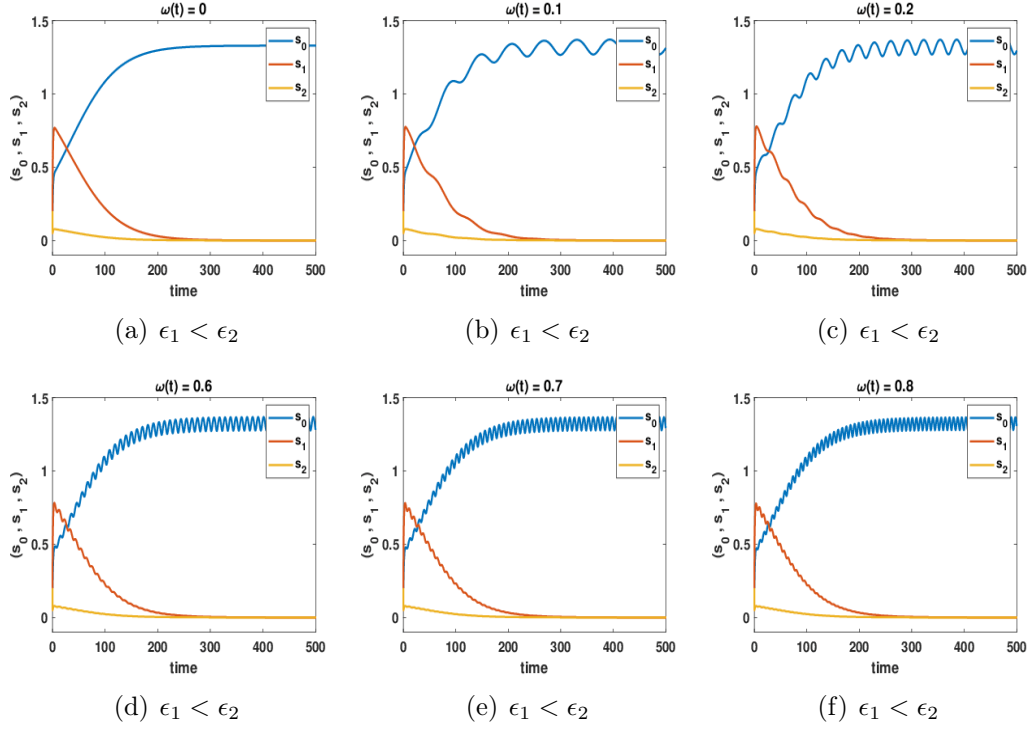


Figure 3.18: Time courses of strains for the 3D bet-hedging model in the fluctuating environment against the varying frequency ( $\omega$ ) values with parameters;  $r_0 = 0.6$ ,  $r_1 = 0.5$ ,  $r_2 = 0.7$ , different values of the transition rates  $\epsilon_i$ , as  $i = 1$  and  $10$  respectively,  $\delta = 0.25$  and the initial values of the bacterial densities  $s_0(0) = s_1(0) = s_2(0) = 0.2$ .

The whole plots obtained in Figures 3.4, 3.11 and 3.19 show the same pattern of results, with the non-switching ( $s_0$ ) strain existing when  $\epsilon_1 < \epsilon_2$ , and  $\epsilon_1 = \epsilon_2$  because of the fluctuations in those environments, but the plots for the non-fluctuating situation in Figure 3.2 show, the non-switching ( $s_0$ ) strain only exists when  $\epsilon_1 < \epsilon_2$ .

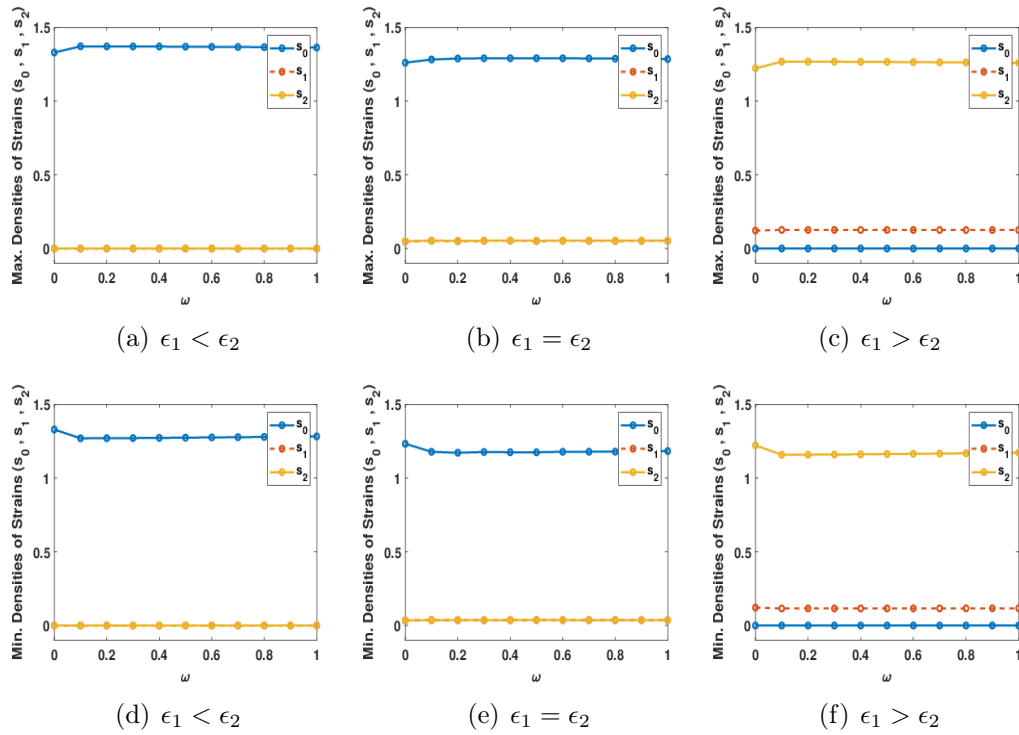


Figure 3.19: The maximum and minimum densities of strains for 3D bet-hedging model in the fluctuating environment against the varying frequency ( $\omega$ ) values with parameters;  $r_0 = 0.6$ ,  $r_1 = 0.5$ ,  $r_2 = 0.7$ , different conditions of the transition rates ( $\epsilon_i$ ), as  $i = 1$  and  $10$  respectively,  $\delta = 0.25$  and the initial values of the bacterial densities  $s_0(0) = s_1(0) = s_2(0) = 0.2$ .

There are some interesting results observed with plots (b) and (e) obtained in Figure 3.20, with a shorter varying frequency ( $\omega$ ) values ( $0 < \omega = 0.1$ ), where the densities for the existing  $s_0$  strain do fluctuate at the lowest frequency ( $\omega$ ) value, which was not observed in the other plots. This creates an avenue for the bacteria to boost its densities from dropping, but the forcing and the dynamics makes it drop as well.



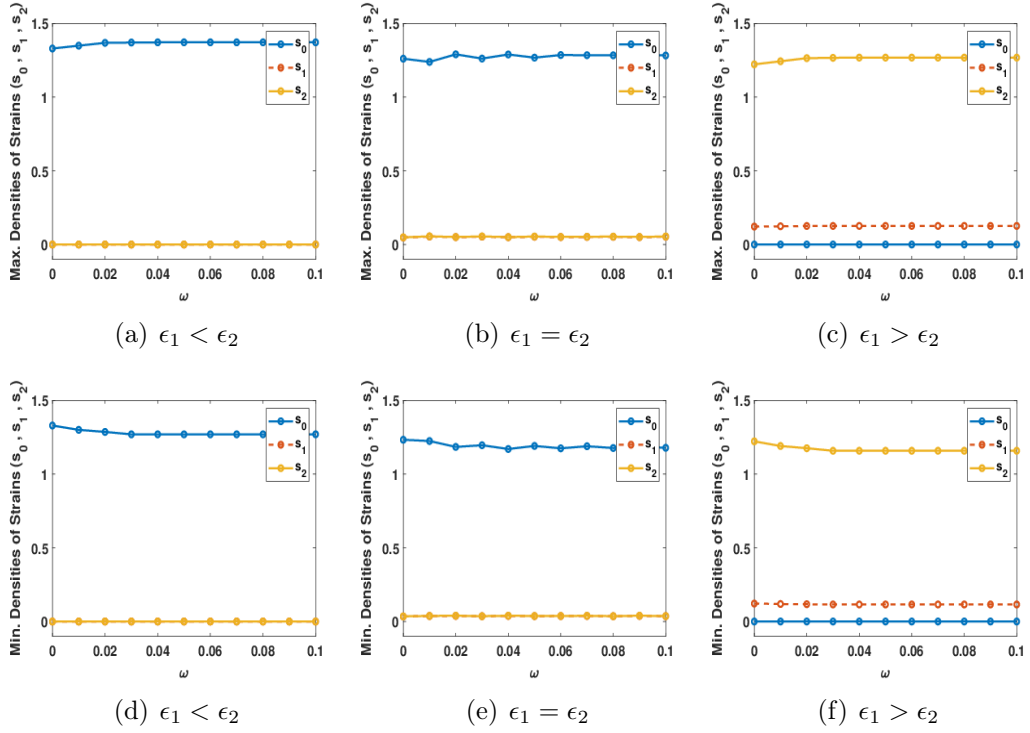


Figure 3.20: The maximum and minimum densities of strains for 3D bet-hedging model in the fluctuating environment against the varying frequency ( $\omega$ ) values with parameters;  $r_0 = 0.6$ ,  $r_1 = 0.5$ ,  $r_2 = 0.7$ , different conditions of the transition rates ( $\epsilon_i$ ), as  $i = 1$  and  $10$  respectively,  $\delta = 0.25$  and the initial values of the bacterial densities  $s_0(0) = s_1(0) = s_2(0) = 0.2$ .

### 3.6.2.4 When the Values of $\beta_0$ , $\beta_1$ and $\beta_2$ are Equal but not a Constant Value, [ $\beta_0 = \beta_1 = \beta_2 \neq 1$ ]

The last aspect we considered in this chapter 3 is when the growth rate ( $\beta_i$ ) values for the non-switching ( $s_0$ ), and the switching ( $s_1$ ,  $s_2$ ) strains are equal, but not equal to a constant value in the strains growth rates ( $\beta_0 = \beta_1 = \beta_2 \neq 1$ ), with varying frequency ( $\omega$ ) values, to also observe if there is anything interesting, which might be different from what were observed in the previous sections with varying frequency ( $\omega$ ) values, or if the same pattern of result will be obtained as well.

By carefully observing the whole plots respectively obtained in Figures 3.3, 3.5 and 3.12, we noticed there is no any difference with the results obtained in Figure 3.21. This clearly show stability is lost at this point, and it is also a stability swapping point between the equilibrium points  $(s_0^*, 0, 0)$  and  $(0, s_1^*, s_2^*)$ .

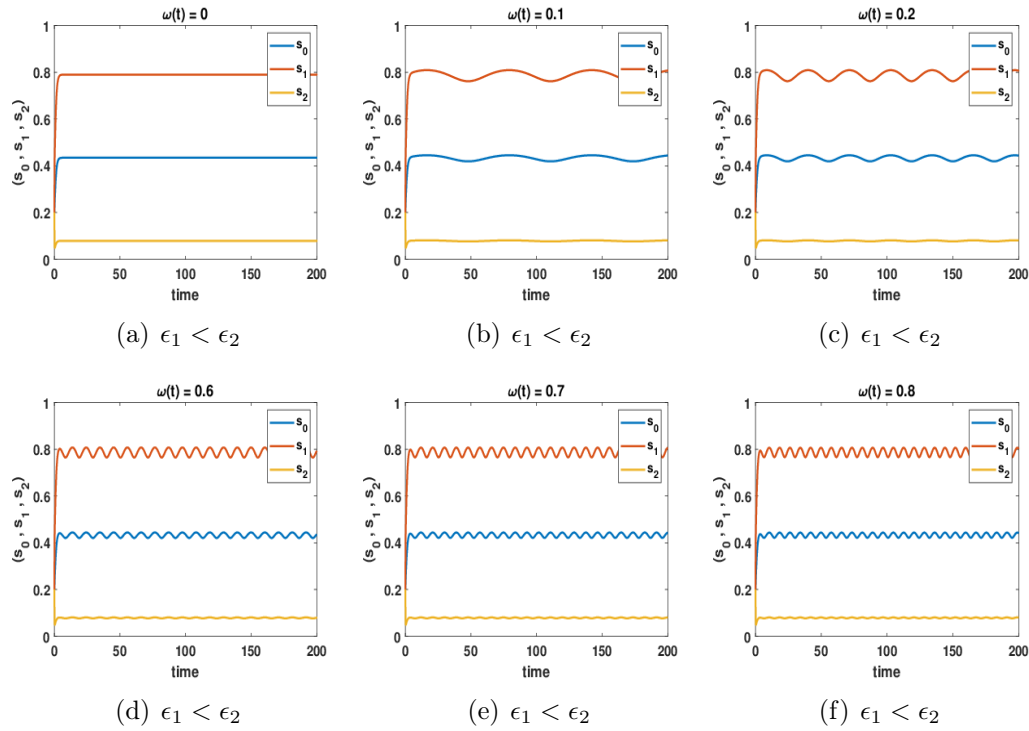


Figure 3.21: Time courses of strains for 3D bet-hedging model in the fluctuating environment against the varying frequency ( $\omega$ ) values with parameters;  $r_0 = r_1 = r_2 = 0.5$ , different values of the transition rates  $\epsilon_i$ , as  $i = 1$  and 10 respectively,  $\delta = 0.25$  and the initial values of the bacterial densities  $s_0(0) = s_1(0) = s_2(0) = 0.2$ , which show the co-existence of all the strains.

Amazingly, the results obtained in Figure 3.13, were having the same pattern of behavior with the results obtained in Figure 3.22. The major differences between the two figures centered on the earlier figure, showing bigger changes in the minimum densities, whereas the latter show no much differences between the maximum and the minimum densities.

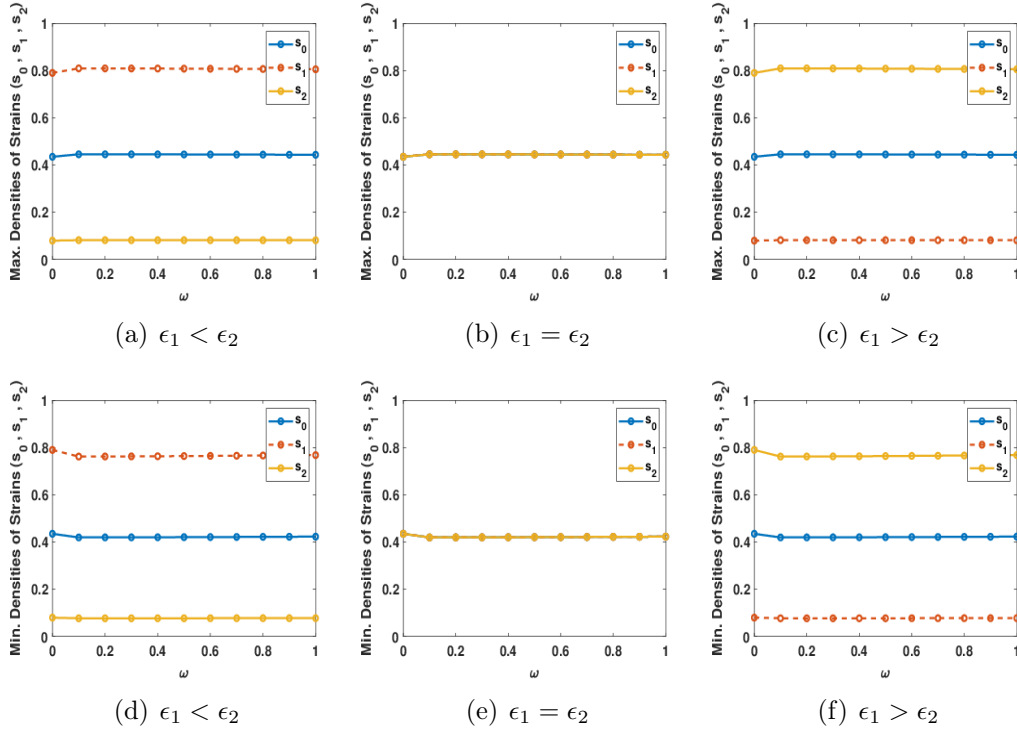


Figure 3.22: The maximum and minimum densities of strains for 3D bet-hedging model in the fluctuating environment against the varying frequency  $(\omega)$  values with parameters;  $r_0 = r_1 = r_2 = 0.5$ , different conditions of transition rates  $(\epsilon_i)$ , as  $i = 1$  and  $10$  respectively,  $\delta = 0.25$  and the initial values of the bacterial densities  $s_0(0) = s_1(0) = s_2(0) = 0.2$ , which show the co-existence of all the strains.

### 3.7 Conclusion

In this chapter we have included the constant ( $s_0$ ) strain to the existing switching ( $s_1, s_2$ ) strains in the model studied in chapter 2, and the results obtained in this chapter after solving the system of the model equations, produced two equilibrium points in the non-fluctuating environment, a zero  $(s_0^*, s_1^*, s_2^*) = (0, 0, 0)$ , and the non-zero  $(s_0^*, s_1^*, s_2^*) = \left(s_0, \frac{(\beta-s_0)\epsilon_2}{\epsilon_T}, \frac{(\beta-s_0)\epsilon_1}{\epsilon_T}\right)$  equilibrium point. The results indicate the strains can't settle at the zero equilibrium point, but they (strains) do always becomes stable at the non-zero equilibrium points in any situation. This means, the existence strain(s) at the steady state might be either a non-switching ( $s_0$ ) strain alone, or might be the switching ( $s_1, s_2$ ) strains alone, or might even be the presence of both the non-switching ( $s_0$ ) and the switching ( $s_1, s_2$ ) strains, depending on their growth rates  $(\beta_i)$ , and the transition rates  $(\epsilon_i)$  values as well. The growth rates  $(\beta_i)$  and the transition rates  $(\epsilon_i)$  values, always determines which among the switching ( $s_1, s_2$ ) strains

will have a high density at the steady state than the other in any situation. Meaning, which among the switching strain performs better or worse in any environment as mentioned earlier.

There is co-existence of both the constant ( $s_0$ ), and the bet-hedgers ( $s_1, s_2$ ) strains when their growth rate values are equal (*i. e.*  $\beta_0 = \beta_1 = \beta_2 = \beta$ ) in any environment, which is a special case and for the vast majority of time, there can be no co-existence. This show stability is lost at that point, and it is a stability swapping point between the non-zero's ( $s_0^*, 0, 0$ ) and ( $0, s_1^*, s_2^*$ ) equilibrium points, but more generally only one type of strain can win at a time, which sometimes depends on its growth ( $\beta_i$ ) and the transition ( $\epsilon_i$ ) rates values as well. This co-existence of the constant ( $s_0$ ) and bet-hedgers ( $s_1, s_2$ ) strains at the same time is very unlikely.

The interesting results noticed in both the non-fluctuating and the fluctuating situations are the non-switching ( $s_0$ ) strain can never invade when the value of  $\beta_0$  is less than the average value of  $\beta_1$  and  $\beta_2$ , that is [ $\beta_0 < \frac{1}{2}(\beta_1 + \beta_2)$ ], and it can never be invaded when the value of  $\beta_0$  is greater than the average value of  $\beta_1$  and  $\beta_2$ , that is [ $\beta_0 > \frac{1}{2}(\beta_1 + \beta_2)$ ] in any environment. But, when the value of  $\beta_0$  is equal to the average value of  $\beta_1$  and  $\beta_2$ , that is [ $\beta_0 = \frac{1}{2}(\beta_1 + \beta_2)$ ], the non-switching ( $s_0$ ) strain only exists when  $\epsilon_1 < \epsilon_2$ , where as the switching ( $s_1, s_2$ ) strains do exists when  $\epsilon_1 = \epsilon_2$ , and  $\epsilon_1 > \epsilon_2$  in the non-fluctuating environment. In the fluctuating environment, the non-switching ( $s_0$ ) strain does exist when  $\epsilon_1 < \epsilon_2$  and  $\epsilon_1 = \epsilon_2$ , while the switching ( $s_1, s_2$ ) strains only exist when  $\epsilon_1 > \epsilon_2$ , and in either case, the growth rates ( $\beta_i$ ) and the transition rates ( $\epsilon_i$ ) values always determines the strain with the high density at the steady state.

The densities of the existing strains changed as we varied the amplitude ( $\delta_i$ ) values of the fluctuating resources. This means increasing the amplitude ( $\delta_i$ ) simply increases the fluctuations, with bigger effects at minimum densities than its maximum densities. This show by varying the values for the amplitude ( $\delta_i$ ) of fluctuations, the bacteria could only keep growth from dropping off and was unable to really boost it up past a threshold, which might be due to the competition between the strains. But when the values of the frequency ( $\omega$ ) were varied there was no clear evidence of resonance, and there was always a rapid increase (change) at relatively lowest values (early time), and the frequency seems to show very little difference in the densities of the strains. These mean there is little interaction between the forcing and the dynamics, and it also show the frequency ( $\omega$ ) makes more difference when  $r_0$  is relatively low.

The whole results obtained in the fluctuating resources describes the ability of the amplitude ( $\delta_i$ ) to affect the behavior of the strains at relatively intermediate values, unlike the frequency ( $\omega$ ) which affects it at relatively lower values, which is almost the same results with the results obtained in chapter 2, when the dynamics of the switching ( $s_1, s_2$ ) strains were investigated separately, with the absence of the non-switching ( $s_0$ ) strain dynamics, with some slight differences in their results usually because of the presence of the non-switching ( $s_0$ ) strain.

In chapter 4 we will introduce the death rates ( $k_i$ ) of the respective strains, and the antibiotic drug ( $D$ ) treatment to the model which included the dynamics of the constant ( $s_0$ ) and the switching ( $s_1, s_2$ ) strains discussed in this chapter, to study the effects of both the death rates ( $k_i$ ), and the antibiotic drug ( $D$ ) treatment on the strains, before we consider the dynamics of the antibiotic drug administration as well in chapter 5.

## CHAPTER 4

# Bacterial Dynamics with Antimicrobial Treatment

---

### 4.1 Introduction

In chapter 3, we basically investigated the behaviors of the bet-hedging dynamics of the switching ( $s_1, s_2$ ) bacterial strains in the presence of the non-switching ( $s_0$ ) constant strain (one strain of bacteria that can 'switch' to specialise in each environment, while the other grows at the same rate in both environments), which was the model structure we studied to understand the benefits of bet-hedging (Müller et al., 2013). The results obtained produced zero  $S^* = (s_0^*, s_1^*, s_2^*) = (0, 0, 0)$ , and non-zero  $S^* = (s_0^*, s_1^*, s_2^*) = \left(s_0, \frac{(\beta-s_0)\epsilon_2}{\epsilon_T}, \frac{(\beta-s_0)\epsilon_1}{\epsilon_T}\right)$  equilibrium points for the constant growth rates of the bacteria in the non-fluctuating environment. For different growth rate values of the bacteria in the non-fluctuating environment, the results also produces a zero  $S^* = (s_0^*, s_1^*, s_2^*) = (0, 0, 0)$ , and three non-zero equilibrium points  $S^* = (s_0^*, s_1^*, s_2^*) = (\beta_0, 0, 0)$ ,  $S^* = (s_0^*, s_1^*, s_2^*) = (0, AA, BB)$ , and  $S^* = (s_0^*, s_1^*, s_2^*) = (0, CC, DD)$ , which like in chapter 2 show, the strains can not be stable at the zero equilibrium point, but they become stable at the non-zero equilibrium points.

We also noticed the results obtained in the fluctuating environment in chapter 3 were the same with those obtained in the fluctuating environment in chapter 2, where the strains are more sensitive to the frequency ( $\omega$ ) at relatively lower values than the amplitude ( $\delta_i$ ), and also the strains are more sensitive to the amplitude ( $\delta_i$ ) at relatively intermediate values than the frequency ( $\omega$ ).

Overall, we noticed the existence of the non-switching ( $s_0$ ) strain when the switching ( $s_1, s_2$ ) strains are extinct, and also the existence of the switching ( $s_1, s_2$ ) strains when the non-switching ( $s_0$ ) strain is extinct, with one of the strains having a higher density at the steady state than the other, due to its growth rate ( $\beta_i$ ), and transition rate ( $\epsilon_i$ ) values. We also noticed the co-existence of all the strains, in the special case when the non-switching ( $s_0$ ),

and the switching  $(s_1, s_2)$  strains have the same growth rates values  $(\beta_0 = \beta_1 = \beta_2 = \beta)$  in any environments, which show stability is lost at that time, and it is a stability swapping point between  $(s_0^*, 0, 0)$ , and  $(0, s_1^*, s_2^*)$  non-zero equilibrium points.

In this chapter 4 we included the death rates  $(k_i)$  of the respective strains, and the antibiotic drug  $(D)$  treatment which is held constant (fixed value) to the model that was investigated in chapter 3, which is one of the main aim of extending the work of (Müller et al., 2013). By including the death rates  $(k_i)$  of the various strains and the antibiotic drug  $(D)$  treatment in their work, we aimed to either curtail the growth of the bacteria, or eliminate them at all. This is definitely a genuinely new work in terms of applying treatment to this model, which makes the work a novel on its own (Ibargüen-Mondragón et al., 2014; Merdan et al., 2017; Ibargüen-Mondragón et al., 2019).

## 4.2 The Model of the Bacterial Dynamics with the Antibiotic Drug $(D)$ Treatment

After studying the models of the bet-hedging dynamics for the switching  $(s_1, s_2)$  strains, with the absence of the non-switching  $(s_0)$  strain in chapter 2, and with its presence in chapter 3, the death rates  $(k_i)$  of the various strains and the antibiotic drug  $(D)$  treatment (which served as the antibiotic treatment to the strains) were introduced to the existing model (Ibargüen-Mondragón et al., 2014; Merdan et al., 2017), in order to observe the dynamical behavior of the strains with their death rates  $(k_i)$  and the antibiotic drug  $(D)$  treatment.

The model equations with the existing strains death rates  $(k_i)$  and the antibiotic drug  $(D)$  treatment were defined as:

$$\begin{aligned} s_0' &= s_0 [\beta_0 (r_0, \alpha_0) - S] - k_0 D s_0 \\ s_1' &= s_1 [\beta_1 (r_1, \alpha_1) - \epsilon_1 - S] + \epsilon_2 s_2 - k_1 D s_1 \\ s_2' &= s_2 [\beta_2 (r_2, \alpha_2) - \epsilon_2 - S] + \epsilon_1 s_1 - k_2 D s_2 \end{aligned} \quad (4.1)$$

where;  $S = s_0 + s_1 + s_2$ ,  $k_i$  as  $(i = 0, 1 \text{ and } 2)$  are the respective death rates for the strains, and  $D$  is the antibiotic drug treatment which is held constant (fixed value), with all other parameters as defined in equation (3.1), and the rate of the bacterial growth  $(\beta_i)$  as defined in equation (2.2) as well.

As it is the norm throughout this research, stability analysis is performed on the model by considering different conditions to check whether the introduction

of the respective strains death rates ( $k_i$ ) and the antibiotic drug ( $D$ ) treatment in the model can affect the behavior of the system or not, by finding the equilibrium point of the system, stability of the model and the eigenvalues of the system from the characteristic equation (2.4).

### 4.3 Constant Growth Rates ( $\beta_i$ ) of the Bacteria

Going by the tradition of this research in chapters 2 and 3, we begin by considering the values of  $r_i$  in equation (4.1) to be zero (*i. e.*  $r_0 = r_1 = r_2 = 0$ ), which implies the growth rates ( $\beta_i$ ) of the whole strains are equal too (*i. e.*  $\beta_0 = \beta_1 = \beta_2 = \beta$ ).

To solve the equation (4.1) with the condition mentioned here, the system produced a zero and three non-zero equilibrium points as;

$$\begin{aligned}
S^* &= (s_0^*, s_1^*, s_2^*) = (0, 0, 0), \\
S^* &= (s_0^*, s_1^*, s_2^*) = (\beta - Dk_0, 0, 0), \\
S^* &= (s_0^*, s_1^*, s_2^*) = (0, EE, FF), \\
S^* &= (s_0^*, s_1^*, s_2^*) = (0, GG, HH)
\end{aligned} \tag{4.2}$$

where;

$$\begin{aligned}
EE &= \frac{- \left[ 2\epsilon_1\epsilon_2 - \beta\epsilon_T - (\beta - \epsilon_T - Dk_1)\sqrt{[D(k_1 - k_2)]^2 + 2D\delta\epsilon(k_1 - k_2) + \epsilon_T^2} \right]}{2D(k_1 - k_2)} \\
&\quad - \frac{[\epsilon_1^2 + \epsilon_2^2 + D\{(Dk_1 - \beta)(k_1 - k_2) - 2\epsilon_1k_1 + k_2\delta\epsilon\}]}{2D(k_1 - k_2)} \\
FF &= \frac{\left[ 2\epsilon_1\epsilon_2 - \beta\epsilon_T - (\beta - \epsilon_T - Dk_2)\sqrt{[D(k_1 - k_2)]^2 + 2D\delta\epsilon(k_1 - k_2) + \epsilon_T^2} \right]}{2D(k_1 - k_2)} \\
&\quad + \frac{[\epsilon_1^2 + \epsilon_2^2 + D\{k_2[D(k_2 - k_1) + 2\epsilon_2] + \beta(k_1 - k_2) + k_1\delta\epsilon\}]}{2D(k_1 - k_2)} \\
GG &= \frac{\beta\epsilon_T - 2\epsilon_1\epsilon_2 - (\beta - \epsilon_T - Dk_1)\sqrt{[D(k_1 - k_2)]^2 + 2D\delta\epsilon(k_1 - k_2) + \epsilon_T^2}}{2D(k_1 - k_2)} \\
&\quad - \frac{[\epsilon_1^2 + \epsilon_2^2 + D\{(Dk_1 - \beta)(k_1 - k_2) + 2\epsilon_1k_1 - k_2\delta\epsilon\}]}{2D(k_1 - k_2)} \\
HH &= \frac{- \left[ \beta\epsilon_T - 2\epsilon_1\epsilon_2 - (\beta - \epsilon_T - Dk_2)\sqrt{[D(k_1 - k_2)]^2 + 2D\delta\epsilon(k_1 - k_2) + \epsilon_T^2} \right]}{2D(k_1 - k_2)} \\
&\quad + \frac{[\epsilon_1^2 + \epsilon_2^2 + D\{k_2[D(k_2 - k_1) + 2\epsilon_2] + \beta(k_1 - k_2) + k_1\delta\epsilon\}]}{2D(k_1 - k_2)}
\end{aligned}$$

$$\epsilon_T = \epsilon_1 + \epsilon_2, \quad \text{and} \quad \delta\epsilon = \epsilon_1 - \epsilon_2$$



To find the eigenvalues of the system, we have to find the Jacobian matrix of equation (4.1) first, which was obtained as;

$$J = \begin{pmatrix} \beta - 2s_0^* - s_1^* - s_2^* - Dk_0 & -s_0^* & -s_0^* \\ -s_1^* & \beta - \epsilon_1 - s_0^* - 2s_1^* - s_2^* - Dk_1 & -s_1^* + \epsilon_2 \\ -s_2^* & -s_2^* + \epsilon_1 & \beta - \epsilon_2 - s_0^* - s_1^* - 2s_2^* - Dk_2 \end{pmatrix} \quad (4.3)$$

We then substituted the zero equilibrium point  $S^* = (s_0^*, s_1^*, s_2^*) = (0, 0, 0)$  from equation (4.2) in the Jacobian matrix obtained in equation (4.3), which resulted to;

$$J = \begin{pmatrix} \beta - Dk_0 & 0 & 0 \\ 0 & \beta - \epsilon_1 - Dk_1 & \epsilon_2 \\ 0 & \epsilon_1 & \beta - \epsilon_2 - Dk_2 \end{pmatrix} \quad (4.4)$$

An identity matrix, together with the Jacobian matrix obtained in equation (4.4) were then substituted in the characteristic equation (2.2), which give us;

$$\begin{vmatrix} \beta - Dk_0 - \lambda & 0 & 0 \\ 0 & \beta - \epsilon_1 - Dk_1 - \lambda & \epsilon_2 \\ 0 & \epsilon_1 & \beta - \epsilon_2 - Dk_2 - \lambda \end{vmatrix} = 0 \quad (4.5)$$

Finally, evaluating the above expression in equation (4.5) by hand, the three eigenvalues were obtained as;

$$\begin{aligned} \lambda_1 &= \beta - Dk_0 \\ \lambda_2 &= \frac{2\beta - [\epsilon_T + D(k_1 + k_2)] - \sqrt{[D(k_1 - k_2)]^2 + 2D\delta\epsilon(k_1 - k_2) + \epsilon_T^2}}{2} \\ \lambda_3 &= \frac{2\beta - [\epsilon_T + D(k_1 + k_2)] + \sqrt{[D(k_1 - k_2)]^2 + 2D\delta\epsilon(k_1 - k_2) + \epsilon_T^2}}{2} \end{aligned} \quad (4.6)$$

where;  $\epsilon_T = \epsilon_1 + \epsilon_2$ , and  $\delta\epsilon = \epsilon_1 - \epsilon_2$

On analysing equation (4.6) we discovered, whenever  $\beta > Dk_0$ , or  $\beta > \frac{[\epsilon_T + D(k_1 + k_2)]}{2}$ , the point will be locally and asymptotically unstable, and the bacteria will not become stable at this equilibrium point of  $(0, 0, 0)$ . But when the value of  $\beta$  is low, that is the opposite of the above mentioned conditions, we realized the zero  $(0, 0, 0)$  equilibrium point can be stable at this stage. Meaning, the extinction of the whole strains can happen, because of the killings by the antibiotic drug ( $D$ ) treatment.

We then continued by considering the first non-zero equilibrium point  $S^* = (s_0^*, s_1^*, s_2^*) = (\beta - Dk_0, 0, 0)$  obtained in equation (4.2), and substituted it

in the Jacobian matrix obtained in equation (4.3), which gave;

$$J = \begin{pmatrix} -\beta + Dk_0 & -\beta + Dk_0 & -\beta + Dk_0 \\ 0 & D(k_0 - k_1) - \epsilon_1 & \epsilon_2 \\ 0 & \epsilon_1 & D(k_0 - k_2) - \epsilon_2 \end{pmatrix} \quad (4.7)$$

The Jacobian matrix obtained in equation (4.7), and its corresponding identity matrix were then substituted in the characteristic equation (2.4), and the result gave;

$$\begin{vmatrix} Dk_0 - \beta - \lambda & Dk_0 - \beta & Dk_0 - \beta \\ 0 & D(k_0 - k_1) - \epsilon_1 - \lambda & \epsilon_2 \\ 0 & \epsilon_1 & D(k_0 - k_2) - \epsilon_2 - \lambda \end{vmatrix} = 0 \quad (4.8)$$

Evaluating the above expression in equation (4.8) by hand, and after performing some careful calculations, the three eigenvalues were obtained as;

$$\begin{aligned} \lambda_1 &= Dk_0 - \beta \\ \lambda_2 &= \frac{2Dk_0 - [\epsilon_T + D(k_1 + k_2)] - \sqrt{[D(k_1 - k_2)]^2 + 2D\delta\epsilon(k_1 - k_2) + \epsilon_T^2}}{2} \\ \lambda_3 &= \frac{2Dk_0 - [\epsilon_T + D(k_1 + k_2)] + \sqrt{[D(k_1 - k_2)]^2 + 2D\delta\epsilon(k_1 - k_2) + \epsilon_T^2}}{2} \end{aligned} \quad (4.9)$$

where;  $\epsilon_T = \epsilon_1 + \epsilon_2$ , and  $\delta\epsilon = \epsilon_1 - \epsilon_2$

Analysis of the eigenvalues obtained in equation (4.9) show whenever  $\beta > Dk_0$ , and  $\left[ \frac{\epsilon_T + D(k_1 + k_2)}{2} \right] > Dk_0$ , and the value obtained from the square root is very small [*i. e.*  $< \frac{\epsilon_T + D(k_1 + k_2)}{2}$ ], the point will be locally and asymptotically stable, and the bacteria will settle at this point.

In plots (a) to (c) of Figure 4.1 below, we considered the death rates ( $k_i$ ) of all the strains to be the same (equal), which show the densities of all the existing strains simultaneously decreased (even though the decrease is very slight to recognise) based on their growth, as the amount of the antibiotic drug ( $D$ ) treatment is increased. This means the effects of the strains death rates ( $k_i$ ) and the antibiotic drug ( $D$ ) treatment towards decreasing the existing strain(s) densities or eliminating them usually depends on the growth of the strains. If there is a presence of high amount of an antibiotic drug ( $D$ ) treatment with the purpose of eliminating the whole strains, we may experience some unexpected behaviors by the strains. Also, the equilibrium densities of the switching ( $s_1, s_2$ ) strains were driven by the values of their growth rate ( $\beta_i$ ) and the transition rates ( $\epsilon_i$ ) in the model.

The results obtained in plots (d) to (f) in the same Figure 4.1 vividly show depending on the density of a particular strain, the strain will definitely extinct at some point in time when its death rates ( $k_i$ ) value is increased. But for the switching ( $s_1, s_2$ ) strains in particular, their death rates ( $k_i$ ) values coupled with their transitions rates ( $\epsilon_i$ ) values from one type to the other, determines the amount of time the strains will take before they extinct, as we noticed in plot (f) extinction of the strain takes almost 10 times the unit-time it takes to extinct in plot (e).

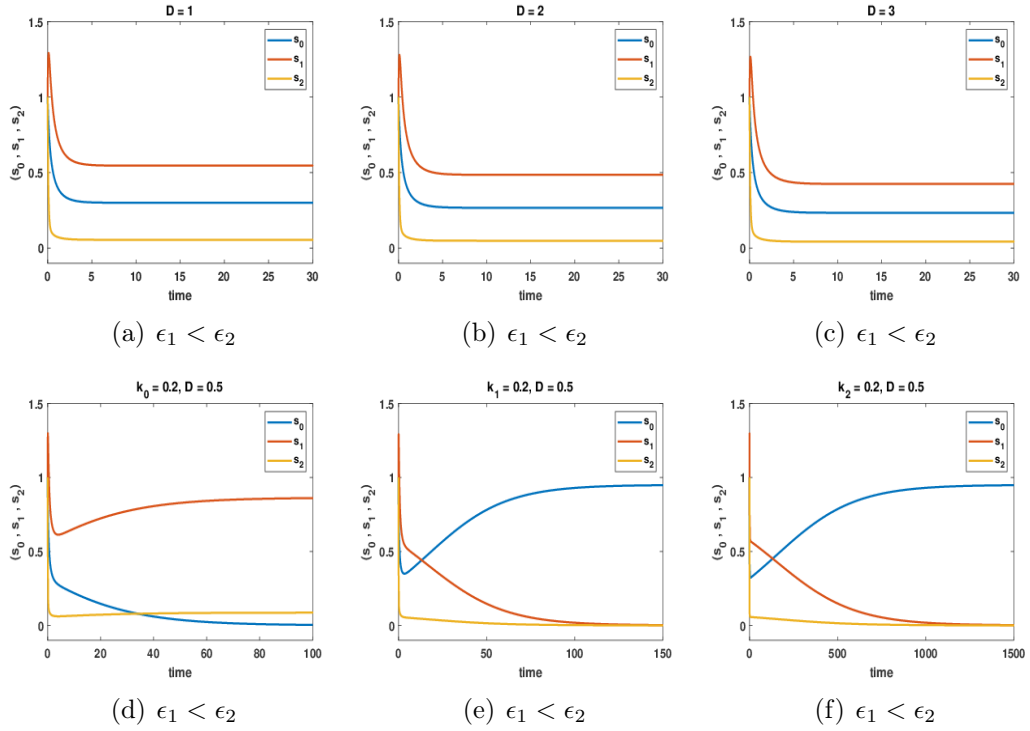


Figure 4.1: The Numerical graphs for the intrinsic dynamics of the 3D bet-hedging model with the antibiotic drug ( $D$ ) treatment and the death rates ( $k_i$ ) of the strains, for the constant growth rates of the bacterial strains:  $\beta_0 = \beta_1 = \beta_2 = \beta = 1$ , the antibiotic drug treatment  $D = 0.5$ , the respective death rates values of the strains:  $k_0 = k_1 = k_2 = 0.1$ , with both strains having the same initial values:  $s_0(0) = s_1(0) = s_2(0) = 1$ , and different transition rate values:  $\epsilon_1 = 1$ , and  $\epsilon_2 = 10$ .

## 4.4 Different Growth Rates ( $\beta_i$ ) Values of the Bacteria

After considering the situation when the values of  $r_i$  in the strains growth rates are zero (*i. e.*  $\beta_0 = \beta_1 = \beta_2 = \beta = 1$ ) in section 4.3, we then considered

a situation when their growth rates are not the same (*i. e.*  $\beta_0 \neq \beta_1 \neq \beta_2$ ), which we did always when we modelled the switching ( $s_1, s_2$ ) strains in the absence and presence of a constant ( $s_0$ ) strain in our chapters 2 and 3 respectively.

The model equations for the non-switching ( $s_0$ ) and the switching ( $s_1, s_2$ ) strains, with the strains death rates ( $k_i$ ), and the antibiotic drug ( $D$ ) treatment based on the aforementioned conditions are governed by;

$$\begin{aligned} s'_0 &= s_0 [\beta_0 (r_0, \alpha_0) - S] - k_0 D s_0 \\ s'_1 &= s_1 [\beta_1 (r_1, \alpha_1) - \epsilon_1 - S] + \epsilon_2 s_2 - k_1 D s_1 \\ s'_2 &= s_2 [\beta_2 (r_2, \alpha_2) - \epsilon_2 - S] + \epsilon_1 s_1 - k_2 D s_2 \end{aligned} \quad (4.10)$$

where;  $S = s_0 + s_1 + s_2$ , with all parameters defined as in equation (4.1).

The same procedures which were applied in finding the solution to the previous situations in equation (4.1) were also applied here. To solve the above equation (4.10) with it current condition, the system produced four equilibrium points, a zero and three non-zeros points as well;

$$\begin{aligned} S^* &= (s_0^*, s_1^*, s_2^*) = (0, 0, 0), \\ S^* &= (s_0^*, s_1^*, s_2^*) = (\beta_0 - Dk_0, 0, 0), \\ S^* &= (s_0^*, s_1^*, s_2^*) = (0, JJ, KK), \\ S^* &= (s_0^*, s_1^*, s_2^*) = (0, LL, MM) \end{aligned} \quad (4.11)$$

where;

$$\begin{aligned} JJ &= \frac{\beta_1^2 + \epsilon_1^2 + \epsilon_2^2 + D[k_1(Dk_1 + \beta_2 + 2\epsilon_1) - \beta_1(2k_1 - k_2) - k_2(\Delta\epsilon + Dk_1)]}{2[\beta_1 - \beta_2 - D(k_1 - k_2)]} \\ &\quad + \frac{\beta_2(\Delta\epsilon - \beta_1) - 2\epsilon_1(\beta_1 - \epsilon_2) - (\beta_1 - \epsilon_T - Dk_1)\sqrt{L}}{2[\beta_1 - \beta_2 - D(k_1 - k_2)]} \\ KK &= \frac{-(\beta_2^2 + \epsilon_1^2 + \epsilon_2^2) - D[k_2(Dk_2 + \beta_1 + 2\epsilon_2) + \beta_2(k_1 - 2k_2) + k_1(\Delta\epsilon - Dk_2)]}{2[\beta_1 - \beta_2 - D(k_1 - k_2)]} \\ &\quad + \frac{\beta_1(\Delta\epsilon + \beta_2) + 2\epsilon_2(\beta_2 - \epsilon_1) + (\beta_2 - \epsilon_T - Dk_2)\sqrt{L}}{2[\beta_1 - \beta_2 - D(k_1 - k_2)]} \\ LL &= \frac{\beta_1^2 + \epsilon_1^2 + \epsilon_2^2 + D[k_1(Dk_1 + \beta_2 + 2\epsilon_1) - \beta_1(2k_1 - k_2) - k_2(\Delta\epsilon + Dk_1)]}{2[\beta_1 - \beta_2 - D(k_1 - k_2)]} \\ &\quad + \frac{\beta_2(\Delta\epsilon - \beta_1) - 2\epsilon_1(\beta_1 - \epsilon_2) + (\beta_1 - \epsilon_T - Dk_1)\sqrt{L}}{2[\beta_1 - \beta_2 - D(k_1 - k_2)]} \\ MM &= \frac{-(\beta_2^2 + \epsilon_1^2 + \epsilon_2^2) - D[k_2(Dk_2 + \beta_1 + 2\epsilon_2) + \beta_2(k_1 - 2k_2) + k_1(\Delta\epsilon - Dk_2)]}{2[\beta_1 - \beta_2 - D(k_1 - k_2)]} \\ &\quad + \frac{\beta_1(\Delta\epsilon + \beta_2) + 2\epsilon_2(\beta_2 - \epsilon_1) - (\beta_2 - \epsilon_T - Dk_2)\sqrt{L}}{2[\beta_1 - \beta_2 - D(k_1 - k_2)]} \end{aligned}$$

$$\epsilon_T = \epsilon_1 + \epsilon_2, \quad \Delta\epsilon = \epsilon_1 - \epsilon_2, \quad \text{and}$$

$$L = [D(k_1 - k_2)]^2 - 2D(k_1 - k_2)[(\beta_1 - \beta_2) - \Delta\epsilon] + (\beta_1 - \beta_2)^2 - 2\Delta\epsilon(\beta_1 - \beta_2) + \epsilon_T^2$$

With the current condition under study, the Jacobian matrix of equation (4.10) was obtained as;

$$J = \begin{pmatrix} \beta_0 - 2s_0^* - s_1^* - s_2^* - Dk_0 & -s_0^* & -s_0^* \\ -s_1^* & \beta_1 - \epsilon_1 - s_0^* - 2s_1^* - s_2^* - Dk_1 & -s_1^* + \epsilon_2 \\ -s_2^* & -s_2^* + \epsilon_1 & \beta_2 - \epsilon_2 - s_0^* - s_1^* - 2s_2^* - Dk_2 \end{pmatrix} \quad (4.12)$$

When we substituted the zero equilibrium point  $S^* = (s_0^*, s_1^*, s_2^*) = (0, 0, 0)$  obtained from equation (4.11) in equation (4.12), the Jacobian matrix becomes;

$$J = \begin{pmatrix} \beta_0 - Dk_0 & 0 & 0 \\ 0 & \beta_1 - \epsilon_1 - Dk_1 & \epsilon_2 \\ 0 & \epsilon_1 & \beta_2 - \epsilon_2 - Dk_2 \end{pmatrix} \quad (4.13)$$

To find the eigenvalues, we substituted the Jacobian matrix obtained in equation (4.13), together with its corresponding identity matrix in the characteristic equation (2.4), which resulted to;

$$\begin{vmatrix} \beta_0 - Dk_0 - \lambda & 0 & 0 \\ 0 & \beta_1 - \epsilon_1 - Dk_1 - \lambda & \epsilon_2 \\ 0 & \epsilon_1 & \beta_2 - \epsilon_2 - Dk_2 - \lambda \end{vmatrix} = 0 \quad (4.14)$$

Resolving the above expression in equation (4.14) by hand, and after performing some simplifications on the results, the three eigenvalues were obtained as;

$$\begin{aligned} \lambda_1 &= \beta_0 - Dk_0 \\ \lambda_2 &= \frac{(\beta_1 + \beta_2) - [\epsilon_T + D(k_1 + k_2)] - \sqrt{B}}{2} \\ \lambda_3 &= \frac{(\beta_1 + \beta_2) - [\epsilon_T + D(k_1 + k_2)] + \sqrt{B}}{2} \end{aligned} \quad (4.15)$$

where;

$$B = [D(k_1 - k_2)]^2 - 2D(\beta_1 - \beta_2)(k_1 - k_2) + 2D\Delta\epsilon(k_1 - k_2) + (\beta_1 - \beta_2)^2 - 2\Delta\epsilon(\beta_1 - \beta_2) + \epsilon_T^2$$

$$\epsilon_T = \epsilon_1 + \epsilon_2, \quad \text{and} \quad \Delta\epsilon = \epsilon_1 - \epsilon_2$$

On analysing equation (4.15) we discovered, whenever  $\beta_0 > Dk_0$ , or  $(\beta_1 + \beta_2) > [\epsilon_T + D(k_1 + k_2)]$ , the point will be locally and asymptotically unstable, and the bacteria will not settle at the zero (0, 0, 0) equilibrium point.

But if  $\beta_0$ ,  $\beta_1$ , and  $\beta_2$  are not high enough, that is the opposite of the above mentioned conditions occur, there will be a full extinction of the whole strains at this zero  $(0, 0, 0)$  equilibrium point, because of killings by the antibiotic drug ( $D$ ) treatment.

We then considered the first non-zero equilibrium point  $S^* = (s_0^*, s_1^*, s_2^*) = (\beta_0 - Dk_0, 0, 0)$  obtained in equation (4.11), and substituted it in the Jacobian matrix obtained in equation (4.12), the result gives;

$$J = \begin{pmatrix} -\beta_0 + Dk_0 & -\beta_0 + Dk_0 & -\beta_0 + Dk_0 \\ 0 & \beta_1 - \beta_0 - \epsilon_1 + D(k_0 - k_1) & \epsilon_2 \\ 0 & \epsilon_1 & \beta_2 - \beta_0 - \epsilon_2 + D(k_0 - k_2) \end{pmatrix} \quad (4.16)$$

Substituting the obtained Jacobian matrix in equation (4.16), and its corresponding identity matrix in the characteristic equation (2.4), the expression became;

$$\begin{vmatrix} -\beta_0 + Dk_0 - \lambda & -\beta_0 + Dk_0 & -\beta_0 + Dk_0 \\ 0 & AB - \lambda & \epsilon_2 \\ 0 & \epsilon_1 & AC - \lambda \end{vmatrix} = 0 \quad (4.17)$$

where;  $AB = \beta_1 - \beta_0 - \epsilon_1 + D(k_0 - k_1)$ , and  $AC = \beta_2 - \beta_0 - \epsilon_2 + D(k_0 - k_2)$

Resolving the above expression obtained in equation (4.17) by hand, and after undergoing series of simplifications and collecting like terms, the results produces the three eigenvalues as;

$$\begin{aligned} \lambda_1 &= Dk_0 - \beta_0 \\ \lambda_2 &= \frac{(\beta_1 + \beta_2) - 2\beta_0 - \epsilon_T + 2Dk_0 - D(k_1 + k_2) - \sqrt{E}}{2} \\ \lambda_3 &= \frac{(\beta_1 + \beta_2) - 2\beta_0 - \epsilon_T + 2Dk_0 - D(k_1 + k_2) + \sqrt{E}}{2} \end{aligned} \quad (4.18)$$

where;

$$E = [D(k_1 - k_2)]^2 - 2D(\beta_1 - \beta_2)(k_1 - k_2) + 2D\Delta\epsilon(k_1 - k_2) + (\beta_1 - \beta_2)^2 - 2\Delta\epsilon(\beta_1 - \beta_2) + \epsilon_T^2$$

$$\epsilon_T = \epsilon_1 + \epsilon_2, \quad \text{and} \quad \Delta\epsilon = \epsilon_1 - \epsilon_2$$

Analysis of equation (4.18) reads, whenever  $\beta_0 > \left[ Dk_0 + \frac{(\beta_1 + \beta_2)}{2} \right]$ , and the value obtained from the square root is very small (*i. e.*  $\sqrt{E} < \beta_0$ ), the point will be locally and asymptotically stable at the non-switching ( $s_0$ ) strain. Else, if the reverse of the condition holds, it will be stable at the switching ( $s_1, s_2$ ) strains, which will be in one of the remaining non-zero equilibrium points (the last one) obtained in equation (4.11) above.

#### 4.4.1 When the Value of $\beta_0$ is Greater than the Average Value of $\beta_1$ and $\beta_2$ , $[\beta_0 > \frac{1}{2}(\beta_1 + \beta_2)]$

Plots (a) to (d) in Figure 4.2 have the same (equal) amount of the antibiotic drug ( $D$ ) treatment, with different values of both the strains death rates ( $k_i$ ), and the transition rates ( $\epsilon_i$ ). In plot (a) we noticed a decrease in the density of the existing ( $s_0$ ) strain than what was obtained in plot (a) of Figure 3.2 in chapter 3 (the equilibrium value was 8), which arises as a result of the strain death rates ( $k_i$ ) and the antibiotic drug ( $D$ ) treatment. When the existing ( $s_0$ ) strain death rate ( $k_0$ ) is increased in plot (b), we notice a decrease in the strain density than we obtained in plot (a) of this Figure 4.2. Even though the death rate ( $k_0$ ) value has effectively doubled, the decrease in the existing strain density is smaller than expected, which indicates both the death rate ( $k_i$ ) and the antibiotic drug ( $D$ ) treatment plays the same role towards decreasing the densities or eradicating the existing strain(s) entirely.

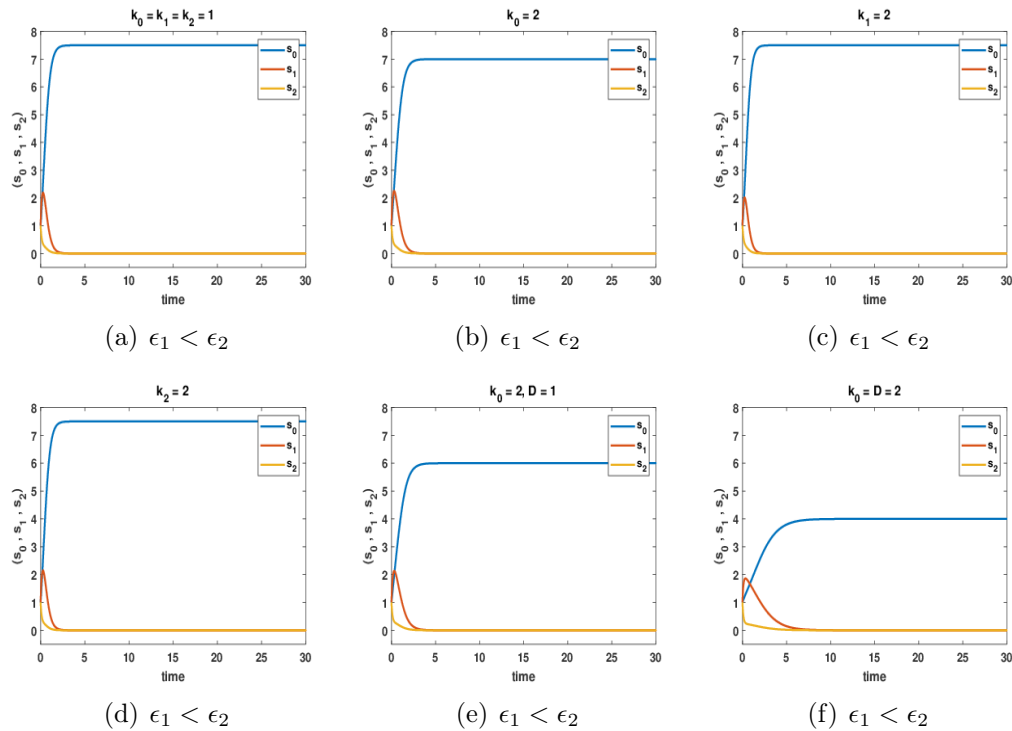


Figure 4.2: The Numerical graphs for the dynamics of the 3D bet-hedging model, with the strains death rates ( $k_i$ ) and the antibiotic drug ( $D$ ) treatment, for  $\beta_0 > \frac{1}{2}(\beta_1 + \beta_2)$ , with both strains having the same initial values ( $s_0(0) = s_1(0) = s_2(0) = 1$ ), different values of the strains growth rates ( $\beta_0 = 8, \beta_1 = 5, \beta_2 = 7$ ), with the antibiotic drug treatment  $D = 0.5$ , and different transition rates values  $\epsilon_1 = 1$ , and  $\epsilon_2 = 10$ .

When the death rate ( $k_i$ ) values of the switching ( $s_1, s_2$ ) strains were respectively increased in plots (c) and (d), we noticed there were not any decreases in the existing strain densities, because the switching ( $s_1, s_2$ ) strains were both extinct anyway. We also noticed a respective decrease in the existing ( $s_0$ ) strain densities in plots (e) and (f) when the death rate ( $k_0$ ) value of the existing strain and the amount of the antibiotic drug ( $D$ ) treatment were respectively increased.

The results obtained in Figure 4.2 above were summarized in Figure 4.3 below, which clearly show if  $k_0$  is increased, this leads to a switch from the  $s_0$  equilibrium to the ( $s_1, s_2$ ) equilibrium as shown in plots (a). But if  $k_1$  or  $k_2$  were increased in plots (b) and (c), there were not any switches between the equilibria, and this is because the ( $s_1, s_2$ ) strains never grow to invade.

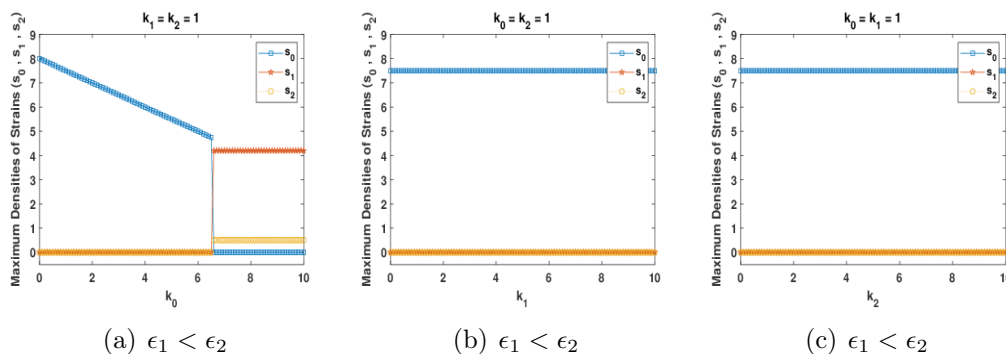


Figure 4.3: The Numerical graphs for the maximum densities of strains for the 3D bet-hedging model with the strains death rates ( $k_i$ ), and the antibiotic drug ( $D$ ) treatment against the different strains death rates ( $k_i$ ) for  $\beta_0 > \frac{1}{2}(\beta_1 + \beta_2)$ , with both strains having the same initial values ( $s_0(0) = s_1(0) = s_2(0) = 0.2$ ), different values of the strains growth rates ( $\beta_0 = 8, \beta_1 = 5, \beta_2 = 7$ ), with the antibiotic drug treatment  $D = 0.5$ , and different transition rates values  $\epsilon_1 = 1$ , and  $\epsilon_2 = 10$ .

#### 4.4.2 When the Value of $\beta_0$ is Less than the Average Value of $\beta_1$ and $\beta_2$ , [ $\beta_0 < \frac{1}{2}(\beta_1 + \beta_2)$ ]

Plots (a) to (d) in Figure 4.4 below also have the same (equal) amount of the antibiotic drug ( $D$ ) treatment, with different values of both the strains death rates ( $k_i$ ), and the transition rates ( $\epsilon_i$ ). Plot (a) show there were decreases in the existing ( $s_1, s_2$ ) strains densities when compared to the plot (d) obtained in Figure 3.2 in the chapter 3 (their equilibrium values were 4.65 and 0.57 respectively), which were caused due to the presence of the antibiotic drug ( $D$ ) treatment and the strains death rates ( $k_i$ ) as well. We also noticed in



plot (b) that increasing the non-switching ( $s_0$ ) strain death rate ( $k_0$ ) does not decrease the densities of the existing ( $s_1, s_2$ ) strains when compared with plot (a) in the same Figure 4.4.

Plot (c) showed there were decreases in the densities of the existing ( $s_1, s_2$ ) strains when the  $s_1$  strain death rate ( $k_1$ ) is increased compared to that of plot (a), but in plot (d) it seems to show not much difference with the result obtained in plot (a) when the  $s_2$  strain death rate ( $k_2$ ) is increased, and these happened as a result of the high transition rate of the  $s_2$  strain than the  $s_1$  strain. But in plots (e) and (f) we respectively noticed a decrease in the existing ( $s_1, s_2$ ) strains densities, when the antibiotic drug ( $D$ ) treatment was increased.

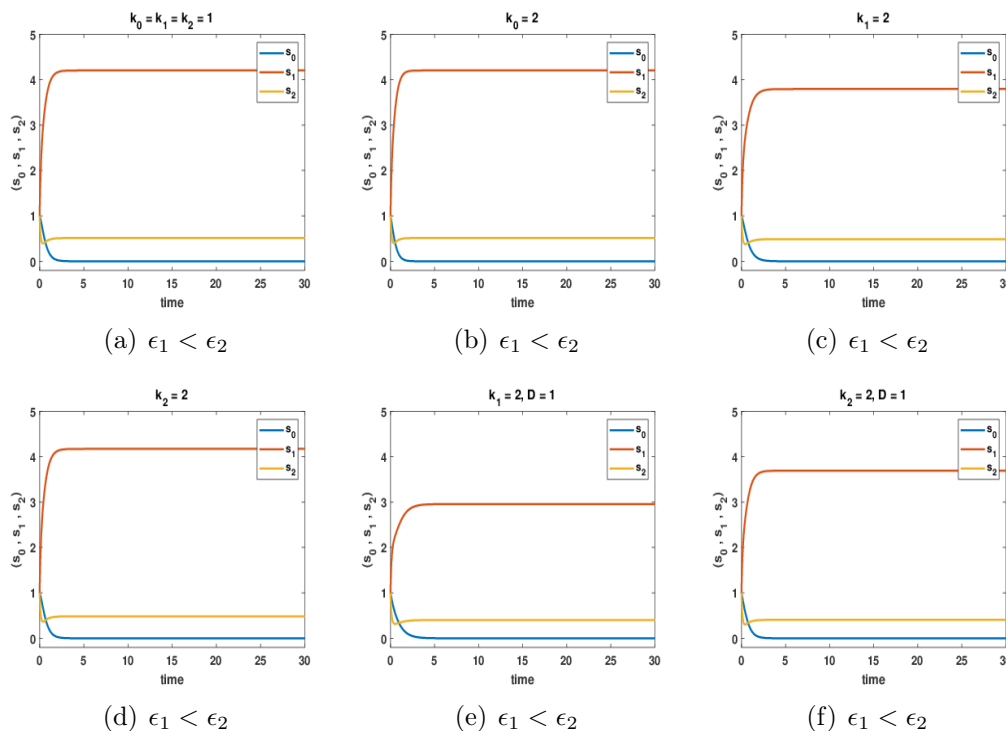


Figure 4.4: The Numerical graphs for the dynamics of the 3D bet-hedging model with the strains death rates ( $k_i$ ), and the antibiotic drug ( $D$ ) treatment for  $\beta_0 < \frac{1}{2}(\beta_1 + \beta_2)$ , with both strains having the same initial values ( $s_0(0) = s_1(0) = s_2(0) = 1$ ), different values of the strains growth rates ( $\beta_0 = 3, \beta_1 = 5, \beta_2 = 7$ ), with the antibiotic drug treatment  $D = 0.5$ , and the different transition rates values  $\epsilon_1 = 1$ , and  $\epsilon_2 = 10$ .

We also noticed a higher decrease in the densities of the existing ( $s_1, s_2$ ) strains in plot (e) than (f), which are caused as a result of the high transitions of the strains from the  $s_2$  to the  $s_1$  strain, coupled with a high death rate ( $k_1$ ) value of the  $s_1$  strain.

The results obtained in Figure 4.4 above were also summarized in Figure 4.5 below, which clearly show if  $k_0$  is increased this does not lead to any switch between the equilibria, because the  $s_0$  strain never grows fast enough to invade as shown in plot (a), but if  $k_1$  is increased this leads to a switch from the  $(s_1, s_2)$  equilibrium to the  $s_0$  equilibrium as shown in plot (b).

There is an interesting result were we are only ever at the switching  $(s_1, s_2)$  equilibrium in plots (c), despite seen some changes within the existing  $(s_1, s_2)$  strains, unlike what we observed in plot (a). This is because for this case also the non-switching  $(s_0)$  strain never grows fast enough to invade, and it is interesting that this is maintained even with very high values of  $k_2$  as shown in plot (c). Even when  $k_2$  was extended to 500, the result remain the same.

We also expect to see a change (swap of densities) between the predominant  $(s_1, s_2)$  strains in plot (c), but couldn't due to the relative large differences in their transition rates  $(\epsilon_i)$  values. If the differences between their transition rates  $(\epsilon_i)$  values is relatively small, we may have seen some changes between the predominant  $(s_1, s_2)$  strains in plot (c).

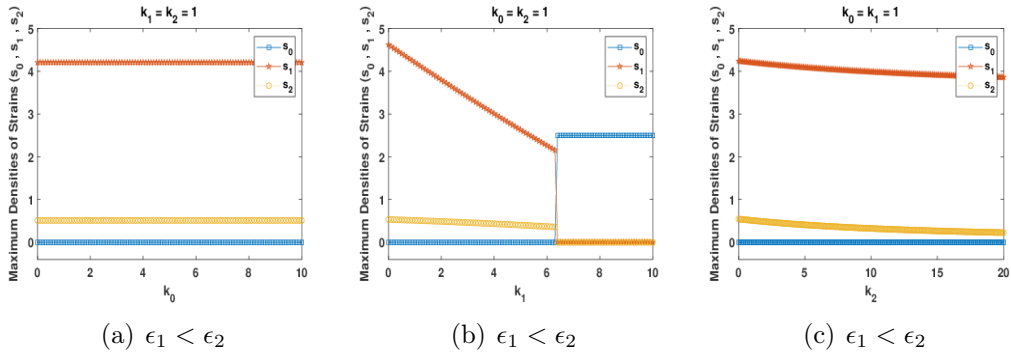


Figure 4.5: The Numerical graphs for the maximum densities of strains for the 3D bet-hedging model with the strains death rates  $(k_i)$  and the antibiotic drug  $(D)$  treatment, against the different strains death rates  $(k_i)$ , for  $\beta_0 < \frac{1}{2}(\beta_1 + \beta_2)$ , with both strains having the same initial values  $(s_0(0) = s_1(0) = s_2(0) = 0.2)$ , different range of values for the strains death rates  $(k_i)$ , different values of the strains growth rates  $(\beta_0 = 3, \beta_1 = 5, \beta_2 = 7)$ , with the antibiotic drug treatment  $D = 0.5$ , and the different transition rates values  $\epsilon_1 = 1$ , and  $\epsilon_2 = 10$ .

#### 4.4.3 When the Value of $\beta_0$ is Equal to the Average Value of $\beta_1$ and $\beta_2$ , $[\beta_0 = \frac{1}{2}(\beta_1 + \beta_2)]$

Plots (a) to (d) in Figure 4.6 below also have the same (equal) amount of the antibiotic drug  $(D)$  treatment, with different values of both the strains' death

rates ( $k_i$ ), and the transition rates ( $\epsilon_i$ ), and the results obtained from those plots were the same with those obtained in Figure 4.2 of this chapter 4. The main differences from the results obtained in Figures 4.2 and 4.6 were in plots (e) and (f), where we noticed a switch of existences from the non-switching ( $s_0$ ) to the switching ( $s_1, s_2$ ) strains when the amount of the antibiotic drug ( $D$ ) treatment is increased in Figure 4.6, unlike in the above Figure 4.2 where we only saw a decreases in the existing  $s_0$  strain, which is because of the non-switching ( $s_0$ ) strain's higher growth rate ( $\beta_i$ ) value.

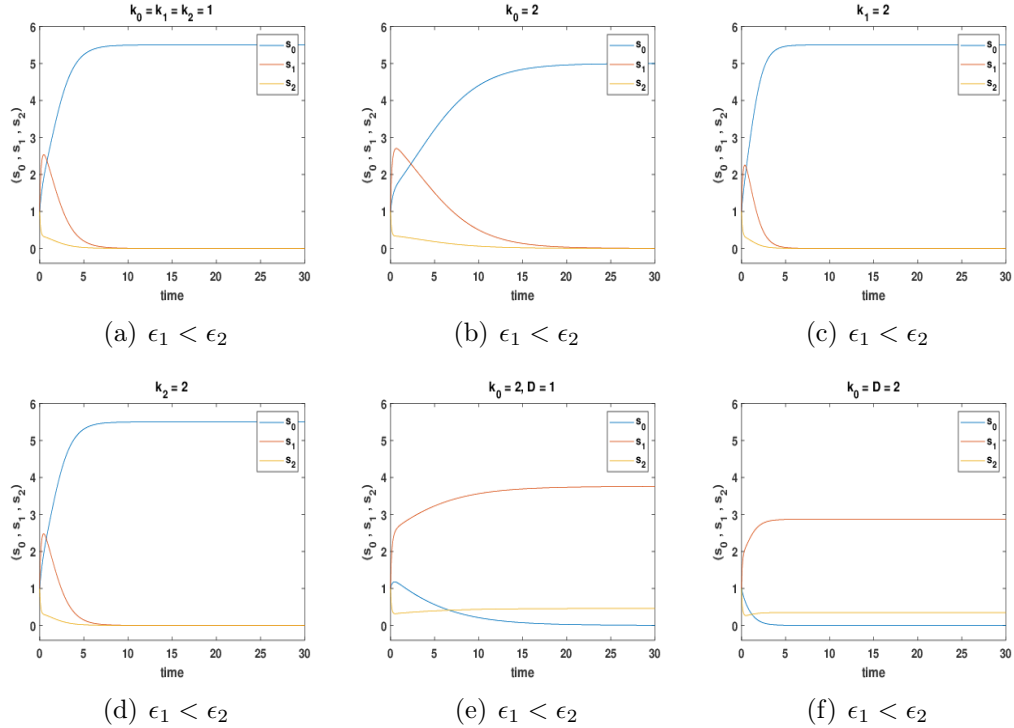


Figure 4.6: The Numerical graphs for the dynamics of the 3D bet-hedging model with the strains death rates ( $k_i$ ) and the antibiotic drug ( $D$ ) treatment for  $\beta_0 = \frac{1}{2}(\beta_1 + \beta_2)$ , with both strains having the same initial values ( $s_0(0) = s_1(0) = s_2(0) = 1$ ), same range of time for each of the plots  $t = 0 : 0.001 : 30$ , different values of the strains growth rates ( $\beta_0 = 6, \beta_1 = 5, \beta_2 = 7$ ), with the antibiotic drug treatment  $D = 0.5$ , and different transition rates values  $\epsilon_1 = 1$ , and  $\epsilon_2 = 10$ .

This show the switch of existence between the strains occurred earlier, when the value of the non-switching ( $s_0$ ) strain's growth rate is equal to the average value of the switching ( $s_1, s_2$ ) strains' growth rates, and the antibiotic drug ( $D$ ) treatment is relatively increased a bit compared to what were obtained in Figure 4.2 above. The results of plots (f) in both Figures 4.2 and 4.6 show

the same behavior with one another, which is a decrease in the densities of the existing strain(s) from what were obtained in plots (e).

The result obtained in Figure 4.6 above when summarized produced the same result with what were obtained in Figure 4.3 above. The main differences is in plot (a), where the switching between the equilibrium occurred earlier than we noticed in Figure 4.3, and this is because the growth rate ( $\beta_0$ ) value of the non-switching ( $s_0$ ) strain used in this situation is lower than what were used in Figure 4.3.

But when the amount of the antibiotic drug ( $D$ ) treatment is increased, the results obtained differed with what were obtained in Figure 4.3, as we noticed in Figure 4.7 below. The results obtained in Figure 4.7 show when  $k_0$  and  $k_1$  were respectively increased in plots (a) and (b), we noticed a switch of the equilibrium between the strains, but the result in plot (c) show we are only ever at the non-switching ( $s_0$ ) equilibrium no matter how largely  $k_2$  is increased, unless if the default value of  $k_1$  is higher than what was used here.

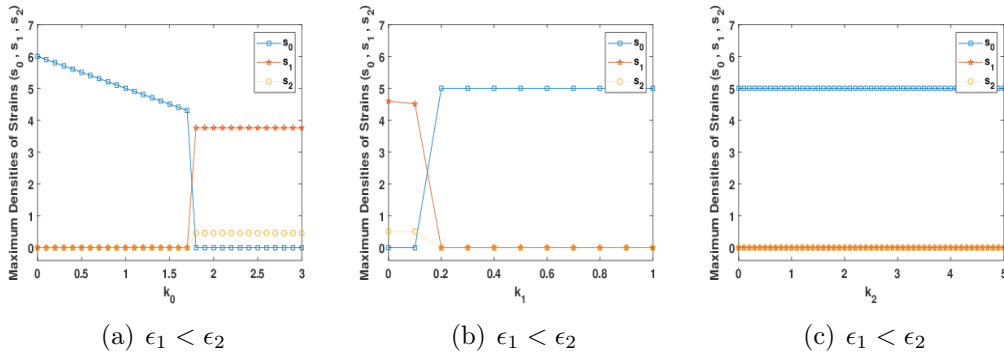


Figure 4.7: The Numerical graphs for the maximum densities of strains for the 3D bet-hedging model with the strains death rates ( $k_i$ ) and the antibiotic drug ( $D$ ) treatment, against the different strains death rates ( $k_i$ ) for  $\beta_0 = \frac{1}{2}(\beta_1 + \beta_2)$ , with both strains having the same initial values  $s_0(0) = s_1(0) = s_2(0) = 0.2$ , different range of values for the strains death rates, different values of the strains growth rates  $\beta_0 = 6$ ,  $\beta_1 = 5$ ,  $\beta_2 = 7$ , with the antibiotic drug treatment  $D = 1$ , and different transition rates values  $\epsilon_1 = 1$ , and  $\epsilon_2 = 10$ .

#### 4.4.4 When the Values of $\beta_0$ , $\beta_1$ , and $\beta_2$ are Equal, $[\beta_0 = \beta_1 = \beta_2 \neq 1]$

The results of the model dynamics obtained in this section 4.4.4 corresponds to the same results obtained in Figure 4.1 above. The main differences in the plots will be for the particular values of the strains' growth rates ( $\beta_i$ ) values

used, and in this context we considered the values of the strains growth rates ( $\beta_i$ ) to be different with those used in Figure 4.1 above, but in either case the growth rates ( $\beta_i$ ) of all the strains are equal to one another.

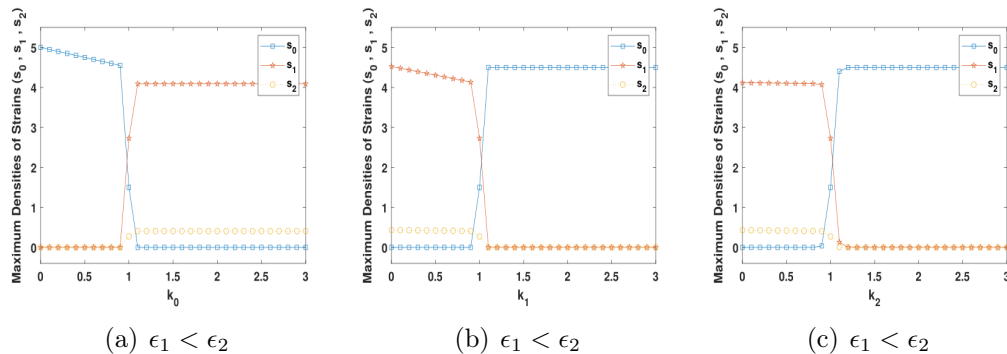


Figure 4.8: The Numerical graphs for the maximum densities of strains for the 3D bet-hedging model with the strains death rates ( $k_i$ ) and the antibiotic drug ( $D$ ) treatment, against the different strains death rates ( $k_i$ ) for  $\beta_0 = \beta_1 = \beta_2 = \neq 1$ , with both strains having the same initial values ( $s_0(0) = s_1(0) = s_2(0) = 0.2$ ), the same range of values for the strains death rates, the same values of the strains growth rates ( $\beta_0 = \beta_1 = \beta_2 = 5$ ), with the antibiotic drug treatment  $D = 0.5$ , and different transition rates values  $\epsilon_1 = 1$ , and  $\epsilon_2 = 10$ .

The results obtained in Figure 4.8 above show there is always a switch between the non-switching ( $s_0$ ) equilibrium and the switching ( $s_1, s_2$ ) equilibrium, which is a very special result compared to what we normally obtained in the previous situations. This also happened because of all the strains having equal values for their growth rates ( $\beta_i$ ).

Plot (a) in Figure 4.8 show a switching from the  $s_0$  equilibrium to the ( $s_1, s_2$ ) equilibrium, with the  $s_1$  strain having a higher density than the  $s_2$  strain, which is caused as a result of the  $s_2$  strain having a higher transition rate ( $\epsilon_i$ ) value than the  $s_1$  strain. But in plots (b) and (c) there are switching from the ( $s_1, s_2$ ) equilibrium to the  $s_0$  equilibrium.

The behaviors of the strains equilibrium in this condition also confirms the results of the model dynamics of a stability swapping point between the non-switching ( $s_0, 0, 0$ ) and the switching ( $0, s_1, s_2$ ) strains.

## 4.5 Fluctuating Resources within the Bacterial Growth Rates ( $\beta_i$ )

In this section 4.5, we considered a situation when the environmental ( $\alpha_i$ ) resources within the strains growth rate ( $\beta_i$ ) fluctuates like we did in chapters 2 and 3. The environmental state ( $\alpha_i$ ) resources that fluctuates within the strains growth rates ( $\beta_i$ ) will be replaced by:  $\alpha_i = \delta_i \sin(\omega t) + 1$ . where;  $\delta_i$  is the amplitude, and  $\omega$  is the frequency of the fluctuating environment.

Based on the aforementioned environmental state resources defined above, the growth rate ( $\beta_i$ ) of the fluctuating resources within the strains growth rate ( $\beta_i$ ) with respect to time ( $t$ ) is defined as in equation (2.26).

As we mentioned in chapters 2 and 3 this problem can not be solved analytically, instead we should study the behavior of this fluctuating situation numerically with respect to time ( $t$ ).

### 4.5.1 When the Value of $\beta_0$ is Greater than the Average Value of $\beta_1$ and $\beta_2$ , [ $\beta_0 > \frac{1}{2}(\beta_1 + \beta_2)$ ]

Plots (a) to (d) in Figure 4.9 below have the same (equal) amount of the antibiotic drug ( $D$ ) treatment, with different values of both the strains death rates ( $k_i$ ) and the transition rates ( $\epsilon_i$ ). In plot (a) we noticed the density of the existing (non-switching) strain decreases compared to what was obtained in plot (a) of Figure 3.4 in chapter 3, which arises as a result of the strains' death rates ( $k_i$ ) and the antibiotic drug ( $D$ ) treatment, and when the existing ( $s_0$ ) strains death rate ( $k_0$ ) is increased in plot (b) we noticed a switch from the non-switching ( $s_0$ ) strain to the switching ( $s_1, s_2$ ) strains.

Also when the death rate values of the switching ( $s_1, s_2$ ) strains were respectively increased in plots (c) and (d), we noticed there is not any decrease in the existing ( $s_0$ ) strain density when compared with that of plot (a), but we realized both the extinction and existence of the non-switching ( $s_0$ ) strain occurred earlier in plot (b) to (d) than the time it takes to exist in plot (a). We also noticed a decrease in the existing strains' densities in plots (e) and (f), when the amount of the antibiotic drug ( $D$ ) treatment was respectively increased in plots (b) and (c).

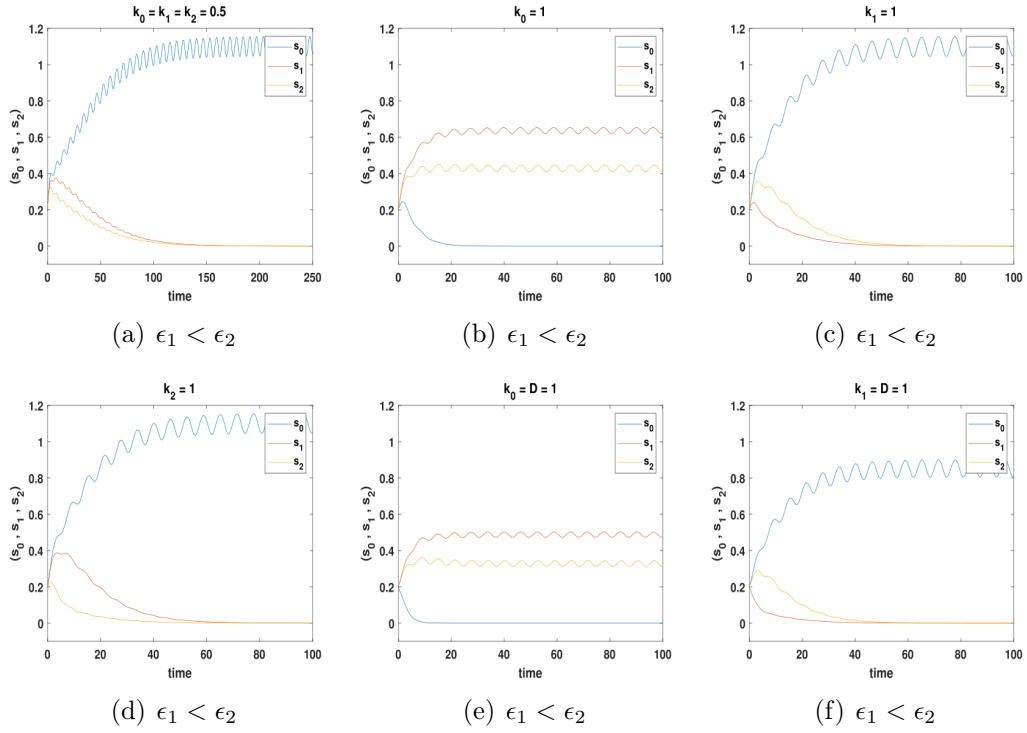


Figure 4.9: The Numerical graphs for the dynamics of the 3D bet-hedging model with the fluctuating growth resources, the strains death rates ( $k_i$ ), and the antibiotic drug ( $D$ ) treatment for  $\beta_0 > \frac{1}{2}(\beta_1 + \beta_2)$ , with both strains having the same initial values ( $s_0(0) = s_1(0) = s_2(0) = 0.2$ ), different ranges of time for the plots, different amount of enzymes in the strains growth rates ( $r_0 = 0.8$ ,  $r_1 = 0.5$ ,  $r_2 = 0.7$ ), with the amplitude  $\delta = 0.25$ , and the frequency of fluctuating resources  $\omega = 1$ , the antibiotic drug treatment  $D = 0.5$ , and different transition rates values  $\epsilon_1 = 0.05$ , and  $\epsilon_2 = 0.1$ .

The results obtained in Figure 4.9 above were summarized in Figure 4.10 below, which clearly show if  $k_0$  is increased this leads to a switch from the  $s_0$  equilibrium to the  $(s_1, s_2)$  equilibrium as shown in plots (a). Likewise, if  $k_1$  and  $k_2$  were respectively increased in plots (b) and (c) they also leads to a switches from the  $(s_1, s_2)$  equilibrium to the  $s_0$  equilibrium, but the strain with a higher density among the switching  $(s_1, s_2)$  strains usually depends on it transition rate ( $\epsilon_i$ ) value.

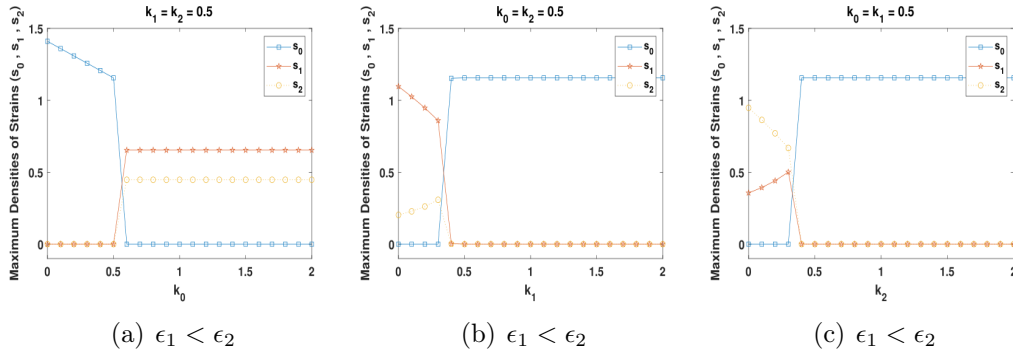


Figure 4.10: The Numerical graphs for the maximum densities of strains for the 3D bet-hedging model and the fluctuating growth resources, with the strains death rates ( $k_i$ ) and the antibiotic drug ( $D$ ) treatment for  $\beta_0 > \frac{1}{2}(\beta_1 + \beta_2)$ , with both strains having the same initial values ( $s_0(0) = s_1(0) = s_2(0) = 0.2$ ), same range of values for the strains death rates in each plots ( $k_i = 0 : 0.1 : 2$ ), different amount of enzymes in the strains growth rates ( $r_0 = 0.8, r_1 = 0.5, r_2 = 0.7$ ), with the amplitude  $\delta = 0.25$ , and the frequency of fluctuating resources  $\omega = 1$ , the antibiotic drug treatment  $D = 0.5$ , and different transition rates values  $\epsilon_1 = 0.05$ , and  $\epsilon_2 = 0.1$ .

#### 4.5.2 When the Value of $\beta_0$ is Less than the Average Value of $\beta_1$ and $\beta_2$ , $[\beta_0 < \frac{1}{2}(\beta_1 + \beta_2)]$

Plots (a) to (d) in Figure 4.11 below have the same (equal) amount of the antibiotic drug ( $D$ ) treatment, with different values of both the strains death rates ( $k_i$ ) and the transition rates ( $\epsilon_i$ ). In plot (a) we noticed the densities of the existing (switching) strains decreases compared to what was obtained in plot (d) of Figure 3.4 in chapter 3, which arises as a result of the strains death rates ( $k_i$ ) and the antibiotic drug ( $D$ ) treatment. When the extinct (non-switching) strain death rate ( $k_0$ ) is increased in plot (b), we noticed the densities of the existing (switching) strains do not decrease at all, but the non-switching ( $s_0$ ) strain goes extinct earlier than the time it takes to extinct in plot (a), and the existing (switching) strains reach a steady state earlier than the time they took to reach the steady state as well in plot (a).

But when the death rate values of the existing (switching) strains were respectively increased in plots (c) and (d), we noticed there is not any switching between the strains but the predominant strains swap their densities, and there are increases in the predominant strain's densities which happened as a result of the strains transition rate ( $\epsilon_i$ ) values. We finally noticed a decrease in the predominant strains' densities in plots (e) and (f), when the amount of the antibiotic drug ( $D$ ) treatment were respectively increased in plots (b) and (c).



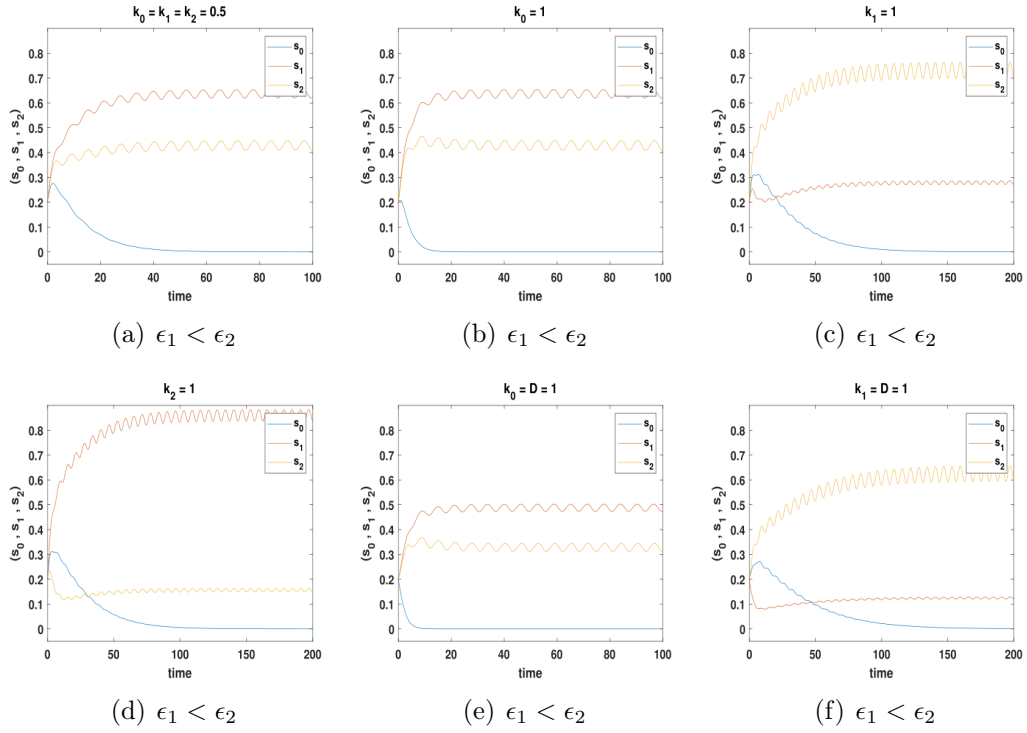


Figure 4.11: The Numerical graphs for the dynamics of the 3D bet-hedging model and the fluctuating growth resources, with the strains death rates ( $k_i$ ) and the antibiotic drug ( $D$ ) treatment for  $\beta_0 < \frac{1}{2}(\beta_1 + \beta_2)$ , with both strains having the same initial values ( $s_0(0) = s_1(0) = s_2(0) = 0.2$ ), different ranges of time for the plots, different amount of enzymes in the strains growth rates ( $r_0 = 0.3$ ,  $r_1 = 0.5$ ,  $r_2 = 0.7$ ), with the amplitude  $\delta = 0.25$ , and the frequency of fluctuating resources  $\omega = 1$ , the antibiotic drug treatment  $D = 0.5$ , and different transition rates values  $\epsilon_1 = 0.05$ , and  $\epsilon_2 = 0.1$ .

The results obtained in Figure 4.11 above were summarized in Figure 4.12 below, which clearly show if  $k_0$  is increased this leads to a switch from the  $s_0$  equilibrium to the  $s_1, s_2$  equilibrium as shown in plot (a). There are a couple of interesting cases where the results were only ever at the  $s_1, s_2$  equilibrium, but the predominant strains swap their densities in plots (b) and (c). This is because for these cases  $r_0$  is very small, and the  $s_0$  strain never grows fast enough to invade. This also happened because the  $(s_1, s_2)$  strains are the bet-hedgers. It is interesting that this is maintained even with very high values of  $k_1$  or  $k_2$  as shown on plots (b) and (c) in Figure 4.12.

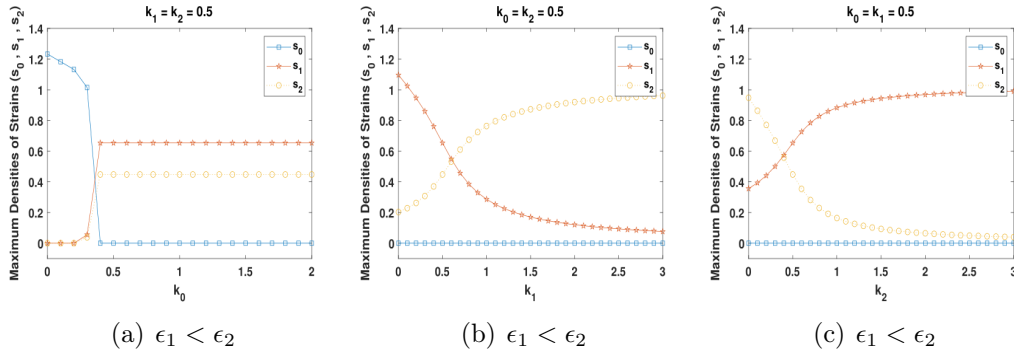


Figure 4.12: The Numerical graphs for the maximum densities of strains for the 3D bet-hedging model and the fluctuating growth resources, with the strains death rates ( $k_i$ ) and the antibiotic drug ( $D$ ) treatment for  $\beta_0 < \frac{1}{2}(\beta_1 + \beta_2)$ , with both strains having the same initial values ( $s_0(0) = s_1(0) = s_2(0) = 0.2$ ), different ranges of the strains death rates in the plots, different amount of enzymes in the strains growth rates ( $r_0 = 0.3$ ,  $r_1 = 0.5$ ,  $r_2 = 0.7$ ), with the amplitude  $\delta = 0.25$ , and the frequency of fluctuating resources  $\omega = 1$ , the antibiotic drug treatment  $D = 0.5$ , and different transition rates values  $\epsilon_1 = 0.05$ , and  $\epsilon_2 = 0.1$ .

### 4.5.3 When the Value of $\beta_0$ is Equal to the Average Value of $\beta_1$ and $\beta_2$ , [ $\beta_0 = \frac{1}{2}(\beta_1 + \beta_2)$ ]

Plots (a) to (d) in Figure 4.13 below have the same (equal) amount of the antibiotic drug ( $D$ ) treatment, with different values of both the strains death rates ( $k_i$ ) and the transition rates ( $\epsilon_i$ ). In plot (a) we noticed the density of the existing (non-switching) strain decreases compared to what was obtained in plot (g) of Figure 3.4 in chapter 3, which arises as a result of the strain death rates ( $k_i$ ) and the antibiotic drug ( $D$ ) treatment. But when the existing ( $s_0$ ) strain death rate ( $k_0$ ) in plot (a) is increased, we noticed in plot (b) there is a change from the non-switching ( $s_0$ ) strain to the switching ( $s_1$ ,  $s_2$ ) strains.

Also, when the death rates of the switching ( $s_1$ ,  $s_2$ ) strains were respectively increased in plots (a), we noticed in plots (c) and (d) there were not any change between the existing strain(s), and the densities of the existing ( $s_0$ ) strain does not decrease at all. Instead, the switching ( $s_1$ ,  $s_2$ ) strains go extinct earlier than the time they took to go extinct in plot (a), and the existing ( $s_0$ ) strain also reaches the steady state earlier than the time it takes to reach the steady state in plot (a) as well, which occurred as a result of the high death rates values of the switching ( $s_1$ ,  $s_2$ ) strain used. Finally we noticed a decrease in the densities of the existing (switching and non-switching) strains in plots (e)

and (f), when the amount of the antibiotic drug ( $D$ ) treatment were increased in plots (b) and (c) respectively.

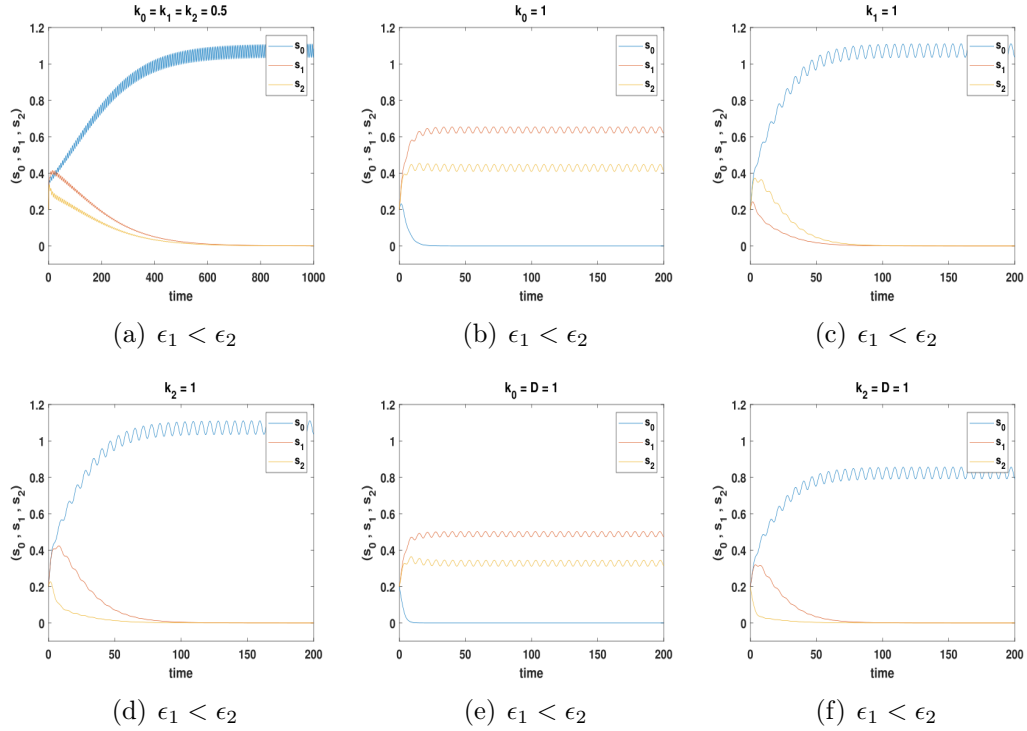


Figure 4.13: The Numerical graphs for the dynamics of the 3D bet-hedging model and the fluctuating growth resources, with the strains death rates ( $k_i$ ) and the antibiotic drug ( $D$ ) treatment for  $\beta_0 = \frac{1}{2}(\beta_1 + \beta_2)$ , with both strains having the same initial values ( $s_0(0) = s_1(0) = s_2(0) = 0.2$ ), different ranges of time for the plots, different amount of enzymes in the strains growth rates ( $r_0 = 0.6, r_1 = 0.5, r_2 = 0.7$ ), with the amplitude  $\delta = 0.25$ , and the frequency of fluctuating resources  $\omega = 1$ , the antibiotic drug treatment  $D = 0.5$ , and different transition rates values  $\epsilon_1 = 0.05$ , and  $\epsilon_2 = 0.1$ .

The results obtained in Figure 4.13 were summarized in Figure 4.14, which clearly show if  $k_0$  is increased, this leads to a switch from the  $s_0$  equilibrium to the  $(s_1, s_2)$  equilibrium as shown in plot (a), but the strain with a higher density between the switching  $(s_1, s_2)$  strains depends on their transition rates ( $\epsilon_i$ ) values. Also if  $k_1$  and  $k_2$  were respectively increased in plots (b) and (c), they also leads to a switch from the  $(s_1, s_2)$  equilibrium to the  $s_0$  equilibrium in both cases.

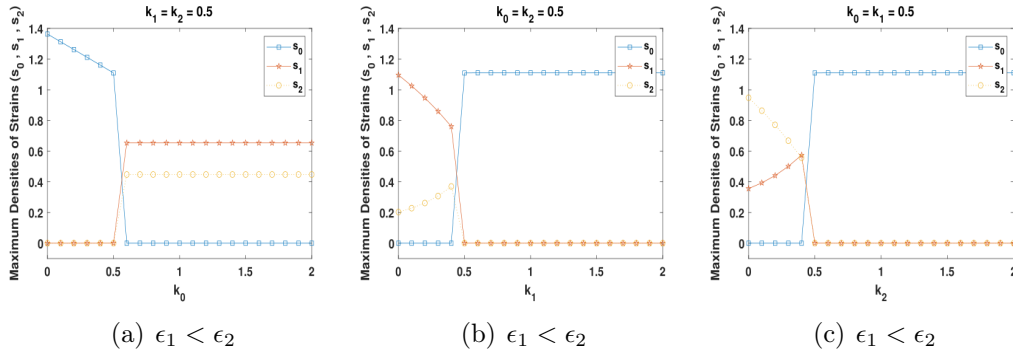


Figure 4.14: The Numerical graphs for the maximum densities of strains for the 3D bet-hedging model and the fluctuating growth resources, with the strains death rates ( $k_i$ ) and the antibiotic drug ( $D$ ) treatment for  $\beta_0 = \frac{1}{2}(\beta_1 + \beta_2)$ , with both strains having the same initial values ( $s_0(0) = s_1(0) = s_2(0) = 0.2$ ), the same ranges of the strains death rates in each plots, different amount of enzymes in the strains growth rates ( $r_0 = 0.6, r_1 = 0.5, r_2 = 0.7$ ), with the amplitude  $\delta = 0.25$ , and the frequency of the fluctuating resources  $\omega = 1$ , the antibiotic drug treatment  $D = 0.5$ , and different transition rates values  $\epsilon_1 = 0.05$ , and  $\epsilon_2 = 0.1$ .

#### 4.5.4 When the Values of $\beta_0, \beta_1$ , and $\beta_2$ are Equal,

$$[\beta_0 = \beta_1 = \beta_2 \neq 1]$$

Plots (a) to (d) in Figure 4.15 have the same (equal) amount of the antibiotic drug ( $D$ ) treatment with different values of both the strains' death rates ( $k_i$ ) and the transition rates ( $\epsilon_i$ ). In plot (a) we noticed a decrease in the densities of the existing (switching and the non-switching) strains, compared to what were obtained in plot (a) of Figure 3.5 in chapter 3, which arises as a result of the strains' death rates ( $k_i$ ) and the antibiotic drug ( $D$ ) treatment.

When the death rate ( $k_0$ ) of the non-switching ( $s_0$ ) strain is increased in plot (b), the non-switching ( $s_0$ ) strain is extinct and the switching ( $s_1, s_2$ ) strains exists. Also, when the death rates ( $k_1$ , and  $k_2$ ) of the switching ( $s_1, s_2$ ) strains were respectively increased in plots (c) and (d), the switching ( $s_1, s_2$ ) strains go extinct and the non-switching ( $s_0$ ) strain exists, with the existing ( $s_0$ ) strain attaining a stable state earlier in plot (c) compared to the time it takes to reach the steady state in plot (d), and the switching ( $s_1, s_2$ ) strains also go extinct earlier in plot (c) compared to the time they took to go extinct in plot (d), which all happened because of the high transition rate ( $\epsilon_i$ ) values of  $s_2$  strain than the  $s_1$  strain. In plots (e) and (f) we noticed a decrease in the densities of the existing (switching and the non-switching) strains, when

the amount of the antibiotic drug ( $D$ ) treatment were respectively increased in plots (b) and (c).

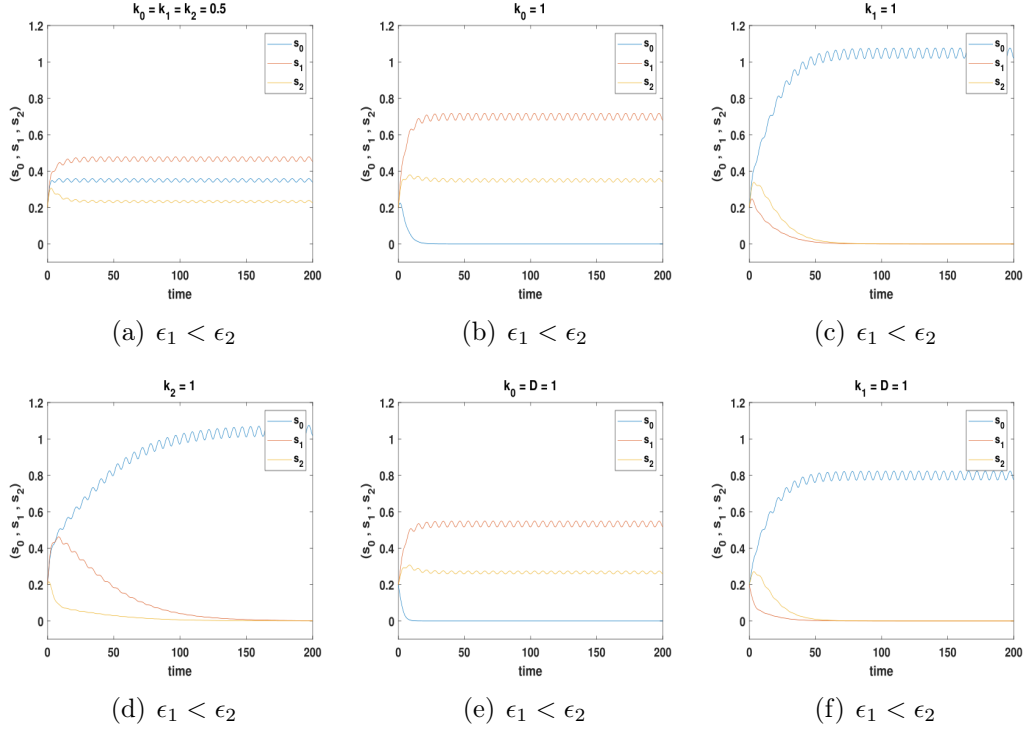


Figure 4.15: The Numerical graphs for the dynamics of the 3D bet-hedging model and the fluctuating growth resources, with the strains death rates ( $k_i$ ) and the antibiotic drug ( $D$ ) treatment for  $\beta_0 = \beta_1 = \beta_2 = \beta$ , with both strains having the same initial values ( $s_0(0) = s_1(0) = s_2(0) = 0.2$ ), the same ranges of time for the plots, the same amount of enzymes in the strains growth rates ( $r_0 = r_1 = r_2 = 0.5$ ), with the amplitude  $\delta = 0.25$ , and the frequency of the fluctuating resources  $\omega = 1$ , the antibiotic drug treatment  $D = 0.5$ , and different transition rates values  $\epsilon_1 = 0.05$ , and  $\epsilon_2 = 0.1$ .

The results obtained in Figure 4.15 were also summarized in Figure 4.16, which clearly show if  $k_0$  is increased, this leads to a switch from the  $s_0$  equilibrium to the  $(s_1, s_2)$  equilibrium as shown in plot (a). Likewise, if  $k_1$  and  $k_2$  were respectively increased in plots (b) and (c), they also leads to a switches from the  $(s_1, s_2)$  equilibrium to the  $s_0$  equilibrium in both cases, but the strain with a high density between the switching ( $s_1, s_2$ ) strains in plot (a), depends on the value of their transition rates ( $\epsilon_i$ ), which also produced the same result like what were obtained in Figure 4.14.

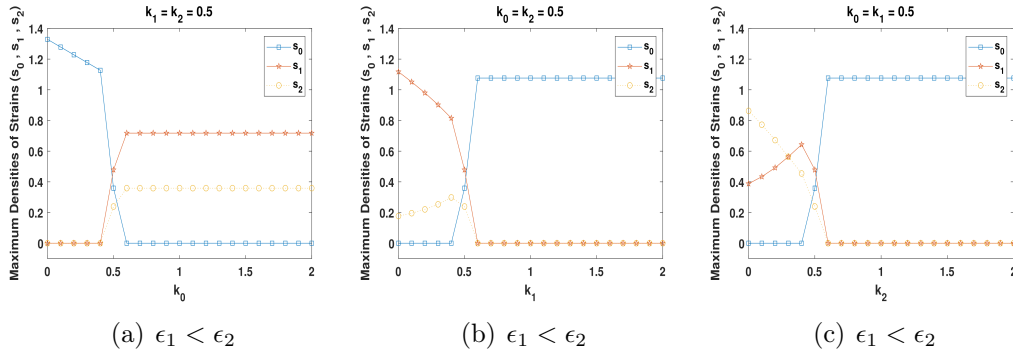


Figure 4.16: The Numerical graphs for the maximum densities of strains for the 3D bet-hedging model and the fluctuating growth resources, with the strains death rates ( $k_i$ ) and the antibiotic drug ( $D$ ) treatment for  $\beta_0 = \beta_1 = \beta_2 = \beta$ , with both strains having the same initial values ( $s_0(0) = s_1(0) = s_2(0) = 0.2$ ), the same ranges of the strains death rates for each plots, the same amount of enzymes in the strains growth rates ( $r_0 = r_1 = r_2 = 0.5$ ), with the amplitude  $\delta = 0.25$ , and the frequency of the fluctuating resources  $\omega = 1$ , the antibiotic drug treatment  $D = 0.5$ , and different transition rate values  $\epsilon_1 = 0.05$ , and  $\epsilon_2 = 0.1$ .

## 4.6 Fluctuating Resources within the Antimicrobial Treatment

Throughout our research both in this chapter 4, and in the previous chapters 2 and 3, we always investigated what happened with the fluctuations within the strains' growth rates ( $\beta_i$ ) in the modelling of the bacterial dynamics, with and without the strains death rates ( $k_i$ ) together with the antibiotic drug ( $D$ ) treatment which is held constant (usually at a fixed value).

In this section 4.6, we investigate what happens if it is the antibiotic drug ( $D$ ) treatment that fluctuates over time ( $t$ ), and compared the results obtained in this section 4.6 with the results obtained in section 4.4 of this chapter 4, for the non-fluctuating resources within the strains growth rates ( $\beta_i$ ), with the strains death rates ( $k_i$ ) and the antibiotic drug ( $D$ ) treatment, to find out if both situations produces the same results, or if there is any differences between their results.

The model of the bacterial dynamics in the presence of a constant strain, with the strains death rates ( $k_i$ ) and the fluctuations within the antibiotic drug ( $D$ ) treatment is given by;

$$\begin{aligned}
s'_0 &= s_0 [\beta_0 (r_0, \alpha_0) - S] - k_0 D [\delta \sin(\omega t) + 1] s_0 \\
s'_1 &= s_1 [\beta_1 (r_1, \alpha_1) - \epsilon_1 - S] + \epsilon_2 s_2 - k_1 D [\delta \sin(\omega t) + 1] s_1 \\
s'_2 &= s_2 [\beta_2 (r_2, \alpha_2) - \epsilon_2 - S] + \epsilon_1 s_1 - k_2 D [\delta \sin(\omega t) + 1] s_2
\end{aligned} \tag{4.19}$$

where;  $S = s_0 + s_1 + s_2$ ,  $\delta$  and  $\omega$  are the amplitude and frequency of fluctuations, with all other parameters remain the same as defined in equations 2.1 at the beginning of chapter 2.

#### 4.6.1 When the Value of $\beta_0$ is Greater than the Average Value of $\beta_1$ and $\beta_2$ , $[\beta_0 > \frac{1}{2}(\beta_1 + \beta_2)]$

Plots (a) to (d) in Figure 4.17 when the antibiotic drug ( $D$ ) treatment fluctuates over time produce the same results like those obtained in plots (a) to (d) of Figure 4.2 above for the non-fluctuating situation, with a differences of fluctuations in the densities of the existing strain in Figure 4.17, which is caused as a result of the fluctuating resources in the antibiotic drug ( $D$ ) treatment, with all the respective plots in both Figures having the same parameter values, and they produced the same points of switching between the strains in either case.

The frequency of oscillations or fluctuations within the densities of the existing ( $s_0$ ) strain is very interesting when the strain death rate ( $k_i$ ) value is increased in plot (c) compared to what was obtained in plot (a), but the density of the existing ( $s_1, s_2$ ) strains in plot (c) decreases because of its high death rate ( $k_0$ ) value, which is expected. This means the frequency of oscillations is linked to the death rate ( $k_i$ ) of the dominant strain. The higher the death rate ( $k_i$ ) value of the dominant strain, the more rapid the fluctuations become, which is due to the rapid turnover causing a high fluctuating competition.

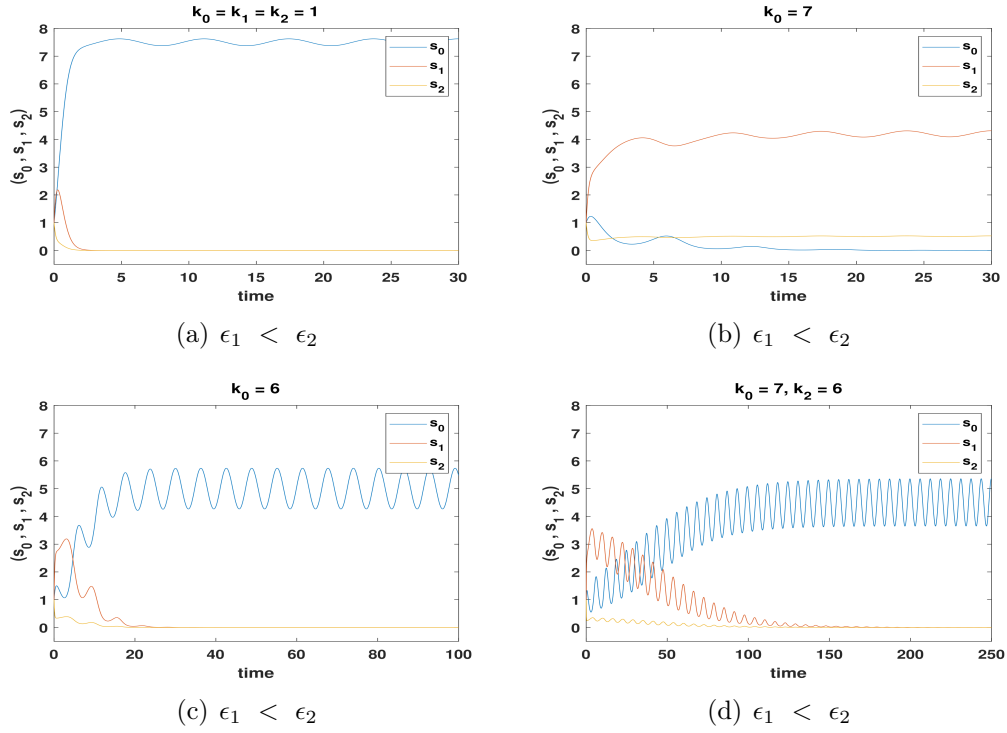


Figure 4.17: The Numerical graphs for the dynamics of the 3D bet-hedging model with the strains death rates ( $k_i$ ), and the fluctuations within the antibiotic drug ( $D$ ) treatment for  $\beta_0 > \frac{1}{2}(\beta_1 + \beta_2)$ , with both strains having the same initial values ( $s_0(0) = s_1(0) = s_2(0) = 1$ ), with different ranges of time for the plots, different strains growth rates values ( $\beta_0 = 8, \beta_1 = 5, \beta_2 = 7$ ), with the amplitude  $\delta = 0.25$ , and the frequency of the fluctuation resources  $\omega = 1$ , the antibiotic drug treatment  $D = 0.5$ , with all other death rate ( $k_i$ ) values not specified in each plot equal to 1 (*i.e.*  $k_i = 1$ , as  $i = 0, 1, 2$ ), and different transition rates values  $\epsilon_1 = 1$ , and  $\epsilon_2 = 10$ .

The results obtained in Figure 4.17 were summarized in Figure 4.18, which clearly show if  $k_0$  is increased, this leads to a switch from the  $s_0$  equilibrium to the  $(s_1, s_2)$  equilibrium as shown in plot (a), but the  $s_1$  strain exists at a higher density than the  $s_2$  strain, because of higher value of the  $s_2$  strain migrating to the  $s_1$  strain. Likewise, if  $k_1$  and  $k_2$  were respectively increased in plots (b) and (c), they also leads to switches from the  $(s_1, s_2)$  equilibrium to the  $s_0$  equilibrium, with different death rate ( $k_i$ ) values of the other strains in each case.



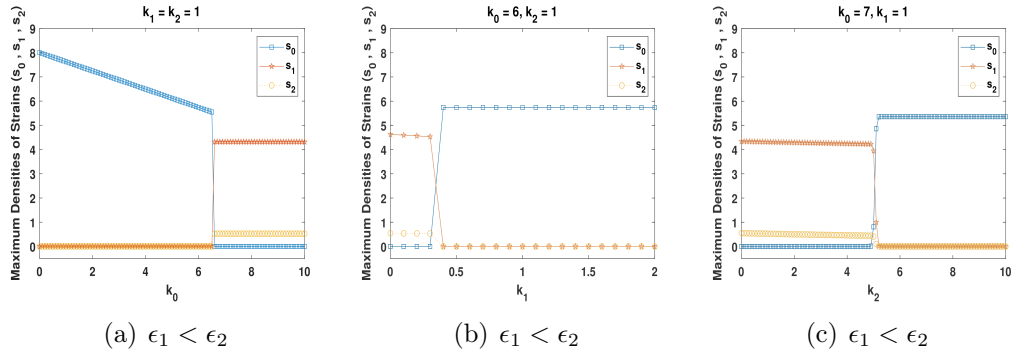


Figure 4.18: The Numerical graphs for the maximum densities of strains for the 3D bet-hedging model, with the strains death rates ( $k_i$ ) and the fluctuations within the antibiotic drug ( $D$ ) treatment for  $\beta_0 > \frac{1}{2}(\beta_1 + \beta_2)$ , with both strains having the same initial values ( $s_0(0) = s_1(0) = s_2(0) = 0.2$ ), different ranges of the strains death rates ( $k_i$ ) for the plots, different values of the strains growth rates ( $\beta_0 = 8, \beta_1 = 5, \beta_2 = 7$ ), with the amplitude  $\delta = 0.25$ , and the frequency of fluctuating resources  $\omega = 1$ , the antibiotic drug treatment  $D = 0.5$ , and different transition rates values  $\epsilon_1 = 1$ , and  $\epsilon_2 = 10$ .

#### 4.6.2 When the Value of $\beta_0$ is Less than the Average Value of $\beta_1$ and $\beta_2$ , $[\beta_0 < \frac{1}{2}(\beta_1 + \beta_2)]$

In Figure 4.19 below it is discovered that the whole plots were the same as those obtained in Figure 4.4 for the non-fluctuating environment. The only difference is the fluctuations within the densities of the existing strains as obtained in section 4.6.1 above, and the oscillations are caused by the fluctuating resources within the antibiotic drug ( $D$ ) treatment.

Like what was observed in section 4.6.1 above, the frequency of oscillations is linked to the death rate ( $k_i$ ) for the dominant strain in this section too. Also in plots (b), (c), and (d) they show different values of the strains death rates ( $k_i$ ) at which switches between the strains occurred.

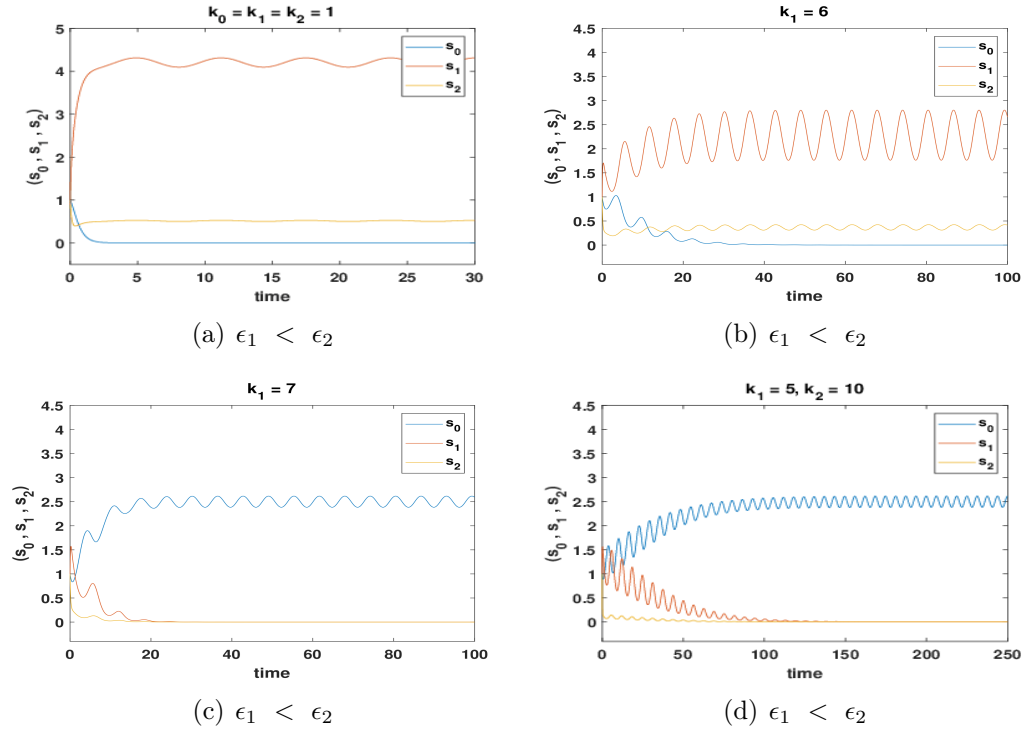


Figure 4.19: The Numerical graphs for the dynamics of the 3D bet-hedging model with the strains death rates ( $k_i$ ), and the fluctuations within the antibiotic drug ( $D$ ) treatment for  $\beta_0 < \frac{1}{2}(\beta_1 + \beta_2)$ , with both strains having the same initial values ( $s_0(0) = s_1(0) = s_2(0) = 1$ ), with different ranges of time for the plots, different strains growth rates values ( $\beta_0 = 3, \beta_1 = 5, \beta_2 = 7$ ), with the amplitude  $\delta = 0.25$ , and the frequency of fluctuation resources  $\omega = 1$ , the antibiotic drug treatment  $D = 0.5$ , with all other death rate ( $k_i$ ) values not specified in each plot equal to 1 (*i. e.*  $k_i = 1$ , as  $i = 0, 1, 2$ ), and different transition rates values  $\epsilon_1 = 1$ , and  $\epsilon_2 = 10$ .

The plots in Figure 4.19 with other plots not shown were summarized in Figure 4.20 below, which show when the non-switching ( $s_0$ ) strain death rate ( $k_0$ ) value is increased, with different values of the other strains death rates ( $k_i$ ), it leads to a switching from the  $s_0$  equilibrium to the ( $s_1, s_2$ ) equilibrium as shown in plot (a), and the  $s_1$  strain existing with a higher density because of the higher value of the  $s_2$  strain transiting to the  $s_1$  strain.

Also when the switching strains' death rates ( $k_1$ ) and ( $k_2$ ) values were increased, they respectively lead to switching from the ( $s_1, s_2$ ) equilibrium to the  $s_0$  equilibrium in plots (b) and (c), with different values of the other strains death rates ( $k_i$ ) as well. And we can easily noticed the switching is at higher ( $k_1, k_2$ ) and lower  $k_0$  values in figure 4.20 below, compared to those obtained in Figure 4.18 where the switching were at higher ( $k_0, k_2$ ) and lower  $k_1$  values.

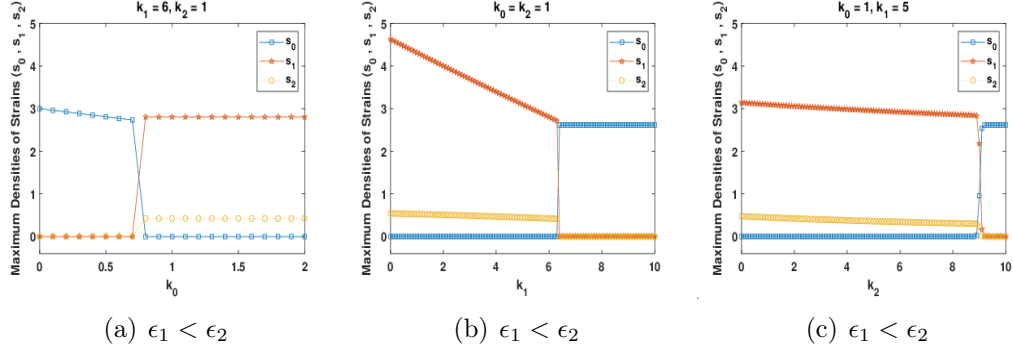


Figure 4.20: The Numerical graphs for the maximum densities of strains for the 3D bet-hedging model, with the strains death rates ( $k_i$ ) and the fluctuations within the antibiotic drug ( $D$ ) treatment for  $\beta_0 < \frac{1}{2}(\beta_1 + \beta_2)$ , with both strains having the same initial values ( $s_0(0) = s_1(0) = s_2(0) = 0.2$ ), different ranges of the strains death rates ( $k_i$ ) for the plots, different values of the strains growth rates ( $\beta_0 = 3, \beta_1 = 5, \beta_2 = 7$ ), with the amplitude  $\delta = 0.25$ , and the frequency of fluctuating resources  $\omega = 1$ , the antibiotic drug treatment  $D = 0.5$ , with all other death rate ( $k_i$ ) values not specified in each plot equal to 1 (*i. e.*  $k_i = 1$ , as  $i = 0, 1, 2$ ), and different transition rates values  $\epsilon_1 = 1$ , and  $\epsilon_2 = 10$ .

### 4.6.3 When the Value of $\beta_0$ is Equal to the Average Value of $\beta_1$ and $\beta_2$ , [ $\beta_0 = \frac{1}{2}(\beta_1 + \beta_2)$ ]

The plots obtained in Figure 4.21 below show the same behavior with what were obtained in Figure 4.6 for the non-fluctuating situation in this chapter 4, with only a difference of fluctuations in the densities of the existing strains, which is quite expected because of the fluctuations within the antibiotic drug ( $D$ ) treatment.

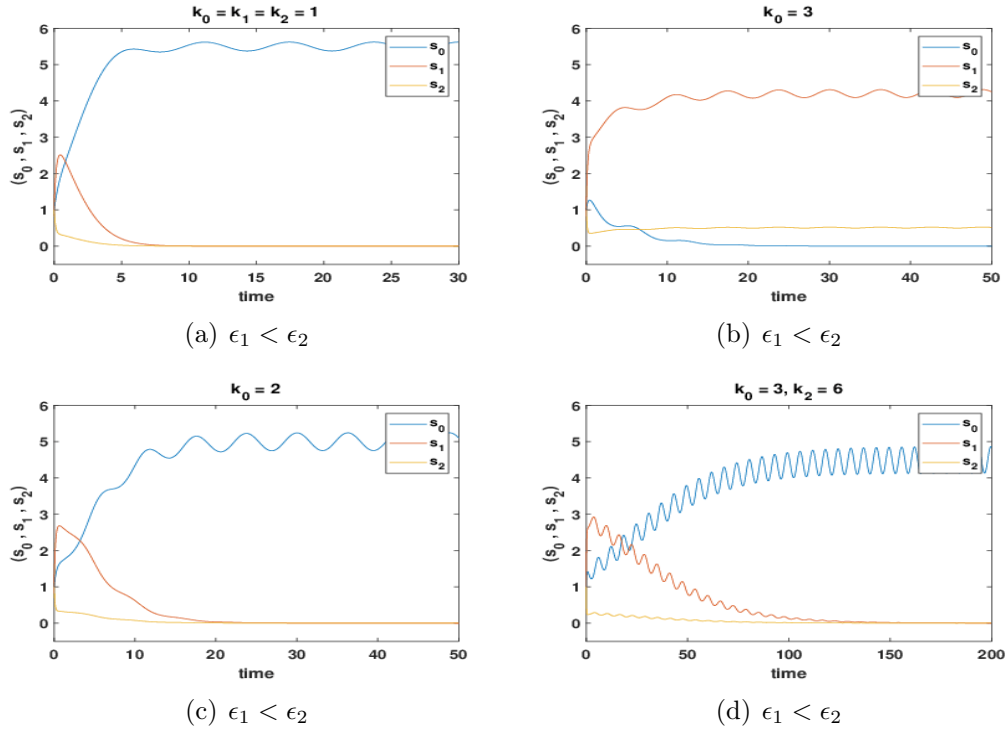


Figure 4.21: The Numerical graphs for the dynamics of the 3D bet-hedging model with the strains death rates ( $k_i$ ), and the fluctuations within the antibiotic drug ( $D$ ) treatment for  $\beta_0 = \frac{1}{2}(\beta_1 + \beta_2)$ , with both strains having the same initial values ( $s_0(0) = s_1(0) = s_2(0) = 1$ ), different ranges of time for the plots, different strains growth rates values ( $\beta_0 = 6, \beta_1 = 5, \beta_2 = 7$ ), with the amplitude  $\delta = 0.25$ , and the frequency of fluctuating resources  $\omega = 1$ , the antibiotic drug treatment  $D = 0.5$ , with all other death rate ( $k_i$ ) values not specified in each plot equal to 1 (*i. e.*  $k_i = 1$ , as  $i = 0, 1, 2$ ), and different transition rates values  $\epsilon_1 = 1$ , and  $\epsilon_2 = 10$ .

Also, Figure 4.22 like other figures summarizes the whole plots obtained in Figure 4.21 and those not shown, which show exactly at what value of the non-switching strain death rates ( $k_0$ ) we obtained a switching from the  $s_0$  equilibrium to the  $(s_1, s_2)$  equilibrium as shown in plot (a). They also show the exact death rates  $k_1$  and  $k_2$  values when the respective switching occurred from the  $(s_1, s_2)$  equilibrium to the  $s_0$  equilibrium in plots (b) and (c).

In those plots we noticed the switches were at higher ( $k_0, k_2$ ) and lower  $k_1$  values compared to what were obtained in Figure 4.18, with an earlier point of switching in plot (a) which was due to the lower growth rate ( $\beta_0$ ) value of the non-switching ( $s_0$ ) strain in this section 4.6.3, compared to the growth rate ( $\beta_0$ ) value used in section 4.6.1 above when  $\beta_0 > \frac{1}{2}(\beta_1 + \beta_2)$ .

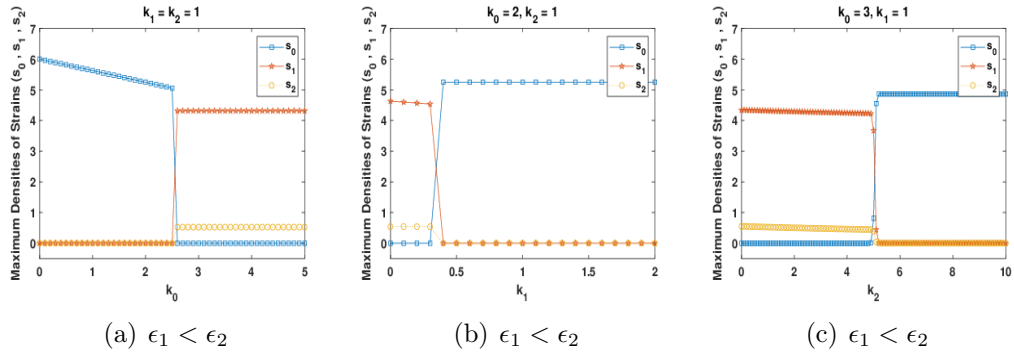


Figure 4.22: The Numerical graphs for the maximum densities of strains for the 3D bet-hedging model, with the strains death rates ( $k_i$ ) and the fluctuations within the antibiotic drug ( $D$ ) treatment for  $\beta_0 = \frac{1}{2}(\beta_1 + \beta_2)$ , with both strains having the same initial values ( $s_0(0) = s_1(0) = s_2(0) = 0.2$ ), different range of strains death rates ( $k_i$ ) for the plots, different values of the strains growth rates ( $\beta_0 = 6, \beta_1 = 5, \beta_2 = 7$ ), with the amplitude  $\delta = 0.25$ , and the frequency of fluctuating resources  $\omega = 1$ , the antibiotic drug treatment  $D = 0.5$ , with all other death rate ( $k_i$ ) values not specified in each plot equal to 1 (*i. e.*  $k_i = 1$ , as  $i = 0, 1, 2$ ), and different transition rates values  $\epsilon_1 = 1$ , and  $\epsilon_2 = 10$ .

#### 4.6.4 When the Values of $\beta_0, \beta_1$ , and $\beta_2$ are Equal, $[\beta_0 = \beta_1 = \beta_2 \neq 1]$

An interesting result was obtained in this section 4.6.4 as expected, where the all strains (the non-switching and the switching) co-exist, as a result of the strains having equal values of their growth rates ( $\beta_i$ ), which were usually the same results obtained in all our previous cases when the strains have equal values of their growth rates ( $\beta_i$ ).

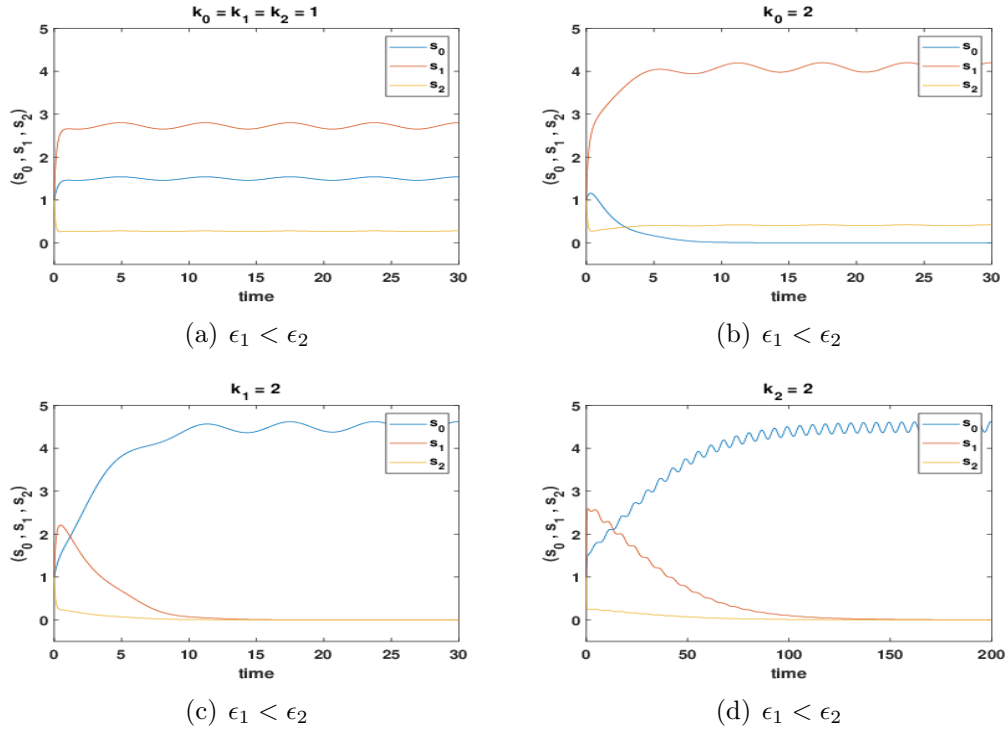


Figure 4.23: The Numerical graphs for the dynamics of the 3D bet-hedging model with the strains death rates ( $k_i$ ), and the fluctuations within the antibiotic drug ( $D$ ) treatment for  $\beta_0 = \beta_1 = \beta_2 = \beta$ , with both strains having the same initial values ( $s_0(0) = s_1(0) = s_2(0) = 1$ ), different ranges of time for the plots, the same strains growth rates values ( $\beta_0 = \beta_1 = \beta_2 = 5$ ), with the amplitude  $\delta = 0.25$ , and the frequency of fluctuations  $\omega = 1$ , the antibiotic drug treatment  $D = 0.5$ , with all other death rate ( $k_i$ ) values not specified in each plot equal to 1 (*i. e.*  $k_i = 1$ , as  $i = 0, 1, 2$ ), and different transition rates values  $\epsilon_1 = 0.05$ , and  $\epsilon_2 = 0.1$ .

Plots (a) to (c) in Figure 4.24 which summarizes the results obtained in figure 4.23 show, when the strains death rates ( $k_i$ , as  $i = 0, 1, 2$ ) values were respectively increased, they leads to a switch from the  $s_0$  equilibrium to the ( $s_1, s_2$ ) equilibrium and vice versa at the same point, which happened because of equal values for the strains growth rate ( $\beta_i$ ).

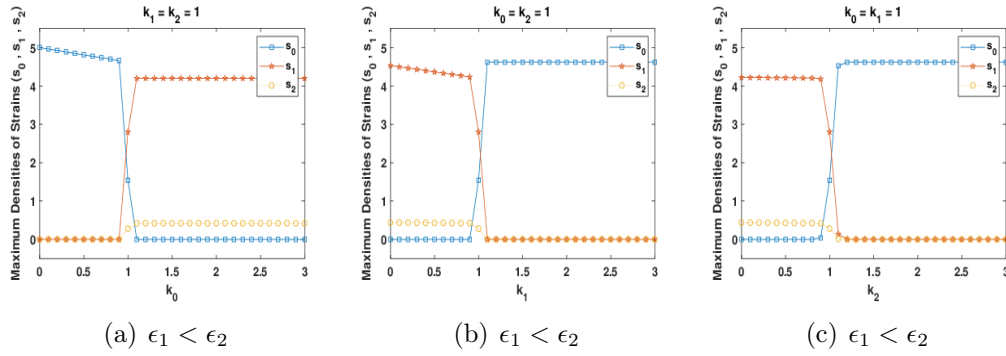


Figure 4.24: The Numerical graphs for the maximum densities of strains for the 3D bet-hedging model, with the strains death rates ( $k_i$ ) and the fluctuations within the antibiotic drug ( $D$ ) treatment for  $\beta_0 = \beta_1 = \beta_2 = \beta$ , with both strains having the same initial values ( $s_0(0) = s_1(0) = s_2(0) = 0.2$ ), the same ranges of strains death rates ( $k_i$ ) for the plots, the same values of the strains growth rates ( $\beta_0 = \beta_1 = \beta_2 = 5$ ), with the amplitude  $\delta = 0.25$ , and the frequency of fluctuating resources  $\omega = 1$ , the antibiotic drug treatment  $D = 0.5$ , with all other death rate ( $k_i$ ) values not specified in each plot equal to 1 (*i. e.*  $k_i = 1$ , as  $i = 0, 1, 2$ ), and different transition rates values  $\epsilon_1 = 1$ , and  $\epsilon_2 = 10$ .

## 4.7 Conclusion

After solving the system of the model equations in this chapter 4, we obtained three equilibrium points for both the constant and different growth rates ( $\beta_i$ ) values of the strains in the non-fluctuating conditions. The overall results show the bacteria will not be stable at the zero  $(0, 0, 0)$  equilibrium point, when the growth rate ( $\beta_i$ ) values of the strains are higher than the interaction between the strains death rates ( $k_i$ ) and the antibiotic drug ( $D$ ) treatment, together with the strains transition rates ( $\epsilon_i$ ) in some situations, and the point will be stable as well when the growth rate ( $\beta_i$ ) of the strains are lower than the conditions mentioned just above (which will be a point of extinction by the strains), and the strain (bacteria) also becomes stable at the non-zero equilibrium points.

The whole results obtained in the non-fluctuating situation in this chapter 4 show there is always a decrease in the densities of the existing strains at the stable point in any conditions when compared with the results obtained in chapter 3, which is caused by the presence of the strains death rates ( $k_i$ ) and the antibiotic drug ( $D$ ) treatment. The level of the decreases in the densities of the existing strains usually depends on the values of the strains death rates ( $k_i$ ) and the antibiotic drug ( $D$ ) treatment.

We also saw a switching between the existing and extinct strains in different conditions, which are usually caused by the strains' growth rates ( $\beta_i$ ), their transition rates ( $\epsilon_i$ ), their death rates ( $k_i$ ), and the antibiotic drug ( $D$ ) treatment values as well. In the cases where we didn't see switching, it could be as a result of either the strains lower growth rate ( $\beta_i$ ), or high transition rate ( $\epsilon_i$ ), or lower death rate ( $k_i$ ) values. The cases we realized in this chapter 4 were mostly caused as a result of either the strains lower death rate ( $k_i$ ), or high transition rate ( $\epsilon_i$ ) values.

In the fluctuating resources within the strains' growth rates ( $\beta_i$ ), we noticed the results obtained were qualitatively the same with those obtained in the non-fluctuating resources situation. We also noticed an interesting result in that situation, where we are only ever at the switching ( $s_1, s_2$ ) equilibrium, but the densities of the predominant strains swapped. This happened because in this case  $r_0$  is very small, and the non-switching ( $s_0$ ) strain has a lower growth rate ( $\beta_i$ ) value, and never grows fast to invade as seen in plots (b) and (c) of Figure 4.12. This also happened because the ( $s_1, s_2$ ) strains are the bet-hedgers. It is also interesting that this is maintained even with very high values of  $k_1$  or  $k_2$ .

Another important aspect we looked at in this chapter 4 is when the antibiotic drug ( $D$ ) treatment fluctuates over time, and we noticed an interesting result in the plots obtained in Figures 4.17, 4.19, 4.21, and 4.23 respectively, showing the higher the death rate ( $k_i$ ) values of the existing strain at the steady state, the more rapid the oscillations become. This means the frequency of oscillations is linked to the death rates ( $k_i$ ) of the existing strain.

In the next chapter 5 we will introduce the dynamics of the antibiotic drug ( $D$ ) treatment in the model, where we will describe the rate at which the antibiotic drug ( $D$ ) treatment is administered, and the degradation term or rate at which the bacteria is being killed, to investigate the behavior and analyze the outcome of the model result as well.



## CHAPTER 5

# Bacterial and the Antimicrobial Treatment Dynamics

---

### 5.1 Introduction

Unlike what was done in chapter 4 where the antibiotic drug ( $D$ ) treatment was held constant or fluctuated over time consistently, in this chapter the dynamics of the antibiotic drug treatment is considered as a dynamic variable. As such we include an administration rate ( $a$ ), and the rate of degrading the drug ( $c$ ) up to when it becomes no longer effective, and the fluctuating resources in this chapter 5 is within the administration rate ( $a$ ) for the dynamics of the antibiotic drug ( $D$ ) treatment. We will investigate whether different results occur with a dynamic treatment compared to the results obtained in chapter 4.

The aim is to compare the results obtained in all the sections in this chapter 5, and to observe how these bacteria are affected by the antibiotic drug ( $D$ ) treatment in each case, and also to investigate if there is any differences in the results obtained with/without fluctuating resources in the bacterial growth rates ( $\beta_i$ ), and also with the results obtained when the fluctuating resources is in the administration rate ( $a$ ) for the dynamics of the antibiotic drug ( $D$ ) treatment.

### 5.2 The Model of the Bacterial and the Antimicrobial Treatment Dynamics

After investigating and analysing the dynamics of the model for the non-switching ( $s_0$ ) and the switching ( $s_1, s_2$ ) bacteria with the antimicrobial ( $D$ ) treatment which is held constant in chapter 4, the research continued by investigating the same model with the inclusion of a new variable for the antimicrobial ( $D$ ) treatment dynamics in the model, which describes the rate ( $a$ ) at

which the antibiotic drug ( $D$ ) treatment is being administered, and the rate ( $c$ ) of degrading the antibiotic drug ( $D$ ) treatment up to when the antibiotic drug ( $D$ ) treatment becomes no longer effective (Ibargüen-Mondragón et al., 2014).

The model equation with the inclusion of the antimicrobial ( $D$ ) treatment dynamics as mentioned earlier is defined as;

$$\begin{aligned}
 s'_0 &= s_0 [\beta_0 (r_0, \alpha_0) - S] - k_0 D s_0 \\
 s'_1 &= s_1 [\beta_1 (r_1, \alpha_1) - \epsilon_1 - S] + \epsilon_2 s_2 - k_1 D s_1 \\
 s'_2 &= s_2 [\beta_2 (r_2, \alpha_2) - \epsilon_2 - S] + \epsilon_1 s_1 - k_2 D s_2 \\
 D' &= a - cD
 \end{aligned} \tag{5.1}$$

where;  $S = s_0 + s_1 + s_2$ ,  $a$  is the rate of the antibiotic drug treatment administration which is a non-fluctuating value here, and  $c$  is the rate of decay of the antibiotic drug ( $D$ ), with all other parameters the same as defined in equations (2.1), (2.2) and (4.1) respectively.

The bacterial growth rate ( $\beta_i$ ), based on the enzymes ( $r_i$ ), and the environment ( $\alpha_t$ ) is defined in equation (2.2) as well.

Beginning by the concept of our research in this project, stability analysis is first performed on the model equations by considering different conditions to check the behavior of the model with the inclusion of the antibiotic drug ( $D$ ) treatment dynamics, through finding the equilibrium point of the system, stability of the model and the eigenvalues of the system from the characteristic equation (2.4).

### 5.3 Constant Growth Rate ( $\beta_i$ ) Values of the Bacteria

As we normally start with throughout this project, once the values of the enzymes ( $r_i$ ) in the bacterial growth rate ( $\beta_i$ ) of equation (2.2) are zero (0), meaning the respective enzymes of the bacteria ( $r_0 = r_1 = r_2 = 0$ ), the strains maintained a constant growth rate, and it implies the growth rates of the whole strains are equal ( $\beta_0 = \beta_1 = \beta_2 = \beta$ ).

Since ( $\beta_0 = \beta_1 = \beta_2 = \beta$ ), the solution to the equation (5.1) yielded four equilibrium points in the form of;

$$\begin{aligned}
S^* &= (s_0^*, s_1^*, s_2^*, D^*) = \left(0, 0, 0, \frac{a}{c}\right) \\
S^* &= (s_0^*, s_1^*, s_2^*, D^*) = \left(\beta - \frac{a}{c}k_0, 0, 0, \frac{a}{c}\right) \\
S^* &= (s_0^*, s_1^*, s_2^*, D^*) = \left(0, P, Q, \frac{a}{c}\right) \\
S^* &= (s_0^*, s_1^*, s_2^*, D^*) = \left(0, R, T, \frac{a}{c}\right)
\end{aligned} \tag{5.2}$$

where;

$$\begin{aligned}
P &= \frac{\beta c [c\epsilon_T + a(k_1 - k_2)] - c [2\epsilon_1(c\epsilon_2 + ak_1) - ak_2\delta\epsilon] - a^2k_1(k_1 - k_2)}{2ac(k_1 - k_2)} \\
&\quad - \frac{\left\{ c^2 (\epsilon_1^2 + \epsilon_2^2) - (\beta c - c\epsilon_T - ak_1) \sqrt{[a(k_1 - k_2)]^2 + 2ac\delta\epsilon(k_1 - k_2) + (c\epsilon_T)^2} \right\}}{2ac(k_1 - k_2)} \\
Q &= \frac{c [2\epsilon_2(c\epsilon_1 + ak_2) + ak_1\delta\epsilon] - \beta c [c\epsilon_T - a(k_1 - k_2)] + a^2k_2(k_2 - k_1)}{2ac(k_1 - k_2)} \\
&\quad + \frac{\left[ c^2 (\epsilon_1^2 + \epsilon_2^2) - (\beta c - c\epsilon_T - ak_2) \sqrt{[a(k_1 - k_2)]^2 + 2ac\delta\epsilon(k_1 - k_2) + (c\epsilon_T)^2} \right]}{2ac(k_1 - k_2)} \\
R &= \frac{\beta c [c\epsilon_T + a(k_1 - k_2)] - c [2\epsilon_1(c\epsilon_2 + ak_1) - ak_2\delta\epsilon] - a^2k_1(k_1 - k_2)}{2ac(k_1 - k_2)} \\
&\quad - \frac{\left\{ c^2 (\epsilon_1^2 + \epsilon_2^2) + (\beta c - c\epsilon_T - ak_1) \sqrt{[a(k_1 - k_2)]^2 + 2ac\delta\epsilon(k_1 - k_2) + (c\epsilon_T)^2} \right\}}{2ac(k_1 - k_2)} \\
T &= \frac{c [2\epsilon_2(c\epsilon_1 + ak_2) + ak_1\delta\epsilon] - \beta c [c\epsilon_T - a(k_1 - k_2)] + a^2k_2(k_2 - k_1)}{2ac(k_1 - k_2)} \\
&\quad + \frac{\left[ c^2 (\epsilon_1^2 + \epsilon_2^2) + (\beta c - c\epsilon_T - ak_2) \sqrt{[a(k_1 - k_2)]^2 + 2ac\delta\epsilon(k_1 - k_2) + (c\epsilon_T)^2} \right]}{2ac(k_1 - k_2)}
\end{aligned}$$

$$\epsilon_T = \epsilon_1 + \epsilon_2, \quad \text{and} \quad \delta\epsilon = \epsilon_1 - \epsilon_2$$

The Jacobian matrix obtained in equation (5.3) below for the present system in equation (5.1), is basically the same with the one obtained in chapter 4 with  $D = \frac{a}{c}$  in this chapter, and that happened because  $D$  is decoupled from the other equations, which makes it different.

$$J = \begin{pmatrix} AD & -s_0^* & -s_0^* & -k_0s_0^* \\ -s_1^* & AE & -s_1^* + \epsilon_2 & -k_1s_1^* \\ -s_2^* & -s_2^* + \epsilon_1 & AF & -k_2s_2^* \\ 0 & 0 & 0 & -c \end{pmatrix} \tag{5.3}$$

where;

$$AD = \beta - 2s_0^* - s_1^* - s_2^* - k_0D^*,$$

$$AE = \beta - \epsilon_1 - s_0^* - 2s_1^* - s_2^* - k_1 D^*,$$

$$AF = \beta - \epsilon_2 - s_0^* - s_1^* - 2s_2^* - k_2 D^*$$

The first equilibrium point  $S^* = (s_0^*, s_1^*, s_2^*, D^*) = (0, 0, 0, \frac{a}{c})$  obtained in equation (5.2) was substituted in the Jacobian matrix in equation (5.3), and we obtained;

$$J = \begin{pmatrix} \beta - \frac{a}{c}k_0 & 0 & 0 & 0 \\ 0 & \beta - \epsilon_1 - \frac{a}{c}k_1 & \epsilon_2 & 0 \\ 0 & \epsilon_1 & \beta - \epsilon_2 - \frac{a}{c}k_2 & 0 \\ 0 & 0 & 0 & -c \end{pmatrix} \quad (5.4)$$

An identity matrix together with the Jacobian matrix obtained in equation (5.4) were substituted in to the characteristic equation (2.4), which gives the below expression as;

$$\begin{vmatrix} \beta - \frac{a}{c}k_0 - \lambda & 0 & 0 & 0 \\ 0 & \beta - \epsilon_1 - \frac{a}{c}k_1 - \lambda & \epsilon_2 & 0 \\ 0 & \epsilon_1 & \beta - \epsilon_2 - \frac{a}{c}k_2 - \lambda & 0 \\ 0 & 0 & 0 & -c - \lambda \end{vmatrix} = 0 \quad (5.5)$$

After evaluating the above expression in equation (5.5) by hand, using the determinant approach method, the four eigenvalues were respectively obtained as;

$$\begin{aligned} \lambda_1 &= -c \\ \lambda_2 &= \beta - \frac{a}{c}k_0 \\ \lambda_3 &= \beta - \left[ \epsilon_1 + \frac{a}{c}k_1 \right] \\ \lambda_4 &= \beta - \left[ \epsilon_2 + \frac{a}{c}k_2 \right] \end{aligned} \quad (5.6)$$

Analysis of equation (5.6) says, if either  $\beta > \frac{a}{c}k_0$ , or  $\beta > \epsilon_1 + \frac{a}{c}k_1$ , or  $\beta > \epsilon_2 + \frac{a}{c}k_2$ , or any two of them, or both three are true, this equilibrium point of  $(0, 0, 0, \frac{a}{c})$  will be locally and asymptotically unstable, and the bacteria will not settle at this point. But with opposite of the above condition as,  $\beta < \frac{a}{c}k_0$ ,  $\beta < \epsilon_1 + \frac{a}{c}k_1$ , and  $\beta < \epsilon_2 + \frac{a}{c}k_2$ , we can get a complete extinction of the strain(s), because of killing the strains by the antibiotic drug ( $D$ ) treatment concentration.

The second equilibrium point  $S^* = (s_0^*, s_1^*, s_2^*, D^*) = (\beta - \frac{a}{c}k_0, 0, 0, \frac{a}{c})$  obtained in equation (5.2) was substituted in the Jacobian matrix in equation

(5.3), and after the usual evaluation of the matrix, we obtained;

$$J = \begin{pmatrix} \frac{a}{c}k_0 - \beta & \frac{a}{c}k_0 - \beta & \frac{a}{c}k_0 - \beta & k_0 \left( \frac{a}{c}k_0 - \beta \right) \\ 0 & \frac{a}{c}(k_0 - k_1) - \epsilon_1 & \epsilon_2 & 0 \\ 0 & \epsilon_1 & \frac{a}{c}(k_0 - k_2) - \epsilon_2 & 0 \\ 0 & 0 & 0 & -c \end{pmatrix} \quad (5.7)$$

As always, the identity matrix together with the Jacobian matrix obtained in equation (5.7) were substituted in the characteristic equation (2.4), and the result obtained gives;

$$\begin{vmatrix} AG - \lambda & \frac{a}{c}k_0 - \beta & \frac{a}{c}k_0 - \beta & k_0 \left( \frac{a}{c}k_0 - \beta \right) \\ 0 & AH - \lambda & \epsilon_2 & 0 \\ 0 & \epsilon_1 & AI - \lambda & 0 \\ 0 & 0 & 0 & -c - \lambda \end{vmatrix} = 0 \quad (5.8)$$

where;  $AG = \frac{a}{c}k_0 - \beta$ ,  $AH = \frac{a}{c}(k_0 - k_1) - \epsilon_1$ , and  $AI = \frac{a}{c}(k_0 - k_2) - \epsilon_2$

Evaluating the expression obtained in equation (5.8) above, we obtained the four eigenvalues as;

$$\begin{aligned} \lambda_1 &= -c \\ \lambda_2 &= \frac{a}{c}k_0 - \beta \\ \lambda_3 &= \frac{a}{c}(k_0 - k_1) - \epsilon_1 \\ \lambda_4 &= \frac{a}{c}(k_0 - k_2) - \epsilon_2 \end{aligned} \quad (5.9)$$

Analysis of the eigenvalues obtained in equation (5.9) says, if  $\beta > \frac{a}{c}k_0$ ,  $\left( \frac{a}{c}k_1 + \epsilon_1 \right) > \frac{a}{c}k_0$ , and  $\left( \frac{a}{c}k_2 + \epsilon_2 \right) > \frac{a}{c}k_0$ , this point will be locally and asymptotically stable at the non-switching ( $s_0$ ) strain. Otherwise, if the opposite for any of the above mentioned conditions is true, one of the remaining non-zero equilibrium points (the last one) obtained in equation (5.2) will be locally and asymptotically stable at the switching ( $s_1, s_2$ ) strains.

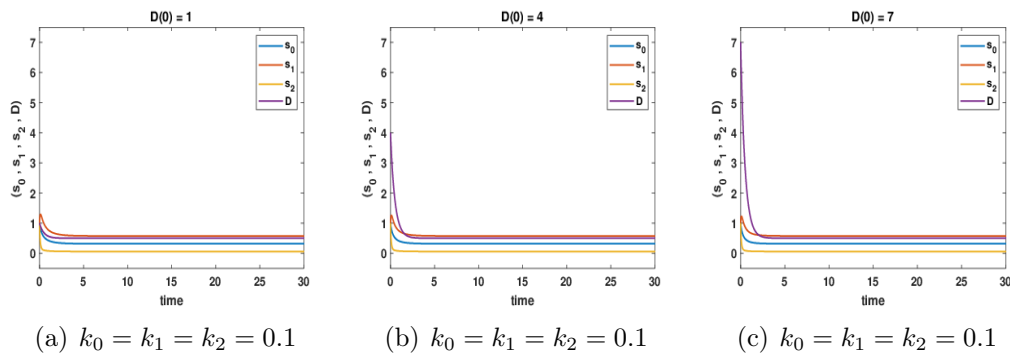


Figure 5.1: The Numerical graphs for the intrinsic dynamics of the 4D bet-hedging model with the dynamics of the antibiotic drug ( $D$ ) treatment, and the respective death rates ( $k_i$ ) of the strains, which has a constant growth rates value for the strain:  $\beta_0 = \beta_1 = \beta_2 = \beta = 1$ , with both the strains and the antibiotic drug ( $D$ ) treatment having the same initial values:  $s_0(0) = s_1(0) = s_2(0) = D(0) = 1$ , the rate of the antibiotic drug administration  $a = 1$ , the rate of the antibiotic drug decay  $c = 2$ , and different transition rate values:  $\epsilon_1 = 1$ , and  $\epsilon_2 = 10$ .

Plots (a) to (c) in Figure 5.1 show the dynamics of the strains with different initial values for the antibiotic drug ( $D$ ) treatment concentration. In plot (a) when the antibiotic drug ( $D$ ) treatment concentration has the same initial values with all the strains, we noticed how the strains were decaying at the beginning before reaching their equilibrium points.

Plots (b) and (c) respectively show much further decaying of the strains at the beginning compared to what was observed in plot (a) when the initial values of the antibiotic drug ( $D$ ) treatment concentration were increased, before both the antibiotic drug and the strains become stable at their respective equilibrium points.

In general the trend show as the initial values of the antibiotic drug ( $D$ ) treatment concentration were increased, the densities of the strains decays much worse at an early time (the beginning) of each plots, compared to what were obtained in the previous plot, until when the antibiotic drug ( $D$ ) treatment reaches it equilibrium point, where all the strains will reach their respective equilibrium points too.

## 5.4 Different Growth Rate ( $\beta_i$ ) Values of the Bacteria

In this section 5.4, we are concerned about investigating the behavior of the strains when their growth rate ( $\beta_i$ ) values are not equal ( $\beta_0 \neq \beta_1 \neq \beta_2$ )

for the strains in the model with the dynamics of the antibiotic drug ( $D$ ) treatment concentration in a non-fluctuating environment.

To achieve that, the model equations (5.1) were solved with the idea of each strain having a different growth rate value ( $\beta_0 \neq \beta_1 \neq \beta_2$ ), and based on that we obtained four equilibrium points from the system of equations, a zero and three non-zero's as;

$$\begin{aligned}
S^* &= (s_0^*, s_1^*, s_2^*, D^*) = \left(0, 0, 0, \frac{a}{c}\right) \\
S^* &= (s_0^*, s_1^*, s_2^*, D^*) = \left(\beta_0 - \frac{a}{c}k_0, 0, 0, \frac{a}{c}\right) \\
S^* &= (s_0^*, s_1^*, s_2^*, D^*) = \left(0, U, V, \frac{a}{c}\right) \\
S^* &= (s_0^*, s_1^*, s_2^*, D^*) = \left(0, W, Z, \frac{a}{c}\right),
\end{aligned} \tag{5.10}$$

where;

$$\begin{aligned}
U &= \frac{c^2 [(\beta_1^2 + \epsilon_1^2 + \epsilon_2^2) - \{\beta_1(\beta_2 + 2\epsilon_1) - \beta_2\Delta\epsilon - 2\epsilon_1\epsilon_2\}] + a^2(k_1^2 - k_1k_2)}{2c[c(\beta_1 - \beta_2) - a(k_1 - k_2)]} \\
&\quad - \frac{c \left\{ a[\beta_1(2k_1 - k_2) - k_1(\beta_2 + 2\epsilon_1) + k_2\Delta\epsilon] + [(\beta_1 - \epsilon_T) - ak_1]\sqrt{M} \right\}}{2c[c(\beta_1 - \beta_2) - a(k_1 - k_2)]} \\
V &= \frac{-c^2 [(\beta_2^2 + \epsilon_1^2 + \epsilon_2^2) + \{\beta_2(\beta_1 + 2\epsilon_2) + \beta_1\Delta\epsilon - 2\epsilon_1\epsilon_2\}] - a^2(k_2^2 + k_1k_2)}{2c[c(\beta_1 - \beta_2) - a(k_1 - k_2)]} \\
&\quad + \frac{c \left\{ a[k_2(\beta_1 + 2\epsilon_2) + \beta_2(k_1 - 2k_2) + k_1\Delta\epsilon] + [(\beta_2 - \epsilon_T) - ak_2]\sqrt{M} \right\}}{2c[c(\beta_1 - \beta_2) - a(k_1 - k_2)]} \\
W &= \frac{c^2 [(\beta_1^2 + \epsilon_1^2 + \epsilon_2^2) - \{\beta_1(\beta_2 + 2\epsilon_1) - \beta_2\Delta\epsilon - 2\epsilon_1\epsilon_2\}] + a^2(k_1^2 - k_1k_2)}{2c[c(\beta_1 - \beta_2) - a(k_1 - k_2)]} \\
&\quad - \frac{c \left\{ a[\beta_1(2k_1 - k_2) - k_1(\beta_2 + 2\epsilon_1) + k_2\Delta\epsilon] - [(\beta_1 - \epsilon_T) - ak_1]\sqrt{M} \right\}}{2c[c(\beta_1 - \beta_2) - a(k_1 - k_2)]} \\
Z &= \frac{-c^2 [(\beta_2^2 + \epsilon_1^2 + \epsilon_2^2) + \{\beta_2(\beta_1 + 2\epsilon_2) + \beta_1\Delta\epsilon - 2\epsilon_1\epsilon_2\}] - a^2(k_2^2 + k_1k_2)}{2c[c(\beta_1 - \beta_2) - a(k_1 - k_2)]} \\
&\quad + \frac{c \left\{ a[k_2(\beta_1 + 2\epsilon_2) + \beta_2(k_1 - 2k_2) + k_1\Delta\epsilon] - [(\beta_2 - \epsilon_T) - ak_2]\sqrt{M} \right\}}{2c[c(\beta_1 - \beta_2) - a(k_1 - k_2)]} \\
M &= [a(k_1 - k_2)]^2 - 2ac(k_1 - k_2)[(\beta_1 - \beta_2) - \Delta\epsilon] + [c(\beta_1 - \beta_2)]^2 - 2c^2\Delta\epsilon(\beta_1 - \beta_2) + (c\epsilon_T)^2 \\
\epsilon_T &= \epsilon_1 + \epsilon_2, \quad \text{and} \quad \Delta\epsilon_T = \epsilon_1 - \epsilon_2
\end{aligned}$$

Based on the condition focused in the research in this section 5.4 for each strain having different values of the growth rate ( $\beta_0 \neq \beta_1 \neq \beta_2$ ), the Jacobian

matrix from the system of equations (5.1) gives;

$$J = \begin{pmatrix} AJ & -s_0^* & -s_0^* & -k_0 s_0^* \\ -s_1^* & AK & -s_1^* + \epsilon_2 & -k_1 s_1^* \\ -s_2^* & -s_2^* + \epsilon_1 & AL & -k_2 s_2^* \\ 0 & 0 & 0 & -c \end{pmatrix} \quad (5.11)$$

where;

$$AJ = \beta_0 - 2s_0^* - s_1^* - s_2^* - Dk_0,$$

$$AK = \beta_1 - \epsilon_1 - s_0^* - 2s_1^* - s_2^* - Dk_1,$$

$$AL = \beta_2 - \epsilon_2 - s_0^* - s_1^* - 2s_2^* - Dk_2$$

After substituting the zero equilibrium point  $S^* = (s_0^*, s_1^*, s_2^*, D^*) = (0, 0, 0, \frac{a}{c})$  obtained in equation (5.10) in the Jacobian matrix in equation (5.11), the matrix was transformed to;

$$J = \begin{pmatrix} \beta_0 - \frac{a}{c}k_0 & 0 & 0 & 0 \\ 0 & \beta_1 - \epsilon_1 - \frac{a}{c}k_1 & \epsilon_2 & 0 \\ 0 & \epsilon_1 & \beta_2 - \epsilon_2 - \frac{a}{c}k_2 & 0 \\ 0 & 0 & 0 & -c \end{pmatrix} \quad (5.12)$$

As usual, the identity matrix together with the Jacobian matrix obtained in equation (5.12), were both substituted in the characteristic equation (2.4), and the outcome of such gave us the below expression as;

$$\begin{vmatrix} AM - \lambda & 0 & 0 & 0 \\ 0 & AN - \lambda & \epsilon_2 & 0 \\ 0 & \epsilon_1 & AP - \lambda & 0 \\ 0 & 0 & 0 & -c - \lambda \end{vmatrix} = 0 \quad (5.13)$$

where;  $AM = \beta_0 - \frac{a}{c}k_0$ ,  $AN = \beta_1 - \epsilon_1 - \frac{a}{c}k_1$ , and  $AP = \beta_2 - \epsilon_2 - \frac{a}{c}k_2$

Evaluating the above expression obtained in equation (5.13) by hand using the determinant method approach, the four eigenvalues were obtained as;

$$\begin{aligned} \lambda_1 &= -c \\ \lambda_2 &= \beta_0 - \frac{a}{c}k_0 \\ \lambda_3 &= \beta_1 - \left[ \epsilon_1 + \frac{a}{c}k_1 \right] \\ \lambda_4 &= \beta_2 - \left[ \epsilon_2 + \frac{a}{c}k_2 \right] \end{aligned} \quad (5.14)$$

Analysis of the above eigenvalues obtained in equation (5.14) says, if either  $\beta_0 > \frac{a}{c}k_0$ , or  $\beta_1 > \left[ \epsilon_1 + \frac{a}{c}k_1 \right]$ , or  $\beta_2 > \left[ \epsilon_2 + \frac{a}{c}k_2 \right]$ , or any of the two, or both of them are true, this equilibrium point will be locally and asymptotically unstable, and the bacteria will not settle at this point. But for the opposites of the above mentioned conditions, this will allow for complete extinction of



all the strains

The second equilibrium point  $S^* = (s_0^*, s_1^*, s_2^*, D^*) = (\beta_0 - \frac{a}{c}k_0, 0, 0, \frac{a}{c})$  obtained in equation (5.10) was substituted in the Jacobian matrix in equation (5.11), and the result obtained show;

$$J = \begin{pmatrix} \frac{a}{c}k_0 - \beta_0 & \frac{a}{c}k_0 - \beta_0 & \frac{a}{c}k_0 - \beta_0 & k_0(\frac{a}{c}k_0 - \beta_0) \\ 0 & \beta_1 - \beta_0 - \epsilon_1 + \frac{a}{c}(k_0 - k_1) & \epsilon_2 & 0 \\ 0 & \epsilon_1 & \beta_2 - \beta_0 - \epsilon_2 + \frac{a}{c}(k_0 - k_2) & 0 \\ 0 & 0 & 0 & -c \end{pmatrix} \quad (5.15)$$

The Jacobian matrix obtained in equation (5.15), together with the identity matrix were both substituted in the characteristic equation (2.4), and the outcome show;

$$\begin{vmatrix} \frac{a}{c}k_0 - \beta_0 - \lambda & \frac{a}{c}k_0 - \beta_0 & \frac{a}{c}k_0 - \beta_0 & k_0(\frac{a}{c}k_0 - \beta_0) \\ 0 & AQ - \lambda & \epsilon_2 & 0 \\ 0 & \epsilon_1 & AR - \lambda & 0 \\ 0 & 0 & 0 & -c - \lambda \end{vmatrix} = 0 \quad (5.16)$$

where;  $AQ = \beta_1 - \beta_0 - \epsilon_1 + \frac{a}{c}(k_0 - k_1)$ , and  $AR = \beta_2 - \beta_0 - \epsilon_2 + \frac{a}{c}(k_0 - k_2)$

After evaluating the above expression in equation (5.16) with hand using the determinant approach method, the four eigenvalues were obtained as;

$$\begin{aligned} \lambda_1 &= -c \\ \lambda_2 &= \frac{a}{c}k_0 - \beta_0 \\ \lambda_3 &= \beta_1 - (\beta_0 + \epsilon_1) + \frac{a}{c}(k_0 - k_1) \\ \lambda_4 &= \beta_2 - (\beta_0 + \epsilon_2) + \frac{a}{c}(k_0 - k_2) \end{aligned} \quad (5.17)$$

Analysis of the above eigenvalues obtained in equation (5.17) says, if  $\beta_0 > \frac{a}{c}k_0$ ,  $[\beta_0 + \epsilon_1 + \frac{a}{c}k_1] > [\beta_1 + \frac{a}{c}k_0]$ , and  $[\beta_0 + \epsilon_2 + \frac{a}{c}k_2] > [\beta_2 + \frac{a}{c}k_0]$ , this point will be locally, and asymptotically stable at the non-switching ( $s_0$ ) strain. Else, if the reverse (opposite) of the above mentioned conditions are all true, one of the remaining non-zero equilibrium points (the last one) obtained in equation (5.10) will be stable at the switching ( $s_1, s_2$ ) strains.

#### 5.4.1 When the Value of $\beta_0$ is Greater than the Average Value of $\beta_1$ and $\beta_2$ , $[\beta_0 > \frac{1}{2}(\beta_1 + \beta_2)]$

Plots (a) and (d) in Figure 5.2 below show some interesting results, with low initial densities of the antibiotic drug ( $D$ ) treatment concentration, where we

realized the system initially appears to go towards the  $(s_1, s_2)$  equilibrium, which allowed the  $(s_1, s_2)$  strains to grow quite large in plots (b), (c), (e), and (f) with relatively high initial densities of the antibiotic drug ( $D$ ) treatment concentration, before eventually flipping to the  $s_0$  equilibrium.

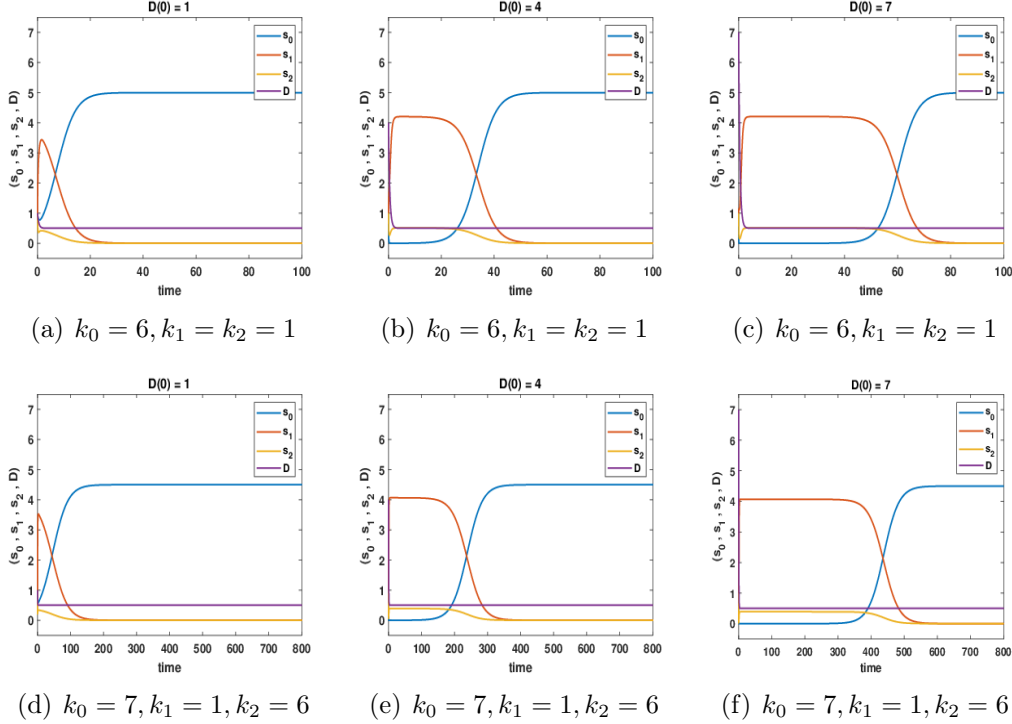


Figure 5.2: The Numerical graphs for the intrinsic dynamics of the 4D bet-hedging model with the dynamics of the antibiotic drug ( $D$ ) treatment for the non-fluctuating growth rate ( $\beta_i$ ) of the strains, and their respective death rates ( $k_i$ ), for  $\beta_0 > \frac{1}{2}(\beta_1 + \beta_2)$  and  $\epsilon_1 < \epsilon_2$ , with both strains having the same initial values:  $s_0(0) = s_1(0) = s_2(0) = 1$ , different initial values for the antibiotic drug ( $D$ ) treatment, different values for the growth rates of the strains:  $\beta_0 = 8$ ,  $\beta_1 = 5$  and  $\beta_2 = 7$ , different values for the strains death rate ( $k_i$ ), the rate of the antibiotic drug administration  $a = 1$ , and the rate of the antibiotic drug decay  $c = 2$ , with different transition rate values:  $\epsilon_1 = 1$ , and  $\epsilon_2 = 10$ .

This show the switching  $(s_1, s_2)$  strains are ultimately unstable in those plots, but the strains can grow quite large for a long frequency of time, depending on the concentration of the antibiotic drug ( $D$ ) treatment, and their death rate ( $k_1, k_2$ ) values, before the eventual flipping of the  $(s_1, s_2)$  strains to where the  $s_0$  equilibrium takes over.

The  $s_0$  strain initially suffered more than the  $(s_1, s_2)$  strains because of the high antibiotic drug ( $D$ ) treatment density, coupled with its high death rate ( $k_0$ ) in plots (a) to (c), causing a lot of damage to the  $s_0$  strain, and

pushing it very close to zero, before the density of the antibiotic drug ( $D$ ) treatment drops, allowing it to slowly recover and take over to become stable at an equilibrium point. But in plots (d) to (f) we realized the  $s_0$  strain takes longer time before it bounced back to take over, caused due to the high density of the antibiotic drug ( $D$ ) treatment together with high death rates of both strains, causing serious competition between them, before the  $s_0$  strain gradually bounce back and win the competition.

This means, the interactions between the densities of the antibiotic drug ( $D$ ) treatment concentration with high death rates ( $k_i$ ) values of any strain(s), and the transition rates ( $\epsilon_i$ ) of the switching strains, partly determines the amount/frequency of unit-time it will take both strains to reach their stable/unstable states as shown in the whole plots.

The strains in the first three plots reach the stable/unstable equilibrium within a few time units, because of the antibiotic drug ( $D$ ) treatment interaction with high death rate ( $k_i$ ) value on the non-switching ( $s_0$ ) strain alone. Unlike in the last three plots, where the amount of time units to reach the stable/unstable equilibrium is almost 8 – 9 times, because of the antibiotic drug ( $D$ ) treatment interaction with high death rates ( $k_i$ ) values on both the switching ( $s_1, s_2$ ) and the non-switching ( $s_0$ ) strains.

In a nutshell, the results show increasing the initial density of the antibiotic drug ( $D$ ) treatment concentration does not affect the equilibrium state of the existing ( $s_0$ ) strain, but it massively delays reaching the equilibrium, which show spending a long time near the other equilibrium.

#### 5.4.2 When the Value of $\beta_0$ is Less than the Average Value of $\beta_1$ and $\beta_2$ , $[\beta_0 < \frac{1}{2}(\beta_1 + \beta_2)]$

In Figure 5.3 below, plots (b), (c), (e), and (f) also show the same behavior compared to the same plots obtained in Figure 5.2, with the same initial high densities of the antibiotic drug ( $D$ ) treatment concentration.

The only difference observed is the switching ( $s_1, s_2$ ) equilibrium that becomes locally stable, instead of the non-switching ( $s_0$ ) equilibrium because of its low growth rate ( $\beta_i$ ) value, allowing the  $s_0$  strain to grow quite large before it is eventually killed off. We also noticed that, the density of the antibiotic drug ( $D$ ) treatment concentration does not depend on the bacterial densities as well.

All other reasons for the bacterial resistance to the antibiotic drug ( $D$ ) treatment, and the ability of the strains taking longer unit-time than others,

before reaching the stable/unstable states by the strains remain the same as mentioned in section 5.4.1 above.

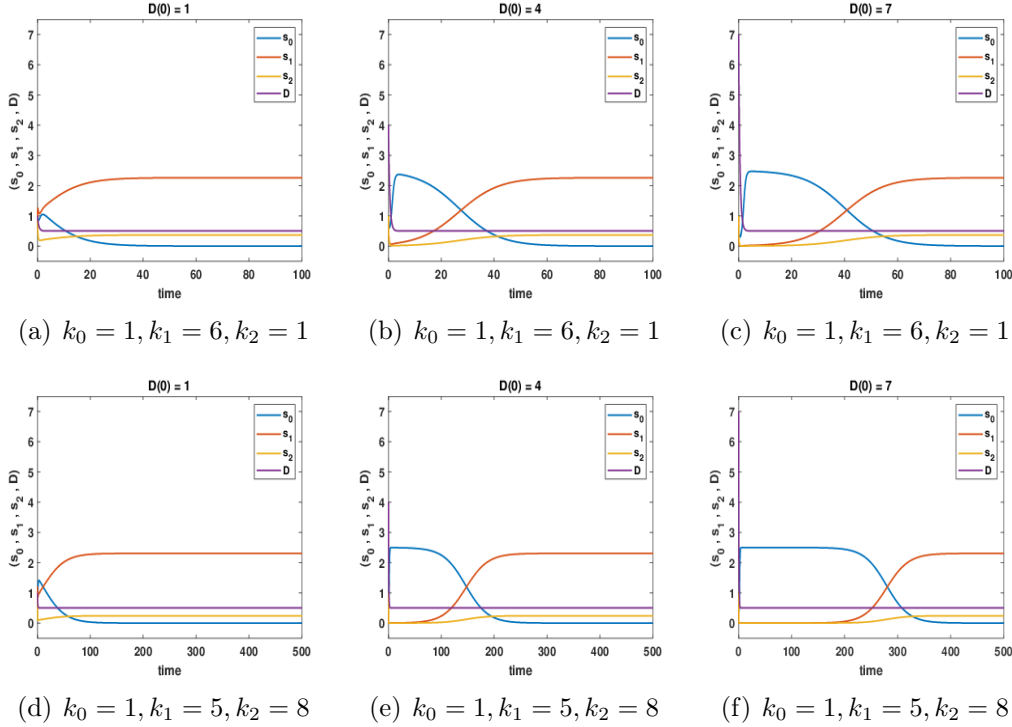


Figure 5.3: The Numerical graphs for the intrinsic dynamics of the 4D bet-hedging model with the dynamics of the antibiotic drug ( $D$ ) treatment for the non-fluctuating growth rate ( $\beta_i$ ) of the strains, and their respective death rates ( $k_i$ ), for  $\beta_0 < \frac{1}{2}(\beta_1 + \beta_2)$  and  $\epsilon_1 < \epsilon_2$ , with both strains having the same initial values:  $s_0(0) = s_1(0) = s_2(0) = 1$ , different initial values for the antibiotic drug ( $D$ ) treatment, different values for the growth rates of the strains:  $\beta_0 = 3$ ,  $\beta_1 = 5$  and  $\beta_2 = 7$ , different values for the strains death rates ( $k_i$ ), the rate of drug administration  $a = 1$ , and the rate of the antibiotic drug decay  $c = 2$ , with different transition rate values:  $\epsilon_1 = 1$ , and  $\epsilon_2 = 10$ .

### 5.4.3 When the Value of $\beta_0$ is Equal to the Average Value of $\beta_1$ and $\beta_2$ , [ $\beta_0 = \frac{1}{2}(\beta_1 + \beta_2)$ ]

The results obtained in this section 5.4.3 are similar to the results obtained in section 5.4.1 above, with the  $s_0$  equilibrium becoming locally stable, because the non-switching ( $s_0$ ) strain growth rate ( $\beta_i$ ) value in this section 5.4.3 is equal (=) to the average value of the switching ( $s_1, s_2$ ) strains growth rate ( $\beta_i$ ), unlike in section 5.4.2 above where the growth rate ( $\beta_i$ ) value of the non-switching ( $s_0$ ) strain is less (<) than the average growth rate ( $\beta_i$ ) value of the switching ( $s_1, s_2$ ) strains.

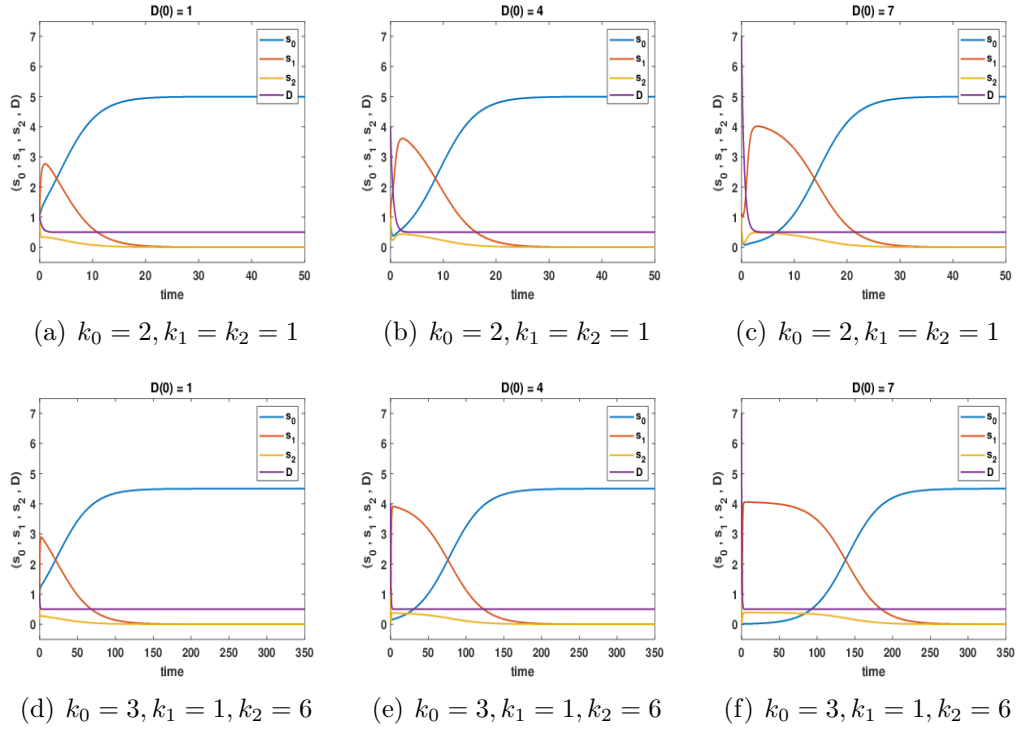


Figure 5.4: The Numerical graphs for the intrinsic dynamics of the 4D bet-hedging model with the dynamics of the antibiotic drug ( $D$ ) treatment for the non-fluctuating growth rate ( $\beta_i$ ) of the strains, and their respective death rates ( $k_i$ ), for  $\beta_0 = \frac{1}{2}(\beta_1 + \beta_2)$  and  $\epsilon_1 < \epsilon_2$ , with both strains having the same initial values:  $s_0(0) = s_1(0) = s_2(0) = 1$ , different initial values for the antibiotic drug ( $D$ ) treatment, different values for the growth rates of the strains:  $\beta_0 = 6$ ,  $\beta_1 = 5$  and  $\beta_2 = 7$ , different values for the strains death rates ( $k_i$ ), the rate of drug administration  $a = 1$ , and the rate of the antibiotic drug decay  $c = 2$ , with different transition rate values:  $\epsilon_1 = 1$ , and  $\epsilon_2 = 10$ .

The main differences observed in the plots obtained in Figure 5.4 above with those obtained in Figure 5.2 is the time taken by the ( $s_1, s_2$ ) strains to stay at the equilibrium state, before reaching a swapping point where the antibiotic drug ( $D$ ) treatment density drops, and the ( $s_1, s_2$ ) strains that were at the equilibrium states are killed off, allowing the  $s_0$  strain to take over and win the competition.

The plots obtained in Figure 5.2 with high densities of the antibiotic drug ( $D$ ) treatment concentration vividly show, the switching ( $s_1, s_2$ ) strains takes longer time before the  $s_0$  strain gradually bounces back and takes over, compared to those obtained in Figure 5.4, which is because of the differences in the respective growth rate ( $\beta_i$ ) values of the non-switching ( $s_0$ ) strain.

## 5.5 Fluctuating Resources within the Strains Growth Rates ( $\beta_i$ )

Having investigated and obtained interesting results in section 5.4 above, without fluctuations in both the strains growth rates ( $\beta_i$ ) and the antibiotic drug treatment administration rate ( $a$ ), we then considered the situation when there is a fluctuation within the strains' growth rates ( $\beta_i$ ).

Since we noticed the weak stability found in section 5.4 above could only be obtained with high growth rates ( $\beta_i$ ) values, and reasonably high death rates ( $k_i$ ) values of the strains as well, we considered the fluctuating resources within the bacterial growth rates ( $\beta_i$ ) in this section 5.5 to be;

$$\beta_i = \beta_c [\delta_i \sin(\omega t) + 1] \quad (5.18)$$

where;  $\beta_c$  is the initial growth rate values used to determined the actual growth rate ( $\beta_i$ ) values of the strains,  $\delta_i$  is the amplitude, and  $\omega$  as the frequency of the fluctuating resources.

The values of the growth rates ( $\beta_i$ ) obtained from the above function in equation (5.18), are not exactly the same as the growth rates ( $\beta_i$ ) values used in section 5.4 above, but are almost the same. The results obtained by using those growth rate ( $\beta_i$ ) values in this section 5.5, are used to compare the results obtained in sections 5.4 of this chapter 5.

Using the above fluctuating resources function for the growth rate ( $\beta_i$ ) values in equation (5.18), together with the exact/same high death rate ( $k_i$ ) values of the strains used in section 5.4 above, we obtained the same pattern of result, which produces the weak stability at an early time before it finally swaps and reached the exact steady state. Unlike the growth rates ( $\beta_i$ ) values obtained from the fluctuating resources function used in chapters 2, 3, and 4, which produces different results without the weak stability.

### 5.5.1 When the Value of $\beta_0$ is Greater than the Average value of $\beta_1$ and $\beta_2$ , $[\beta_0 > \frac{1}{2}(\beta_1 + \beta_2)]$

As we can see, the results of the whole plots obtained in Figure 5.5 below produces the same pattern of results obtained in Figure 5.2 of this chapter 5, by using almost the same growth rate ( $\beta_i$ ) values, the same death rate ( $k_i$ ) values, the same transition rates ( $\epsilon_i$ ) values of the strains, the same administration rate ( $a$ ) value, and the same killing rate ( $c$ ) value of the antibiotic drug ( $D$ ) treatment concentration.

The results show the ability of the switching ( $s_1, s_2$ ) strains to stay at the equilibrium state at an early time for a long frequency of time, with initial high densities of the antibiotic drug ( $D$ ) treatment concentration in plots (b), (c), (e), and (f) before the non-switching ( $s_0$ ) strain gradually takes over and win the competition, which were noticed earlier in section 5.4.1 above, which is similar to this section 5.5.1.

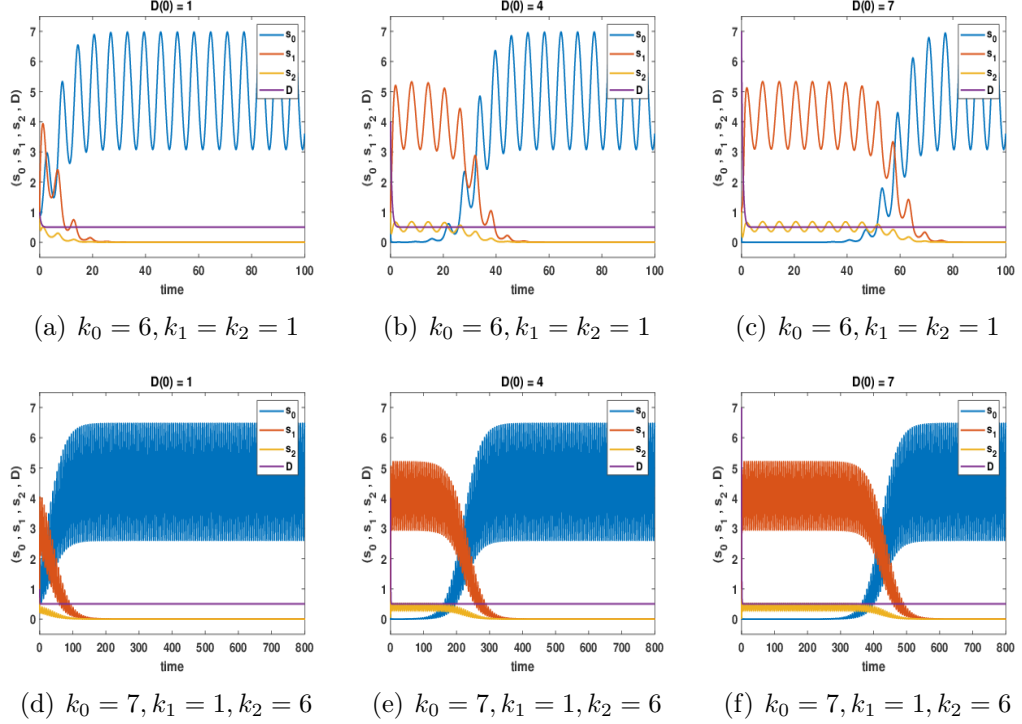


Figure 5.5: The Numerical graphs for the intrinsic dynamics of the 4D bet-hedging model with the dynamics of the antibiotic drug ( $D$ ) treatment for the fluctuating growth rate ( $\beta_i$ ) of the strains and their respective death rates ( $k_i$ ), for  $\beta_0 > \frac{1}{2}(\beta_1 + \beta_2)$  and  $\epsilon_1 < \epsilon_2$ , with both strains having the same initial values:  $s_0(0) = s_1(0) = s_2(0) = 1$ , different initial values for the antibiotic drug ( $D$ ) treatment, different values for the growth rates of the strains:  $\beta_0 = 8, \beta_1 = 5$  and  $\beta_2 = 7$ , different values for the strains death rates ( $k_i$ ), the rate of drug administration  $a = 1$ , and the rate of the antibiotic drug decay  $c = 2$ , with different transition rate values:  $\epsilon_1 = 1$ , and  $\epsilon_2 = 10$ .

The only differences with the results obtained in Figure 5.5 and those obtained in Figure 5.2 are the fluctuations in the existing strains densities, with all other results (the unit-time taking by the switching ( $s_1, s_2$ ) strains to stay at the equilibrium state before the non-switching ( $s_0$ ) strain takes over to win the competition, and other results obtained) are the same as obtained in section 5.4.1 above.

### 5.5.2 When the Value of $\beta_0$ is Less than the Average Value of $\beta_1$ and $\beta_2$ , $[\beta_0 < \frac{1}{2}(\beta_1 + \beta_2)]$

Interestingly as expected the whole plots obtained in Figure 5.6 below produces the same results which were obtained in Figure 5.3, by using the same parameter values used in section 5.4.2 above.

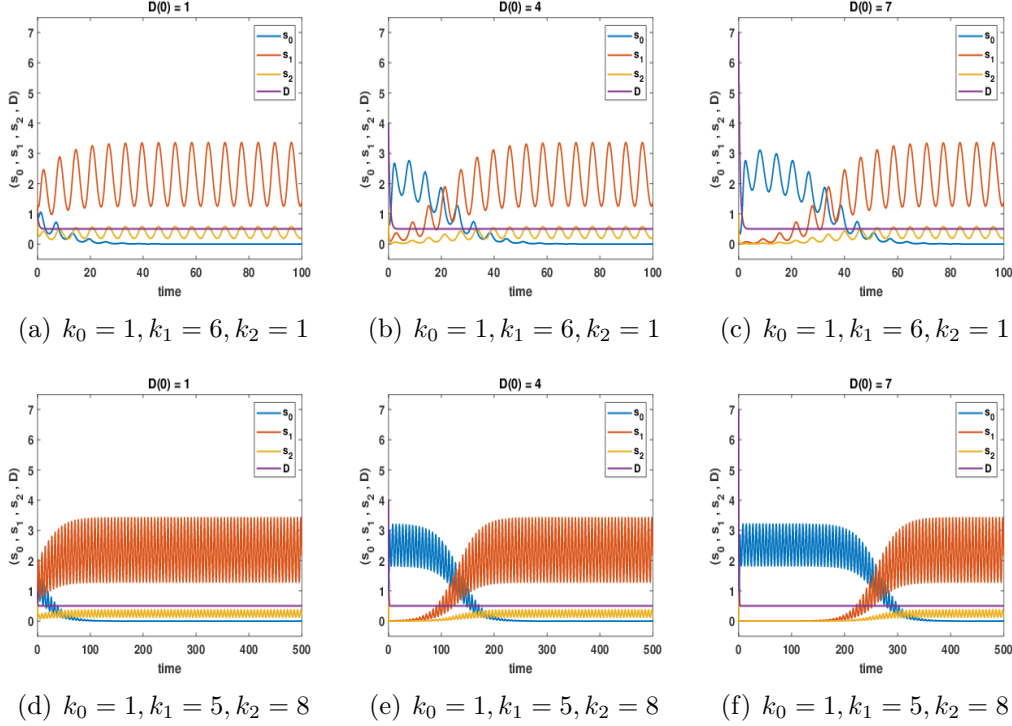


Figure 5.6: The Numerical graphs for the intrinsic dynamics of the 4D bet-hedging model with the dynamics of the antibiotic drug ( $D$ ) treatment for the fluctuating growth rate ( $\beta_i$ ) of the strains and their respective death rates ( $k_i$ ), for  $\beta_0 < \frac{1}{2}(\beta_1 + \beta_2)$  and  $\epsilon_1 < \epsilon_2$ , with both strains having the same initial values:  $s_0(0) = s_1(0) = s_2(0) = 1$ , different initial values for the antibiotic drug ( $D$ ) treatment, different values for the growth rates of the strains:  $\beta_0 = 3$ ,  $\beta_1 = 5$  and  $\beta_2 = 7$ , different values for the strains death rates ( $k_i$ ), the rate of drug administration  $a = 1$ , and the rate of the antibiotic drug decay  $c = 2$ , with different transition rate values:  $\epsilon_1 = 1$ , and  $\epsilon_2 = 10$ .

The behavior of the plots obtained in this section 5.5.2, which includes the ability of the non-switching ( $s_0$ ) strain to stay at the equilibrium state, the time it takes to stay near the equilibrium state, before the switching ( $s_1, s_2$ ) strains takes over gradually to win the competition, and all other results are the same (equal) with the results obtained in Figure 5.3.



### 5.5.3 When the Value of $\beta_0$ is Equal to the Average Value of $\beta_1$ and $\beta_2$ , $[\beta_0 = \frac{1}{2}(\beta_1 + \beta_2)]$

The results obtained in Figure 5.4 and those obtained in Figure 5.7 below are the same, which produced the same pattern of behavior showing the existence of the non-switching ( $s_0$ ) strain at the equilibrium state, and the extinction of the switching ( $s_1, s_2$ ) strains after growing quite large and stays at the equilibrium states in plots (b), (c), (e), and (f) for long frequency of time before they are eventually killed off.

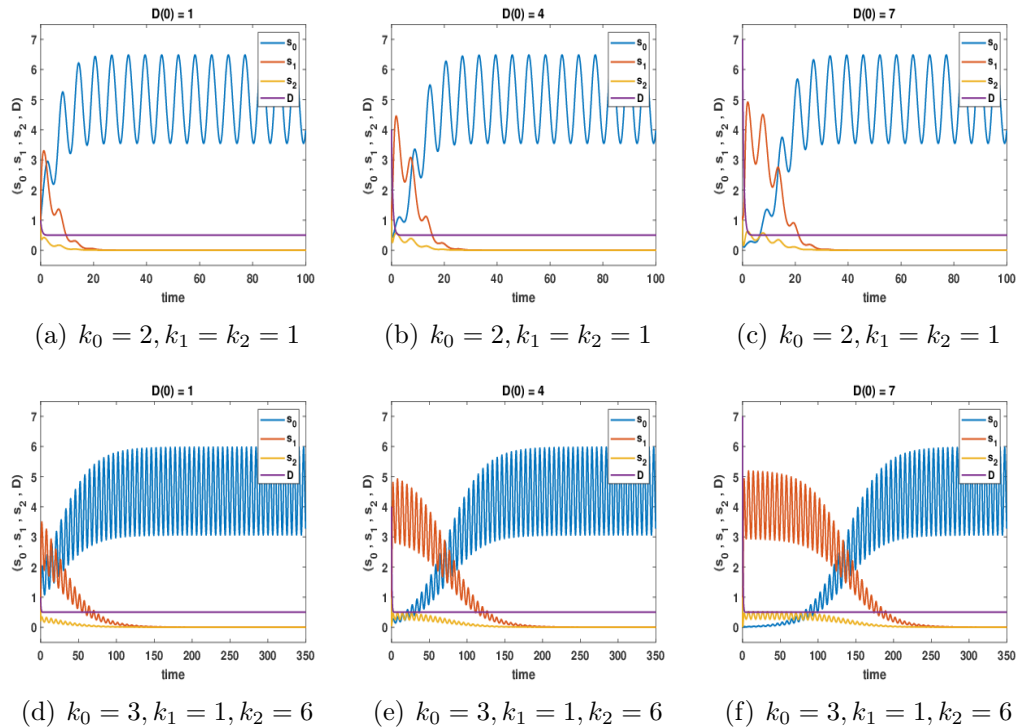


Figure 5.7: The Numerical graphs for the intrinsic dynamics of the 4D bet-hedging model with the dynamics of the antibiotic drug ( $D$ ) treatment for the fluctuating growth rate ( $\beta_i$ ) of the strains and their respective death rates ( $k_i$ ), for  $\beta_0 = \frac{1}{2}(\beta_1 + \beta_2)$  and  $\epsilon_1 < \epsilon_2$ , with both strains having the same initial values:  $s_0(0) = s_1(0) = s_2(0) = 1$ , different initial values for the antibiotic drug ( $D$ ) treatment, different values for the growth rates of the strains:  $\beta_0 = 6$ ,  $\beta_1 = 5$  and  $\beta_2 = 7$ , different values for the strains death rates ( $k_i$ ), the rate of drug administration  $a = 1$ , and the rate of the antibiotic drug decay  $c = 2$ , with different transition rate values:  $\epsilon_1 = 1$ , and  $\epsilon_2 = 10$ .

The overall results obtained in this section 5.5 show, the fluctuations within the strains growth rates ( $\beta_i$ ), does not affect the density of the antibiotic drug ( $D$ ) treatment.

## 5.6 Fluctuating Resources within the Antimicrobial Treatment Administration Rate ( $a$ )

Our fluctuating resources in this section 5.6 is on the antibiotic drug administration rate ( $a$ ), unlike in chapter 4 when the antibiotic drug ( $D$ ) treatment fluctuates over time.

The aim is to investigate the results obtained for the behavior of the strains with fluctuations in the antibiotic drug administration rate ( $a$ ), and compare them with the results obtained when there is no fluctuations in both growth rates ( $\beta_i$ ) and the antibiotic drug administration rate ( $a$ ), and also when the fluctuations is on the strains growth rate ( $\beta_i$ ) only.

To achieve that, we set our fluctuating resources within the antibiotic drug administration rate ( $a$ ) to be;

$$a = \delta \sin(\omega t) + 1 \quad (5.19)$$

where;  $\delta$  is the amplitude, and  $\omega$  as the frequency of the fluctuating resources.

To give room for proper comparison between the results obtained in this section 5.6, with the other results obtained from sections 5.4, and 5.5 above in this chapter 5, we used the same high growth rates ( $\beta_i$ ) and high death rates ( $k_i$ ) values used in those sections mentioned, and investigate if there is presence of a weak stability at an early time by the strains before reaching the equilibrium point, or not.

### 5.6.1 When the Value of $\beta_0$ is Greater than the Average Value of $\beta_1$ and $\beta_2$ , [ $\beta_0 > \frac{1}{2}(\beta_1 + \beta_2)$ ]

The whole plots obtained in Figure 5.8 below, show exactly the same pattern of behaviors with the results obtained in Figures 5.2 and 5.5, which clearly show with high density of the antibiotic drug ( $D$ ) treatment concentration, the switching ( $s_1, s_2$ ) strain stays at the equilibrium state for a long frequency at an early time in plots (b), (c), (e), and (f), before the non-switching ( $s_0$ ) strain takes over where the switching ( $s_1, s_2$ ) strains are eventually killed off, which were all expected.

The time it takes the switching ( $s_1, s_2$ ) strains in this section 5.6.1 to stay at the equilibrium state, before the non-switching ( $s_0$ ) strain takes over were almost the same, compared to the one's obtained in sections 5.4.1 and 5.5.1 above, since we used the same or almost the same parameter values with those sections mentioned.

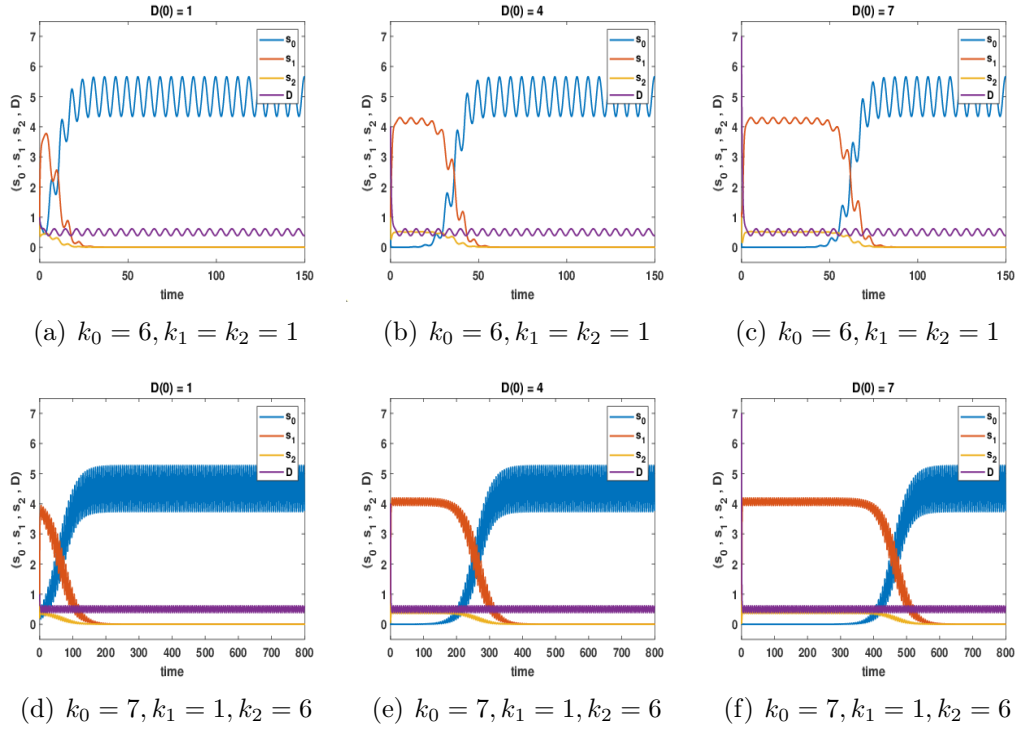


Figure 5.8: The Numerical graphs for the intrinsic dynamics of the 4D bet-hedging model with the dynamics of the antibiotic drug ( $D$ ) treatment for the fluctuating antibiotic drug administration rate (a), and the respective death rates ( $k_i$ ) of the strains, for  $\beta_0 > \frac{1}{2}(\beta_1 + \beta_2)$  and  $\epsilon_1 < \epsilon_2$ , with both strains having the same initial values:  $s_0(0) = s_1(0) = s_2(0) = 1$ , different initial values for the antibiotic drug ( $D$ ) treatment, different values for the growth rates of the strains:  $\beta_0 = 8$ ,  $\beta_1 = 5$  and  $\beta_2 = 7$ , different values for the strains death rates ( $k_i$ ), the rate of drug administration  $a = 1$ , and the rate of the antibiotic drug decay  $c = 2$ , with different transition rate values:  $\epsilon_1 = 1$ , and  $\epsilon_2 = 10$ .

### 5.6.2 When the Value of $\beta_0$ is Less than the Average Value of $\beta_1$ and $\beta_2$ , $[\beta_0 < \frac{1}{2}(\beta_1 + \beta_2)]$

Nothing different is expected from the results obtained in Figure 5.9 below, compared to those obtained in Figures 5.3 and 5.6 above, because they all have the same growth rates ( $\beta_i$ ), and the same high death rates ( $k_i$ ) values in each case.

The behavior of the non-switching ( $s_0$ ) strain of growing quite large to stay at the equilibrium state in plots (b), (c), (e), and (f) with high densities of the antibiotic drug ( $D$ ) treatment concentration in Figure 5.9, and the time taken by the switching ( $s_1, s_2$ ) strains before bouncing back to exists at the equilibrium points, were all the same with those obtained in the Figures 5.3,

and 5.6 respectively.

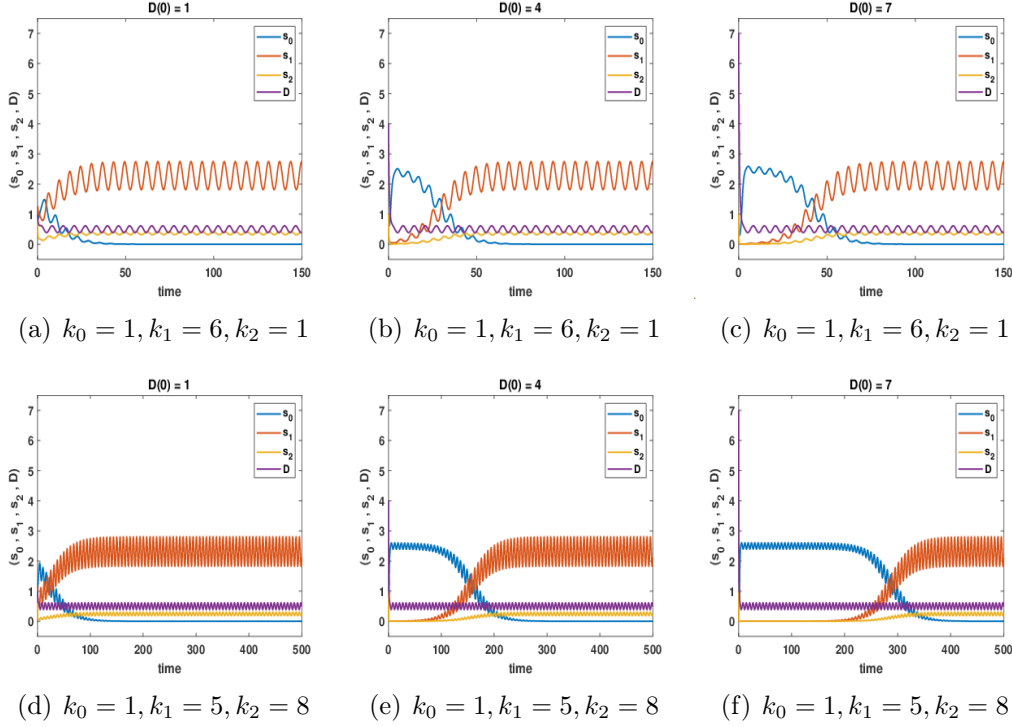


Figure 5.9: The Numerical graphs for the intrinsic dynamics of the 4D bet-hedging model with the dynamics of the antibiotic drug ( $D$ ) treatment for the fluctuating antibiotic drug administration rate (a), and the respective death rates ( $k_i$ ) of the strains, for  $\beta_0 < \frac{1}{2}(\beta_1 + \beta_2)$  and  $\epsilon_1 < \epsilon_2$ , with both strains having the same initial values:  $s_0(0) = s_1(0) = s_2(0) = 1$ , different initial values for the antibiotic drug ( $D$ ) treatment, different values for the growth rates of the strains:  $\beta_0 = 3$ ,  $\beta_1 = 5$  and  $\beta_2 = 7$ , different values for the strains death rates ( $k_i$ ), the rate of drug administration  $a = 1$ , and the rate of the antibiotic drug decay  $c = 2$ , with different transition rate values:  $\epsilon_1 = 1$ , and  $\epsilon_2 = 10$ .

### 5.6.3 When the Value of $\beta_0$ is Equal to the Average Value of $\beta_1$ and $\beta_2$ , [ $\beta_0 = \frac{1}{2}(\beta_1 + \beta_2)$ ]

Since the whole results obtained in this chapter 5 have the same pattern of behaviors because of using the same parameter values, we shouldn't expect a different results here too.

We noticed the results of plots (b), (c), (e), and (f) in Figure 5.10 below, coincides with the results obtained in Figures 5.4 and 5.7, with a differences of fluctuations in the densities of the antibiotic drug ( $D$ ) treatment, which are different from what were obtained in Figures 5.4, and 5.7 respectively.

In the results we observed the switching ( $s_1, s_2$ ) strain grows quite large when the initial density of the antibiotic drug ( $D$ ) treatment concentration is high, before they are eventually killed off at the stable equilibrium, where the non-switching ( $s_0$ ) strain takes over.

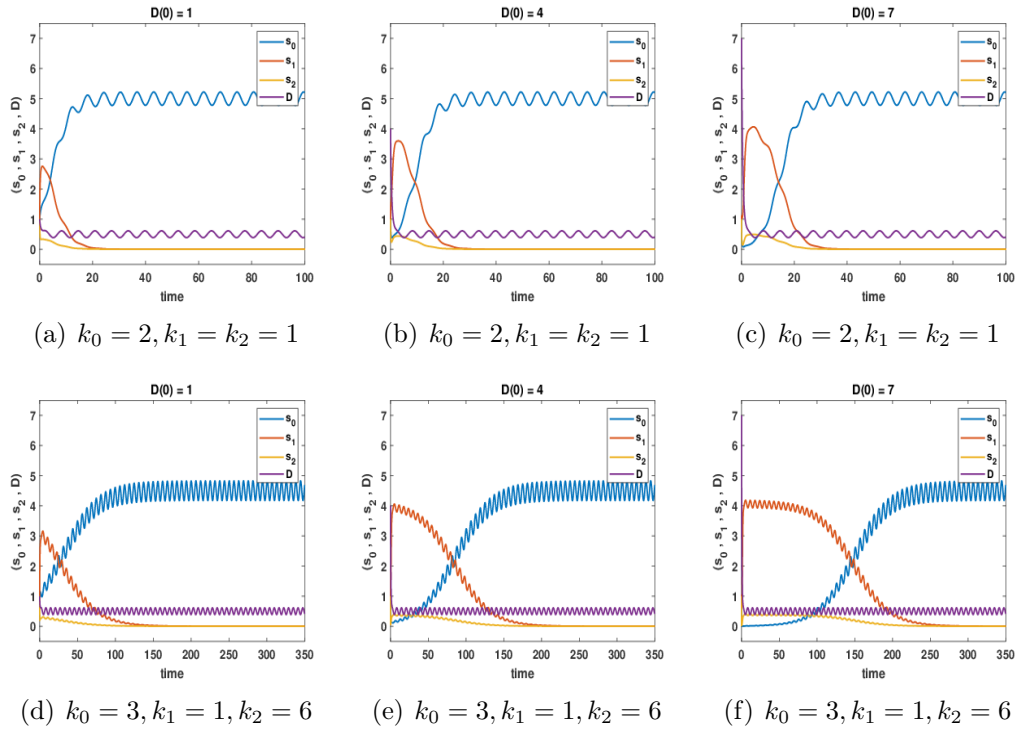


Figure 5.10: The Numerical graphs for the intrinsic dynamics of the 4D bet-hedging model with the dynamics of the antibiotic drug ( $D$ ) treatment for the fluctuating antibiotic drug administration rate (a), and the respective death rates ( $k_i$ ) of the strains, for  $\beta_0 = \frac{1}{2}(\beta_1 + \beta_2)$  and  $\epsilon_1 < \epsilon_2$ , with both strains having the same initial values:  $s_0(0) = s_1(0) = s_2(0) = 1$ , different initial values for the antibiotic drug ( $D$ ) treatment, different values for the growth rates of the strains:  $\beta_0 = 6$ ,  $\beta_1 = 5$  and  $\beta_2 = 7$ , different values for the strains death rates ( $k_i$ ), the rate of drug administration  $a = 1$ , and the rate of the antibiotic drug decay  $c = 2$ , with different transition rate values:  $\epsilon_1 = 1$ , and  $\epsilon_2 = 10$ .

The major differences observed in the whole plots obtained in this section 5.6, compared to those obtained in sections 5.4 and 5.5 above, are the presence of fluctuations in both the densities of the antibiotic drug ( $D$ ) treatment and in the densities of the existing strains, which are driven by the fluctuating resources in the antibiotic drug administration rate ( $a$ ). Unlike the results obtained in section 5.5 above, which show the fluctuating resources in the strains growth rates ( $\beta_i$ ), does not cause any fluctuations in the densities of the antibiotic drug ( $D$ ) treatment.

## 5.7 Conclusion

The results obtained in this chapter 5 show there are unexpected behavior by the strain(s) at an early time, when there are high density of antibiotic drug ( $D$ ) treatment concentration, coupled with the growth rates ( $\beta_i$ ) and reasonably high death rates ( $k_i$ ) values of the strains. Instead of the whole strains to start crashing out at an early time when there is a high density of the antibiotic drug ( $D$ ) treatment concentrations as seen in Figure 5.1 of this chapter 5, we noticed a sudden unexpected growth by some strain(s), which grow quite large and stay for long frequencies of time near the unstable equilibrium state in the results, before the other strain(s) takes over to win the competition.

In Figures 5.2, 5.4, 5.5, 5.7, 5.8, and 5.10, instead of the switching ( $s_1, s_2$ ) strain to start decaying out at an early time in plots (b), (c), (e), and (f), because of a high densities of the antibiotic drug ( $D$ ) treatment concentration, they respectively grow quite large in those plots, thereby staying at the equilibrium state for long frequency of time, before the non-switching ( $s_0$ ) strain bounce back and takes over to win the competition. We also noticed the same behavior of staying for a long frequency of time at the equilibrium state in Figures 5.3, 5.6, and 5.9 by the non-switching ( $s_0$ ) strain, and growing quite large at the inceptions in plots (b), (c), (e), and (f) as well, with high densities of the antibiotic drug ( $D$ ) treatment concentration, before the switching ( $s_1, s_2$ ) takes over to win the competition.

One very important thing to be cognizant about, is the time taken by the appearance of the unexpected strain(s) to stay at the equilibrium state in those plots, before the eventual taken over by the expected strain(s). In those plots mentioned above we observed that the time taken by the appearance of the unexpected strain(s) and staying for a long frequency of time at an equilibrium state, before the expected strain(s) takes over, are derived by the interactions of high densities of the antibiotic drug ( $D$ ) treatment concentration, coupled with the strains' growth rates ( $\beta_i$ ) values, high death rates ( $k_i$ ) values of the strains, and the values of the strains transition rates ( $\epsilon_i$ ) as well.

The investigations in this chapter 5 also testified that, increasing the initial densities of the antibiotic drug ( $D$ ) treatment concentration, does not affect the steady state of the existing strains in all the plots produced, but it only affects the densities of the strains at an early stage before reaching the steady state.

Another important aspect discovered in the results obtained in Figures 5.8, 5.9, and 5.10, are the presence of fluctuations in both the densities of the existing strains and the antibiotic drug ( $D$ ) treatment concentration, which are caused due to the fluctuations in the antibiotic drug administration rate ( $a$ ). Unlike what were obtained in Figures 5.5, 5.6, and 5.7, where the fluctuations within the strains growth rates ( $\beta_i$ ) does not cause any fluctuations for the densities of the antibiotic drug ( $D$ ) treatment concentration, but it caused the fluctuations for the existing strain(s) only.

# CHAPTER 6

## Conclusions

---

### 6.1 Overview of Thesis

In this thesis, I have been studying models relevant to antimicrobial resistant (AMR) treatment, which focuses on examining a model about bet-hedging. The model has been looked at in terms of evolution by (Müller et al., 2013) for the constant ( $s_0$ ) and switching ( $s_1, s_2$ ) strains, which explore the evolution of bet-hedging model within a population that experiences a stochastically changing environment, but needed a full examination of the underlying model using a deterministic approach method.

In chapter 2 we looked at the model dynamics for the switching ( $s_1, s_2$ ) strains, which formed a basis of study for this thesis. The research considers a situation when the growth rates of the strains are equal ( $\beta_1 = \beta_2 = \beta$ ), and when their growth rates are not equal ( $\beta_1 \neq \beta_2$ ) in the non-fluctuating and fluctuating environments. The concept of time courses, and densities of strains for varying values of the fluctuating resources parameters were looked into which describes the behavior of the strain(s).

In chapter 3, the constant ( $s_0$ ) strain was included in the dynamics of the model discussed in chapter 2, which was the full model published in the paper of (Müller et al., 2013), which looked at the evolution and stochastic simulation of the model in their work, but ours is different because we looked at the underlying model using a deterministic approach, in the fluctuating and non-fluctuating situations. The same methods, approach, and techniques used in chapter 2 to investigate the behavior of the strains when their growth rates are equal ( $\beta_0 = \beta_1 = \beta_2 = \beta$ ), and when their growth rates are not equal ( $\beta_0 \neq \beta_1 \neq \beta_2$ ) for both the non-fluctuating and fluctuating situations were adopted in this chapter. Also, the concept of time courses, and densities of strains for varying values of the fluctuating resources parameters for the new model equations was addressed in this chapter, like it was done in chapter 2.



The aim is to find out whether the behavior of the strains changes in both situations, when the constant ( $s_0$ ) strain is included in the underlying model discussed in chapter 2, or if there are any differences in the behavior of the strains that occurred as a result of new strain inclusion.

In chapter 4, the death rates ( $k_i$ ), as ( $i = 0, 1$ , and  $2$ ) for the respective strains and the antibiotic drug ( $D$ ) treatment which is held constant (fixed value) were included in the dynamics of the strains discussed in chapter 3, which wasn't discussed in the paper of (Müller et al., 2013) under review by this research in a different approach. The effect of the death rates ( $k_i$ ) and the antibiotic drug ( $D$ ) treatment were noticed in this chapter. The behavior of the non-switching ( $s_0$ ) strain together with the switching ( $s_1, s_2$ ) strain(s), with/without fluctuating resources within their growth rates ( $\beta_i$ ), and when the antibiotic drug ( $D$ ) treatment fluctuates over time were also looked into.

In chapter 5, the dynamics of the antibiotic drug ( $D$ ) treatment with its administration rate ( $a$ ), and the degradation rate ( $c$ ) was included in the dynamics of the model discussed in chapter 4. Apart from investigating the behavior of the strains with/without fluctuating resources within their growth rates ( $\beta_i$ ), and when the antibiotic drug ( $D$ ) treatment fluctuates over time in chapter 4, the behavior of the strains when the fluctuating resources is within the administration rate ( $a$ ) of the antibiotic drug ( $D$ ) treatment was investigated too, and the results obtained in that situation were completely different, with those obtained in the other situations.

## 6.2 Discussion of Results

In this section we will discuss the results obtained in various chapters, and compare the outcome of the results with those obtained in other chapters, in order to observe the impact of what is added to the existing model.

### 6.2.1 Chapter 2

The results obtained in chapter 2 for the constant (equal), and different (unequal) growth rates ( $\beta_i$ ) of the strain(s) produced two equilibrium points, a zero and non-zero equilibrium points in both situations, which in all cases show the strains become unstable at the zero equilibrium point, and stable at the non-zero equilibrium point. In the fluctuating environment, we noticed the behavior for the densities of the strains are the same compared to what were obtained in the non-fluctuating situation, but the only differences is the

oscillations in the strains densities for the fluctuating environment, which isn't there in the non-fluctuating situation. The results also show the transition rates ( $\epsilon_i$ ) appear to have a bigger effect, or a greater impact on the densities of the strains, than their growth rates ( $\beta_i$ ) in both the non-fluctuating and the fluctuating situations.

We also noticed in the results that once the values of the amplitude ( $\delta_i$ ) are increased in the time courses, the densities of oscillations in the strains are increased too, with the minimum showing a greater changes than the maximum. Meaning the amplitude ( $\delta_i$ ) makes surprisingly little difference to the maximum/minimum densities, suggesting some strong intrinsic regulation. Also a rapid increase in the strains densities at the early time between  $\omega = 0$  and  $\omega = 0.1$  at the steady state were observed, and a rapid decrease in their densities as well between  $\omega = 0.1$  and  $\omega = 0.2$  at the steady state, but the rapid decrease is not as high as the rapid increase, when the frequency ( $\omega$ ) value of the fluctuating resources is increased. Meaning that, the frequency ( $\omega$ ) makes a bigger differences at the early time, with amplitudes ( $\delta_i$ ) peaking at very low frequency.

## 6.2.2 Chapter 3

The results obtained in chapter 3 after solving the system of model equations in the non-fluctuating environment, with the inclusion of the constant ( $s_0$ ) strain produced two equilibrium points, a zero and non-zero equilibrium (with a continuum of equilibria) points for the constant (equal) growth rates ( $\beta_i$ ) of the strains, which is quite different with what were obtained in chapter 2. The results indicates the strains can't settle at the zero equilibrium point, but they can/can't becomes stable at the non-zero equilibrium point, depending on the situation for the continuum equilibria. Any attempt for the continuum equilibria to move slightly towards the positive value of what was obtained in equation (3.9), the equilibria will be locally and asymptotically unstable, and we will notice an extinction of the whole strains.

The result also produced four equilibrium points, a zero and three non-zero's (with none co-existence) equilibrium points for the different (unequal) growth rates ( $\beta_i$ ) of the strains, which show the behavior of the equilibrium points are ultimately different compared to what were obtained from the model equations discussed in chapter 2. This means the existence strain(s) at the steady state might be either a non-switching ( $s_0$ ) strain alone, or might be the switching ( $s_1, s_2$ ) strains alone, or might even be the presence of both the

non-switching ( $s_0$ ) and switching ( $s_1, s_2$ ) strains, depending on their growth rates ( $\beta_i$ ) and transition rates ( $\epsilon_i$ ) values.

The growth rates ( $\beta_i$ ) and the transition rates ( $\epsilon_i$ ) values always determines which among the switching ( $s_1, s_2$ ) strains will have a higher density at the steady state than the other in any situation. Meaning, which among the switching strain performs better or worse in any environment as mentioned earlier.

There is a co-existence of both the constant ( $s_0$ ), and the bet-hedgers ( $s_1, s_2$ ) strains when their growth rate ( $\beta_i$ ) are equal (*i. e.*  $\beta_0 = \beta_1 = \beta_2 = \beta$ ) in any environment which is a special case, and for the vast majority of time there can be no co-existence of the strains. This show stability is lost at that point, and it is a stability swapping point between the non-zero's ( $s_0^*, 0, 0$ ) and ( $0, s_1^*, s_2^*$ ) equilibrium points, but more generally only one type of strain can win at a time, which sometimes depends on its growth ( $\beta_i$ ) and the transition ( $\epsilon_i$ ) rates as well.

Also, the densities of the existing strains changed as we varied the amplitude ( $\delta_i$ ) values of the fluctuating resources. This means increasing the amplitude ( $\delta_i$ ) simply increases the fluctuations of the existing strain(s), with bigger effects at minimum densities than its maximum densities. This show by varying the values for the amplitude ( $\delta_i$ ) of fluctuations, the bacteria could only keep growth from dropping off and was unable to really boost it up past a threshold, which might be due to the competition between the strains. But when the values of the frequency ( $\omega$ ) were varied there was no clear evidence of resonance, and there was always a rapid increase (change) at relatively low values (early time), and the frequency seems to show very little difference in the densities of the strains. These mean there is little interaction between the forcing and the dynamics, and it also show the frequency ( $\omega$ ) makes more difference when  $r_0$  is relatively low.

This means the whole results obtained in the fluctuating resources describes the ability of the amplitude ( $\delta_i$ ) to affect the behavior of the strains at relatively intermediate values, unlike the frequency ( $\omega$ ) which affects it at relatively lower (early) values, which is almost the same results compared to the results obtained in chapter 2.

### 6.2.3 Chapter 4

After solving the system of model equations in chapter 4, we obtained four equilibrium points as well, a zero and three non-zero's (with none co-existence)

equilibrium points for both the constant, and different growth rates ( $\beta_i$ ) of the strains in the non-fluctuating environment, which is quite different compared to what were obtained in chapter 3 for constant growth rates, but the same type of result compared to what were obtained for different growth rates. As we obtained in the results of chapter 3, the zero (0) equilibria will be unstable if the growth rate ( $\beta$ ) value is high, and it will be stable if the growth rate ( $\beta$ ) value is very low in both situations in this chapter. Meaning the bacteria will be extinct at a stable point because of the killings by the antibiotic drug ( $D$ ) treatment.

The whole results obtained in the non-fluctuating situation in this chapter show there is always a decrease in the densities of the existing strains at the stable point in any conditions when compared with the results obtained in chapter 3, which is caused by the presence of the strains death rates ( $k_i$ ) and the antibiotic drug ( $D$ ) treatment. The level of the decreases in the densities of the existing strains usually depends on the values of the strains death rates ( $k_i$ ) and the antibiotic drug ( $D$ ) treatment.

We also saw a switching between the existing and extinct strains in different conditions, which are usually caused by the strains' growth rates ( $\beta_i$ ), their transition rates ( $\epsilon_i$ ), their death rates ( $k_i$ ), and the antibiotic drug ( $D$ ) treatment values as well. In the cases where we didn't see a switching, it could be as a result of either the strains lower growth rate ( $\beta_i$ ), or high transition rate ( $\epsilon_i$ ), or lower death rate ( $k_i$ ) values. The cases we realized in this chapter were mostly caused as a result of either the strains lower death rate ( $k_i$ ), or high transition rate ( $\epsilon_i$ ) values.

In the fluctuating resources within the strains' growth rates ( $\beta_i$ ), we noticed the results obtained were qualitatively the same with those obtained in the non-fluctuating resources situation. We also noticed an interesting result in that situation, where we are only ever at the switching ( $s_1, s_2$ ) equilibrium, but the densities of the predominant strains swapped. This happened because in this case  $r_0$  is very small, and the non-switching ( $s_0$ ) strain has a lower growth rate ( $\beta_i$ ) value, and never grows fast to invade. This also happened because the ( $s_1, s_2$ ) strains are the bet-hedgers. It is also interesting that this is maintained even with very high values of  $k_1$  or  $k_2$ .

We also noticed an interesting result when the antibiotic drug ( $D$ ) treatment fluctuates over time, showing the higher the death rate ( $k_i$ ) values of the existing strain at the steady state, the more rapid the oscillations become.

This means the frequency of oscillations is linked to the death rates ( $k_i$ ) of the existing strain(s).

## 6.2.4 Chapter 5

The results obtained in this chapter when the dynamics of the antibiotic drug ( $D$ ) treatment with its administration rate ( $a$ ), and its degradation rate ( $c$ ) were included in the existing model studied in chapter 4, were the same compared to the results obtained in that chapter. The only differences between the equilibrium points obtained is the inclusion of the antibiotic drug ( $D$ ) treatment solution as  $D = \frac{a}{c}$  in this chapter.

The results of this chapter indicate that whenever the antibiotic drug ( $D$ ) treatment is administered to the bacteria, the strain(s) which suppose to be extinct unexpectedly/surprisingly happens to have a lesser impact of killing by the antibiotic drug ( $D$ ) treatment attack, thereby growing quite large when the concentration (density) of the antibiotic drug ( $D$ ) treatment is high and staying at the equilibrium state for a long frequency of time, while the strain which supposed to exist(s) at the equilibrium state initially experiences a greater loss due to the killing by the antibiotic drug ( $D$ ) treatment attack for the same frequency of time. By the time the density (concentration) of the antibiotic drug ( $D$ ) treatment drops, the strain(s) which supposed to exist(s) at the equilibrium state gradually start growing, and finally takes over to win the competition.

One very important thing to be cognizant about, is the time taken by the appearance of the unexpected strain(s) to stay at the equilibrium state, before the eventual taken over by the expected strain(s). In the results obtained we observed that, the time taken by the appearance of the unexpected strain(s) and staying for a long frequency of time at an equilibrium state, before the expected strain(s) takes over, are derived by the interactions of high densities of the antibiotic drug ( $D$ ) treatment concentration, coupled with the strains growth rates ( $\beta_i$ ) values, high death rates ( $k_i$ ) values of the strains, and the values of the strains transition rates ( $\epsilon_i$ ) as well.

The investigations in this chapter also testified that, increasing the initial densities of the antibiotic drug ( $D$ ) treatment concentration, does not affect the steady state of the existing strains, but it only affects the densities of the strains at an early stage before reaching the steady state.

Another important aspect discovered in the results obtained in chapter 5, are the presence of fluctuations in both the densities of the existing strain(s)

and the antibiotic drug ( $D$ ) treatment concentration, which are caused due to the fluctuations in the antibiotic drug administration rate ( $a$ ). Unlike what were obtained when the fluctuations is within the strains growth rates ( $\beta_i$ ), when it doesn't cause any fluctuations for the densities of the antibiotic drug ( $D$ ) treatment, but it caused the fluctuations for the existing strain(s) only.

### 6.3 Future work

In this thesis I have formulated an extensions to the adaptive dynamics model which was initially developed by (Müller et al., 2013), by including the death rates ( $k_i$ ) of the respective strains together with the antibiotic drug ( $D$ ) treatment which was held constant (fixed value), and also by including the dynamics of the antibiotic drug ( $D$ ) treatment administration rate ( $a$ ), and its degradation rate ( $c$ ) in the model mentioned.

Categorically, I have investigated the impact of using the deterministic approach on the strains of (Müller et al., 2013) model and the dynamics of the antibiotic drug ( $D$ ) treatment, and have explored the effect of using different initial densities of the antibiotic drug ( $D$ ) treatment, and other parameter values. The models also consider a deterministic fluctuation on the growth rates ( $\beta_i$ ) of the strains, the antibiotic drug ( $D$ ) treatment which fluctuates over time ( $t$ ), and the fluctuations on the administration rate ( $a$ ) of the antibiotic drug ( $D$ ) treatment concentration. During the course of this research, I have not come across any studies that uses a deterministic approach on the (Müller et al., 2013) model involving the constant ( $s_0$ ) and bet-hedgers ( $s_1, s_2$ ) strains, but have come across so many studies on sensitive and resistant strains, with antibiotic drug treatment which are held constant and its dynamics. In view of the aforementioned this thesis seems novel because of its content, and can be extended for further research.

- An important aspect to be considered relevant for future work is the dynamic of the antibiotic drug ( $D$ ) treatment in a quadratic form, like the works of (Blanchet et al., 2011; Delfour and Garon, 2011).
- Another aspect to consider is the dynamic of the  $i^{th}$  antibiotic drug treatment concentration supplied at a constant rate, and being taken up at a constant rate too, like what were found in (Ibargüen-Mondragón et al., 2014; Daşbaşı and Öztürk, 2016).

- Fluctuation of the antibiotic drug ( $D$ ) treatment over time ( $t$ ) for the dynamics of the strains and the antibiotic drug treatment (4D model).
- Fluctuation within the degradation rate of the antibiotic drug ( $D$ ) treatment (4D model).
- Adding the death rates ( $k_i$ ) of the strains and the antibiotic drug ( $D$ ) treatment which is held constant (fixed) value for the switching ( $s_1, s_2$ ) strains discussed in chapter 2.
- Also to include the dynamics of the antibiotic drug ( $D$ ) treatment in chapter 2 with its administration and degradation rates, like it was done in chapter 5.

## Bibliography

---

---

- Agusto, F. (2016), ‘Optimal control of methicillin-resistant staphylococcus aureus transmission in hospital settings’, *Applied Mathematical Modelling* **40**(7-8), 4822–4843.
- Agusto, F., Knight, K. and Jones, M. (2015), ‘Modeling of community-and hospital-acquired methicillin-resistant staphylococcus aureus transmission in hospital settings’, *BIOMATH* **4**(2), 1511161.
- Allison, K. R., Brynildsen, M. P. and Collins, J. J. (2011), ‘Metabolite-enabled eradication of bacterial persisters by aminoglycosides’, *Nature* **473**(7346), 216–220.
- Appelbaum, P. C. (2012), ‘2012 and beyond: potential for the start of a second pre-antibiotic era?’, *Journal of Antimicrobial Chemotherapy* **67**(9), 2062–2068.
- Austin, D. and Anderson, R. (1999), ‘Studies of antibiotic resistance within the patient, hospitals and the community using simple mathematical models’, *Philosophical Transactions of the Royal Society of London. Series B: Biological Sciences* **354**(1384), 721–738.
- Austin, D. J., Kristinsson, K. G. and Anderson, R. M. (1999), ‘The relationship between the volume of antimicrobial consumption in human communities and the frequency of resistance’, *Proceedings of the National Academy of Sciences* **96**(3), 1152–1156.
- Balaban, N. Q., Merrin, J., Chait, R., Kowalik, L. and Leibler, S. (2004), ‘Bacterial persistence as a phenotypic switch’, *Science* **305**(5690), 1622–1625.
- Bhunu, C. (2011), ‘Mathematical analysis of a three-strain tuberculosis transmission model’, *Applied mathematical modelling* **35**(9), 4647–4660.



- Bigger, J. et al. (1944), ‘Treatment of staphylococcal infections with penicillin by intermittent sterilisation.’, *Lancet* pp. 497–500.
- Blanchet, G., Delfour, M. C. and Garon, A. (2011), ‘Quadratic models to fit experimental data of paclitaxel release kinetics from biodegradable polymers’, *SIAM Journal on Applied Mathematics* **71**(6), 2269–2286.
- Blower, S. M. and Gerberding, J. L. (1998), ‘Understanding, predicting and controlling the emergence of drug-resistant tuberculosis: a theoretical framework’, *Journal of molecular medicine* **76**(9), 624–636.
- Castillo-Chavez, C. and Feng, Z. (1997), ‘To treat or not to treat: the case of tuberculosis’, *Journal of mathematical biology* **35**(6), 629–656.
- Chow, K., Wang, X., Curtiss III, R. and Castillo-Chavez, C. (2011), ‘Evaluating the efficacy of antimicrobial cycling programmes and patient isolation on dual resistance in hospitals’, *Journal of biological dynamics* **5**(1), 27–43.
- Chu, D. and Barnes, D. J. (2016), ‘The lag-phase during diauxic growth is a trade-off between fast adaptation and high growth rate’, *Scientific reports* **6**(1), 1–15.
- Cooper, N. G. and Julius, A. A. (2011), Bacterial persistence: mathematical modeling and optimal treatment strategy, in ‘Proceedings of the 2011 American Control Conference’, IEEE, pp. 3502–3507.
- Das, S., Das, P. and Das, P. (2020), ‘Dynamics and control of multidrug-resistant bacterial infection in hospital with multiple delays’, *Communications in Nonlinear Science and Numerical Simulation* **89**, 105279.
- Daşbaşı, B. and Öztürk, İ. (2016), ‘Mathematical modelling of bacterial resistance to multiple antibiotics and immune system response’, *SpringerPlus* **5**(1), 1–17.
- Delfour, M. C. and Garon, A. (2011), Quadratic ode and pde models of drug release kinetics from biodegradable polymers, in ‘IFIP Conference on System Modeling and Optimization’, Springer, pp. 13–24.
- Demerec, M. (1945a), ‘Genetic aspects of changes in staphylococcus aureus producing strains resistant to various concentrations of penicillin’, *Annals of the Missouri Botanical Garden* **32**(2), 131–138.

- Demerec, M. (1945*b*), ‘Production of staphylococcus strains resistant to various concentrations of penicillin’, *Proceedings of the National Academy of Sciences of the United States of America* **31**(1), 16.
- Demerec, M. (1948), ‘Origin of bacterial resistance to antibiotics’, *Journal of bacteriology* **56**(1), 63–74.
- Fair Richard, J. and Yitzhak, T. (2014), ‘Antibiotics and bacterial resistance in the 21st century. perspect’, *Med. Chem* **6**, 25–64.
- Friedman, G., McCarthy, S. and Rachinskii, D. (2014), ‘Hysteresis can grant fitness in stochastically varying environment’, *PLoS One* **9**(7), e103241.
- Fudenberg, D. and Imhof, L. A. (2012), ‘Phenotype switching and mutations in random environments’, *Bulletin of mathematical biology* **74**(2), 399–421.
- Garber, A. M. (1987), ‘Antibiotic exposure and resistance in mixed bacterial populations’, *Theoretical population biology* **32**(3), 326–346.
- Gardete, S., Wu, S., Gill, S. and Tomasz, A. (2006), ‘Role of vrasr in antibiotic resistance and antibiotic-induced stress response in staphylococcus aureus’, *Antimicrobial agents and chemotherapy* **50**(10), 3424–3434.
- Geritz, S. A., Kisdi, E., Metz, J. A. et al. (1998), ‘Evolutionarily singular strategies and the adaptive growth and branching of the evolutionary tree’, *Evolutionary ecology* **12**(1), 35–57.
- Godlee, F. (2013), ‘Antimicrobial resistance—an unfolding catastrophe, british medical journal, vol. 346, article f1663, 2013’.
- Gumel, A. B. and Song, B. (2008), ‘Existence of multiple-stable equilibria for a multi-drug-resistant model of mycobacterium tuberculosis’, *Mathematical Biosciences & Engineering* **5**(3), 437.
- Heins, A.-L. and Weuster-Botz, D. (2018), ‘Population heterogeneity in microbial bioprocesses: origin, analysis, mechanisms, and future perspectives’, *Bioprocess and biosystems engineering* **41**(7), 889–916.
- Hiramatsu, K. (2001), ‘Vancomycin-resistant staphylococcus aureus: a new model of antibiotic resistance’, *The Lancet infectious diseases* **1**(3), 147–155.
- Huang, C. and Fan, A. (2014), Antimicrobial resistance within host: a population dynamics view, *in* ‘Abstract and Applied Analysis’, Vol. 2014, Hindawi.

- Ibargüen-Mondragón, E., Mosquera, S., Cerón, M., Burbano-Rosero, E. M., Hidalgo-Bonilla, S. P., Esteva, L. and Romero-Leitón, J. P. (2014), ‘Mathematical modeling on bacterial resistance to multiple antibiotics caused by spontaneous mutations’, *Biosystems* **117**, 60–67.
- Ibargüen-Mondragón, E., Romero-Leitón, J. P., Esteva, L., Gómez, M. C. and Hidalgo-Bonilla, S. P. (2019), ‘Stability and periodic solutions for a model of bacterial resistance to antibiotics caused by mutations and plasmids’, *Applied mathematical modelling* **76**, 238–251.
- Jia, C., Qian, M., Kang, Y. and Jiang, D. (2014), ‘Modeling stochastic phenotype switching and bet-hedging in bacteria: stochastic nonlinear dynamics and critical state identification’, *Quantitative Biology* **2**(3), 110–125.
- Joyner, M. L., Manning, C. C. and Canter, B. N. (2012), ‘Modeling the effects of introducing a new antibiotic in a hospital setting: A case study’, *Mathematical Biosciences & Engineering* **9**(3), 601.
- Kebriaei, R., Lev, K., Morrisette, T., Stamper, K. C., Abdul-Mutakabbir, J. C., Lehman, S. M., Morales, S. and Rybak, M. J. (2020), ‘Bacteriophage-antibiotic combination strategy: An alternative against methicillin-resistant phenotypes of staphylococcus aureus’, *Antimicrobial Agents and Chemotherapy* **64**(7), e00461–20.
- Kuok, C.-F., Hoi, S.-O., Hoi, C.-F., Chan, C.-H., Fong, I.-H., Ngok, C.-K., Meng, L.-R. and Fong, P. (2017), ‘Synergistic antibacterial effects of herbal extracts and antibiotics on methicillin-resistant staphylococcus aureus: A computational and experimental study’, *Experimental Biology and Medicine* **242**(7), 731–743.
- LaFleur, M. D., Qi, Q. and Lewis, K. (2010), ‘Patients with long-term oral carriage harbor high-persister mutants of candida albicans’, *Antimicrobial agents and chemotherapy* **54**(1), 39–44.
- Lawrence, B., Mummert, A. and Somerville, C. (2010), ‘A model of the number of antibiotic resistant bacteria in rivers’, *arXiv preprint arXiv:1007.1383*.
- Lewis, K. (2007), ‘Persister cells, dormancy and infectious disease’, *Nature Reviews Microbiology* **5**(1), 48–56.
- Luria, S. E. and Delbrück, M. (1943), ‘Mutations of bacteria from virus sensitivity to virus resistance’, *Genetics* **28**(6), 491.

- Makrythanasis, P., Nelis, M., Santoni, F. A., Guipponi, M., Vannier, A., Béna, F., Gimelli, S., Stathaki, E., Temtamy, S., Mégarbané, A. et al. (2014), ‘Diagnostic exome sequencing to elucidate the genetic basis of likely recessive disorders in consanguineous families’, *Human mutation* **35**(10), 1203–1210.
- McCluskey, C. C. and Muldowney, J. S. (1998), ‘Bendixson-dulac criteria for difference equations’, *Journal of Dynamics and Differential Equations* **10**(4), 567–575.
- Meads, M., Ory, E. M., Wilcox, C. and Finland, M. (1945), ‘Penicillin sensitivity of strains of six common pathogens and of hemophilus hemolyticus’, *The Journal of Laboratory and Clinical Medicine* **30**(9), 725–730.
- Merdan, M., Bekiryazici, Z., Kesemen, T. and Khaniyev, T. (2017), ‘Comparison of stochastic and random models for bacterial resistance’, *Advances in Difference Equations* **2017**(1), 1–19.
- Mostefaoui, I. (2014), ‘Mathematical analysis of a model describing the number of antibiotic resistant bacteria in a polluted river’, *Mathematical Methods in the Applied Sciences* **37**(13), 1956–1973.
- Müller, J., Hense, B. A., Fuchs, T. M., Utz, M. and Pötzsche, C. (2013), ‘Bet-hedging in stochastically switching environments’, *Journal of theoretical biology* **336**, 144–157.
- Murray, J. D. (2002), *Mathematical Biology I. An Introduction*, Springer.
- North, E., Christie, R. et al. (1945), ‘Observations on the sensitivity of staphylococci to penicillin.’, *Medical Journal of Australia* **2**(2), 44–6.
- Oakberg, E. F. and Luria, S. (1947), ‘Mutations to sulfonamide resistance in staphylococcus aureus’, *Genetics* **32**(3), 249.
- Osuna, O. and Villaseñor, G. (2011), ‘On the dulac functions’, *Qualitative Theory of Dynamical Systems* **10**(1), 43–49.
- Pirommas, T. and Farida, C. (2021), ‘Modeling bacterial resistance to antibiotics: bacterial conjugation and drug effects’, *Advances in Difference Equations* **2021**(1).
- Ripa, J., Olofsson, H. and Jonzén, N. (2010), ‘What is bet-hedging, really?’, *Proceedings of the Royal Society B: Biological Sciences* **277**(1685), 1153.

- Rodrigues, P., Gomes, M. G. M. and Rebelo, C. (2007), ‘Drug resistance in tuberculosis—a reinfection model’, *Theoretical population biology* **71**(2), 196–212.
- Stewart, G. R., Robertson, B. D. and Young, D. B. (2003), ‘Tuberculosis: a problem with persistence’, *Nature Reviews Microbiology* **1**(2), 97–105.
- Takahashi, H., Oshima, T., Hobman, J. L., Doherty, N., Clayton, S. R., Iqbal, M., Hill, P. J., Tobe, T., Ogasawara, N., Kanaya, S. et al. (2015), ‘The dynamic balance of import and export of zinc in escherichia coli suggests a heterogeneous population response to stress’, *Journal of the Royal Society Interface* **12**(106), 20150069.
- Tuscherr, L., Kreis, C., Hoerr, V., Flint, L., Hachmeister, M., Geraci, J., Bremer-Streck, S., Kiehntopf, M., Medina, E., Kribus, M. et al. (2016), ‘Staphylococcus aureus develops increased resistance to antibiotics by forming dynamic small colony variants during chronic osteomyelitis’, *Journal of Antimicrobial Chemotherapy* **71**(2), 438–448.
- Van den Driessche, P. and Watmough, J. (2002), ‘Reproduction numbers and sub-threshold endemic equilibria for compartmental models of disease transmission’, *Mathematical biosciences* **180**(1-2), 29–48.
- Wu, J. A., Kusuma, C., Mond, J. J. and Kokai-Kun, J. F. (2003), ‘Lysostaphin disrupts staphylococcus aureus and staphylococcus epidermidis biofilms on artificial surfaces’, *Antimicrobial agents and chemotherapy* **47**(11), 3407–3414.
- Zhou, Y., Khan, K., Feng, Z. and Wu, J. (2008), ‘Projection of tuberculosis incidence with increasing immigration trends’, *Journal of theoretical biology* **254**(2), 215–228.